Instrumentation of the US Grant Bridge for Monitoring of Fabrication, Erection, In-Service Behavior, and to Support Management, Maintenance, and Inspection

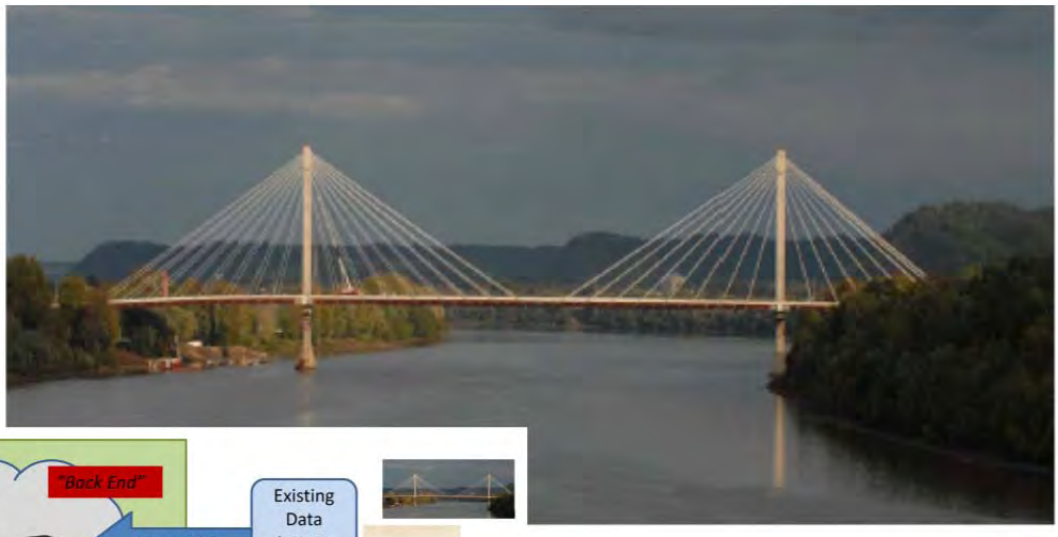

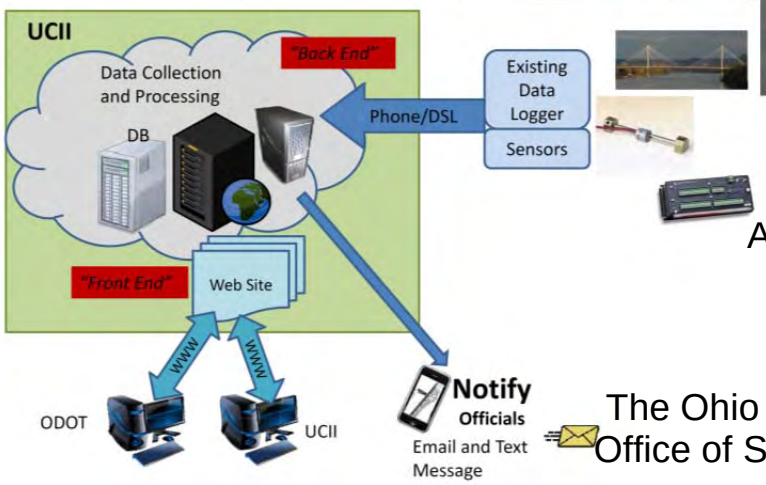

Prepared by:
Arthur Helmicki and Victor Hunt
University of Cincinnati

Prepared for:
The Ohio Department of Transportation,
Office of Statewide Planning & Research

State Job Number 14805

December 2013

Final Report

Technical Report Documentation Page

1. Report No.	2. Government Accession No.	3. Recipient's Catalog No.
FHWA/OH-2013/23		

4. Title and Subtitle	5. Report Date
Instrumentation of the US Grant Bridge for Monitoring of Fabrication, Erection, In-Service Behavior, and to Support Management, Maintenance, and Inspection	**December 2013**
	6. Performing Organization Code

7. Author(s)	8. Performing Organization Report No.
Arthur Helmicki and Victor Hunt	

9. Performing Organization Name and Address	10. Work Unit No. (TRAIS)
University of Cincinnati **Infrastructure Institute** **ML 0030** **Cincinnati, OH 45221-0030**	
	11. Contract or Grant No.
	SJN 14805

12. Sponsoring Agency Name and Address	13. Type of Report and Period Covered
Ohio Department of Transportation **1980 West Broad Street, MS 3280** **Columbus, Ohio 43223**	**Final Report**
	14. Sponsoring Agency Code

15. Supplementary Notes

16. Abstract

The replacement of the US Grant Bridge over the Ohio River in Portsmouth, OH, was initiated in 2001 when the original bridge was closed and demolished, and its substitute opened in 2006. The new design is a steel cable stay design with steel girders and floor-beams supporting a post-tensioned concrete deck system nearly 65' wide carrying one lane of traffic in each direction. The combination of epoxy-coating, grout filling, and outer tubing provides protection for the all-important structural cabling suspension system from both weather and corrosion. Ironically, however, these same features make it impossible to gain direct access to either the cables or the interior of the anchorages which, in turn, presents special challenges for inspection and rehabilitation of these critical bridge components on bridges of this type. It was envisioned that its long-term behavior and any associated changes in its structural condition could be best understood with the aid of a longitudinal study beginning during bridge construction, one that includes instrumented monitoring of both construction/erection and in-service phases of the life of this bridge. Such an approach, integrated with traditional bridge management techniques, would help lead to a safe and economical realization of the 100-year design life of this structure. A health monitoring system for the bridge would be designed, planned, and implemented, with data collection and archival throughout its construction and ultimately an automated, user-friendly interface on a dedicated website.

17. Keywords	18. Distribution Statement
Bridge Monitoring, Condition Assessment, Structural Identification, Truckload Test, Modal Test, Load Rating, Nondestructive Evaluation	**No restrictions. This document is available to the public through the National Technical Information Service, Springfield, Virginia 22161**

19. Security Classification (of this report)	20. Security Classification (of this page)	21. No. of Pages	22. Price
Unclassified	**Unclassified**		

Form DOT F 1700.7 (8-72) **Reproduction of completed pages authorized**

Instrumentation of the US Grant Bridge for Monitoring of Fabrication, Erection, In-Service Behavior, and to Support Management, Maintenance, and Inspection

Prepared by:
Arthur Helmicki and Victor Hunt
University of Cincinnati

December 2013

Prepared in cooperation with the Ohio Department of Transportation
and the U.S. Department of Transportation, Federal Highway Administration

Acknowledgments

The authors would like to acknowledge the Ohio Department of Transportation (ODOT) and the Federal Highway Administration (FHWA) for their cooperation and funding of this project. Without the assistance of forward thinking agencies such as these, development of new technologies and methods would advance at a much slower rate. Special thanks go to ODOT personnel at the district office in Chillicothe and the main office in Columbus for help with design plans, analysis reports, truck support, coordination, etc. The authors specifically acknowledge the support, advice, and direction of Greg Baird, Max Francis, Tom Barnitz, Brad Montgomery, Jeremy Buckle, Tim Keller, Mike Loeffler, Amjad Waheed, the ODOT Technical Panel members, and many others. Throughout the project, the management and tradespersons provided support, insight into the construction process and patience as the instrumentation was installed and data collected. Finally, without the support of numerous people at the district level in coordinating field support for the testing, this project could not have been a success. Though they are too numerous to name individually, their support is gratefully acknowledged. Matt Shamis of Ohio FHWA has also extended his confidence and support for this project for which we are grateful. We also acknowledge the valuable input provided by FHWA Headquarters, the Turner-Fairbank Highway Research Center, and the Office of Research at Washington, D.C.

The work documented within this report is largely the result of a combined effort of many people. Those include Mahdi Norouzi, Jason Kumpf, Scott Kangas, Shashank Chauhan, Jaspal Singh Saini, Robert Sexton, Jim Swanson, and many others.

U.S. Grant (USG) Bridge Final Report

The organization of USG final report is presented herein as follows:

Chapter 1: Introduction and Objectives

The replacement of the US Grant Bridge over the Ohio River in Portsmouth, OH, was initiated by the Ohio Department of Transportation (ODOT) in 2001 when the original bridge was closed and demolished, and its substitute opened on October 16, 2006.

Chapter 2: Proposed and Implementation Plans

The initial tasks for the research project included modeling, sensor suite design and ordering of supplies and equipment. The first phase was to involve instrumentation of the towers at the traffic and cable anchor elevations as the construction process reached these locations. As the instrumented sections were erected, University of Cincinnati Infrastructure Institute (UCII) researchers worked with the contractor to route and connect the sensor cabling through a network of conduit and junction boxes to the main cabinet. Also, dead-load effects would be recorded and long-term monitoring would begin as the sensors were connected to the data systems. In this manner, the responses to transverse and longitudinal post-tensioning of the panels would be measured and the stressing of the cable stays would be tracked for the given section and with successively erected sections of the bridge. Similarly, a set of dynamic experiments would be conducted to characterize the structure's response to truckload, ambient (e.g. wind) forces and effects, and to it.

Chapter 3: Preliminary Design

A health monitoring system for the bridge was designed, planned, and implemented for the U.S. Grant bridge, with data collection and archival throughout its construction and ultimately an automated, user-friendly interface on a dedicated website. The primary criteria for selecting the instrumented segments were the predicted stresses and rating factors using the analytical data provided by the designer. Bridge Plans Addendum and Construction Contract Bid Documents were developed to document the monitor design.

Chapter 4: Bridge Modeling and Analysis

The chapter objective was to use the measured response of the bridge against construction live loads and programmed truck load tests to develop a field calibrated finite element model of the bridge simulating the end of construction and initial in-service behavior. This field calibrated model captures baseline information of the bridge before it was opened to traffic.

Chapter 5: Analytical and Experimental Stress during Construction

This chapter compares the experimental stresses through the end of construction (EOC) derived from the health monitoring strain gages to the calculated stresses that were anticipated during design. Thereafter, daily and seasonal environmental effects are measured, the effect of the pulldown retrofits are examined, and other longer term effects are discussed.

Chapter 6: Truckload Testing Results

This chapter covers the designing and executing a truck test, performing the initial data reduction and assessment of the bridge response. After construction, testing was performed to determine the elastic bridge response using truck load tests whereby a number of heavily loaded vehicles are driven across the structure in an attempt to determine bridge response under design loads and to accurately predict live load response for the bridge.

Chapter 7: Pulldown Instrumentation and Testing

This chapter focuses on instrumentation and monitoring system for the new upstream and downstream pull downs and at the Kentucky abutment wall.

Chapter 8: Experimental Load Rating and Analysis

An inventory HS25 rating using both the allowable stress and load factor methods was formulated for both the composite and noncomposite or cracked case for each section as defined by the stations used by both HNTB and B&T. Each section was analyzed by each method at the bottom flange, top flange, cast-in-place (CIP) decking immediately above the edge girder, and for the deck panel adjacent to the edge girder which is to include the effect of the post tensioning (PT) force reported by B&T. In addition, each of these members was analyzed under both the positive and negative liveload moment reported by HNTB.

Chapter 9: Stay Vibration

This chapter focuses on the stay testing program that was employed on this project. Several experiments were performed during various stages of construction to determine the capability of using traditional vibration techniques to estimate cable tensions with the non-traditional cable sheathing system of this structure.

Chapter 10: Modal Analysis

This chapter focuses on the operational modal analysis program that was employed on this project. The magnitude and direction of structural vibrations may be monitored/measured at critical locations through the use of mounted accelerometers to identify the characteristic modal shapes and frequencies of the bridge.

Chapter 11: Website Design and Documentation

This chapter focuses on the long term instrumentation package, data collection system and web site which is used to monitor and evaluate the long term environmental effects on the structure. This system provided the ability to plot strain and temperature information about the bridge in a data-form which can easily be plotted over periods of time for multiple locations. The data collection and warehousing of gage readings means not only can officials do further analysis of the bridges health but a historical archive of bridge performance is recorded. High speed connectivity allows for frequent data collection which enables fault detection and the ability to automatically send warning notifications.

Chapter 12: Conclusions and Future Work.

A general increase in understanding of the inspection, maintenance, and bridge management issues associated with cable-stayed bridges by key personnel in the state.

Table of Contents

Chapter 1 Introduction and Objectives

1.1 Overview of the Project

The replacement of the US Grant Bridge over the Ohio River in Portsmouth, OH, was initiated by the Ohio Department of Transportation (ODOT) in 2001 when the original bridge was closed and demolished, and its substitute opened on October 16, 2006. Initially, it was a suspension bridge, and opened to traffic as a toll bridge in 1927. It was the only automobile bridge in Scioto County to cross the Ohio River, but became a nightmare when the bridge closed for repairs in 1978. Subsequent maintenance work, and a long-range study to determine the cost effectiveness of sustained rehabilitation in 1992, showed that a new structure would be cheaper in the long-run.

Now completed, and in service since 2006, the new structure consists of 9 spans, including a 875' main span crossing the Ohio River, for an overall bridge length of 2,155' (Figure 1.1). The design of this replacement structure is a steel cable stay design with steel girders and floor-beams supporting a post-tensioned concrete deck system nearly 65' wide carrying one lane of traffic in each direction. Each of the two main pylons/support towers are 288' above the waterline and the main span deck sits more than 85' above the Ohio River.

The US Grant Bridge, serving US Route 23, represents a key transportation link in the southeastern part of the state, and it is a highly visible monument for the City of Portsmouth, the surrounding communities and the state of Ohio. In addition, the main span unit is Ohio's first long-span, cable-stayed bridge and one of only a few dozen such bridges in service in the nation at this writing (Helmicki, 2002). As such, this structure is vastly different from the types of structures that are currently in the Ohio bridge inventory. In fact, bridges of this design type, together with the set of associated construction technologies necessary to build them, have been used extensively around the world only for the past 2 decades.

The distinctive feature of the cable-stayed bridge type is that the decking system is suspended directly from pylons/towers by straight diagonals that typically consist of cables encased in stiff pipes or tubes (Figure 1.2). These cables have specialized anchorages at the deck interface and may be either anchored at the pylon or continuous over it. The remaining super-structural and sub-structural components of cable stayed bridges (towers, shafts, abutments, deck systems, etc.) are, in general, otherwise similar to those used on more common bridge types.

1.2 Significance of Monitoring and Testing

The US Grant Bridge design calls for a radial arrangement of a system of 32 cables consisting each of 19 seven-wire strands with anchorages at both deck (floor-beam web) and pylon. The combination of epoxy-coating, grout filling, and outer tubing provides protection for the all-important structural cabling suspension system from both weather and corrosion. Ironically, however, these same features make it impossible to gain direct access to either the cables or the interior of the anchorages which, in turn, presents special challenges for inspection and rehabilitation of these critical bridge components on bridges of this type.

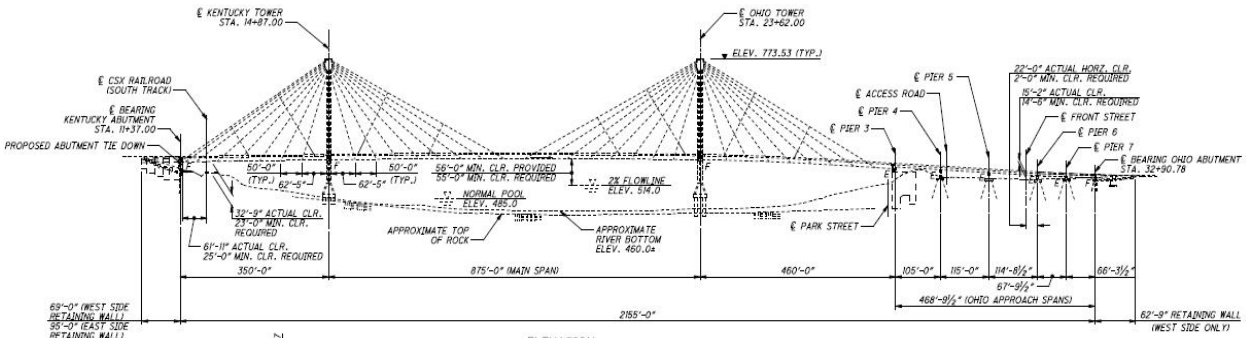

Figure 1.1: Elevation View of the US Grant Bridge

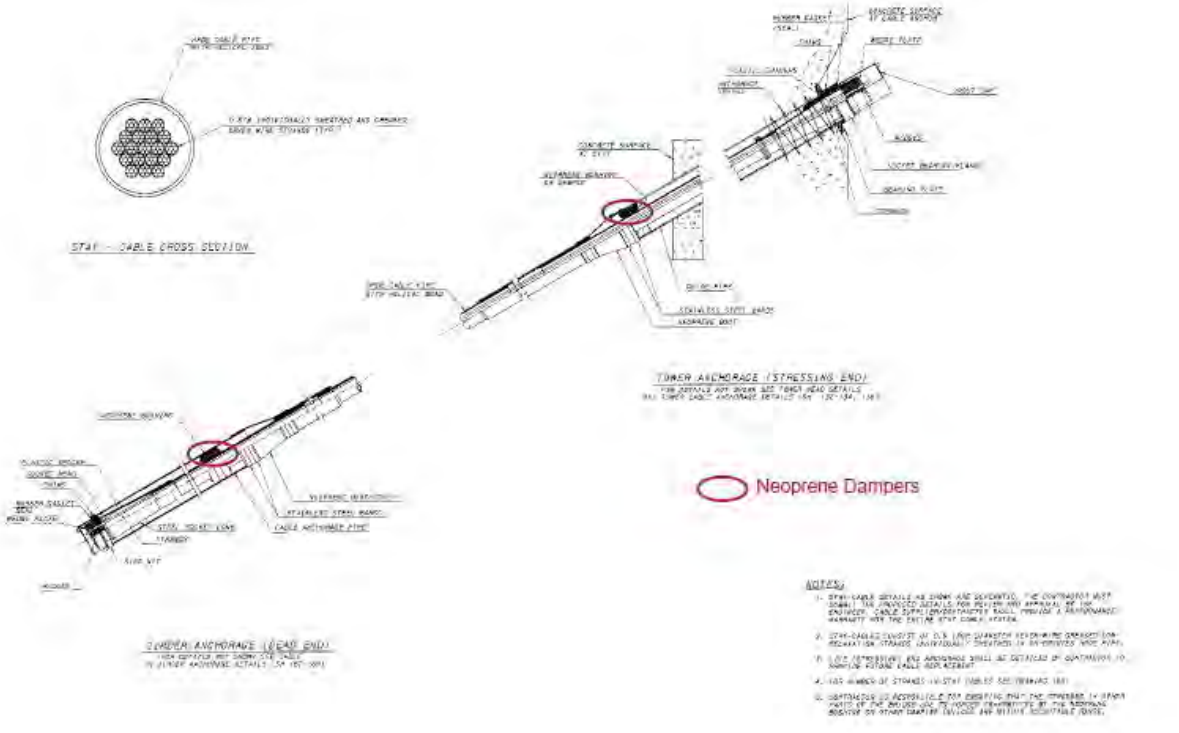

Figure 1.2: Stay-cable Details of the US Grant Bridge

In addition, vibration of the stay cable system is an issue that is unresolved for bridges of this type although passive damping systems are part of their standard components, including the US Grant Bridge (Figure 1.3). This problem is primarily a wind-induced phenomenon that excites lower modes of tensioned cables much like the plucking of a guitar string (Helmicki, 2002). Other environmental phenomena like rain, wind direction, and cable harping pattern contribute to previously observed vibration magnitudes of up to six feet peak-to peak on many bridges. Also, biaxial vibrations mean that vibrations may not be confined to a single plane perpendicular to the axis of the stay-cable. Ultimately, vibrations lead to fatigue and damage in the stay cables and anchorages. Worse still is the fact that the causes and circumstances that create this problem are not yet fully understood.

Figure 1.3: Artistic Impression of the US Grant Bridge

Based on the discussions above, it is important that issues related to maintenance and bridge management be addressed early on with an effective bridge monitoring system. The main shortcoming of current bridge management, monitoring, and inspection methods is that they involve subjective decisions/evaluations. Moreover, certain critical parameters cannot be measured visually and, consequently, visual inspection reports provide incomplete information. This is especially true of the encased, grouted stay cable systems that form the key structural component of cable stayed bridges in general, and of the new US Grant Bridge in particular.

Hence, long-term behavior of the new US Grant and any associated changes in structural condition can be best understood with the aid of a longitudinal study beginning during bridge construction, one that includes instrumented monitoring of both construction/erection and in-service phases of the life of this bridge. Such an approach, integrated with traditional bridge management techniques, will lead to safe and economical realization of the 100-year design life of this structure.

Over the past decade, Ohio Department of Transportation (ODOT) has supported numerous projects aimed at investigating bridge behavior through instrumentation, nondestructive field testing, and structural modeling/identification. These projects have revealed the advantages of

incorporating monitoring and testing in dealing with a wide variety of maintenance and management issues covering dozens of bridges of various types (e.g., steel girder, truss, concrete, etc.) throughout the state. The key feature of this approach is that it provides a solid, objective database of information that can be put to a variety of uses including: verification of design assumptions and analyses, monitoring of construction processes and methods, tracking of bridges responses at key locations for rating, support of inspection and maintenance practices, long term monitoring of structural behavior, etc. Table 1 shows a detailed comparison of the advantages/disadvantages of visual inspection-based evaluations and instrumented/field test-based evaluations.

	VISUAL INSPECTION	**INSTRUMENTATION/FIELD TESTING**
Live and Wind Load Induced Stresses/ Vibrations	Cannot evaluate stress levels, magnitude of vibrations, and magnitude of vibration-induced stresses.	Stress/strain levels due to respective loads/vibrations can be monitored at mounted sensor locations.
Thermally Induced Stresses	Cannot evaluate thermal stress levels and their variations.	Thermal stress/strain levels and variations can be monitored at mounted sensor locations.
Connection Integrity	Section loss, quantity of rust, bolt-integrity, rivet-integrity, weld-integrity, and pin/hinge-integrity, all subjectively evaluated through visual observations. Cannot evaluate force transfer through the connection.	Sensors mounted on connection plates, pins, and hinges can be used to evaluate how effectively force/load is transferred through the connection as well as what stress levels are within critical connection components.
Structural Member Rating	Interpretation of visually observed section loss, rust, cracking, corrosion, etc. used to evaluate load-carrying ability of structural member.	Field measurements reflect true load-carrying ability of structural member. This information used to evaluate capacity of member as well as live load effects on member.

Table 1: Comparison of maintenance/inspection approaches

1.3 Objectives of the Study and its Phases

The project sought to identify an appropriate instrumentation and field testing program to support management of the US Grant Bridge. This program augments the traditional visual inspection program to provide objective, quantitative data for use by ODOT in assessing the status of the structure. It was anticipated that the instrumentation plan will be designed to allow

researchers and ODOT officials capture key aspects of the behavior of the bridge during both the fabrication and erection phase as well as during in-service use.

In the initial phase, proper arrangements were made with the construction contractor for necessary on-site assistance in installing gages to monitor the bridge's response to construction loadings (responses accumulated through erection, etc). Subsequently, environmental loadings (from wind, temperature, etc) and traffic/in-service loadings were employed, after construction, without requiring the need for contractor assistance. All instrumentations were operated by a computer-controlled, digital data-acquisition system located on-site, and accessible tele-remotely via direct modern/telephone connection. The goal was to achieve a high degree of monitoring intelligence so that the system would be user friendly and would alert ODOT officials of anomalous structural events.

The project also proposed the development of detailed instrumentation and testing plan designs in close consultation with ODOT officials, bridge designers, and construction contractors. It was expected that existing design calculations and upcoming erection analyses would be used to fine-tune the sensor suite and testing plan. A summary description of various aspects of the instrumentation/monitoring/testing plan is given as follows:

Key Construction Parameters

The first task of the project focused on working with ODOT to secure the assistance of the contractor in gaining proper access to the site during the construction period so that construction events could be monitored. Key variables of interests included

1. Weather conditions throughout erection including temperature, precipitation, and wind direction and velocity.
2. Thermal cross-section of pylons, exterior girders, and concrete-decking sections, over time, to resolve the environmental responses and internal strains of the structural components.
3. Stress levels (longitudinal and tangential), at pylon cable anchorages, as they are erected, and as deck sections are added.
4. Tip displacement of the outermost-decking sections in response to thermal, wind, and dead load, as erection proceeds, in order to ensure proper alignment.
5. Cable acceleration and displacement, during erection, in response to accumulated dead loads, thermally induced responses, and wind loads. Loads and stresses were then determined in order to ensure proper tensioning and positioning.

Throughout construction, the authors coordinated with the contractor to ensure maximum synergy between data sets and avoid collection of redundant data. Upon completion of construction, well-defined loads were applied to the bridge, and the authors ran test sequences to confirm the structural behavior, proper operation of the instrumentation, and validate pre-built computer models.

Key In-Service Parameters (Environmental and Traffic Related)

Once the bridge was put into service, it was expected that gages placed during the erection process would be maintained and some additional, traffic-related measurements taken as follows:

1. Weather conditions (i.e., temperature, precipitation, and wind direction and velocity).
2. Thermal cross-section of pylons, exterior girders, and concrete-decking sections, over time, to resolve the environmental responses and internal strains of the structural components, and separate them from traffic responses.
3. Stress levels (longitudinal and tangential) at selected pylon cable anchorages, to continually monitor settlement and live load effects (wind and traffic).
4. Acceleration of selected deck sections (particularly at abutments, pylons, and mid-span) in response to thermal, wind, and traffic load.
5. Longitudinal stress of selected exterior girder and deck sections, particularly at abutments, pylons, and mid-span (high moment regions), in response to thermal, wind, and traffic load. These were to be used to monitor movement of the neutral axis of the deck section in order to obtain the information on integrity of the pre-stressing tendons in the deck sections.
6. Cable acceleration in response to thermal, wind and traffic loads in order to characterize vibration levels and mechanisms, as well as calculate loads and stresses.

It was proposed that a schedule of controlled truckload tests and ambient cable-vibration studies would be developed for the purposes of structural identification. These tests would make use of the aforementioned sensor suites and would yield the information necessary to calibrate Finite Element (FE) models of the bridge.

Inspection/Maintenance Support

In the case of the US Grant Bridge, the inspection/maintenance support focused on measuring (1) Accumulated and incremental stresses at all gaged locations. (2) Neutral axis location as an indicator of composite action and pre-stressing tendon integrity. (3) Cable acceleration in response to thermal, wind and traffic loads in order to characterize vibration levels and mechanisms, and facilitate load rating.

1.4 Expected Benefits and Deliverables

The benefits of the overall project, proposed, were twofold:

1. A database of field measurements, together with structural interpretations, which would serve to provide objective information for use as part of the bridge management process specific to the US Grant Bridge.

2. A deeper understanding of the general behavior and performance of cable-stayed bridges - one that could be used on, and transferred to, other cable-stayed bridges being constructed and/or planned in Ohio (i.e. Veterans Glass City Skyway, Pomeroy-Mason, etc).

These would help facilitate the management of this portion of the ODOT bridge inventory, and help make it possible to reach the expected service life of 100 years in an economical manner. Other specific benefits included:

1. Formation of a team with the knowledge and personnel to support ODOT's efforts in effectively managing cable-stayed bridges.
2. General increase in understanding of the inspection, maintenance, and bridge-management issues associated with cable-stayed bridges by key personnel in Ohio state (universities, ODOT and the industry at large).
3. Development of field-ready monitoring strategies, aimed at supporting inspection and maintenance/management activities, and reducing life-cycle costs.
4. Implementation and continued operation of a monitor, using the aforementioned strategies at the US Grant Bridge.
5. Collection and archival of a comprehensive information bank, based on instrumentation and field observations of the US Grant structure, together with recommendations for possible actions to be taken during construction and service.

1.5 Anticipated Research Results

At the completion of the project, the following research products/results were expected:

1. An analytical FE model of the US Grant Bridge main span system, complete with analysis/simulation results, indicating all critical load carrying members and load paths for sensor suite design and placement.
2. A detailed instrumentation of the US Grant Bridge's most critical members/locations with instrumentation protection suitable for long-term, reliable operation over the next 3-5 years. Instrumentation plan would allow for future truck-loading tests to take place intermittently at ODOT's discretion.
3. A database of all field test data obtained on the US Grant Bridge, including baseline and a regular regimen of truck-load tests, ambient vibration tests, and long-term environmental monitoring.
4. A detailed analysis of all data obtained from field testing operations to reveal member/ connection load carrying capacities at all instrumented locations.
5. A detailed, written reporting of all activities and findings obtained by UCII in the course of conducting this project.
6. A dynamic bridge-health monitor, incorporating hardware and software on the bridge at the completion of the project, as well as weigh-in-motion scales for real-time monitoring and statistical documentation of every wheel/axle weights, speeds and classification,

real-time online capacity assessment of the instrumented members/locations, real-time instantaneous control actions including electronic paging/email, variable message signs (VMS) and video camera surveillance.

7. A dedicated website for community access to the bridge history, general description, selected bridge/traffic conditions, future plans, email feedback, etc.

References

1. A. Helmicki and V. Hunt, “Instrumentation of the US Grant Bridge for Monitoring of Fabrication, Erection, In-service Behavior, and to Support Management, Maintenance, and Inspection,” Bridge No. SCI-23-0.00, Proposal to ODOT and FHWA by University of Cincinnati Infrastructure Institute, 2002.

Chapter 2 Proposed Implementation Plan

2.1 Work Plan

Implementing a customized, integrated and synergistic plan of testing and evaluation, to provide ODOT with detailed information about construction, traffic, wind, thermal and other bridge responses at the most critical members/connections of the bridge, would require the following aspects of the problem to be addressed:

a. Modeling
b. Sensor suite
c. Data acquisition
d. System design
e. Installation
f. Dead-load, and (where possible), other constructions
g. Event monitoring
h. Regimen of truck-load testing
i. Ambient vibration testing
j. Environmental monitoring
k. Data analysis

At the outset of the project, demolition of the existing bridge was already complete, and construction of the new one was about to commence. The initial tasks for the research project included modeling, sensor suite design and ordering of supplies and equipment. After adequate access to the fabrication and construction facilities, for instrumentation installation, was guaranteed, it was envisioned that all operations could be conducted in tandem and without interruption to the contractor(s).

Hence, the first phase was to involve instrumentation of the towers at the traffic and cable anchor elevations as the construction process reached these locations. A select set of precast panels were chosen to be instrumented at the fabrication shop and critical steel frames at the staging yard near the construction site. The proposed design was such that a main cabinet for the on-site dedicated data systems would be installed at a secured and accessible location on the bridge, while a weather station would be installed at/upon one of the towers to characterize the environmental conditions at the structure. The first frame and panel was expected to be erected in July, 2002 and the final frame and panel in March, 2003. As the instrumented sections were erected, University of Cincinnati Infrastructure Institute (UCII) researchers worked with the contractor to route and connect the sensor cabling through a network of conduit and junction boxes to the main cabinet.

Also, dead-load effects would be recorded and long-term monitoring would begin as the sensors were connected to the data systems. In this manner, the responses to transverse and longitudinal post-tensioning of the panels would be measured and the stressing of the cable stays would be tracked for the given section and with successively erected sections of the bridge. Similarly, a set of dynamic experiments would be conducted to characterize the structure’s response to ambient (e.g. wind) forces and effects, and to it.

Based on the project timeline, the main spans of the US Grant Bridge were scheduled to be completed in May 2003, with the installation of the overlay, pavement, drainage, railing and permanent cable ties. Completion of the approach spans, either Ohio or Kentucky, would require a full diagnostic schedule to be conducted in the summer of 2003, consisting of truckload, modal/vibration, and ambient monitoring tests. Finally, as the bridge began its service to the community, the on-site dedicated data systems would continue collecting response measurements to, any and all, long-term forces and effects. Gradual degradation or shifts of a permanent nature would be observed in the data, downloaded to the lab computers at the Infrastructure Institute, processed, and reported to the Department of Transportation on a regular basis until the contract expired.

A more detailed description of some of the proposed tasks for the project, developed during the planning stages, is included below:

Task 1: Work with ODOT and Contractor to secure needed support for Field Instrumentation Installation and Construction Event Monitoring

Earlier discussions propose the design and installation of a dual purpose instrumentation effort; one that would capture and monitor both construction and in-service effects for the US Grant Bridge. However, it is clear that in order to conduct the gaging necessary to capture construction effects, contractor involvement and support will be needed**.** A draft copy of a change order outlining the necessary interaction with and support from the contractor is contained in Appendix 2 of the original proposal. It was prepared by UCII research team members, in conjunction with ODOT colleagues both at the Central Office and District levels, and was reviewed by the contractor. UCII eventually finalized an agreement for contractor involvement, so that all aspects for the proposed research could be carried out. Table 2 shows the proposed work plan for the project.

Table 2 Project Work Plan

Task Item	**Implementation Group**
Task 2 - Obtain drawings, design calculations, etc.	UCII
Task 3 - Develop Finite Element model	UCII
Task 4 - Design Instrumentation Package	UCII
Task 5 - Establish field test plan • Environmental monitoring	 UCII UCII

• Ambient vibration monitoring • Truck-load testing	UCII
Task 6 - Develop detailed sensor/cable layout plan	UCII
Task 7 - Instrumentation installation • Conduit/junction box/cabinet installation • Utility installation and maintenance • Sensor installation • Provide access (lift, snooper, bucket, etc.) • Provide traffic control (if needed)	 Contractor Contractor UCII Contractor Contractor
Task 8 - Construction monitoring	UCII
Task 9 - Ambient/environmental monitoring	UCII
Task 10 - Baseline field testing • Conduct testing • Provide lane closure/traffic control • Provide access (snooper, bucket, etc.)	 UCII ODOT ODOT
Task 11 - Data analyses and reporting	UCII

Task 2: Obtain Copies of all Design and Construction Drawings, Calculations, Manuals, etc.

A survey of the complete set of information regarding the design and construction of the bridge will give UCII researchers a better understanding of the expected work plan and performance of the structure. Survey information will provide details on geometry, dimensions, and timeline that will be needed for the planning of instrumentation including such items as amount of conduit and cabling needed, routing of conduit, etc. In addition, it will provide details on structural characteristics (such as sectional properties, expected stress/moment ranges, etc.) needed to conduct the modeling and structural analysis as per Task 3 below that will drive the ultimate design of the sensor package for monitoring and testing phases of the project.

Task 3: Develop Three-Dimensional (3D) Analytical Model of Bridge

A 3D model of the stay system will be developed using the information provided in the drawings. The model will reflect the characteristics of the sectional properties and will be adjusted to compensate for any reported changes to the plans during construction. This model will be used to simulate the structural response of the bridge due to each member's dead-load, expected loading by the stay cables, unexpected cable loss, intended scenario for cable replacement, wind loads, and the HS25-44 truck and lane loadings for both capacity and fatigue as per AASHTO Specifications. The results will be analyzed to determine critical-load-carrying members, and load paths, and to bound expected response levels and characteristics. These findings will, in turn, be used as one of the inputs to the sensor suite design and controlled test design described below in Tasks 4 and 5. In addition, the model will be adjusted to compensate for possibly undetected anomalies or for previously unexplored conditions at cable-stay locations and supports (e.g., varying degrees of fixity, axial forces upon the exterior girders, etc.). Again, the above loading simulations will be run to consider the effects of these hypothetical or worst-case scenarios, and these modified simulations will be used to explore other possible locations/members for which monitoring may be indicated. Model validation will occur in two phases: (1) the model will be validated against the independent design calculations provided by the designer to ODOT, and (2) once sensors are in place and data is obtained from actual field measurements, these measurements will be compared against theoretically expected model output and used to tune the model.

Task 4: Determine Members, Connections, Stay-cables, etc. to be instrumented

UCII researchers will make an initial indication as to which members and cables are to be instrumented as well as what the particular instrument configurations (e.g., numbers and types of sensors) are to be used. The inputs which will drive the selection process include the following:

- modeling analysis results from Task 3,
- critical members, connections, cable details specified within the design plans and construction manuals
- members, connections, details indicated by consultation with the design engineers, the contractor, other noted designers, specialists in the field of cable stay assessment, and
- members, connections, details indicated by ODOT as regions of concern

Based on UCII's past field-testing experiences, the sensor suite is likely to consist of vibrating wire strain/temperature gages (used to obtain reliable long-term environmental response characteristics) and resistive-based, high speed strain gages (used to obtain low noise, dynamic load response characteristics). Additional gaging (i.e., accelerometers) will be used for ambient vibration studies. A weather station will be erected to monitor wind speeds in three dimensions, rainfall, temperature, and humidity.

Task 5: Establish Test Schedule

In conjunction with the analysis and sensor suite design activities of Task 4, parallel design activities will be conducted to develop the following bridge tests:

- **Truck-load testing:** Both static and crawl speed tests will be considered. Truck-load configurations and transit paths will be developed, and several loaded and weighed tandem or larger trucks will be required to force a measurable response from the structure and the installed sensors.
- **Ambient vibration monitoring:** An ambient modal test will be designed to evaluate vibration characteristics in the selected members/connections. The results of this testing will serve to further clarify the loading environment by wind, traffic, vibration patterns of the cable response, member and connection responses, and possible fatigue-prone regions within the system. It is important to note that this approach will provide mode frequencies and shapes, but not necessarily any scaling due to the difficulties in assigning the relative effect of each ambient load upon the measured response.
- **Long-term environmental monitoring:** An automated data acquisition system will be designed to interface with that portion of the sensor suite, developed to track the long-term environmental response of the bridge. This system will be configured to run continuously in the standalone mode to sample and record measurements at fixed intervals (e.g., every 15-30 minutes) without human intervention. Periodically, the data will be downloaded to UCII labs for analysis and to clear the data acquisition system memory for more measurements. The download operation will be handled remotely through the use of telephone lines and modem connections. Finally, red-line limits on gage readings will be established and the long-term monitor will have the capability to page ODOT/UCII personnel in the event that a gage reading limit is exceeded, indicating a possibly significant structural response (as in the case for excessive overload, cable loss, accident, damage event, etc.)

Task 6: Establish Sensor and Cable Layouts

The detailed instrumentation plan developed in Tasks 4 and 5 would be finalized in terms of cabling and conduit layouts, placement of sensors, and placement of all connections and data acquisition hardware. This will provide a “blueprint” for the installation phase of the project (e.g., what types of sensors, how many of each type, when and where they will be positioned, protection methods; cable lengths, how will cables be secured to bridge, cable protection methods, etc.). UCII researchers will work closely with the contractor and/or ODOT officials to choreograph the installation process, and make the most efficient use of manpower and resources. All requirements for successful/safe complete sensor installation will be established and reviewed with the contractor and/or ODOT. Also, contingency plans for system maintenance will be established in the event of sensor damage, and an installation timeline/schedule will be developed and reviewed with the contractor and/or ODOT.

Task 7: Sensor Installation

With the detailed, finalized instrumentation plan from Task 6 as a guide, UCII researchers, in conjunction with the contractor and/or ODOT personnel, will install all gages for controlled field testing and long-term environmental monitoring. Due to contractor involvement, the installation would take place in conjunction and concert with construction activities with the minimum possible impact on construction operations. Scheduling will be coordinated with ODOT, as will issues associated with access, and safety, utilities, etc. (see Table 2).

All sensors, cabling, protection/covers/conduits, and data acquisition hardware will be installed according to the timeline established in Task 6. All systems will be tested and debugged to guarantee satisfactory operation. Here it is assumed that all necessary access and safety measures will be provided by the contractor and/or ODOT. Scaffolding, rigging, or other means of access may be required. Alternatively, the contractor and/or ODOT personnel trained in climbing such structures may be assigned to handle tasks that are not reachable otherwise. All necessary instructions and training needed for proper sensor placement will be administered to construction/ODOT personnel by the researchers. In addition, the researchers will oversee that portion of the installation when, and if, it is conducted by non-university personnel.

Task 8: Construction Event and Ambient Monitoring

In order to validate the design steps for both the structure and its monitoring system in Tasks 1 through 7 above, UCII proposed to immediately begin the regular (e.g., every 15-30 minutes) and automated data acquisition, with a permanent data system for the first and successively installed sensors. In addition, a high-speed data system would be used temporarily to collect dynamic ambient (e.g., wind, construction) measurements from the appropriate sensors, by the research team on day trips to the construction site. The data obtained from this monitoring would be used for the following purposes:

- validate (by comparison of theoretical estimates from modeling and actual field measurements) the results obtained from the analytical modeling studies, upon which the sensor suite and testing plan designs were based,
- provide definitive information on expected signal levels and frequency content so that the proper sensors, signal conditioning algorithms, and data acquisition components can be specified and ordered,
- obtain preliminary data on some of the critical locations to initiate the procedures for data post-processing and analysis for member capacity, etc., and
- debug field operations specific to the site, installation methods, access issues, etc.

All data collected would be analyzed and the results would be reviewed with ODOT. If indicated, any necessary modifications would be made to the proposed instrumentation and/or testing plans. The instrumentation and testing plans would then be finalized. Long-term monitoring would continue its regular and automated data collection throughout construction and into the service life for the bridge. It was envisioned that a high-speed data system for dynamic ambient monitoring would be temporarily installed into the main cabinet for dynamic ambient monitoring, when the necessary utilities (e.g., clean power, phone line, temperature control) are provided for its operation.

Task 9: Field Testing for Baseline and Service Condition Assessment

Truck-load testing will consist of an initial baseline test to track any changes in bridge state in response to live loadings. The truck-load test will take several days to complete and require several loaded, pre-weighed tandem or larger trucks of a known axle configuration. It was assumed that all necessary access and safety measures would be provided by the contractor and/or ODOT, and when appropriate, lane or bridge closure, traffic control, and the loaded trucks would also be provided. Scaffolding, rigging, snooper truck, or other means of access was going to be required for the repair/replacement of any damaged sensors, cabling, or other portions of the data system. Full bridge closure was also necessary during portions of the test.

Ambient vibration monitoring will, similarly, take several days to establish the vibration levels and characteristics of the structure. After the stay cables have been grouted within their conduits, accelerometers would be temporarily bonded to a select subset of stay cable conduits, at certain intervals along their length, in order to record their response profiles to ambient loading. Bridge traffic will provide input excitation for the structure and so the bridge was expected to remain open to traffic for most of the test. However, identification of the bridge response to wind loading required full closure of the bridge and was to be conducted just before the bridge went into service.

Long-term environmental monitoring will continuously run in the background, collecting strain data at selected locations. Data will be periodically downloaded to UCII labs via a remote telephone/modem connection.

Task 10: Data Analysis/Reporting

All test data will be post-processed at UCII and findings delivered to ODOT. Intermediate results and findings will be reviewed with ODOT on a continual basis, as they become available. Findings would include: breakdown of construction, truckload and ambient bridge member responses, comparative analysis of bridge member response both temporally and spatially, verification of design calculations, and capacity rating of instrumented members. In order to reduce life-cycle costs, recommendations will be made for actions to take during the service inspection, maintenance and management activities for the US Grant Bridge, in particular, and for cable stay bridges in general.

Data analyses to be performed include:

- Evaluation of member/cable/connection performances, using long-term environmental monitoring, to determine dead-load stress at the instrumented locations, peak and cumulative stress from all construction at instrumented locations, thermal induced stress/cycles, and thermal effects on instrumented locations
- Evaluation of member/cable/connection performances, using dynamic ambient monitoring, to determine load-carrying/transfer capability to ambient loading, maximum measured stresses to both traffic and wind loading (within members/connections and where such measured stresses occur), maximum vibration amplitude (g's) at instrumented locations, natural frequencies and vibration (mode) shapes from both traffic and wind loading
- Evaluation of member/cable/connection performances using baseline and service field tests to determine load-carrying/transfer capability for controlled loading, maximum measured stresses

(within members/connections and where such measured stresses occur), maximum vibration amplitude (g's) at instrumented locations, natural frequencies, and vibration (mode) shapes, HS25-44 load and fatigue rating of instrumented members.

In addition to the normal communication of findings as described above, the research team would formally submit quarterly progress reports to ODOT in the required format. Six months prior to the completion of the contract, the research team would submit, for ODOT's review, a draft of the project's final report. This report would fully describe the activities undertaken on the project, incorporate all results and findings obtained, as well as any recommendations for actions to take during the service inspection, maintenance and management activities for the US Grant Bridge in particular and for cable stay bridges in general.

After review of the report, ODOT comments and suggestions would be incorporated in a final version of the project report, which would be officially submitted to ODOT.

References

1. A. Helmicki and V. Hunt, "Instrumentation of the US Grant Bridge for Monitoring of Fabrication, Erection, In-service Behavior, and to Support Management, Maintenance, and Inspection," Bridge No. SCI-23-0.00, Proposal to ODOT and FHWA by University of Cincinnati Infrastructure Institute, 2002.

Chapter 3 Preliminary Design

3.1 Design of Instrumentation Plan

Proper arrangements were made with the general contractor for the necessary assistance and access at the site, while minimizing any disruption to the construction work or its schedule. However, environmental loadings (i.e. wind, temperature, etc.), and traffic/in-service loadings were employed after construction without any need for contractor assistance. Detailed instrumentation and testing plan designs were developed in close consultation with ODOT officials, bridge designers, and construction contractors. Where possible, the researchers employed proven, off-the-shelf, turn-key components to assemble the pieces of the proposed monitor. This was to minimize monitor development time and maximize reliability.

In order to meet stated objectives, a weather station, together with a suite of vibrating wire and resistive strain gages, and accelerometers, were used at selected critical sections as shown in Figure 3.1. Where possible, all gaging were placed embedded in (i.e., attached to rebar, etc.) or affixed on (i.e. tack-welded or epoxied to steel surfaces, etc.) the structure as construction proceeded.

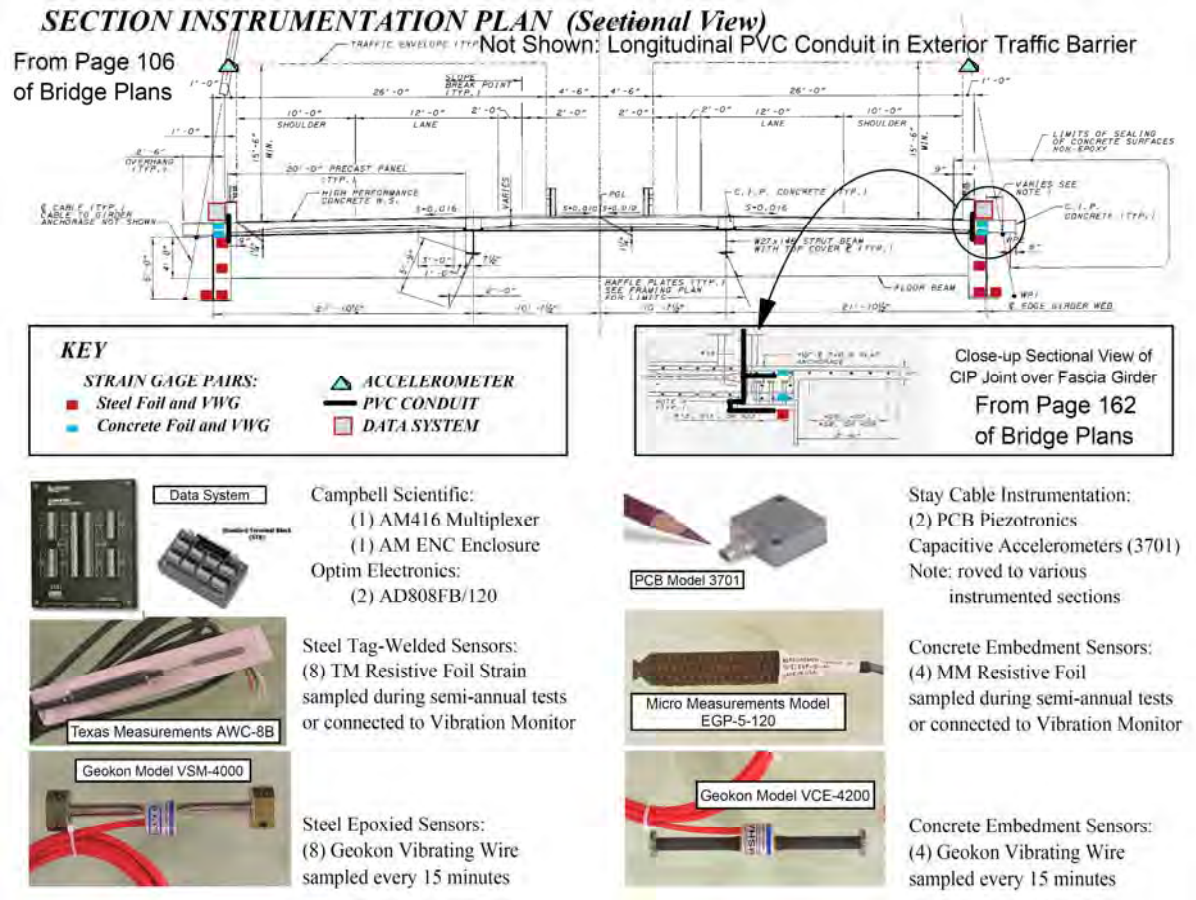

Figure 3.1: Sensor Plan for Selected Critical Sections of U.S. Grant Bridge (Hunt, 2005)

From the sensor plan of Figure 3.1, key variables that were monitored include:

- Weather conditions (i.e., temperature, precipitation, and wind direction and velocity).
- Cable acceleration in response to thermal, wind and traffic loads, in order to characterize vibration levels and mechanisms. Loads and stresses were calculated in order to ensure proper tensioning and positioning.
- Acceleration of selected deck sections in response to thermal, wind, and traffic load to compare with the designed frequencies of its movement, and to resolve any coupling with the stay movements themselves.
- Longitudinal stress of selected exterior girder and deck sections, particularly at abutments, pylons, and mid-span (high moment regions), in response to thermal, wind, and traffic load. These were used to monitor stress levels as compared to the design values and movement of the neutral axis of the section, and to obtain information on the integrity of the designed level of composite action.
- Thermal cross section of exterior girders and decking sections, over time, to resolve the environmental responses and internal strains of the structural components, and separate them from traffic responses.

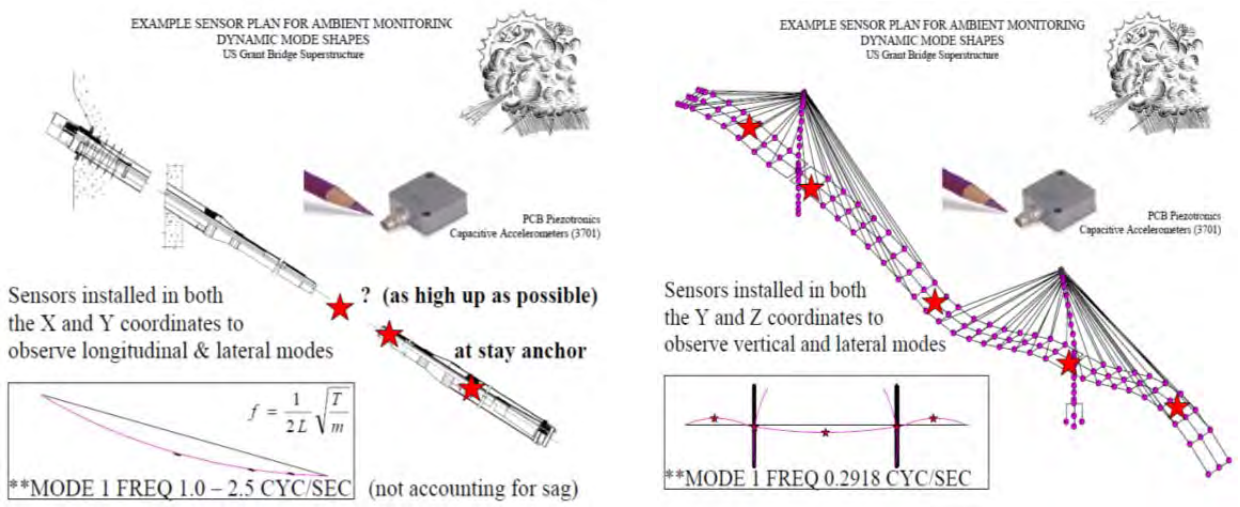

Figure 3.2: Example Sensor Plan for Ambient Monitoring of Dynamic Mode Shapes (Helmicki, Hunt, 2004)

A schedule of regular and automated monitoring, controlled truckload tests, and ambient cable vibration studies were also developed for the purposes of structural identification. The monitor and controlled tests/studies utilized installed sensor suites, and yielded the necessary information for comparison with design values as well as to calibrate finite element models of the structure. Such models were useful in determining the bridge response, globally, and interpolating responses at locations where gages were not mounted, developing trend lines for bridge response over time to understand long term behavior of structural systems, and provide a response-prediction tool which can be used for rating and issuance of overload permits, etc.

3.2 Selection of Critical Sections

UCII researchers prioritized the many possible events of concern that may occur throughout the construction and service of this bridge, and winnowed the critical sections down to only five due to budget constraints. Existing design calculations [2] and erection analyses [3] were used to specifically identify the five critical sections to instrument, test, and monitor these variables during the life of the bridge. Allowable stress rating of the exterior girder section identified three minima of concern for the bottom flange in terms of positive moment (Figure 3.2) and three for the cast-in-place (CIP) joint/decking above the girder in terms of negative moment (Figure 3.3). There was three of each, corresponding to each span of the structure. They do not necessarily coincide with each other, due to the very nature of a stayed structure and its staged construction; however, the middle and Ohio spans are proximate.

The Kentucky span is not coincident due to large negative moment occurring near the end of construction when the bridge is weighed down and tied at the abutment in order to achieve the designed vertical profile for the structure. The ratings were also important because they enabled the identification of sections which may actually be classified as “cracked” (according to the designer) or non-composite. Note that the ratings for the pre-cast deck panels are also shown in Figure 3.3, which includes the post-tensioning to considerably improve the rating over the CIP joint/decking.

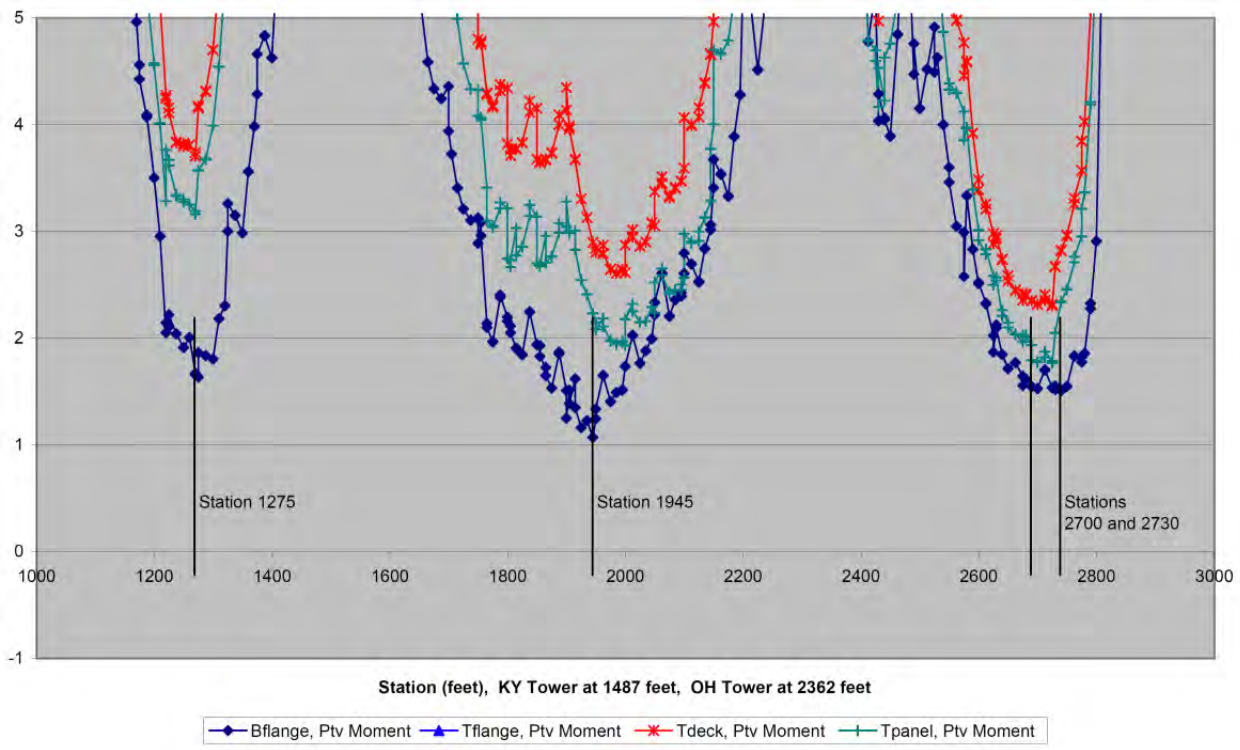

Figure 3.2: Allowable Stress Rating +M Live Load (Hunt, 2005)

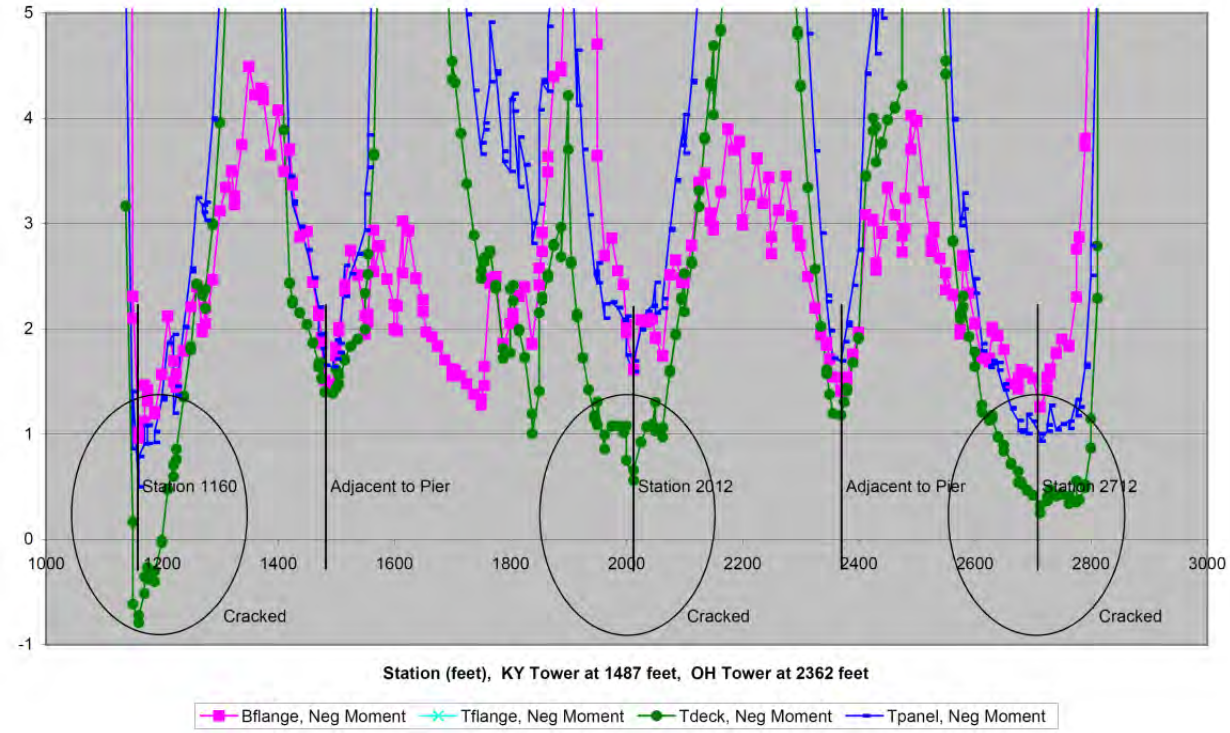

Figure 3.3: Allowable Stress Rating -M Live Load (Hunt, 2005)

For a “cracked” or non-composite section, the sectional modulus for the top flange to resist bending, and the sectional area to resist axial force, were greatly reduced (Figures 3.4 and 3.5, respectively) [5, 2]. This dramatically increased the stress in a section for a given moment and axial load, and decreased the capacity to the girder alone. Further, the top flange extended to only one side of the girder’s web and failed the compactness test [10.48.1.1a, 1]; hence, the yield moment for the top flange was considered as the ultimate capacity in the case of negative moment.

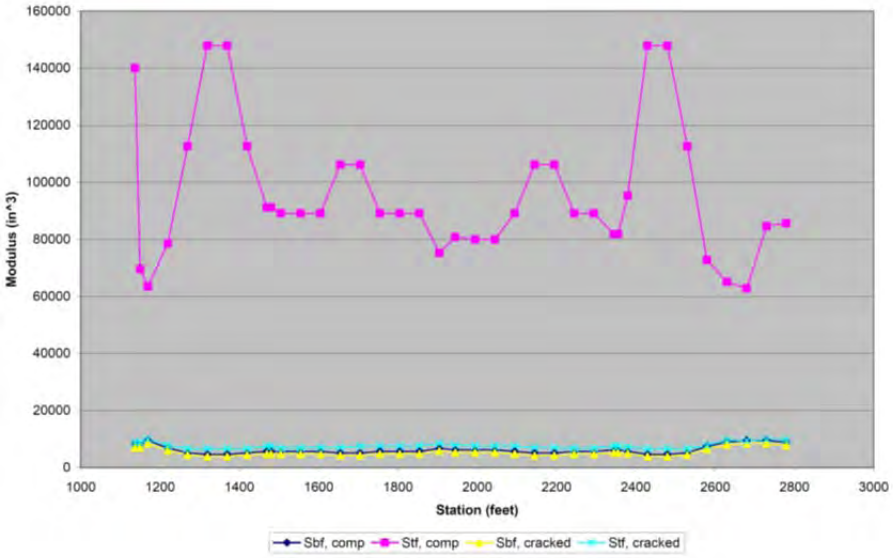

Figure 3.4: Section Modulus for a Cracked or Non-Composite Section (Hunt, 2005)

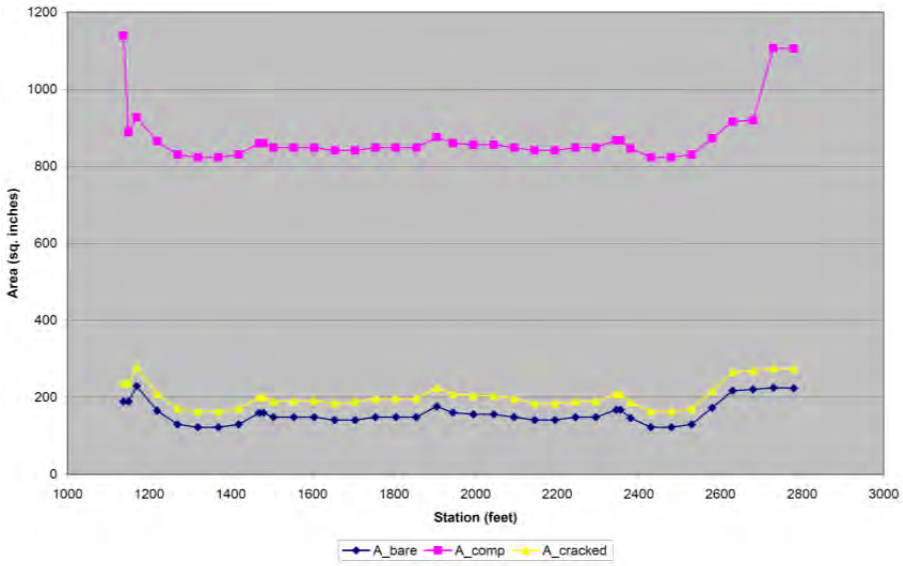

Figure 3.5: Section Area for a Cracked or Non-Composite Section (Hunt, 2005)

Load factor rating of the exterior girder section identified three minima of concern in terms of positive moment (Figure 3.6) and five in terms of negative moment (Figure 3.7). Note that axial force was not considered in deriving the load factor rating. The section was assumed to act composite in positive moment and “cracked” or non-composite in negative moment. The derived results corresponded to each span and pier of the structure.

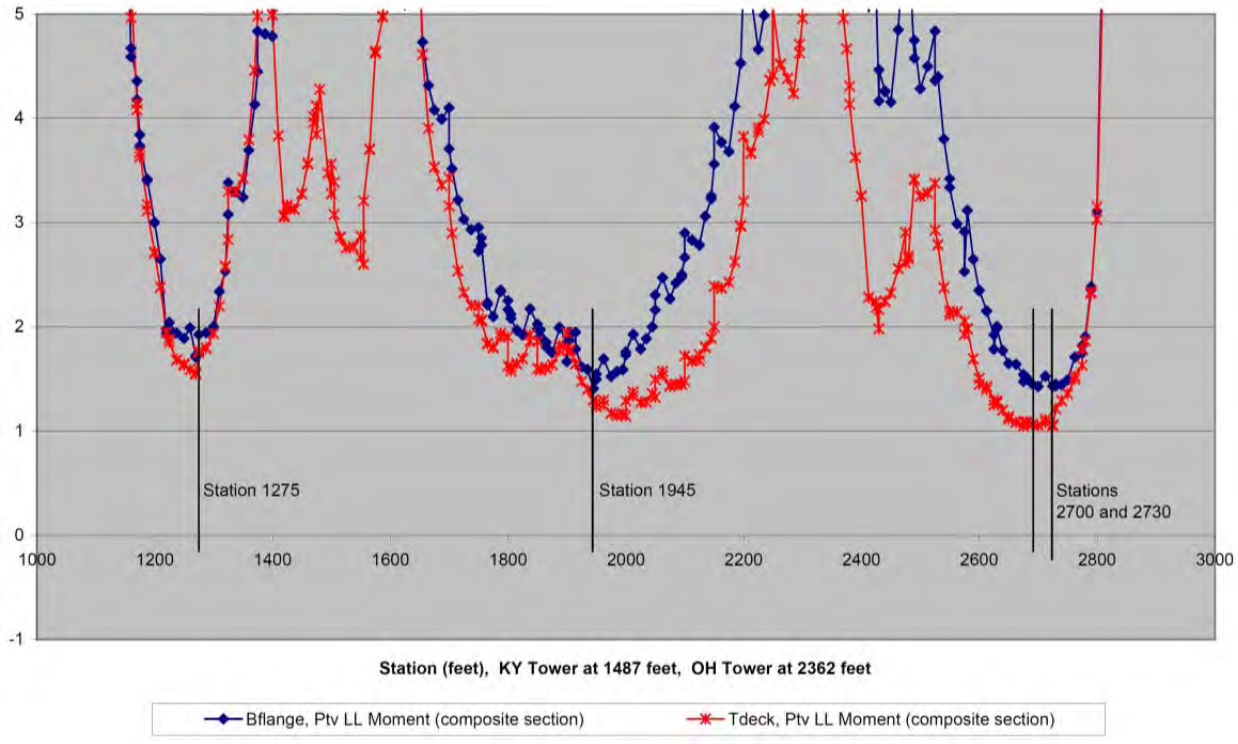

Figure 3.6: Load Factor Rating +M Live Load (Hunt, 2005)

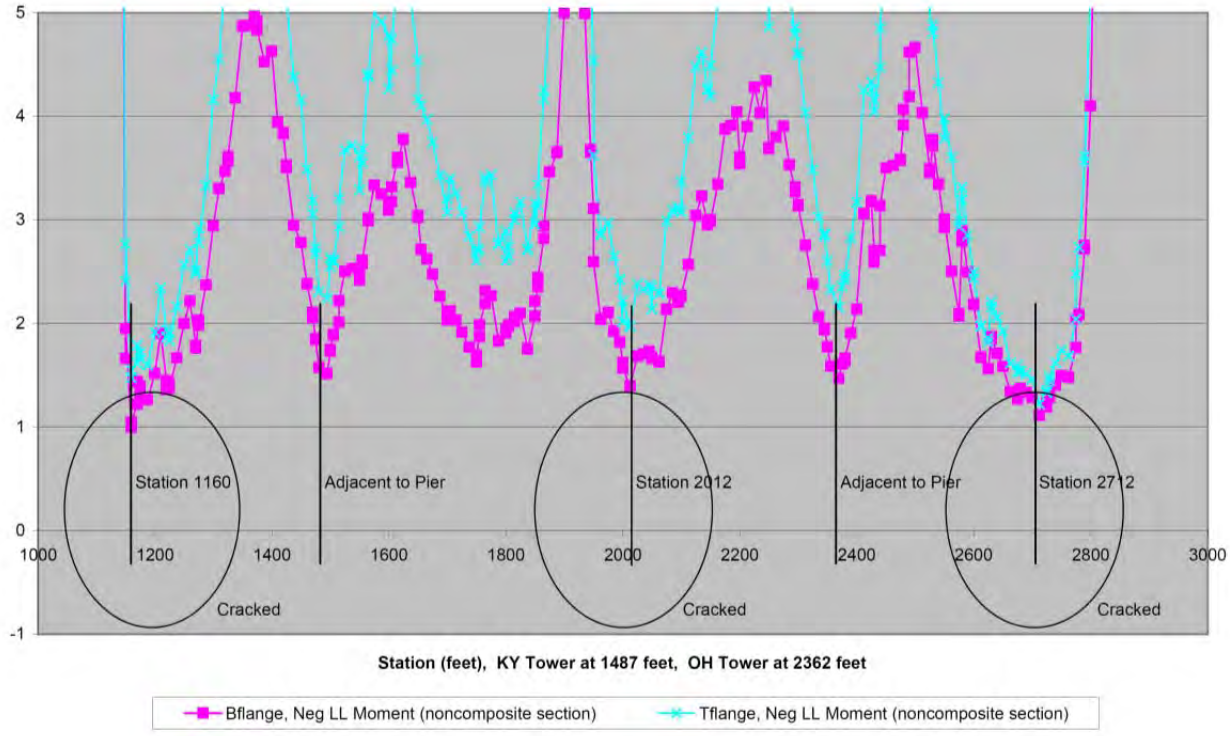

Figure 3.7: Load Factor Rating -M Live Load (Hunt, 2005)

Figure 3.8 summarizes the sections or stations of concern according to the various analyses of the structure. The two methods for live load rating identified three stations of concern for positive moment loading (P1, P2, and P3) and five stations for negative moment (N1 – N5). These results were combined with those from the erection analysis.

The erection analysis identified several stations of concern at specific stages of the construction [3]. As framing began to cantilever out from the towers, there was a concern of torsional cracking for the stub/table beams at the piers. Similarly, as the construction proceeded nearer to the abutments, there was a concern of negative moment at the temporary bents (e.g., N6) until the framing actually reached the abutments for support.

There was also a significant negative moment imparted at N1 when the bridge was tied at the abutment, to achieve the designed vertical profile for the structure. Note that all but the temporary bent was already a station of concern from the live load rating analysis. Hence, the total number of critical sections identified was nine (i.e., P1-3, N1-6), but only five could be permanently monitored. A temporary installation was designed for the Ohio bent in order to monitor it only during construction, while it was decided to instrument only one pier (and remove N4 from the list) since the selection criteria were identical. N3 and N5 were removed due to proximity of the positive and negative moment stations in their respective spans.

The instrumentation at P2 and P3 would still provide sufficient information about the negative moment case for these spans, especially for the case of N5; to this end, the final station for P3 was chosen to also accommodate N5. The final selection of stations is shown in Figure 3.8; a check mark indicates that the chosen stations will be able to monitor the specific concerns of the live load and erection analyses. Figure 3.9 shows the location of temporary bents on segment/panels 4N and 4S.

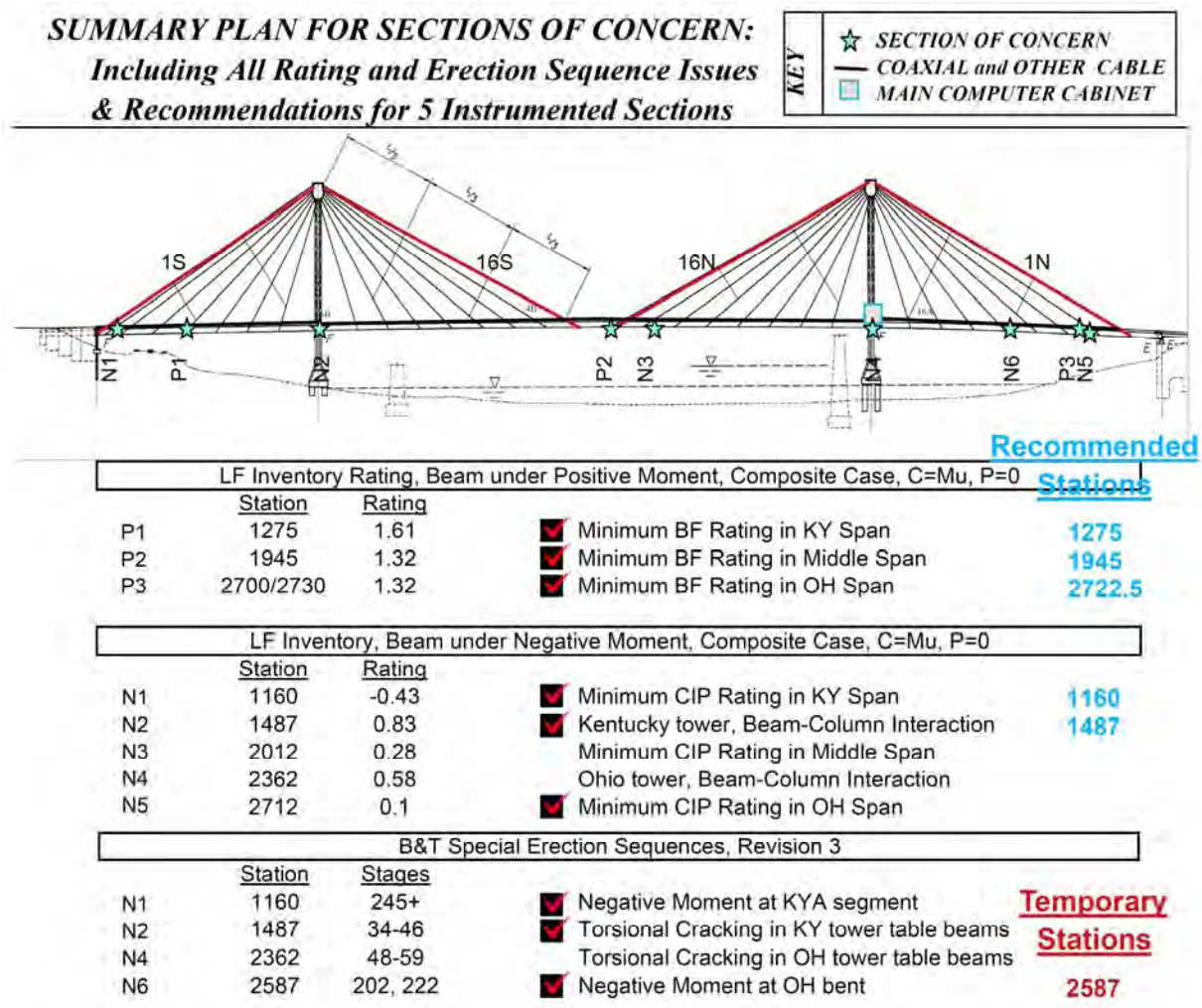

Figure 3.8: Final Selected Critical Stations for U.S. Grant Bridge (Hunt, 2005)

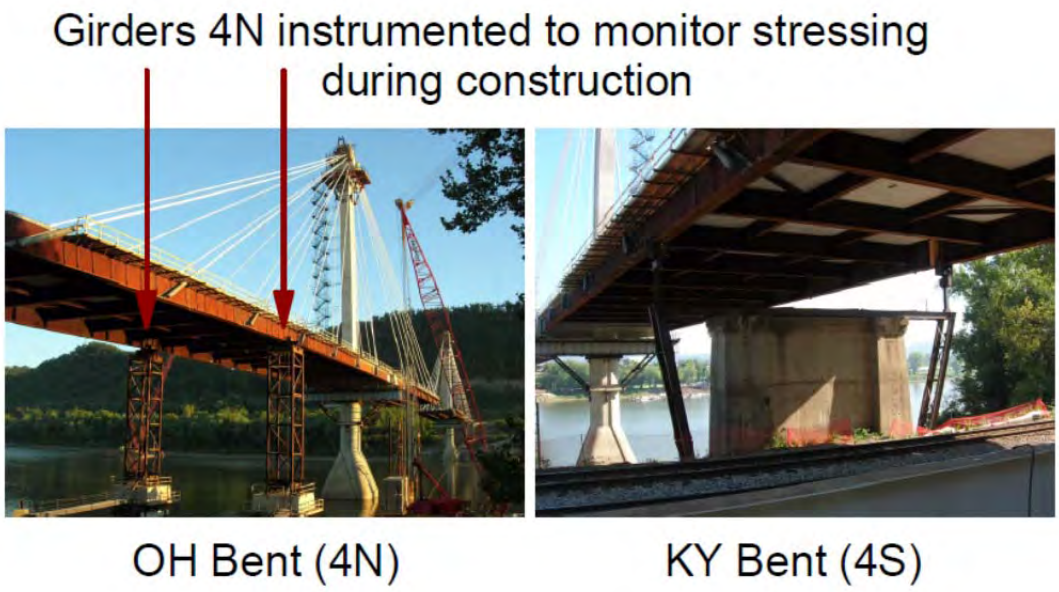

Figure 3.9: Location of Temporary Bents on Segment/Panels 4N and 4S (Helmicki, Hunt, 2004)

REFERENCES

1. V. Hunt, A. Helmicki, and J. Swanson, “Instrumentation and Monitoring of the US Grant Bridge,” *Proceedings of ASNT Structural Materials Technology VI: An NDT Conference,* Columbus, OH, October, 2005.
2. Howard, Needles, Tammen, and Bergendoff (HNTB), Design Calculations for the U.S. Grant Bridge, 2000.
3. Buckland & Taylor (B&T), Superstructure Erection Submission for U.S. Grant Bridge, Rev. 3, 2004.
4. A. Helmicki, and V. Hunt, “Instrumentation of the US Grant Bridge for Monitoring of Fabrication, Erection, In-service Behavior, and to Support Management, Maintenance, and Inspection,” Project Review, ODOT Central Office, 2004.
5. C.S. Cai, J. Nie, and Y. Zhang, “Composite Girder Design of Cable-Stayed Bridges.” Structural Design and Construction, ASCE, Vol. 3, No. 4, November 1998: 158-163.

Chapter 3 Appendix or Notes Regarding Rating Calculations

In order to better document our approach and methods, the calculation of the design ratings presented as the basis for our location of the sensors is detailed here. For further details, please see the spreadsheet "Edge Girder Ratings, B&T Deadload, HNTB Liveload, v3d3, modified LFR, P=0.XLS" or contact the authors directly.

GIVEN VALUES USED

Geometric properties by Member by Section were found in the bridge plans by HNTB.

Sectional Area, Centroid, and Inertia of the Bare Steel alone were calculated using these.

Note that there is a slight discrepancy between HNTB and B&T regarding the thickness of the deck panels (i.e., 10" and 9", respectively). It is assumed that the erection engineer would know best as to which deck panel thickness was actually employed.

Sectional Centroid was then compared to that given by B&T in version 3 of their input file "g_sec_JH, rev3.csv" for erection analysis. These two values were generally within a few inches (less than 5% of section height).

Composite sectional area, centroid, and inertia were given by B&T in version 3 of their input file "g_sec_JH, rev3.csv" for erection analysis.

Composite sectional modulus at bottom flange, top flange, and top of decking were given by B&T in version 3 of their input file "g_sec_JH, rev3.csv" for erection analysis.

Prestress force and area were given by B&T in version 3 of their input file "g_sec_JH, rev3.csv" for erection analysis.

Reinforcement quantities, size, and location were found in the bridge plans by HNTB, including some additional reinforcement added in later revisions to the plans. This information was used to adjust (i.e., increase) the sectional properties for the bare steel case above to determine the final values for the Noncomposite (or Cracked) Sectional properties. Nonomposite (or Cracked) sectional modulus at bottom flange, top flange, and top of decking were calculated accordingly (i.e., S = I/y).

Note that both a bottom and top flange modulus are considered (e.g., for noncomposite case) because the steel section is not vertically symmetric.

Note that there were significant discrepancies between HNTB and B&T in regards to various analytical assumptions such as effective width in bending (i.e., 96" and 201", respectively) and under axial force (they differ in areas of low axial force, at the ends and middle of the bridge).

See Figures 3.4 and 3.5, respectively, for illustrations of these differences. These differences in basic assumptions would affect a variety of things including sectional properties such as centroid, inertia, and modulus, as well as other concepts such as the depth of the stress block for the compactness check in positive moment.

DEADLOADS USED

As there was considerably more information available from B&T (see above), and since the erection engineer would probably have more knowledge of how the bridge would actually be built, we decided to use the deadload forces and moments from B&T in this analysis.

The erection engineering analysis was performed using the sequence generation program ERC95 and their in-house non-linear analysis program CAMIL. See the U.S. Grant Bridge, Demolition Submission, Volume 1 of 2, May, 2001, by B&T for complete details on these.

At every stage of construction, B&T provides not only the total or net axial force, bending moment, and shear for a given section but also for all of its constituent parts (e.g., Dead Load LC 0, Cast-In-Deformation LC -11, Time Dependent Creep and Shrinkage Effects LC -12, Bare Section Forces At Casting, Forces to get same composite deformation, Starting Forces for Composite Sections, etc.). These are found in file "DECK-TOWER-CABLE FORCES REV3.XLS".

Since we are monitoring the construction with strain gages, we need to convert these forces and moments into stress and then ultimately strain for comparison with the gage readings. The most convenient way to do this is by using the sectional properties (found above) for the various conditions of the section during construction (i.e., bare, composite, and possibly noncomposite).

The B&T values for "Bare Section Forces At Casting" are used with the sectional area and modulus for the bare steel to calculate the trapped or built-in stress at both the bottom and top flange, accordingly. Note that B&T applies the axial force at their model's origin which then imparts a moment at the centroid of the section under consideration which must be removed; hence, the calculation of deadload stress for the bare steel would look like this:

$$\sigma_{DL} = \frac{N_{DL}}{A_{Bare}} + \frac{M_{DL}}{S_{Bare}} - \frac{y_{Bare} N_{DL}}{S_{Bare}}$$

Likewise, a calculation for the superimposed deadload stress on the composite section is similarly obtained.

$$\sigma_{SDL} = \frac{N_{SDL}}{A_{Comp}} + \frac{M_{SDL}}{S_{Comp}} - \frac{y_{Comp} N_{SDL}}{S_{Comp}}$$

Since B&T does not directly supply these forces and moments for the superimposed deadload, one must calculate from other values that they do provide. Superimposed deadloads are found by adding Dead Load LC 0, Cast-In-Deformation LC -11, and Time Dependent Creep and Shrinkage Effects LC -12 for the given stage of construction, and then subtracting the Starting Forces for Composite Sections.

Finally, an adjustment stress which is transferred due to axial straining of the steel is applied to each section at both the top and bottom flanges equally. All three of these stresses are added together at each stage of construction to tabulate the total stress accumulated at each member. Both the adjustment and total stresses are included in the output file for each stage. In general, the error between the reported and calculated analytical stress for bottom and top flanges were less than one percent. This was important to verify our understanding of their analysis, and to be able to then use this same procedure on the noncomposite case.

Note that the calculation for strain in the concrete deck becomes much more involved, with additional terms required to account for the various time dependencies and boundary conditions imposed upon the creep effects. Instead, we did not attempt to calculate the analytical stress in the deck and simply used the B&T estimates of strain found in their output file for each stage.

The calculation for the superimposed deadload stress on the noncomposite or cracked section is obtained by using the noncomposite or cracked section properties in the above calculation. Anywhere the subscript says “Comp”; instead, change the subscript to “Cracked”. Note that this does not affect the deadload stress, which is based upon the section of bare steel alone.

LIVELOADS USED

HNTB provided estimates for HS20 liveload moment, axial force, and shear response. Note that B&T applies the axial force at their model's centroid of the section under consideration such that it does not impart an additional moment to the section; hence, the calculation of liveload stress for the bare steel, composite section, and noncomposite or cracked section would follow the above calculations but not include the third term (i.e., yN/S). Note that no adjustment for axial straining or other creep effects needs to be included in the calculation of liveload. Since B&T did not provide any estimates for liveload response, we had to calculate the deck stress, but this was simplified considerably by the lack of creep effects to consider under liveload. Lane load was found to control, as is typical of large structures, and is the only liveload included in our spreadsheet and figures.

For rating purposes, this liveload is later scaled by a variety of factors: the result is scaled by 1.25 to represent an HS25 liveload as intended by its design, scaled by a distribution factor of 1.74 to account for lateral effects not included in the two dimensional, finite element model used in the design, and scaled by an impact factor of 1.1 for the controlling lane load.

Note that HNTB and B&T used different naming schemes in defining and reporting their results for bridge members and nodes. Stations were used as a common method of reconciling and aligning the liveloads by HNTB with the deadloads by B&T.

CAPACITIES USED

Allowable stress for the steel is fy =50ksi, and for the concrete is f'c = 7ksi.

Many of the sections have a bottom flange whose dimensions are such that the section will fail the compression flange check for compact and even braced sections. For example, a flange that is 30" wide by 1" thick has a ratio of 30, which is not less than the test for compactness of a braced section (i.e., AASHTO Specification 10.48.2, where the test is 4400/sqrt(Fy) = 19.7).

Many of the sections have lateral bracing (e.g., floorbeams) which does not meet the specification for the compression flange of a compact and even braced sections (i.e., see AASHTO Specification 10.48.2.1, where the spacing should be less than 160" or 13.3' for the 30" x 1" flange and depth of bare steel girder is approximately 75").

Both of the above concerns are with regards to negative moment case.

The above was noted at various presentations and discussions with ODOT. A teleconference was held between UC and HNTB, and various email correspondence was conducted, but there was little resolved in this matter. It was decided by all parties to shelve any further discussion and proceed with the following method to calculate capacities for rating purposes.

Negative Ultimate Moment for the unbraced section (see above) was then assumed to be equal to that of the Yield Moment of the steel alone (i.e., girder and reinforcement), irregardless of the status of the composite action for the section. It was understood that this represents an upper bound on capacity in negative moment, and it would need to be reduced to the lateral torsional buckling moment (found in Eq. 10-103c) limit if it were lower than the yield moment, but that this required further clarification on section properties and the intent of the designer, which had not been forthcoming. For sensor locations, this assumption would suffice since most of the structure was controlled by positive moment.

Positive Ultimate Moment for a composite section was calculated according to stress block concept (i.e., AASHTO Specification 10.50.1 where the compactness check is found in Eq. 10-129b). Based upon the effective width by B&T, all the composite sections pass and the ultimate moment is set to the plastic limit (Mu = Mp). Here, the maximum strength of the section in bending is the first moment of all forces about the neutral axis, taking all forces and moment arms as positive quantities. Alternatively, since the compressive and tensile forces in the section are equal but opposite, the capacity can be calculated using the tensile force in the steel and the distance between the opposing moment arms (i.e., distance between the centroid of the bare steel under tension and the concrete stress block under compression).

RATING ASSESSMENT USED

An inventory HS25 rating using both the allowable stress and load factor methods was formulated for both the composite and noncomposite or cracked case for each section as defined by the stations used by both HNTB and B&T. Note that the bridge was designed by load factor design (LFD) method; however, assessment by allowable stress design (ASD) methods will allow consideration of material capacity limits (e.g., cracking of the concrete deck). Those sections where the concrete experiences a state of stress that approaches its allowable limit should not be considered composite but instead as noncomposite or “cracked”.

Each section was analyzed by each method at the bottom flange, top flange, cast-in-place (CIP) decking immediately above the edge girder, and for the deck panel adjacent to the edge girder which is to include the effect of the post tensioning (PT) force reported by B&T. Note that the deck and panel ratings are not calculated for the noncomposite or cracked section.

In addition, each of these members was analyzed under both the positive and negative liveload moment reported by HNTB.

Note that all rating formulations were conducted in terms of stresses for consistency. For allowable stress formulation of the composite section, it was possible that the top flange could have either sign convention (since it was very near the neutral axis), so the equation requires an IF statement to account for the sign.

Initially, the rating formulations were conducted with both bending moment and axial force stresses added together; this allowed both effects to be considered simultaneously. In addition, the axial force is greatly diminished near the abutments and centerline of the structure, which also happens to be the locations of the lowest rated sections of the bridge; so, axial force was only somewhat reducing the controlling rating values.

However, load factor design has commonly separated bending moment and axial force effects in the standard rating calculation. Upon review of the design manuals by HNTB, it seemed that this convention was also intended in the design of this bridge; clarification was requested, but this was not forthcoming. Given that the axial force was only somewhat effecting the controlling rating values, it was decided that this rating formulation should follow convention.

Hence, all axial forces and effects were set to zero in the spreadsheet, such that the ratings would be based solely upon bending moment. Accordingly, the deadload and liveload axial forces and the adjustment stress which is transferred due to axial straining of the steel were deleted from the spreadsheet. Deleting numeric values is equivalent to zeroing in Excel. In the title of the file, and in the title of its figures, we appended the phrase “P=0” to signify this step.

An interaction or combined rating was also formulated (AASHTO Specification 10.54.2) for compression members with a reduced capacity for buckling concerns. This particular rating was intended for analyzing columns under compression; however, the superstructure of a stay bridge can be considered as such given the axial forces that occur during construction. Again, the buckling stress was assumed to be the yield stress, as above. Interaction ratings were calculated for both top and bottom flange for a composite section and found not to control. Since the axial force was zeroed, this rating is not included in the spreadsheet "Edge Girder Ratings, B&T Deadload, HNTB Liveload, v3d3, modified LFR, P=0.XLS".

Note that the Overload case used by the Load Factor Design method (AASHTO Specification 10.57) is not considered in this analysis. It quite often will control rating for structures in the negative moment region, but was not considered here in determining sensor locations in order to maintain consistency in the method.

REFERENCES

1. V. Hunt, A. Helmicki, and J. Swanson, "Instrumentation and Monitoring of the US Grant Bridge," *Proceedings of ASNT Structural Materials Technology VI: An NDT Conference,* Columbus, OH, October, 2005.
2. Howard, Needles, Tammen, and Bergendoff (HNTB), Design Calculations for the U.S. Grant Bridge, 2000.
3. Buckland & Taylor (B&T), Superstructure Erection Submission for U.S. Grant Bridge, Rev. 3, 2004.
4. A. Helmicki, and V. Hunt, "Instrumentation of the US Grant Bridge for Monitoring of Fabrication, Erection, In-service Behavior, and to Support Management, Maintenance, and Inspection," Project Review, ODOT Central Office, 2004.
5. C.S. Cai, J. Nie, and Y. Zhang, "Composite Girder Design of Cable-Stayed Bridges." Structural Design and Construction, ASCE, Vol. 3, No. 4, November 1998: 158-163.

Chapter 4 Bridge Modeling and Analyses

4.1 Introduction

Mathematical modeling of any structure is a critical task since the model represents the real structure as closely as possible. Hence, accuracy of the adopted modeling strategy ensures accuracy of the predicted response. Modeling procedures for static analysis of the structures are essentially directed at obtaining an estimate of the global response, while the methodology adopted for conducting a dynamic analysis ensures that component-level response is also extracted in addition. This becomes much more important in case of stay bridges, wherein the localized cable response is as important as global bridge response.

The ultimate goal of this chapter was the development of a finite element model and its subsequent calibration. For calibration in general, the steps are

1) Select type (two dimensional or three dimensional), and develop preliminary model
2) Conduct load tests and monitor the responses
3) Simulate the load test on the model and compare the model's output against the measured response
4) Make changes in the model so that the model's output correlates with the measured response.

It would not have been possible to simulate the test load configurations with a two dimensional model and get an output that correlates well with the measured response, and predicts static and dynamic responses. Thus, a three dimensional model, able to represent the real bridge geometry accurately, as well as having the ability to simulate symmetrical and unsymmetrical loading, was needed. Two finite element analysis packages were used depending on the desired response. The initial part of the research was conducted using SAP2000 version 7.44 (and version 10.0 later on) and the latter part of the study was conducted in ABAQUS, owing to limitations of SAP2000 to handle the involved complexities of the problem.

4.2 Model Description

Besides the bridge deck, which behaves as a very stiff planar diaphragm, all components of the bridge are essentially linear elements. Therefore, the bridge components were idealized using linear elements, be it beam or truss. The beams at the deck level (i.e. longitudinal girders, cross beams and stringer beams) were modeled using three-dimensional BEAM elements, while the bridge deck was modeled using SHELL element with modifications to account for the fact that the girders carry all the axial forces, and nothing goes into the deck (Saini 2007). The centerlines of the girder cross-section and the bridge deck are not aligned at the same horizontal plane, but the finite element model was developed assuming that both lie at the same plane. This simplification facilitates modeling efforts, but also leads to modeling deviations since the differences in the center of mass and center of rigidity of the bridge deck section are not reflected. This deviation primarily arises out of the eccentricity of the girder center line from the deck center line as shown in Figure 4.1.

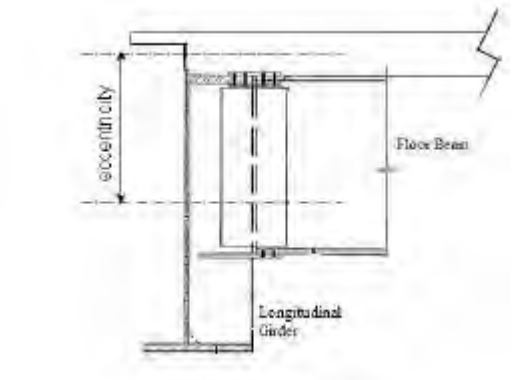

Figure 4.1 Eccentricity between Girder and Deck

The stiffness contribution due to the offset of the longitudinal girders from the center-line of the deck was accounted for by computing equivalent increased stiffness of the longitudinal girders as presented in Appendix A of Saini's thesis. Also, the beam-beam shear connections were modeled as appropriate moment releases, ensuring that no moment are transferred between beams.

The pylons were modeled as three-dimensional beam elements, starting off at the pile-cap level, and cables were modeled as either One Element Cable Stay (OECS) or the Multi Element Cable Stay (MECS) formulation depending on the utility of the analysis. In SAP2000, OECS enabled the study of various installation effects for the tuned mass dampers' global response, while both OECS and MECS were used for frequency extraction, computations involving cable vibrations, dynamic interaction effects, and dynamic sequence analysis in ABAQUS. When conducting a dead load analysis and eigenvalue extraction studies, as observed for the USG Bridge, it was sufficient to model the deck panels using single SHELL elements. For an equivalent static version of moving load analysis, however, it became imperative to model the deck panels using multiple deck elements, in order to allow accurate placement of truck loads (Saini 2007).

4.3 Loading

The primary loading on a cable-stayed bridge comes from the self weight of the various elements, the cable pre-tensions and the vehicular loading, while the dynamic component arises due to the lateral loads associated with wind or seismic activity. For static analysis, the dead loads of the beam/truss elements were included in the analysis by specifying the appropriate material densities (concrete with unit weight of 150 lb/ft^3 and steel with unit weight of 490 lb/ft^3). Also, the self-weight of the bridge deck panels was computed and assigned to the adjacent supporting beam elements using the tributary area concept. The self-weight of components that were not modeled explicitly, like railings and parapets, were included by assigning the computed load as line loading on the girders supporting them. Figure 4.2 shows the finite element model of the bridge with loads distributed to the supporting girders.

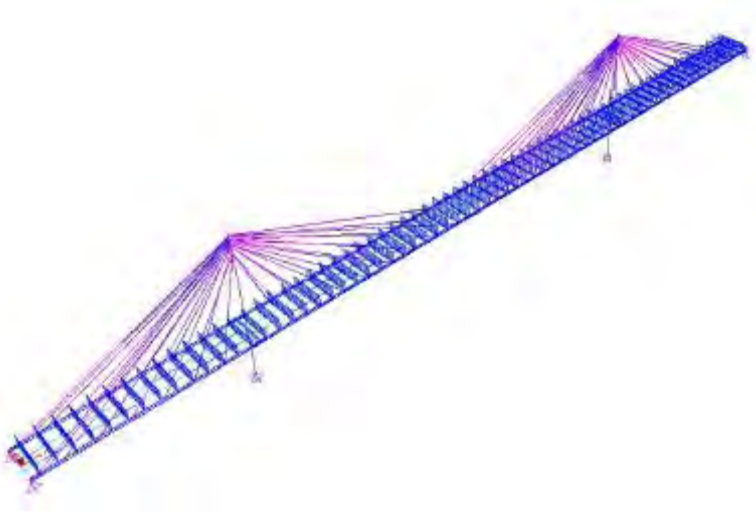

Figure 4.2 Loading on the US Grant Bridge for dead load analysis

For cable pre-tensions, SAP2000 enabled their direct application as the element loading. Similarly, equivalent strains, corresponding to the pre-tension values, were applied, but on a limited basis. Live load on the bridge consisted of HS20 truck and lane loading as per AASHTO standard specifications (AASHTO 2002). For experimental testing requirements, as was the case with the USG Bridge, the maxima or minima of the different responses did not occur at the same location. For this purpose, an equivalent static moving load analysis was preferred, wherein the truck load was applied as concentrated loads at multiple locations along the length of the bridge.

In order to obtain accurate results, the equivalent static live load analysis was conducted with 97 load locations. The response from the various load cases were then overlapped appropriately to arrive at a realistic envelope of element responses. For dynamic analyses, the weights of the linear elements were included automatically because of their density specification, while the weights of deck and railings/parapets were lumped at the node locations on the main girders and the stringers.

4.4 One Element Cable Stay (OECS) Model

The nonlinearity associated with the inclination and sag of the cables was accounted for, by replacing the actual cable catenaries with equivalent straight chord members as depicted in Figure 4.3. Since straight members were to be idealized, each cable was then modeled as an individual member, making the approach relatively less-computationally intensive.

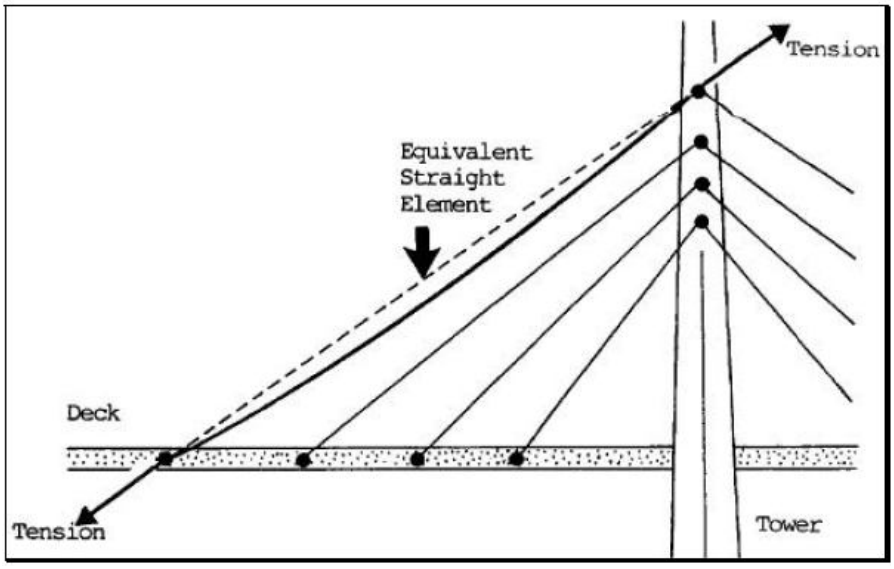

Figure 4.3 One Element Cable Stay methodology (Nazmy and Abdel-Ghaffar 1990)

In SAP2000, the girders and pylons were idealized as three-dimensional beam elements, while the deck was modeled coarsely using SHELL elements, neglecting their in-plane stiffness component in the longitudinal direction. The adopted mesh refinement for the shell elements depended on the ease of conducting the analysis. For dead-load, eigenvalue analysis and built-in SAP2000 moving load analysis, each deck panel was modeled using individual shell element, while for equivalent live load analysis, each deck panel was modeled using multiple shell elements. Since the deck thickness was variable, an equivalent uniform thickness was computed based on equivalence of total mass.

The typical deck panel was also modeled as a three-dimensional object and the total mass was computed using the modeling software. This mass was then used to compute the equivalent thickness of the shell element. The adopted approach used in computing the equivalent shell parameters is shown in Figure 4.4 below:

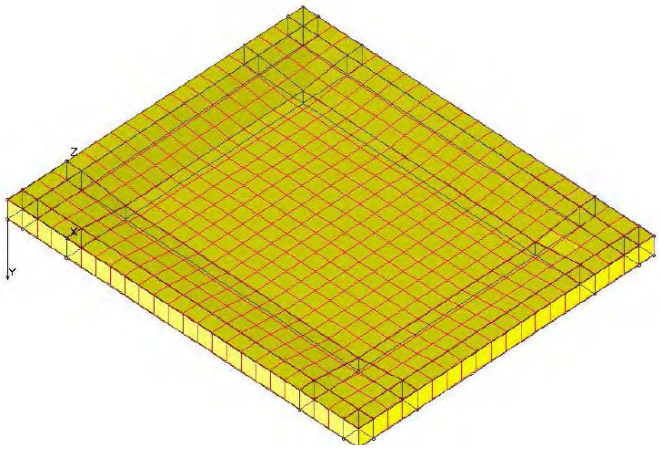

Figure 4.4 Solid model of deck panel with variable thickness (shown upside down)

Due to the fact that SAP2000 had no truss element in its library, beam elements, with appropriate section stiffness modifiers and end moment releases, were used to simulate truss behavior.

4.5 Dead Load Analysis

From the axial force diagram in Figure 4.5, it was observed that although the response from the conducted SAP2000 analysis followed the profile predicted by the designer, the numbers did not match. The difference in the results was higher on the Kentucky side (South Tower) as compared to the Ohio side (North Tower). The shear force diagram's profile of Figure 4.6 also showed some variations, especially at the forty-six Kentucky abutment, while for the bending moment response, variations occurred at the Kentucky abutment, near South and North towers, and near the closure segment in the middle of the bridge.

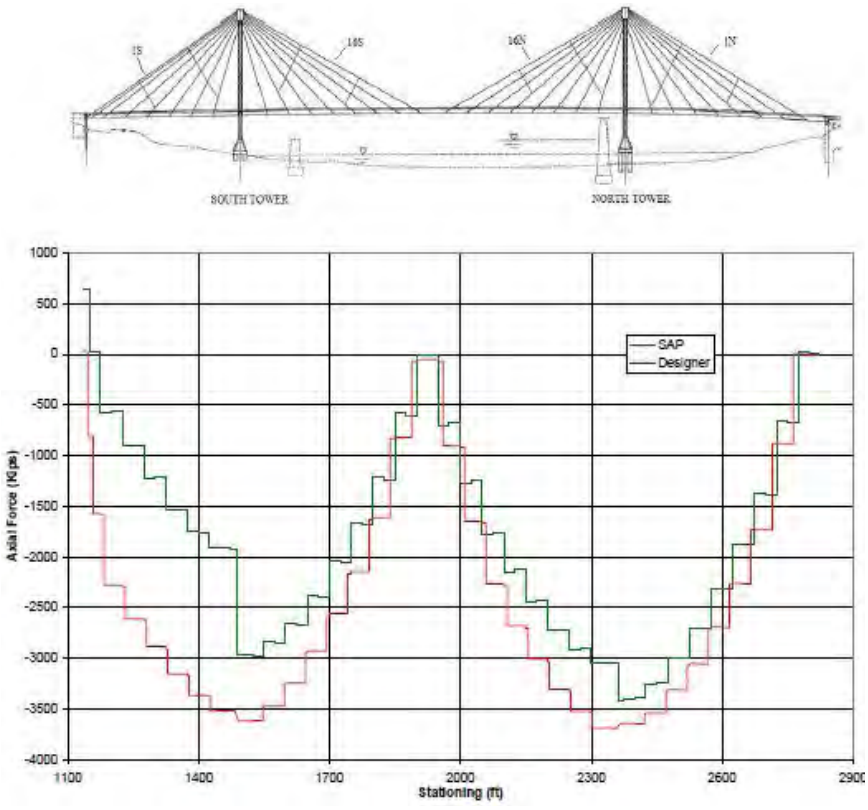

Figure 4.5 Axial Force Diagram for Longitudinal Girder

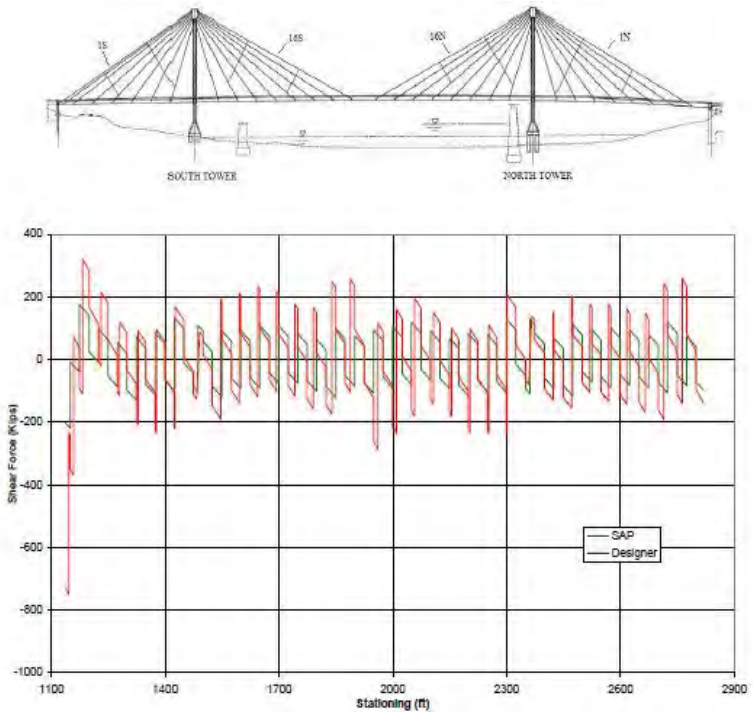

Figure 4.6 Shear Force Diagram for Longitudinal Girder

The deviations in the results of conducted analysis from designer results were attributed to the following:

a. Simplifications to the finite element model, both in the conducted SAP2000 analysis and designer model.
b. Designer having accounted for the effects of construction sequence on static response, while the SAP2000 analysis was based on the completed geometry of the bridge
c. Designer considering the long term creep and shrinkage effects, which was not accounted for in the SAP2000 analysis.

Similarly, the Kentucky abutment witnessed increased shear and bending moments in the longitudinal girders because its end was tied down as the construction process drew to a close. The increased differences in the axial force response was due to the fact that the construction began from the South Tower, and the effects of construction sequence and creep/shrinkage effects became more significant, as compared to other parts of the bridge. The construction sequence and creep/shrinkage produced maximum bending moment effect on the bending response of the longitudinal girders, which are the primary force transfer mechanism used at the closure segment, and were not to be properly simulated in the conducted analysis.

4.6 Moving Load Analysis

The SAP2000 moving load analysis consisted of the following (SAP 2004):

1. Modeling
2. Definition of traffic lanes and vehicle classes
3. Analysis

Since the frame element response was of interest, the US Grant Bridge model used for the dead load analysis was adapted for moving load analysis. Traffic lanes were defined with reference to the longitudinal edge girders, specifying appropriate eccentricities. In order to consider the criticality of different responses, all possible lane configurations were used to compute response parameters.

Chapter four of Saini's thesis explained the use of a HS20 truck and lane load to specify vehicle classes and load assignments. Based on the lane definitions shown in Figure 4.7, three load cases were considered:

a. Lanes 1 and 4 loaded
b. Lanes 2 and 3 loaded
c. All 4 lanes loaded 51

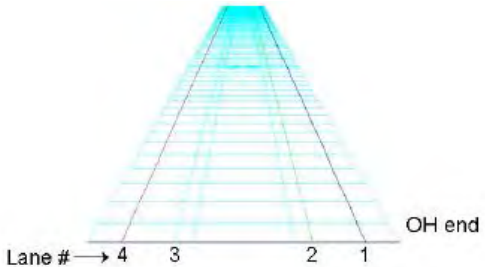

Figure 4.7 Perspective view showing the traffic lanes

Figures 4.8 and 4.9 show the moment response envelope for an edge girder for the truck load and lane responses, wherein the four lanes' load responses from the SAP2000 analysis were compared with the designer's responses. It was observed that slight discrepancies occurred at few locations, which were attributed to the modeling assumptions both by the designer and in the analysis. Also, an equivalent moving load analysis (Saini 2007) was developed to compute strain profile for the longitudinal girders at the end of bridge construction. The strain profiles acted as an indicator of available safety margins.

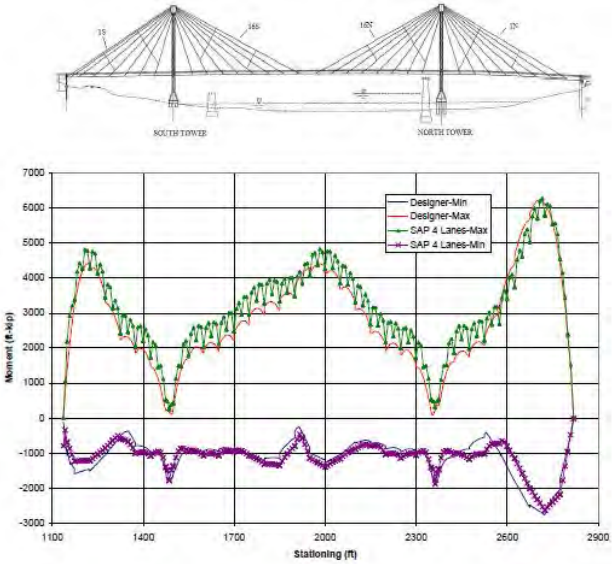

Figure 4.8 Bending moment envelope for Truck Load

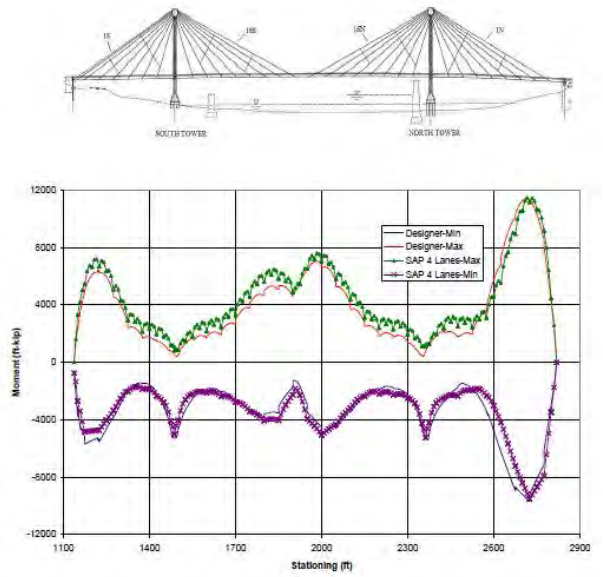

Figure 4.9 Bending moment envelope for Lane load

4.7 Frequency Analysis

The OECS model enabled the computation of superstructure frequencies and the corresponding modes. It was observed that the frequencies for the bending modes and corresponding mode shapes matched fairly well as compared to that of the torsional mode which had less correlation. Figure 4.10 shows the frequency correlation trend line (FCTL) plot (Ewins 2000; Wang 2005) between the two set of results for two cases, one including both the bending and torsion modes and the other wherein only bending modes are included. Both the slope of the line and R-squared values exceeded 0.9, which indicated a good match between the two data sets.

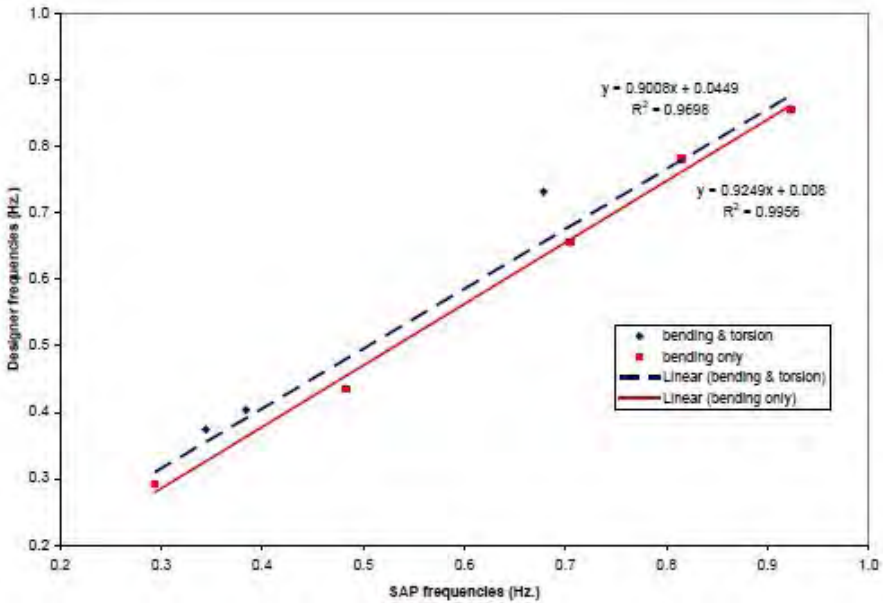

Figure 4.10 FCTL plot between SAP and designer's results

For the US Grant Bridge, Operational Modal Analysis (OMA) tests were designed primarily to extract the structural frequencies accurately, while gathering some information on mode shapes. An array of 65 accelerometers was installed on bridge deck, with the arrangement designed to provide information on both the bending as well as torsion modes. Some preliminary tests were conducted to ascertain the suitability of the sensors and the adopted procedure (Chauhan et al. 2007), and then a final test was conducted with the sensor layout shown in Figure 4.11.

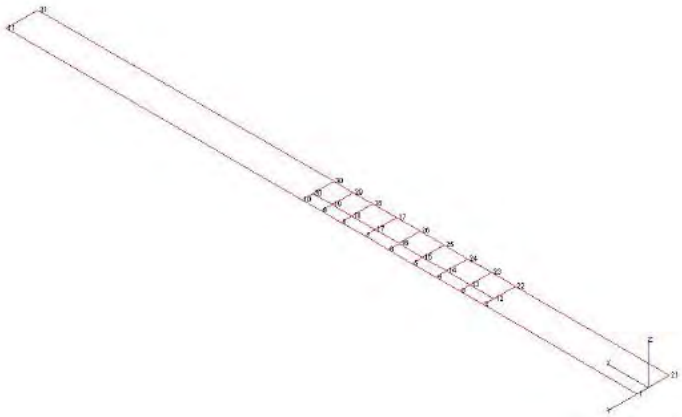

Figure 4.11 Sensor layout for the OMA test (Chauhan et al. 2007)

Table 4.1 presents a comparison of the obtained frequencies from the finite element analysis and the OMA test. Again, the frequencies and mode shapes of the bending modes matched very well, but the torsion modes did not, for earlier-mentioned reasons. Also, the tower sway and anti-sway modes were not reflected in the OMA test since the accelerometers were installed only on the bridge deck. From the SAP2000 analysis, it was observed that the bending modes were more significant than torsion modes in terms of their effect on the overall response. Therefore, only the bending modes were taken up for detailed comparison.

Table 4.1: Comparison of FEM with OMA results

Mode #	Frequency (Hz.)		Mode Description
	SAP2000	OMA	
1	0.2936	0.3100	Bending-1
2	0.3443	-	Tower Sway
3	0.3842	-	Tower AntiSway
4	0.4827	0.4747	Bending-2
5	0.6786	0.7383	Torsion-1
6	0.7052	0.6863	Bending-3
7	0.7971	0.9227	Torsion-2
8	0.8150	0.8359	Bending-4
9	0.8391	1.1064	Torsion-3
10	0.9230	0.9193	Bending-5
11	0.9511	-	Torsion-4
12	1.0201	-	Torsion-5
13	1.0855	1.1189	Bending-6
14	1.1678	-	Torsion-6
15	1.1749	1.2055	Bending-7
16	1.2571	-	Torsion-7
17	1.4233	1.5019	Bending-8
18	1.5113	-	Torsion-8
19	1.5122	-	Bending-9

The modal displacement information from six bending modes were also used to compute the Modal Assurance Criteria (MAC) value, which is an accurate indicator of the mode shape comparison and is the most widely used model validation criteria. The MAC takes into account comparison of mode shape vectors rather than comparison of frequencies as is done in FCTL, and forms a numerical as well as graphical basis of comparison.

4.8 MECS Approach for US Grant Bridge

The strategy adopted for application of the MECS approach to the US Grant Bridge model is shown in Figure 4.12 below:

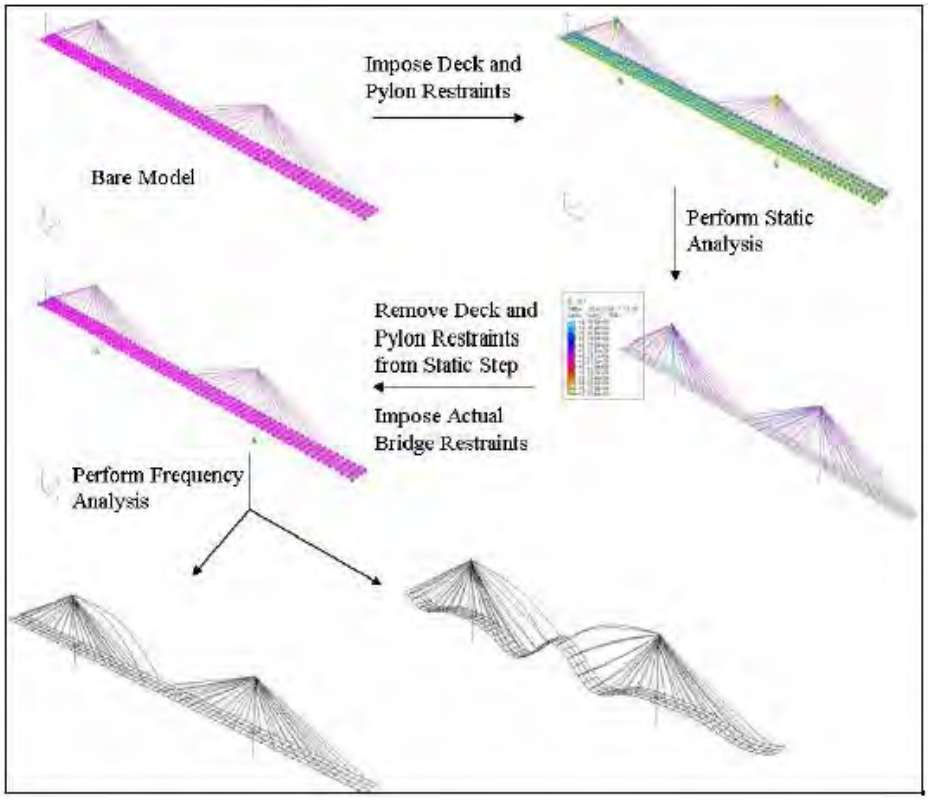

Figure 4.12 Multi Element Cable Stay approach for US Grant Bridge

The results of the frequency analysis, using the MECS model, were evaluated by comparing the superstructure's responses with the design values and the OMA results, while the cable-only modes were compared with the results from the individual cables. It was observed that there were many local modes giving rise to a large number of total modes. There were more than 800 modes up to 10 Hz frequency, and the closely spaced modes arose more for the cables. This was attributed to the fact that there was always some sort of interaction among the cables and the deck, and owing to the relatively flexible nature of the cables, the deck participation was less.

Table 4.2 lists the frequencies with the mode description from the MECS model, the designer's model, OMA test and the OECS model. The computed frequencies from various

sources matched each other, within error limits. Based on these plots, it can be seen that a good match was obtained between the MECS results and other available results.

Table 4.2: Superstructure frequencies from various sources

Mode #	Frequency (Hz.)				Mode Description
	OECS	Designer	OMA	MECS	
1	0.2936	0.2918	0.3100	0.3089	Bending-1
2	0.3443	0.3740	-	0.3978	Tower Sway
3	0.3842	0.4034	-	0.4318	Tower AntiSway
4	0.4827	0.4348	0.4747	0.4936	Bending-2
5	0.6786	0.7321	0.7383	0.7135	Torsion-1
6	0.7052	0.6550	0.6863	0.7115	Bending-3
7	0.7971	-	0.9227	0.7962	Torsion-2
8	0.8150	0.7811	0.8359	0.8198	Bending-4
9	0.8391	-	1.1064	0.8399	Torsion-3
10	0.9230	0.8550	0.9193	0.9252	Bending-5
11	0.9511	-	-	0.9405	Torsion-4
12	1.0201	-	-	1.0190	Torsion-5
13	1.0855	-	1.1189	1.0880	Bending-6
14	1.1678	-	-	1.1752	Torsion-6
15	1.1749	-	1.2055	1.1885	Bending-7
16	1.2571	-	-	1.2589	Torsion-7
17	1.4233	-	1.5019	1.4270	Bending-8
18	1.5113	-	-	1.5198	Torsion-8
19	1.5122	-	-	1.5504	Bending-9

References

1. J.S. Saini, “Effects of Nonlinearities due to Geometry, Cables and Tuned Mass Dampers on the Analysis of Cable-stayed Bridges,” MS Thesis, Department of Civil and Environmental Engineering, University of Cincinnati, Cincinnati, OH, 2007.
2. AASHTO, “Standard Specifications for Highway Bridges,” American Association for State Highway and Transportation Officials, 17th Ed., Washington, DC, 2002.
3. A. S. Nazmy, and A. M. Abdel-Ghaffar, “Three-dimensional Nonlinear Static Analysis of Cable-stayed Bridges.” Computers & Structures, 34(2), 257-271, 1990.
4. SAP2000®, CSI Analysis Reference Manual, Version 10.0. Computers and Structures Inc., Berkeley, CA, 2004.
5. D. J. Ewins, *Modal testing: theory, practice and application*. 2nd Ed., Research Studies Press, Hertfordshire, England, 2000.
6. X. Wang, “Structural Condition Assessment of Steel Stringer Highway Bridges.” *Ph.D. Dissertation*, Department of Civil and Environmental Engineering, University of Cincinnati, 2005.
7. S. Chauhan, J. S. Saini, S. Kangas, R. Sexton, A. J. Helmicki, V. J. Hunt, and J.A. Swanson, “Operational modal analysis of the US Grant Bridge at Portsmouth, OH.” SEM Annual Conference & Exposition, Springfield, MA, 2007.

Chapter 5 Analytical and Experimental Stress during Construction

5.1 Introduction

A significant amount of effort was expended in this project to measure, record, and interpret the behavior of the steel framing and composite concrete decking system during construction. This included monitoring the induced stresses and strains, where and when they occurred, and investigating causative effects. The main components of the framing system, namely the edge girders and the cast-in-place concrete strip directly above them, were comprehensively instrumented and continuously monitored during the construction of the bridge (see Figure 3.8). Instrumented monitoring commenced immediately before the segment was erected onto the bridge, through any temporary stressing or profiling with the stays or post-tensioning strands, placement of the precast concrete deck panels, during the concrete pour and curing of the cast-in-place strips, and as other segments were installed on either side of its respective tower, throughout most stages of its construction and into (and beyond) service on October 16, 2006.

The framing and decking systems were monitored during construction for several reasons. One reason was to try to evaluate the causative effects that influence the behavior of the bridge during construction. Construction techniques used to build the bridge, or specific details of the bridge design can be evaluated to determine how they affect the final behavior of the structure. In addition, some sensors were actually added to be specifically monitored for construction events of concern. For example, after review of the erection plans (see Figure 5.1), there were some overstressing concerns at the temporary bent located at Segment 4N near the end of construction when a significant number of segments were to be cantilevered north of it. By adding these sensors to the original plan (see Figure 3.9), we were able to monitor these stresses during construction and verify that they were under control as intended.

Another important reason was to address the significant knowledge gap that exists between the design and in-service performance of such systems. In particular, the manner in which typical events that occur during construction affect the stress levels in stay bridges is not well documented. For example, dead load stresses are estimated during the design, but the actual stress levels in the members of the completed structure are probably somewhat different. This project will give some idea of the actual stress levels in this typical structure after it is constructed. For this bridge in particular, we actually measured the true deadload (and superimposed deadload) effect, which allowed direct comparison to its design and erection predictions, and document such for future analysis (e.g., liveload rating). There was some contention between erection and design analysis about the expected moments (e.g., that caused by the Kentucky pulldowns, see Figure 5.2) and the effective width of the decking (see Figure 5.3), which translated into differences in section properties, and together this lead to differences in predicted stresses between the two analyses (see Figure 5.4, where we have assumed the moments and forces predicted by B&T, but used the two different effective widths to calculate the respective stress).

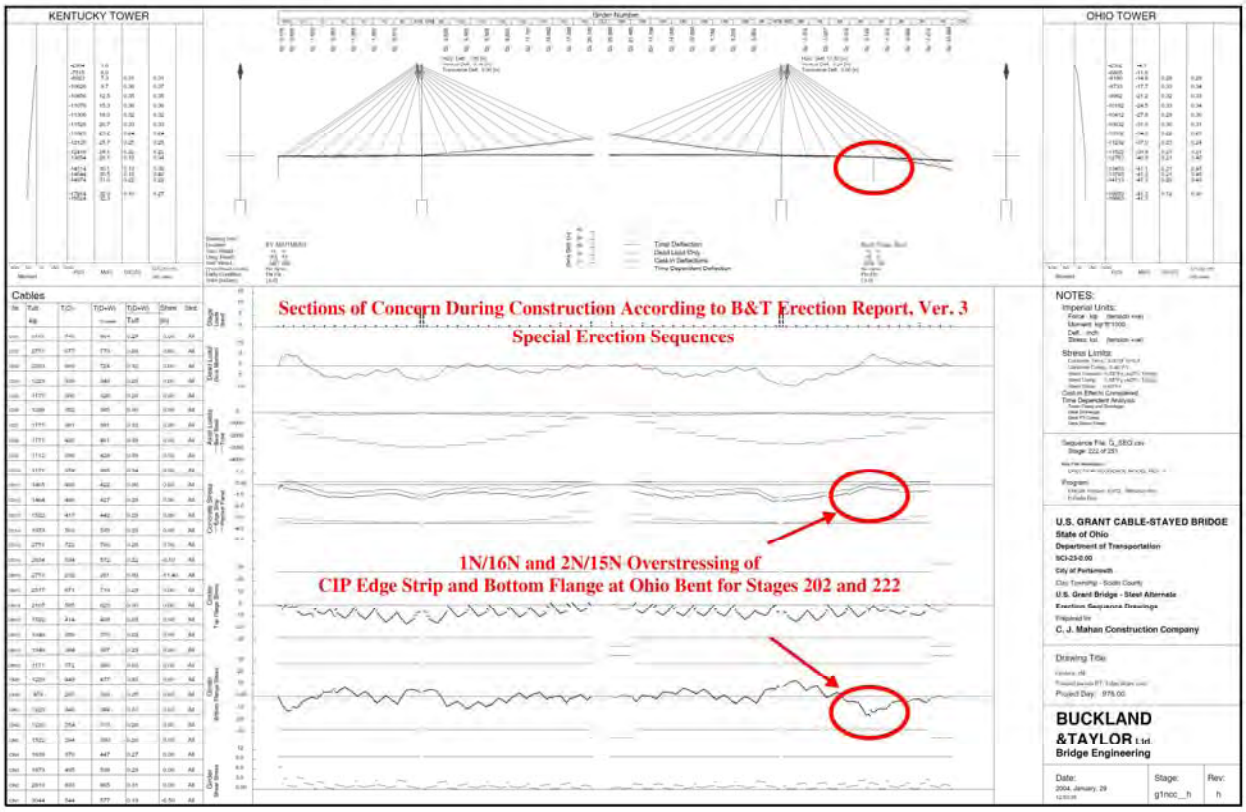

Figure 5.1: Overstress Concerns, Construction Stage 222 of 251, Segment 4N (B&T, 2004)

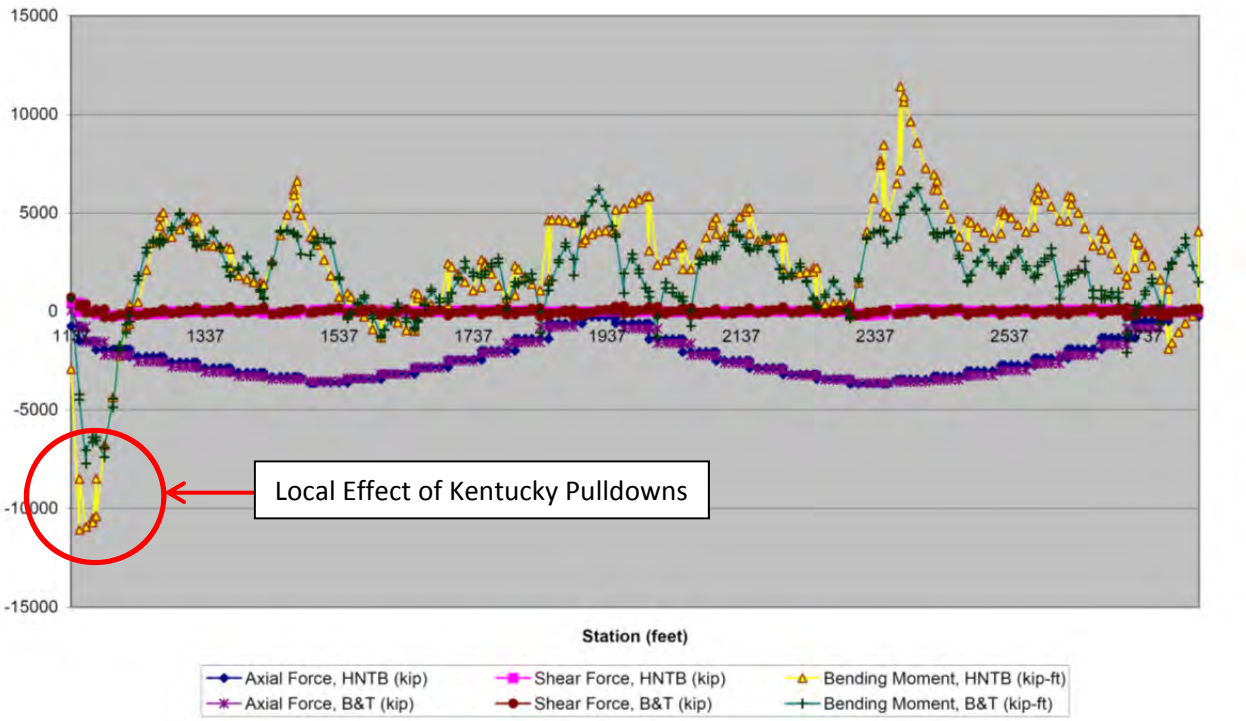

Figure 5.2: Deadload Forces and Moments, USG (HNTB, 2000 and B&T, 2004)

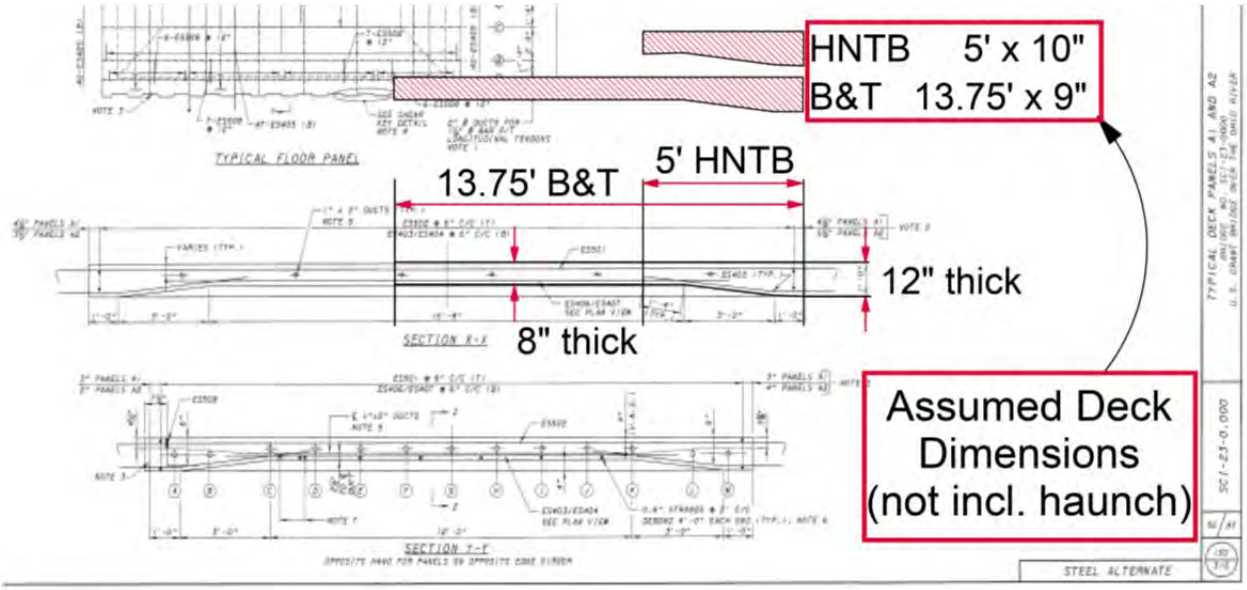

Figure 5.3: Differences in Effective Deck Width, USG (HNTB, 2000 and B&T, 2004)

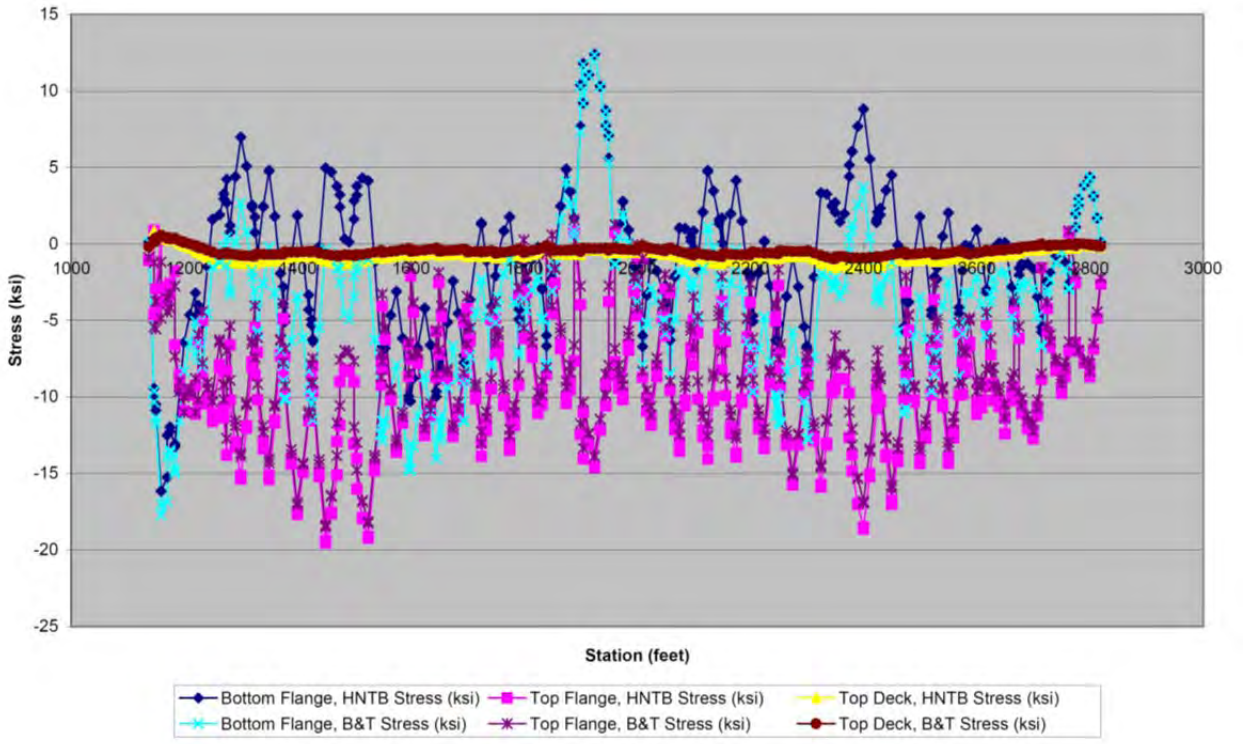

Figure 5.4: Deadload Stress using Two Values for Effective Width, USG (UCII, 2004)

It should be noted here that every effort was made to document and assess the analysis conducted by both the designer and the erection engineer. The designer provided a large box of paper reports, each chapter collecting the various handwritten and spreadsheet output of the work product required to assess and validate the various components of the bridge; however, digital output, assessment of stage construction, and an overall manual or assessment of the entire design was not available. On the other hand, each of several versions of the staged erection analysis was submitted as digital input and output files of their in-house software. The erection engineering analysis was performed using the sequence generation program ERC95 and their in-house non-linear analysis program CAMIL. A full manual for their software was provided, which detailed the format of the input and output files, but also the analytical methods, equations, and assumptions used in the calculations. In addition, a summary PDF sheet was provided for every stage of construction to provide an overall continuous assessment of the structure (e.g., see Figure 5.1). As there was considerably more information available from B&T (see the Appendix to Chapter 3 for more details on these), and since the erection engineer would probably have more knowledge of how the bridge would actually be built, we decided to use the staged deadload forces and moments from B&T in this analysis. The ratings manual by HNTB ultimately used the deadload forces and moments from B&T in their analysis.

One conclusion that was clear from any analysis of this structure was a concern regarding the ultimate effect and response due to the pulldowns at the Kentucky abutment (see Figure 5.5).

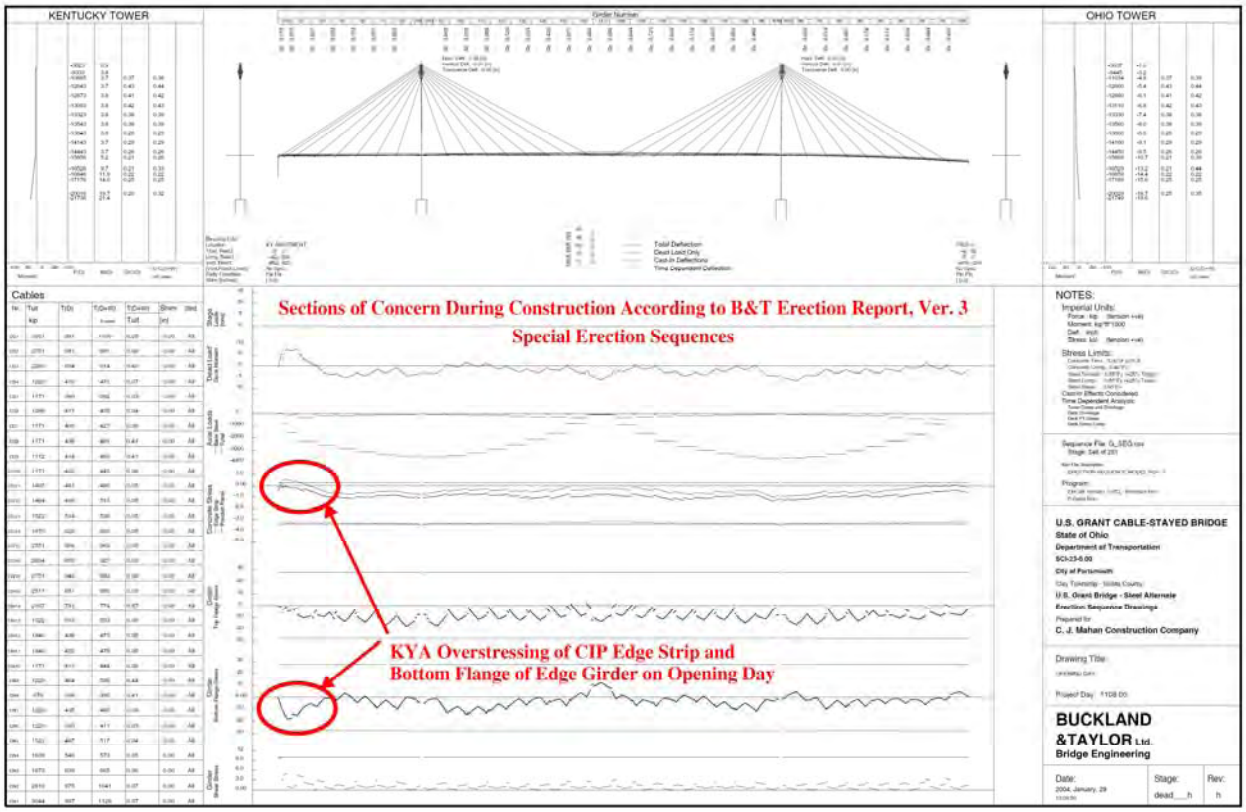

Figure 5.5: Overstress Concern from Pulldown, Segment 2S, USG (B&T, 2004)

5.2 Instrumentation and Data Acquisition during Construction

An instrumentation scheme was developed for the framing system during the initial planning stages of the project. This instrumentation design was guided by the stated objectives for the project: observing and documenting behavior and corresponding causative effects for a stay bridge during construction, observing and documenting the behavior and corresponding causative effects for the same bridge during service, and laying the groundwork for further development of intelligent bridge monitoring applications. To fulfill these objectives, two types of instrumentation were planned for monitoring the framing system. Vibrating wire strain gages (i.e., slow speed, long term reliability) were installed to monitor global changes in the structure, such as magnitudes of stress induced by construction or environmental effects. Traditional foil strain gages (i.e., high speed, short term stability) were installed for use in monitoring traffic responses.

The placement of the sensors in each location was according to one common pattern: two strain gages on the bottom flange, one on the web and top flange, and one at each layer of the deck reinforcement. The bottom flange has two gages for averaging and corroboration purposes, as this location provides the most sensitive and critical response for load rating, given the composite nature of the section. The top flange has only one gage because the behavior of the entire flange is restrained by the deck haunches and sits very near the neutral axis (i.e., zero liveload response) for the composite section. The deck gaging allows us to verify continuity of the section profile into the concrete and for estimation of the effective width of the deck used in the composite section. Gaging on the web also allows verification of continuity of the section profile, but also to clearly observe out-of-plane behavior which may become possible with the unsymmetrical anchoring of the stay cables. The gages were located on the interior side of these beams to minimize disruption to construction and to the overall aesthetics of the bridge. At all locations mentioned above, both a vibrating wire and a traditional foil strain gage were installed (see Figure 5.6). Some tweaking of the proposed sensor locations was required (see Figure 5.7) to avoid stay and floorbeam details and other construction concerns.

The Campbell Scientific CR-10X data acquisition system was used for monitoring the vibrating wire strain gages throughout construction. These loggers were housed in white fiberglass enclosures and literally tethered to the gages by their own sensor cables. This allowed some flexibility in the exact location of the enclosure so as to avoid construction efforts, but also some level of protection from the very same concern. The data acquisition system was set to scan each gage in half-hour increments during most of the construction. Regular visits to the bridge allowed us to download the collected data into our laptop and to change the 12V battery powering the system.

Near the end of construction, a conduit spine was installed by the contractor down the length of both parapets and connected to a main cabinet located in the Ohio tower at roadway level. The batteries were then connected to and continuously charged by standard 120VAC power and the loggers were networked to the UCII labs by various communication services (i.e., initially by analog phone modem, then by digital ADSL router).

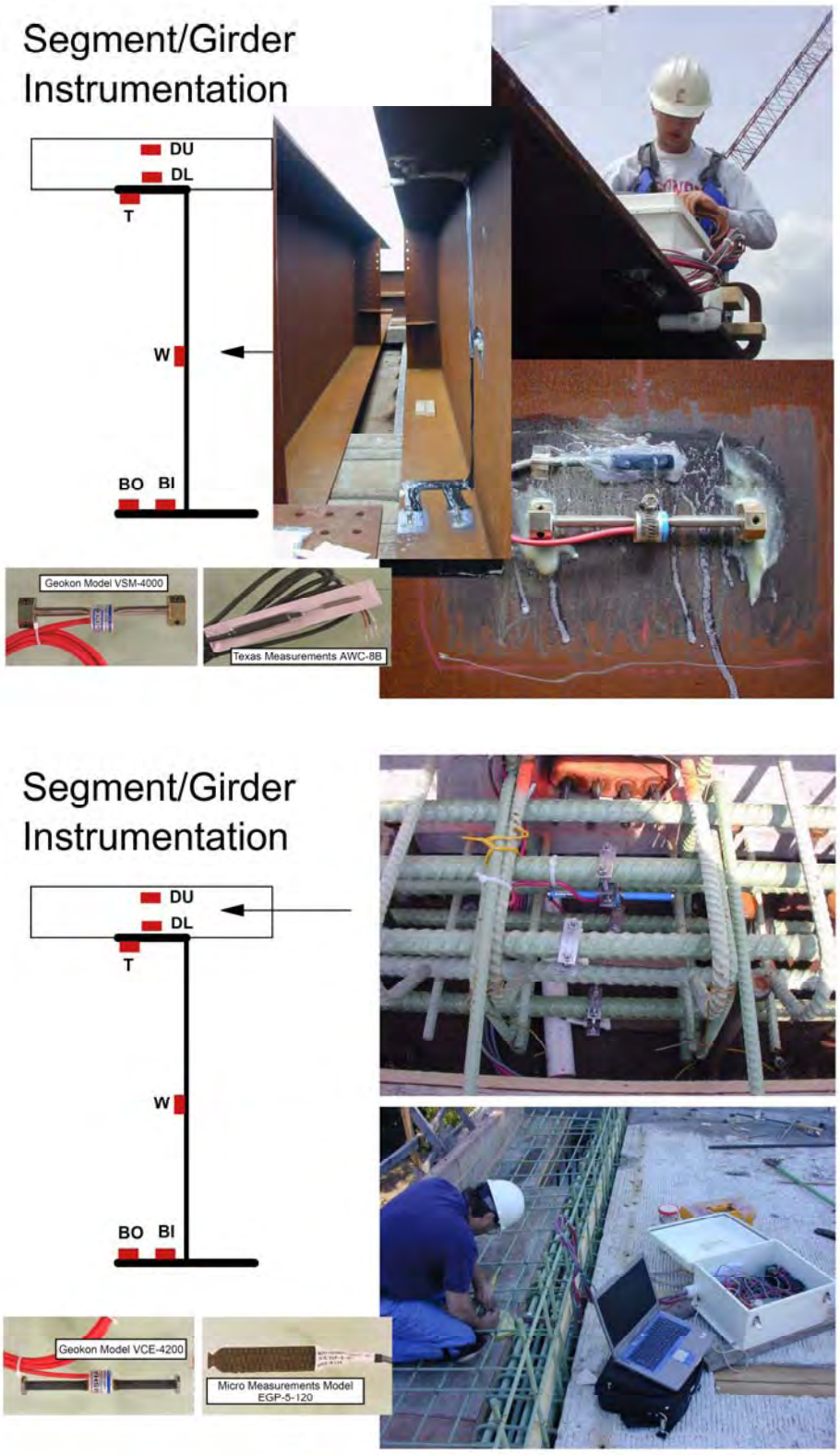

Figure 5.6: Typical Sensor Installations, USG (UCII, 2004)

Revised Sensor Stations based upon Construction Requirements

Location Checks:

1 Sensor must be 6 feet closer to tower than stay/feature work point to avoid anchor

2 Sensor must be 10 feet further away from tower than stay/feature work point to avoid anchor and splice joint

Sensor	Proposed Station	Nearest Stay/Feature	Nearest Work Points Away From Tower	Nearest Work Points Nearest Tower	Location Check 10' Further	Location Check 6' Closer	Revised Station
N1	1160	2S	1149.5	1160.24		N	1164
P1	1275	4S	1274.5	1281.56		N	1264.5
N2	1487	STM	1499.5	1487	N		1510
P2	1945	16N	1949.5	1962.55	N		1933.5
P3/N5	2722.5	2N	2724.5	2712.5		N	2706

Sensor	Controlling Rating Factor at Proposed Station	Controlling Rating Factor at Revised Station	Comments:
N1	1	1.08	LFR Neg Moment, Bottom Flange, "Cracked" condition, moved towards tower
P1	1.61	1.67	LFR Ptv Moment, Bottom flange, moved towards tower
N2	1.55	1.95	LFR Neg Moment, Top Flange, "Cracked" condition, moved 5' past the starter girder splice
P2	1.32	1.59	LFR Ptv Moment, Bottom flange, moved away from tower and closer to bridge center
P3/N5	1.32/1.33	1.36/1.35	LFR Ptv Moment, Bottom flange / LFR Neg Moment, Top Flange, "Cracked" condition

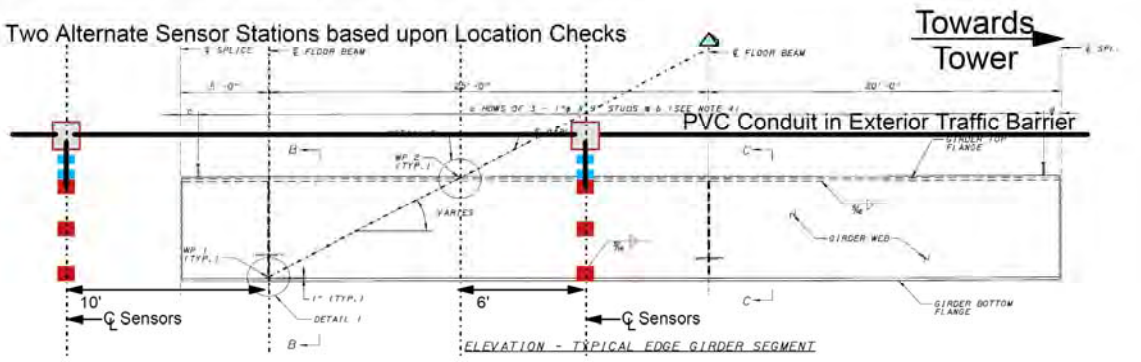

Figure 5.7: Revised Sensor Stations, USG (UCII, 2006)

5.3 Thermal Response of the Sensor and Structure

An important characteristic of the vibrating wire strain gages is temperature compensation. For example, the vibrating wire strain gage is made of the very same material (i.e., steel) as the exterior beams upon which they are installed; hence, they have the very same temperature coefficient (i.e., response to temperature). So, when the gage and the steel host are at the same temperature, and both are completely free to move, the gage will indicate no change in strain reading. Note that this is not exactly true for steel gages embedded in concrete and some post-processing and additional assumptions are required for such; however, similar results to the steel-on-steel case study are found for the deck gages as well. The result is that a temperature compensated gage will not exhibit any response not related to stress; or, in other words, a change in reading by a compensated strain gage infers that there is stress in the member upon which it is installed.

While monitoring the steel framing system during construction, the strain responses of both bottom and web gages regularly indicated increased compressive strain behavior during the middle of the day, and tensile response at night. There is a slightly delayed relationship between increasing temperature and increasing compressive strain, and vice versa, at these locations. This behavior was repeated daily and an example of this behavior is illustrated in Figure 5.8. Note that the top flange sensor has the opposite relationship with temperature. The gages on the bottom flange have a larger thermal response than those located under the top flange, no doubt due to the presence of the concrete deck for shading. In addition, the top and bottom gages indicate less temperature response than the web gages, as the web receives significant direct sunlight to warm it. Last, the eastern gages are first in the day to exhibit this behavior, with the western gages delayed until the sun reaches the western sky.

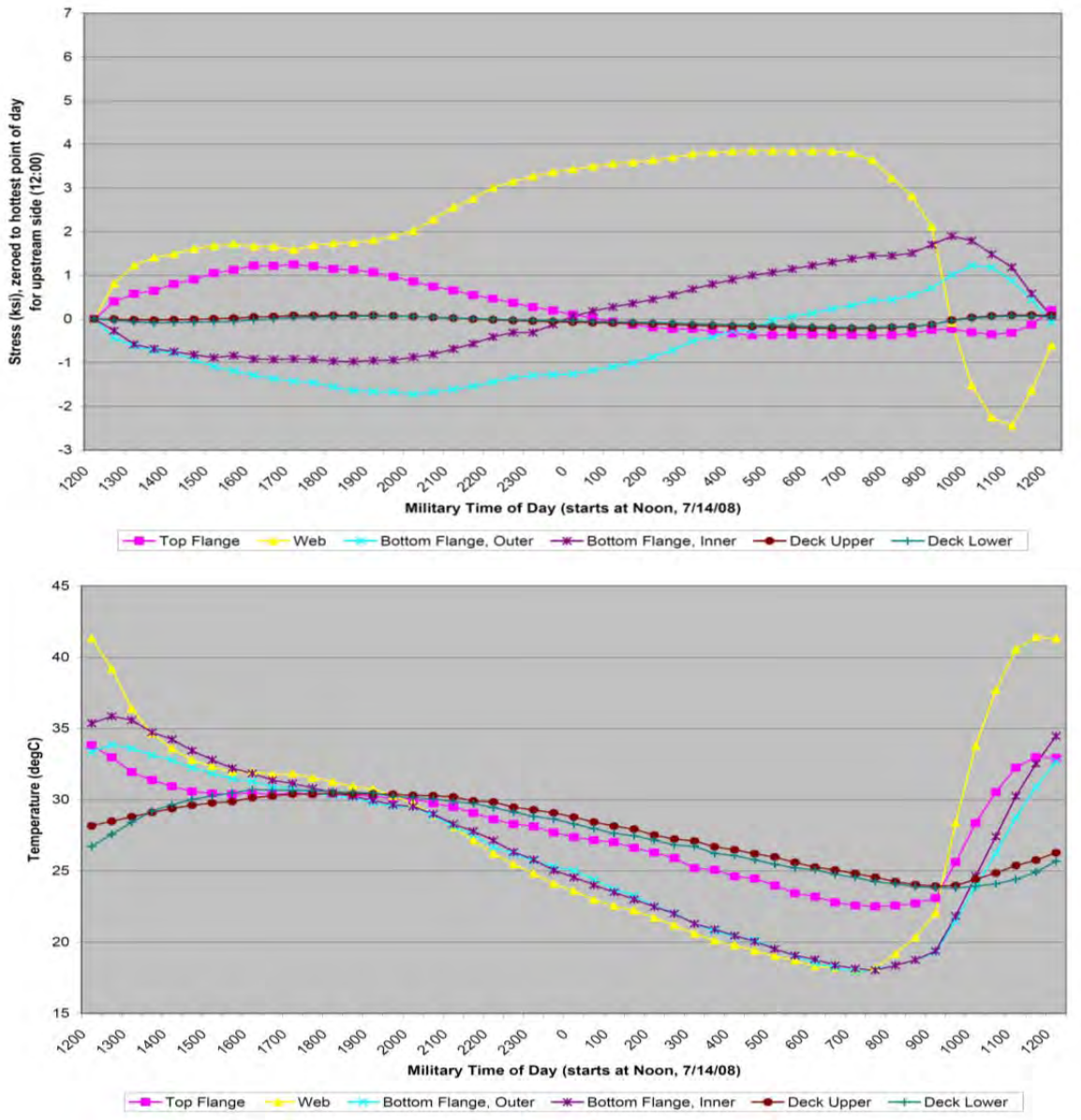

Figure 5.8: Typical Daily Response of the Sensors, Upstream, Station 2S, USG

Figure 5.8 also demonstrates what is believed to be apparent strain response from the sensors. If the temperature is similar for both the beam and gage (e.g., at night, when the sun is not a factor), the bottom gage will experience tensile strains with a decrease in temperature, because its free compression is resisted by a beam that is somehow not completely free to move. Similarly, during the day, a bottom gage will experience compressive strains with an increase in temperature, because its free extension is resisted again by a beam not completely free to move. Now, a bridge is generally designed with some support defined as "free" to move; however, in practice, there are a variety of reasons how some resistance to this may occur (e.g., friction, dirt, material defects, surface roughness, misalignment, difference in the temperature coefficient of steel and concrete, etc.). Note that the web response is dramatically different from the other gage responses, which would be indicative of the large radiative heating of the exterior steel surface from the Sun; hence, some bowing of the web occurs every day, where the exterior face tenses in relation to the interior shaded face of the web. The top gage acts opposite to the bottom gage response to temperature, which indicates some bending that occurs at this station near the Kentucky abutment. This daily relationship between each gage and temperature is captured in Figure 5.9 as well for the month of July in 2008.

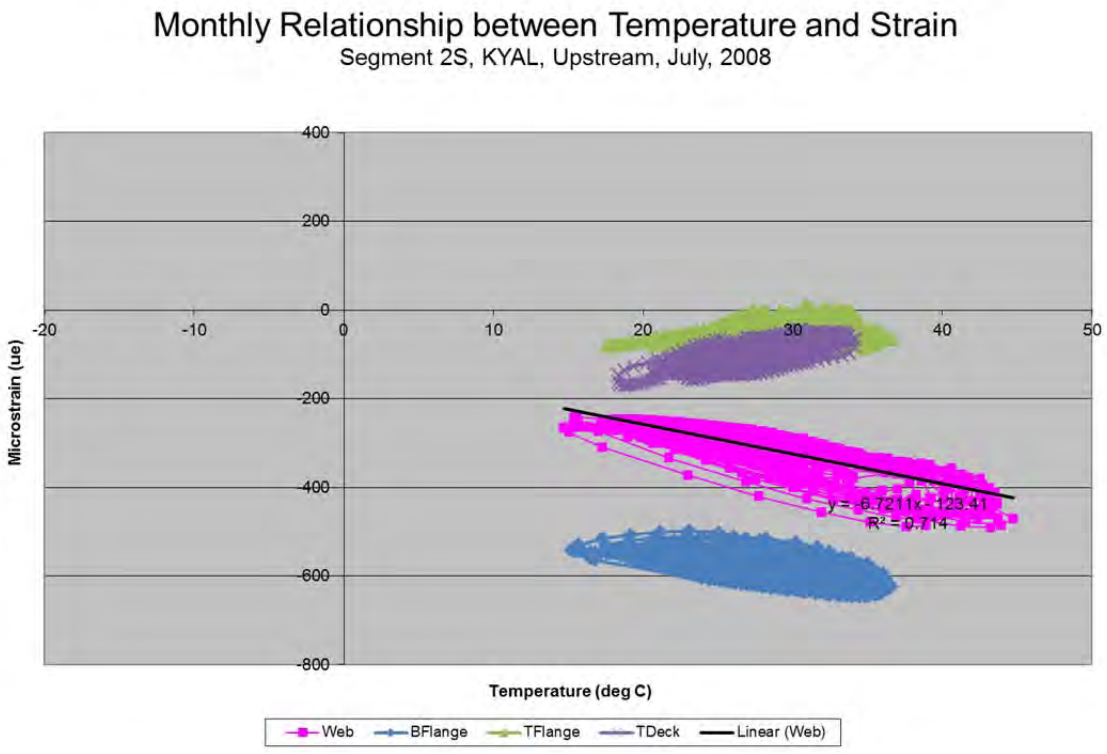

Figure 5.9: Strain vs. Temperature Response, Upstream, Station 2S, USG, July, 2008

Figure 5.10 illustrates how the daily relationship between strain and temperature is somewhat continued throughout the annual cycle of seasons. The x axis is now more populated by the annual range of temperatures over 2007 and 2008; hence, the web response no longer dominates the others in the amount of strain observed. It becomes less obvious how to fit a line to a year's worth of data, due to the inherent nonlinear behavior involved. However, there remains a negative relationship for the bottom and web gages, and a positive relationship for the deck gages with temperature; hence, the bending at this station with temperature is observed over the year. The top gage becomes less responsive to temperature (i.e., almost a flat line) over a year's worth of data, similar to its neutral axis response to liveload.

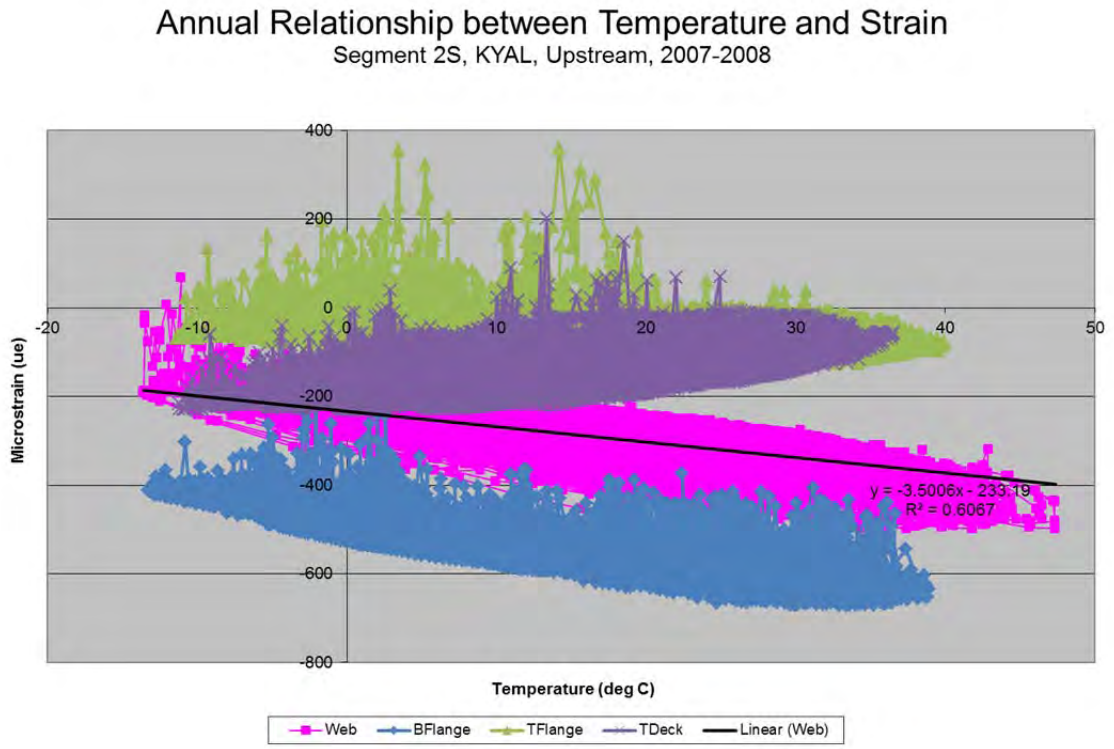

Figure 5.10: Strain vs. Temperature Response, Upstream, Station 2S, USG, 2007-2008

Nevertheless, these measured strains due to temperature are actually manifested as stress in the member upon which they are installed. As such, these daily and seasonal stresses add to the deadload stress as additional forces which subtract from the full capacity of the beam or member to resist liveload; hence, these "long-term" stresses should be documented and somehow used in the traditional rating process of the structure so as to account for same.

5.4 Examples of Construction Monitoring

5.4.1. Initial Data from Tower Sensors Compared to Design

As a simple example of the steps required for comparison of measured field data with analytical design values, we begin with the first few months of sensor data for the embedded vibrating wire strain gages installed at the Ohio tower just above the roadway (see Figure 5.11). First, the raw sensor data must be post processed in order to subtract the initial value bias (i.e., we only want to examine the change in reading since installation) and also attempt to remove the apparent effect of temperature. For steel gages in concrete, this becomes a bit of trial and error in that the actual temperature coefficient of the concrete is approximate to steel but can vary quite a bit depending upon various conditions (e.g., mix recipe, moisture content, fineness, age, etc.); hence, some initial fine tuning is conducted to achieve the result of a known load case (e.g., no load should have a flat line response for a member that is completely free to move). Next, we need to account for changes in the construction schedule from that assumed by the analytical design or erection model (e.g., in Figure 5.11, the tower construction was first ahead of schedule and then later behind schedule over the course of just a few months).

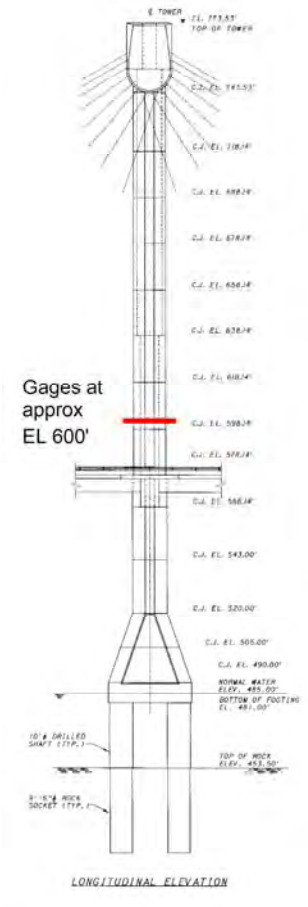

Construction Event	Actual Date	Actual Elapsed Time (days)	Projected Elapsed Time B&T, rev. 3 (days)
OHT598	10/06/03	0	0
Gages Installed	11/11/03	-	-
OHT618	12/20/03	75	74
OHT638	1/20/04	106	129
OHT658	2/17/04	134	143
Data Acquisition System Installed	2/24/04	-	-
OHT678	3/02/04	148	157
OHT698	3/19/04	165	171
OHT718	3/29/04	175	185
OHT743	5/08/04	215	198
Data Collected	6/23/04		

Database of measurements available

Campbell Scientific CR-10X Datalogger System stored in OH Tower at tabletop level

Figure 5.11: Instrumentation of the Ohio Tower, USG (UCII, 2004)

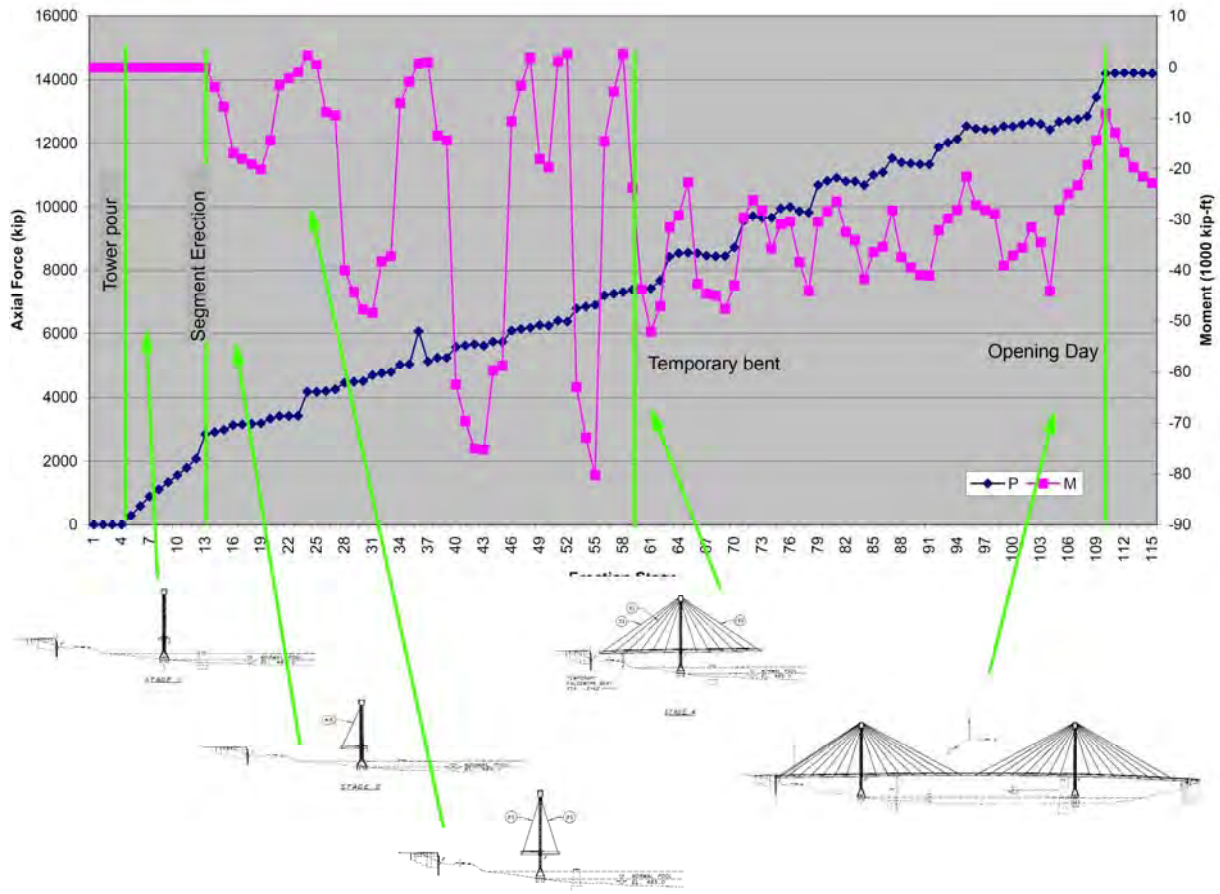

Figure 5.12: Moment and Axial Forces During Erection, EL600, Ohio Tower, USG (B&T, 2004)

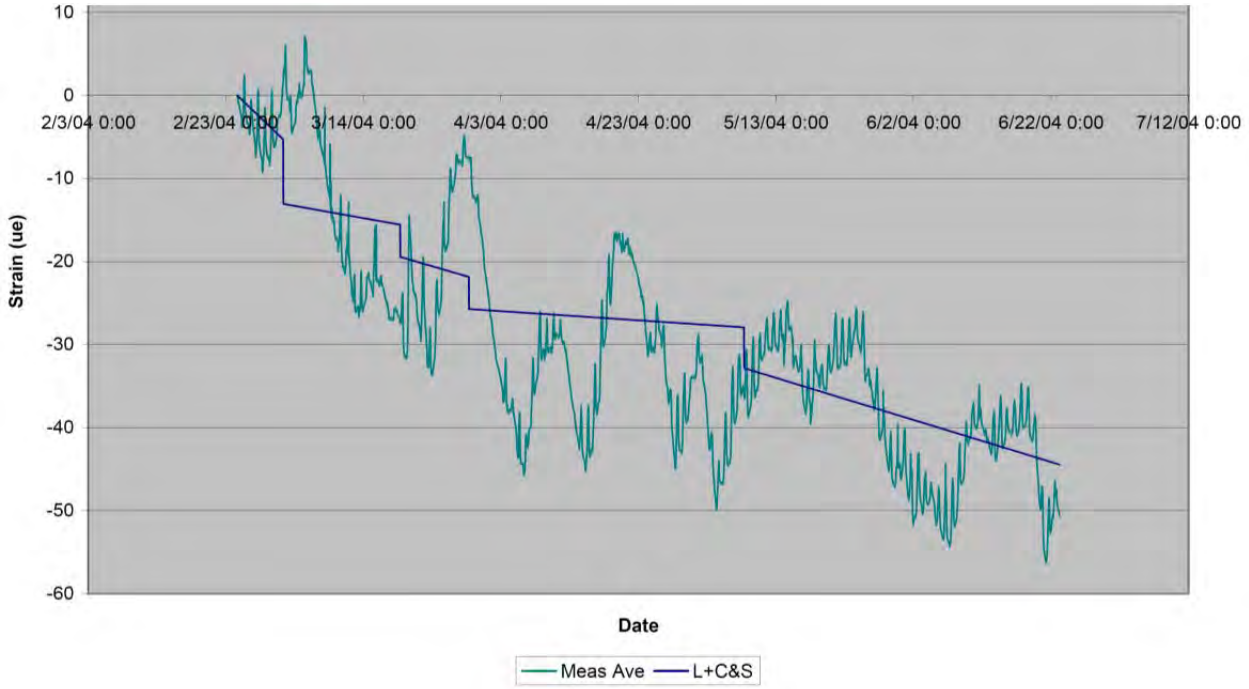

Figure 5.13: Measured vs Predicted Strain, EL600, Ohio Tower Pour, USG

In Figure 5.13, the measured sensor data after post processing is plotted against the analytical predictions after adjustment for the actual construction calendar of the Ohio tower at elevation 600. These first few months of data cover just the first few stages of construction for this location (e.g., see Tower Pour event, Figure 5.12). Here, the measured value is an average of all six strain gages installed at this elevation of the tower, as only axial force is assumed. Even with post processing, the measured data still exhibits some effect from the seasonal thermal swing and the daily thermal spikes as the tower is not a homogenous structure. The analytical values include the summation of both the expected deadload (L) response from upper segments of the tower, along with the predicted effect from creep and shrinkage (C&S). As this is a fairly straightforward exercise with few events and processes involved, this exemplifies a decent fit or comparison between measured and predicted values for the bridge monitor.

5.4.2. Initial Data from Girder Sensors Compared to Design

As another example of the steps required for comparison of measured field data with analytical design values, we next review with the first few months of sensor data for the vibrating wire strain gages installed on segment 2S (also known as KYAL) near the Kentucky abutment (see Figure 5.14). Again, the raw sensor data must be post processed in order to subtract the initial value bias (i.e., we only want to examine the change in reading since installation) and also attempt to remove the apparent effect of temperature. For steel gages epoxied directly to the steel edge girder, this becomes unnecessary, as both sensor and member are crafted from steel. For the steel gages embedded within the cast-in-place concrete strip above the edge girder, some trial and error is again required in that the actual temperature coefficient of the concrete is approximate to steel but can vary quite a bit depending upon various conditions. Next, we need to account for changes in the construction schedule from that assumed by the analytical design or erection model. In Figure 5.14, we adjust the dashed line of estimated values taken from the erection analysis by B&T by aligning the staged predictions with when they actually occurred on the calendar. The stages of construction shown in Figure 5.14 are (from left/first to right/last): 1) structural steel KYAL erected, 2) pre-cast panels and tie-downs installed, 3) infill joints cast, 4) edge strip cast, 5) structural steel 15S erected (i.e., the corresponding segment on the opposite side of the Kentucky tower), 6) Kentucky Bent removed, and 7) Stay 2S stressed (i.e., the stay for this instrumented segment). This represents most of the immediate stages of construction for this segment; however, it does not include the effect of the final segment installation (see Figure 5.15). Note how there is a fairly decent match between several of the gages with their analytical predictions: Top flange (T) vs T(est); Bottom flange, inner (BI) vs B(est); and either Deck gage, upper (DU) or lower (DL) vs predicted D(est). There is a noted bias on the outer bottom flange as compared to the inner bottom flange which causes it to differ from the predicted deadload value by -4.0ksi. The cause of this bias is unknown, but is probably due to the manner in which the segment is supported in this interim stage of construction.

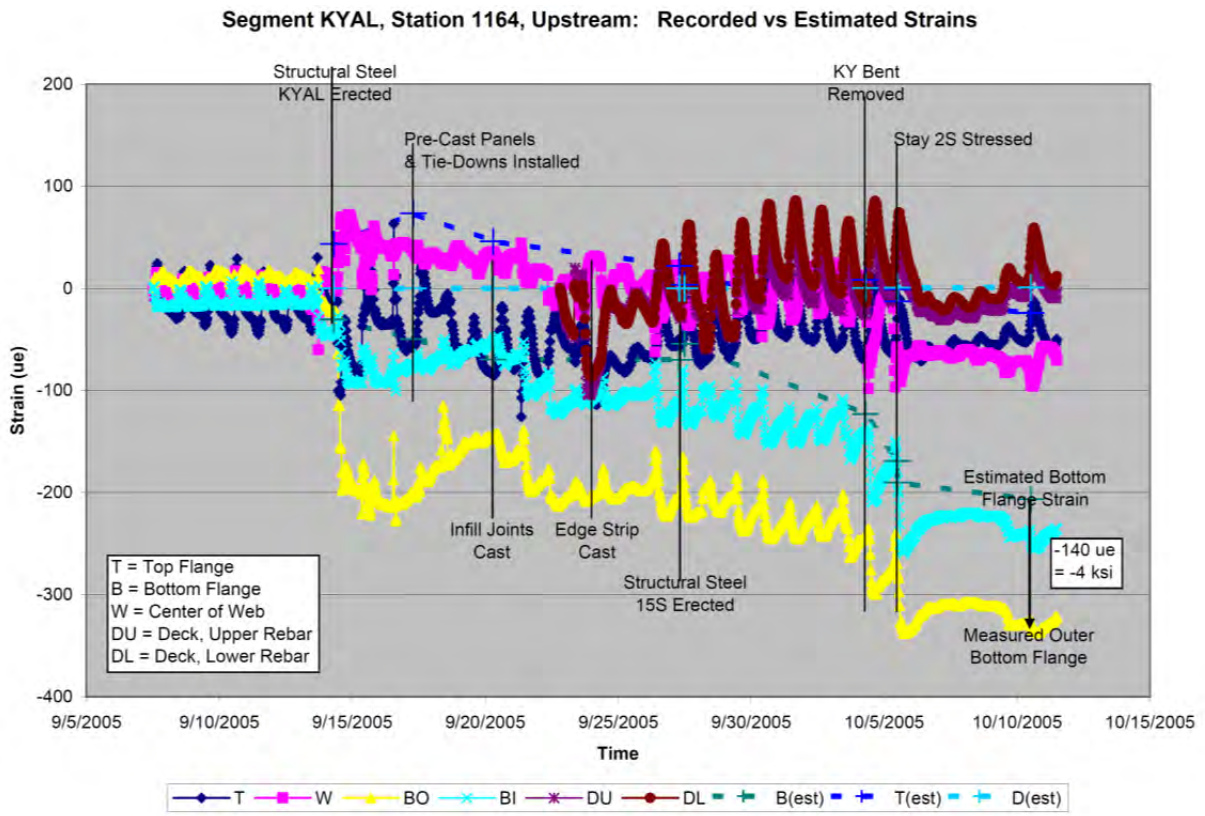

Figure 5.14: Measured vs Predicted, Station 2S, Upstream, USG, Sept., 2005 (UCII, 2005)

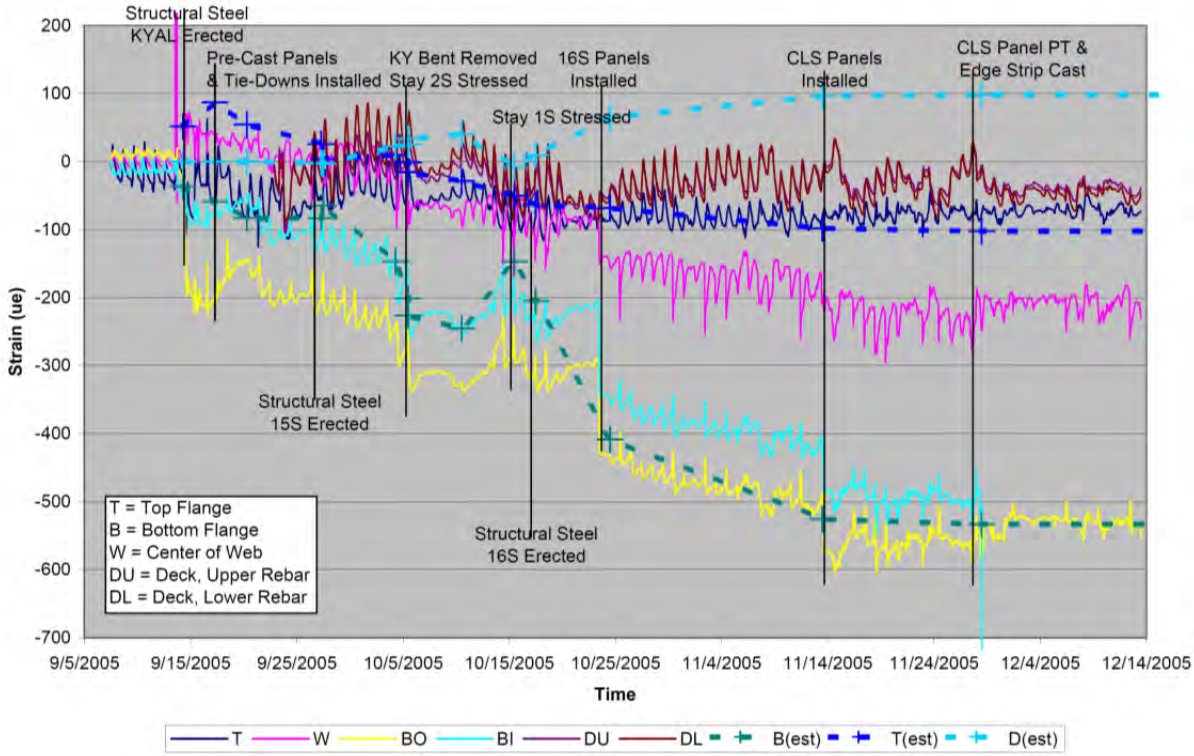

Figure 5.15: Measured vs Predicted, Station 2S, Upstream, USG, 2005 (UCII, 2006)

In Figure 5.15, we show the effect of the remaining significant stages of construction on segment 2S. Here, we again adjust the dashed line of estimated values taken from the erection analysis by B&T by aligning the staged predictions with when they actually occurred on the calendar. The additional stages of construction shown in Figure 5.15 are (from left/first to right/last, starting from those shown in Figure 5.14): 8) Stay 1S stressed, 9) structural steel 16S erected, 10) 16S panels installed, 11) CLS panels installed, and 12) CLS panel PT and edge strip cast. Note how the bias between bottom flange gages is slowly removed as construction proceeded. This represents most of the significant stages of construction for this segment and essentially captures the true deadload effect through end of construction (EOC). The superimposed deadload was added in the Summer of 2006 and included the parapet, the median, and the overlay, as well as final adjustments to the stays to achieve profile (not shown).

In Figures 5.16 through 5.20, we show the effect of the significant stages of construction through 2005 on the other instrumented segments of the upstream (right) side of the bridge. Most show small (i.e., 3ksi) to no difference from the predicted analytical values from B&T; however, there is significantly large difference (i.e., +11ksi for bottom flange, -6ski for top flange) for segment 9S near the Kentucky tower. The cause for this essentially positive moment is unknown; however, since this is a negative moment region for liveload, it is a boon.

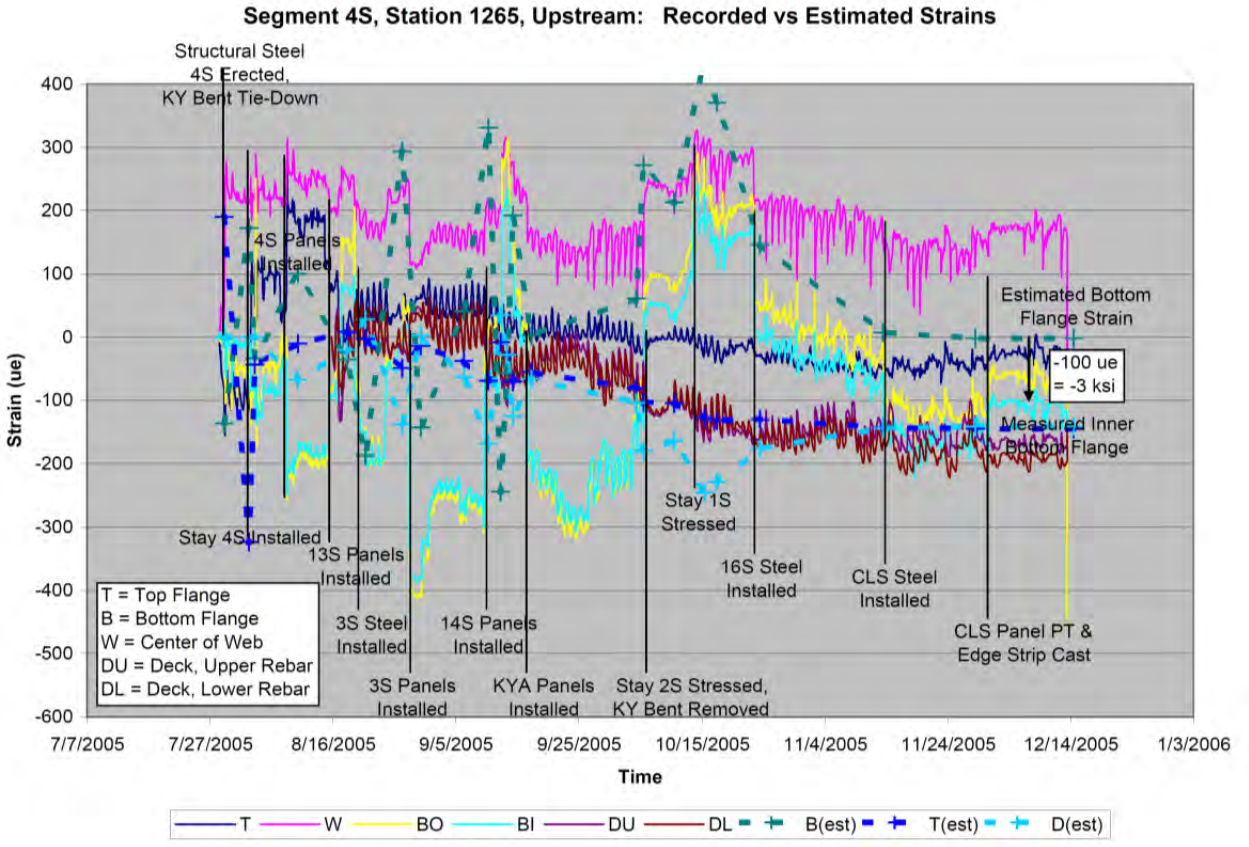

Figure 5.16: Measured vs Predicted, Station 4S, Upstream, USG, 2005 (UCII, 2006)

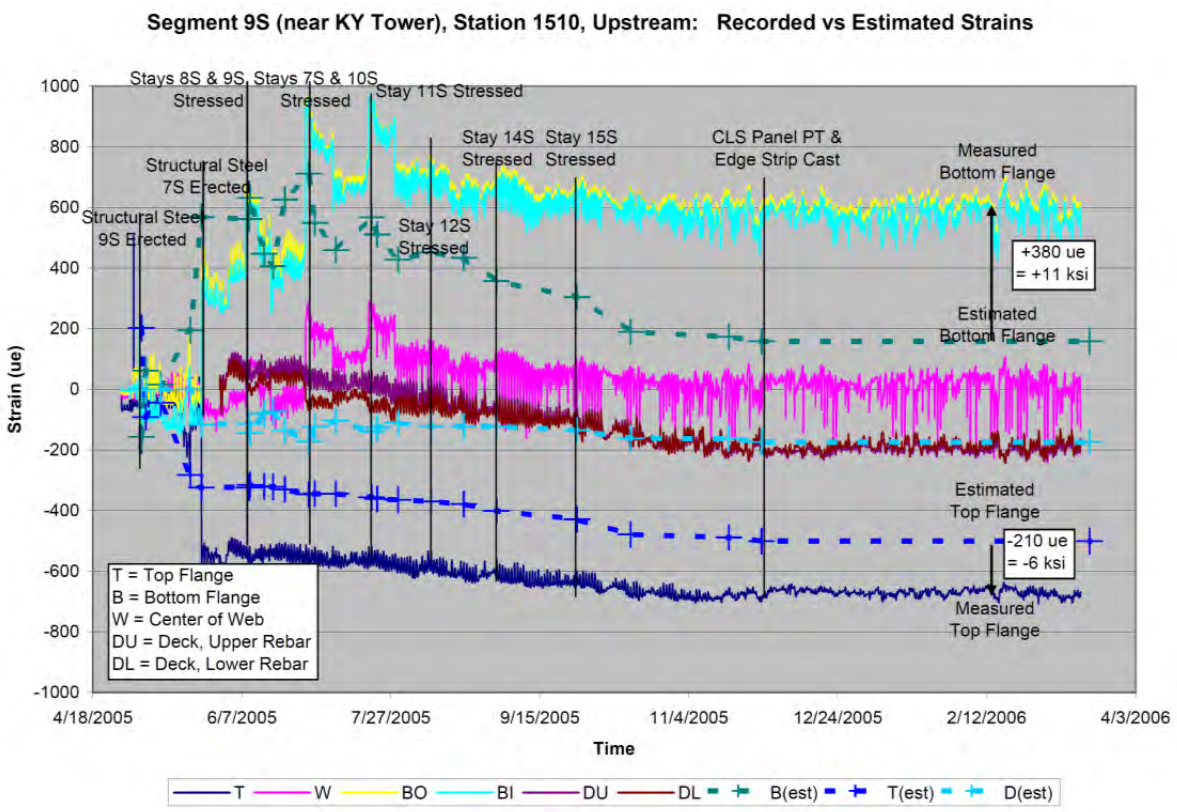

Figure 5.17: Measured vs Predicted, Station 9S, Upstream, USG, 2005 (UCII, 2006)

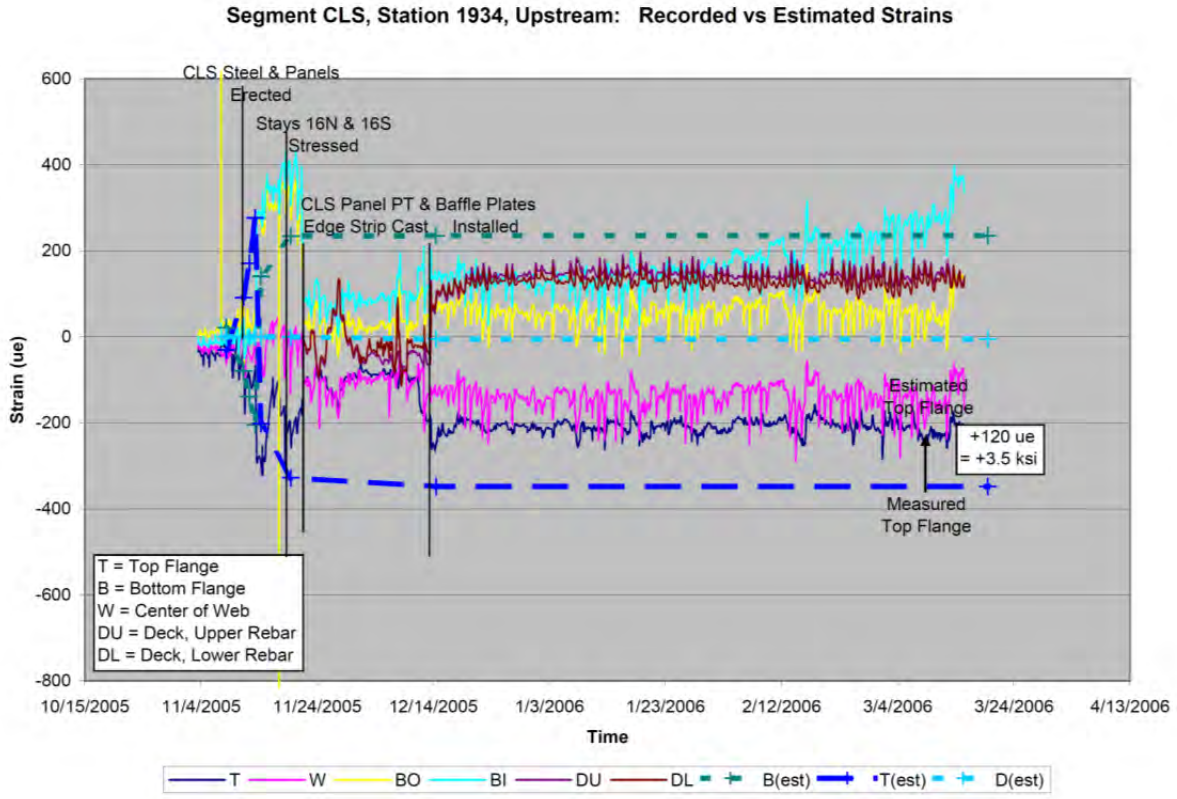

Figure 5.18: Measured vs Predicted, Station 16N, Upstream, USG, 2005 (UCII, 2006)

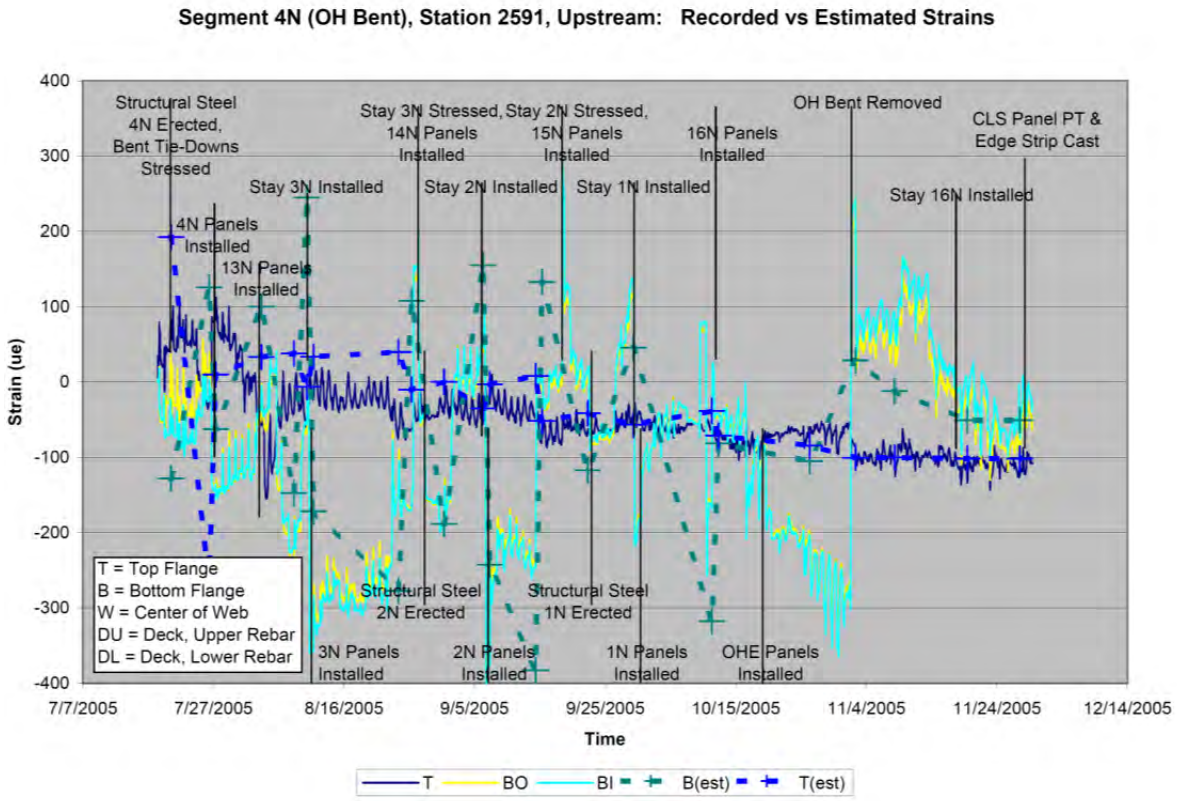

Figure 5.19: Measured vs Predicted, Station 4N, Upstream, USG, 2005 (UCII, 2006)

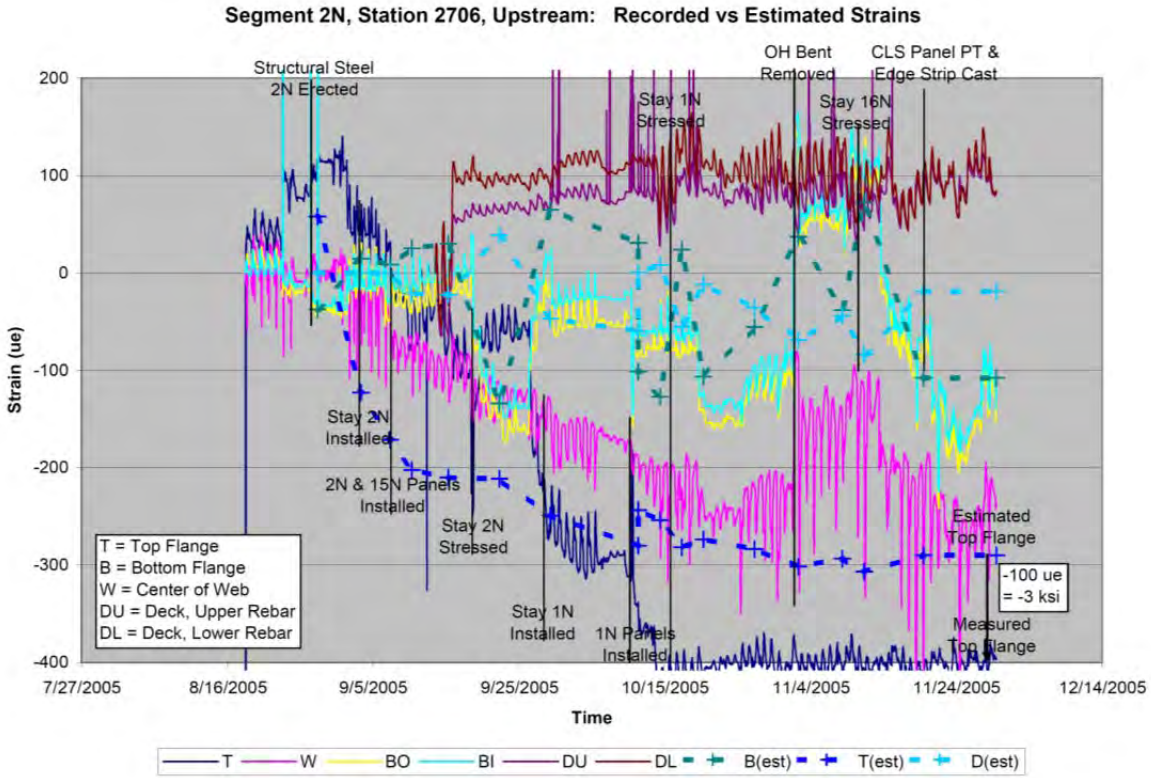

Figure 5.20: Measured vs Predicted, Station 2N, Upstream, USG, 2005 (UCII, 2006)

5.5 Summary Tables of Deadload and Other Long-Term Effects

In Table 5.1, the measured deadload strain/stress observed by the end of construction in 2006 are tabulated and compared to the equivalent deadload predictions by B&T. These values would include not only deadload (as illustrated in Figures 5.15 through 5.20), but also the superimposed deadload of the items installed in the Summer of 2006 (e.g., parapet, median, overlay, etc.). Since both stresses are treated the same by the Load Factor Method of analysis, we combine them here. Note that for most of the instrumented segments there is relative agreement between measured and estimated values, with two exceptions: segment 9S, which we discussed above, and segment 16N. Segment 16N exhibited a very large tensile response at the bottom flange which occurred after the stays were adjusted for profile. This is of concern since this is a positive moment region under liveload. Subsequent monitoring of this location showed that this condition was relaxed over time and fell more in line with predictions (see Tables 5.2 and 5.3).

US Grant Bridge, End of Construction Stresses, October 10, 2006

	Measured EOC DL Stress			B&T EOC DL Stress, Ver. 3			
	Gage	DWN	UPstream				
Section	DU	+50ue	+20ue	DU	-20ue		
2N	TF	-375ue	-430ue	TF	-341ue	?	-M LL
	BF	-175ue	-175ue = -5.1ksi	BF	-150ue = -4.4ksi		
4N	TF	-220ue	-160ue	TF	-147ue	?	+M LL
	BF	0ue	-200ue = 0ksi	BF	-98ue = -2.8ksi		
16N	DU	119ue	111ue	DU	-57ue		
	TF	-229ue	-408ue	TF	-387ue	?	+M LL
	BF	638ue	297ue = 18.5ksi	BF	351ue = 10.2ksi		
9S	DU	-279ue	-217ue	DU	-147ue		
	TF	-935ue	-733ue	TF	-538ue	✓	-M LL
	BF	203ue	418ue = 5.9ksi	BF	-47ue = -1.4ksi		
4S	DU	-224ue	-218ue	DU	-154ue		
	TF	-256ue	-136ue	TF	-187ue	✓	+M LL
	BF	-153ue	-40ue = -1.2ksi	BF	-30ue = -0.9ksi		
2S	DU	-78ue	49ue	DU	126ue		
	TF	36ue	-57ue	TF	-157ue	✓	-M LL
	BF	-526ue	-509ue = -15.3ksi	BF	-623ue = -18.1ksi		

✓ = Difference between Measured and Estimated is Helpful in terms of Liveload Rating

Table 5.1: Measured vs Predicted Deadloads, USG, End of Construction (UCII, 2007)

In Table 5.2, the measured long-term strain/stress observed in March, 2009 are tabulated and compared to the equivalent deadload predictions by B&T. These values would include not only deadload (as illustrated in Figures 5.15 through 5.20) and the superimposed deadload of the items installed in the Summer of 2006 (e.g., parapet, median, overlay, etc.), but also any and all other long-term effects that are evident (e.g., creep, shrinkage, degradation, initial repairs to the Kentucky pulldowns, etc.). Since all such stresses are treated the same by the Load Factor Method of analysis, we combine them here. Note that for most of the instrumented segments there is relative agreement between measured and estimated values. Also note how the two exceptions to this comparison in 2006 (i.e., segments 9S and 16N) have somehow worked out most of these differences with the analytical predictions in the intervening years.

US Grant Bridge, Deadload (+Long Term) Stresses, March, 2009

	Measured EOC DL Stress			B&T EOC DL Stress, Ver. 3			
Section	Gage	DWN	UPstream				
2N	DU	+150ue	+50ue	DU	-20ue		-M LL
	TF	-375ue	-430ue	TF	-341ue		
	BF	n/a	-260ue = -7.5ksi	BF	-150ue =	-4.4ksi	
4N	TF	-305ue	-305ue	TF	-147ue		+M LL
	BF	50ue	-175ue = 1.5ksi	BF	-98ue =	-2.8ksi	
16N	DU	0ue	-200ue	DU	-57ue		+M LL
	TF	0ue	n/a	TF	-387ue		
	BF	438ue	257ue = 12.7ksi	BF	351ue =	10.2ksi	
9S	DU	-279ue	-75ue	DU	-147ue		-M LL
	TF	-935ue	n/a	TF	-538ue		
	BF	-75ue	-350ue = -2.2ksi	BF	-47ue =	-1.4ksi	
4S	DU	-350ue	n/a	DU	-154ue		+M LL
	TF	-356ue	-350ue	TF	-187ue		
	BF	-153ue	0ue = 0 ksi	BF	-30ue =	-0.9ksi	
2S	DU	n/a	+100ue	DU	126ue		-M LL
	TF	+100ue	0ue	TF	-157ue		
	BF	-675ue	-700ue = -20.3ksi	BF	-623ue =	-18.1ksi	

Table 5.2: Measured vs Predicted Deadloads and Long-Term Effects, USG, 2009 (UCII, 2009)

In Figures 5.21 through 5.26, we show 7 years of long-term monitoring data for the upstream (right) side of the bridge. This includes the effect of the significant stages of construction in 2005, the superimposed deadload and other final stages of construction in 2006, and the intervening effect of long-term processes (e.g., daily and seasonal thermal cycles, environmental effects, cracking and initial repairs at Kentucky abutment, creep, shrinkage, etc.) through 2011 Most show small to no difference from the values listed in Table 5.2; however, there is significantly large differences (i.e., see Figure 5.21, Table 5.3) near the Kentucky abutment that occurred due to the installation of the permanent external pulldowns in the Summer of 2011. The cause for this essentially positive moment is known and was predicted in the design by HNTB; however, since this is a negative moment region for liveload, it is a boon.

Aside from the obvious daily and seasonal effects (and the local effect of the Kentucky pulldown), most of the gages show little to no long-term change since 2007. This is in stark contrast to the predicted effect of creep and shrinkage predicted by B&T (see Table 5.3), where it was assumed some tension would occur in the decking which would cause some compression on the bottom flange due to the composited design of the edge girders. Note that some deck gages show a compressive trend (e.g., 11642SDU) which is more indicative of deterioration or damage to the embedded sensor and/or its cable and not actual structural response like creep. Most are essentially trending sideways in Figures 5.21 through 5.26.

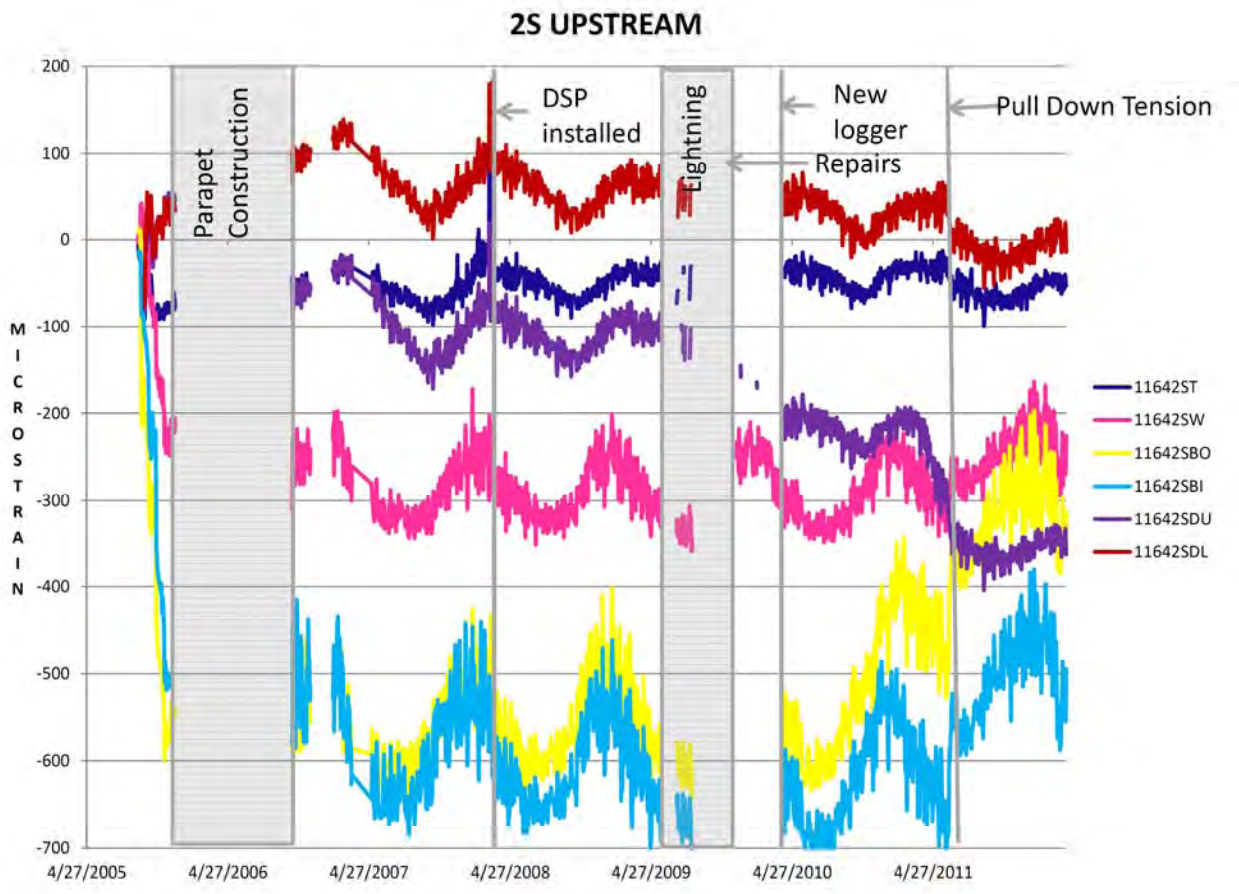

Figure 5.21: Measured vs Predicted, Station 2S, Upstream, USG, 2011 (UCII, 2012)

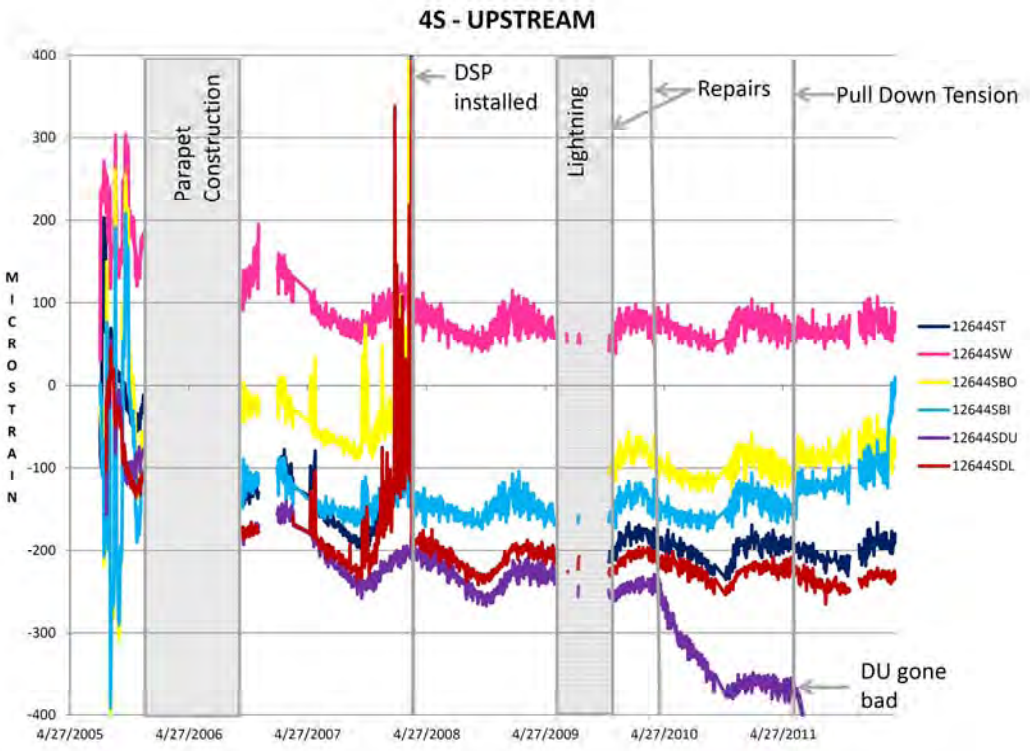

Figure 5.21: Measured vs Predicted, Station 4S, Upstream, USG, 2011 (UCII, 2012)

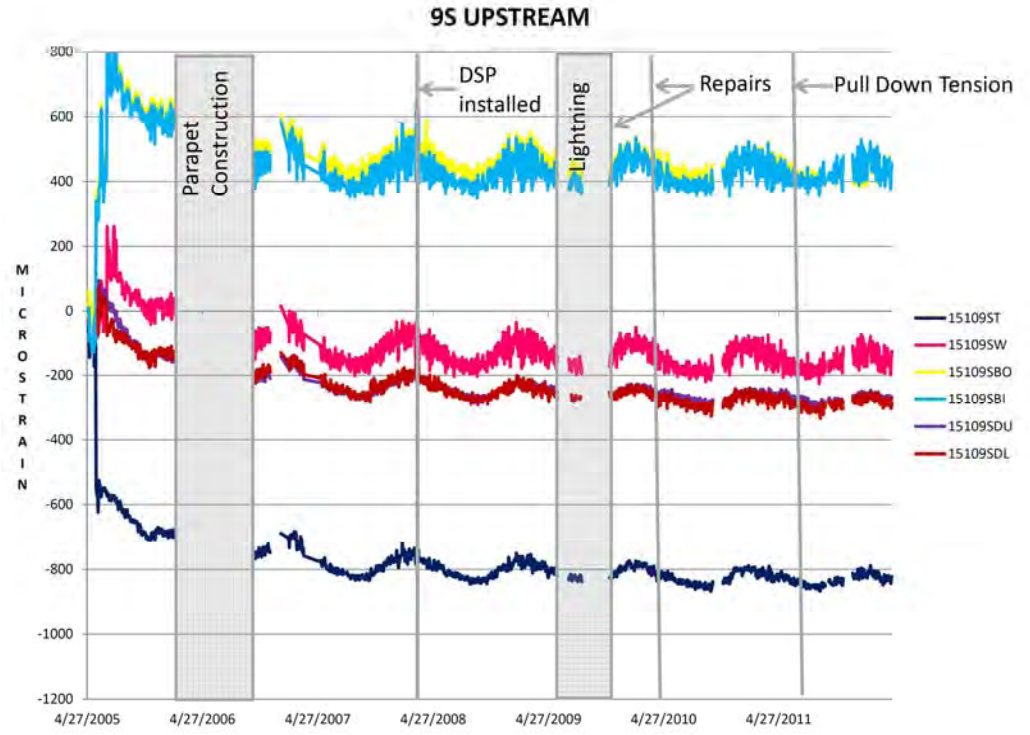

Figure 5.21: Measured vs Predicted, Station 9S, Upstream, USG, 2011 (UCII, 2012)

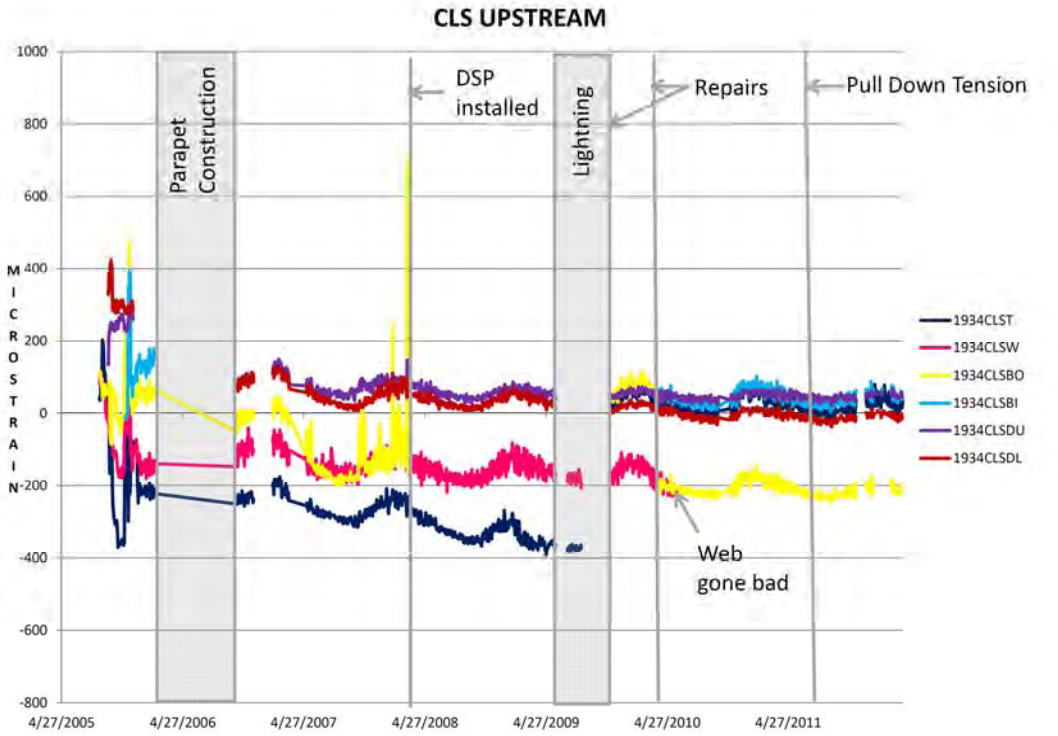

Figure 5.21: Measured vs Predicted, Station 16N, Upstream, USG, 2011 (UCII, 2012)

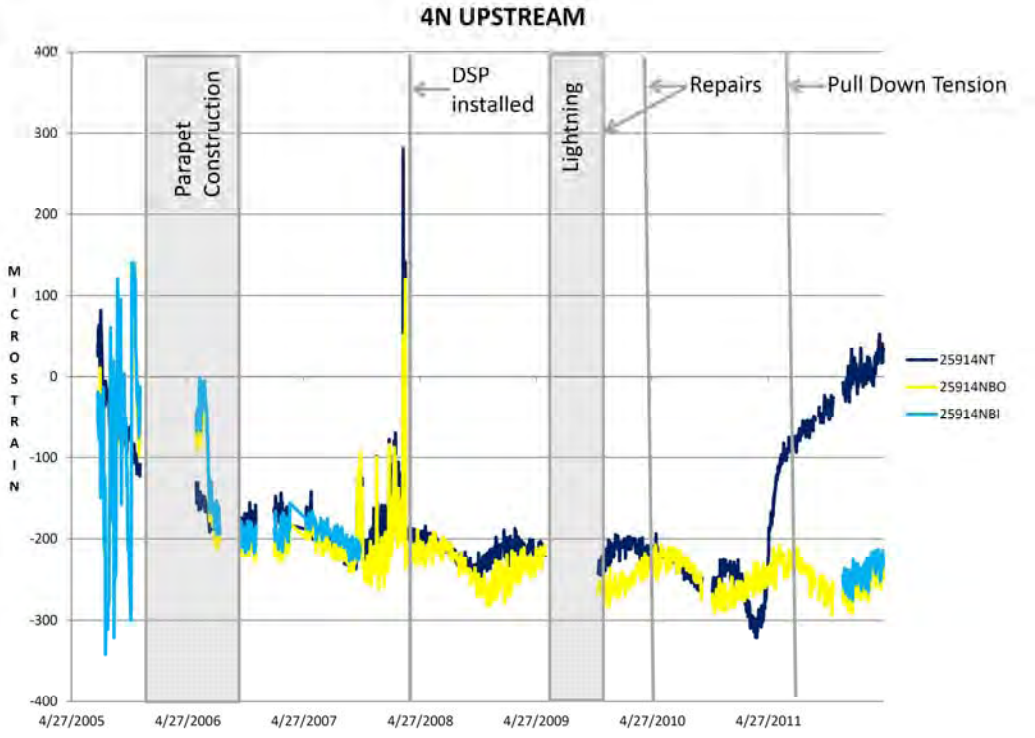

Figure 5.21: Measured vs Predicted, Station 4N, Upstream, USG, 2011 (UCII, 2012)

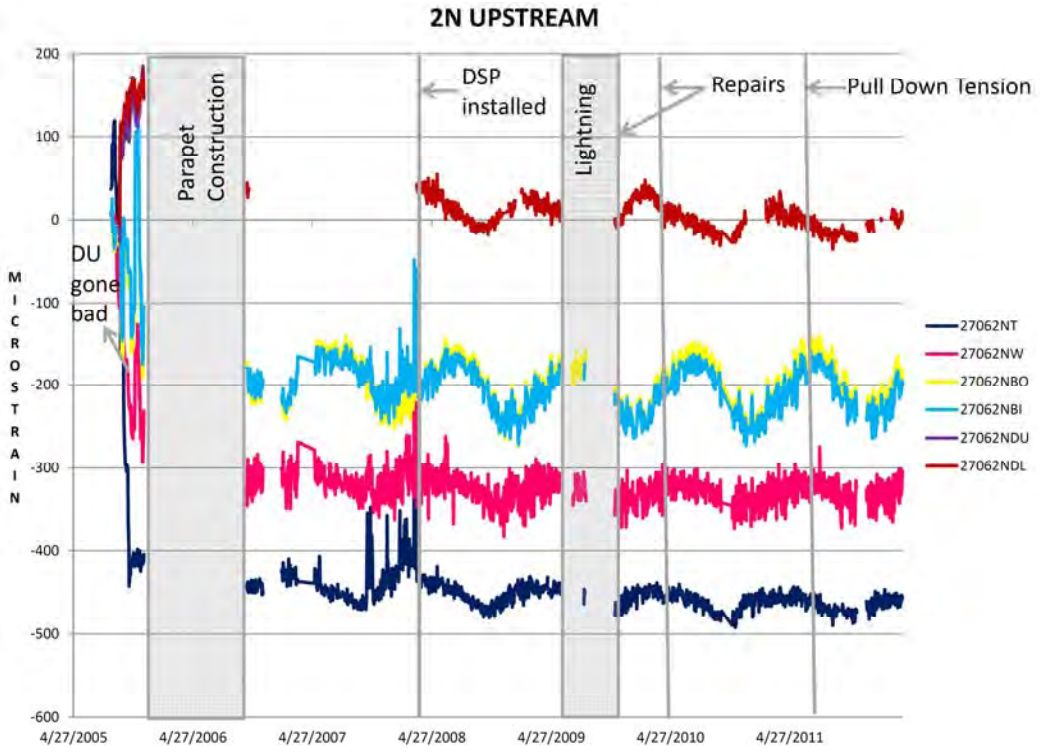

Figure 5.21: Measured vs Predicted, Station 2N, Upstream, USG, 2011 (UCII, 2012)

US Grant Bridge, Bottom Flange, Deadload (+ Long Term) Stresses (ksi)

Segment	2006 (EOC)	2009	2012 (Day 2000)	B&T (EOC)	B&T (Day 2500)
2N	-5.1	-7.5	-7.5	-4.4	-6.4
4N	0	+1.5	+3.6	-2.8	-6.2
CLS	+18.5	+12.7	+13.6	+10.2	+8.3
9S	+5.9	-2.2	-2.2	-1.4	-4.1
4S	-1.2	0	0	-0.9	-2.4
2S	-15.3	-20.3	-17.4	-18.1	-16.0

Higher Rating

Effect of creep

2006, Bridge Opened to Service
2009, Following Initial Repairs at KYA
2012, Following Pulldowns at KYA

B&T = Buckland & Taylor Analysis
EOC = End of Construction

Table 5.3: Measured vs Predicted Deadloads and Long-Term Effects, USG, 2011 (UCII, 2012)

5.6 Conclusions and Recommendations

A significant amount of effort was expended in this project to measure, record, and interpret the behavior of the steel framing and composite concrete decking system during construction. This included monitoring the induced stresses and strains, where and when they occurred, and investigating causative effects. The main components of the framing system, namely the edge girders and the cast-in-place concrete strip directly above them, were comprehensively instrumented and continuously monitored during the construction of the bridge (see Figure 3.8). Instrumented monitoring commenced immediately before the segment was erected onto the bridge, through any temporary stressing or profiling with the stays or post-tensioning strands, placement of the precast concrete deck panels, during the concrete pour and curing of the cast-in-place strips, and as other segments were installed on either side of its respective tower, throughout most stages of its construction and into (and beyond) service on October 16, 2006.

Table 5.1 summarizes the measured deadload effects at essentially the end of construction (EOC). In Table 5.2, the measured long-term strain/stress observed in March, 2009 are tabulated and compared to the equivalent deadload predictions by B&T. These values would include not only deadload (as illustrated in Figures 5.15 through 5.20) and the superimposed deadload of the items installed in the Summer of 2006 (e.g., parapet, median, overlay, etc.), but also any and all other long-term effects that are evident (e.g., creep, shrinkage, degradation, initial repairs to the Kentucky pulldowns, etc.). Since all such stresses are treated the same by the Load Factor Method of analysis, we combine them here. Note that for most of the instrumented segments there is relative agreement between measured and estimated values.

The long-term results depicted in Figures 5.21 through 5.26 are summarized and compared to past design and measured values (e.g., Table 5.2) in Table 5.3. As noted above, little to no change was observed in the average long-term value for each gage between 2009 and 2012 results; however, there was a positive moment induced locally near the Kentucky abutment due to the installed exterior pulldowns in 2011. There is little to no effect from creep (or any other long-term effect except the obvious seasonal response cycle) which contradicts the expected negative moment due to creep as predicted by the analysis of B&T.

REFERENCES

1. Howard, Needles, Tammen, and Bergendoff (HNTB), Design Calculations for the U.S. Grant Bridge, 2000.
2. Buckland & Taylor (B&T), Superstructure Erection Submission for U.S. Grant Bridge, Rev. 3, 2004.
3. Howard, Needles, Tammen, and Bergendoff (HNTB), Ratings Manual for the U.S. Grant Bridge, 2013.
4. A. Helmicki, and V. Hunt, "Instrumentation of the US Grant Bridge for Monitoring of Fabrication, Erection, In-service Behavior, and to Support Management, Maintenance, and Inspection," Project Review, ODOT Central Office, 2004.
5. C.S. Cai, J. Nie, and Y. Zhang, "Composite Girder Design of Cable-Stayed Bridges." Structural Design and Construction, ASCE, Vol. 3, No. 4, November 1998: 158-163.
6. A. Helmicki, and V. Hunt, "Instrumentation of the US Grant Bridge for Monitoring of Fabrication, Erection, In-service Behavior, and to Support Management, Maintenance, and Inspection," Project Review, ODOT Central Office, 2006.
7. A. Helmicki, and V. Hunt, "Instrumentation of the US Grant Bridge for Monitoring of Fabrication, Erection, In-service Behavior, and to Support Management, Maintenance, and Inspection," Project Review, ODOT Central Office, 2007.
8. J.S. Saini, "Effects of Nonlinearities due to Geometry, Cables and Tuned Mass Dampers on the Analysis of Cable-stayed Bridges," MS Thesis, Department of Civil and Environmental Engineering, University of Cincinnati, Cincinnati, OH, 2007.
9. A. Helmicki, and V. Hunt, "Instrumentation of the US Grant Bridge for Monitoring of Fabrication, Erection, In-service Behavior, and to Support Management, Maintenance, and Inspection," Project Review, ODOT Central Office, 2009.
10. A. Helmicki, and V. Hunt, "Instrumentation of the US Grant Bridge for Monitoring of Fabrication, Erection, In-service Behavior, and to Support Management, Maintenance, and Inspection," Project Review, ODOT Central Office, 2012.
11. Essegby, J., *Piece-wise Linear Approximation for Improved Detection in Structural Health Monitoring*, Masters Thesis, School of Electronics and Computing Systems, University of Cincinnati, Cincinnati, OH, 2012.
12. Lenett, M., Hunt, V., Helmicki, A., "Instrumentation, Testing and Monitoring of a Newly Constructed Reinforced Concrete Deck-On-Steel Girder Bridge – Phase III." University of Cincinnati Infrastructure Institute, Cincinnati, OH, 2001.
13. Levi, A. *Instrumented Monitoring & Diagnostic Load Testing For Condition Assessment And Evaluation Of Bridges.* Doctoral Dissertation, Department of Civil and Environmental Engineering, University of Cincinnati, Cincinnati, OH, 1997.
14. Grimmelsman, K. *Instrumented Monitoring of a Reinforced Concrete Slab on Steel Stringer Highway Bridge Through Construction: Steel Elements*, Masters Thesis, Department of Civil and Environmental Engineering, University of Cincinnati, Cincinnati, OH, 1997.
15. Barrish, R. *Instrumented Monitoring of a Reinforced Concrete Slab on Steel Stringer Highway Bridge Through Construction: Concrete Elements*, Masters Thesis, Department of Civil and Environmental Engineering, University of Cincinnati, Cincinnati, OH, 1997.

Chapter 6 Truckload Testing Results and Comparison with Design

6.1 Introduction

Structural identification testing has been defined as the art of analytically conceptualizing, modeling, and designing experiments to measure and quantify structural behavior, and the phenomena that affect it, as a basis for subsequent engineering decisions. Structural behavior and the phenomena that affect it are quantified using strain data, displacement data, tilt or rotation data, modal frequencies, or different combinations of these. Objective identification and characterization of a structure's global state are the essence of structural identification testing.

Several discrete structural identification tests were conducted after construction was complete but before the bridge was opened to traffic. The conduct and timing of these tests served several critical objectives. The first was to establish the constructed-state baseline of the bridge. Another was to corroborate or provide a sanity check of the instrumented monitoring readings obtained during construction. Finally, the testing was conducted to provide additional experimental data with which to evaluate the efficacy of the structural identification testing procedure.

There are two basic types of truck tests: (1) crawl speed testing, and (2) static load testing. During a crawl speed test, one or more loaded and pre-weighed trucks drive along the longitudinal dimension of the bridge at a fairly slow speed, generally 20 miles per hour, and the bridge response is measured. The speed is kept slow to minimize dynamic effects in the sensor responses. The process may be repeated for several longitudinal lines, usually the marked traffic lanes and shoulders, across the width of the bridge. The main advantage associated with this technique is that it provides a continuous record of all sensor responses as the truck crosses the bridge. This test is also somewhat faster than static testing and therefore minimizes disruption of traffic flow on the bridge. The instrumentation and data acquisition systems used for this test must be capable of performing high-speed measurements to accurately determine the complete record of structural response.

In static load tests, trucks are positioned in various patterns on the bridge for a brief amount of time, on the order of seconds to several minutes, and the corresponding bridge response is measured and recorded. The instrumentation and data acquisition systems do not necessarily need to function at high speeds given the static nature of the test. An advantage of this test is that it can be used to directly evaluate bridge response to various discrete load cases and permits multiple readings to be taken for each position. The static load test method was used to test the bridge because the vibrating wire gages cannot be read at high speeds, requiring about two seconds to read each gage. In addition, because the bridge had yet to be commissioned, disruption to traffic was not a concern for the baseline tests.

Truck tests are generally used for diagnostic or rating purposes. For either purpose, the crawl test or static test technique may be utilized. A diagnostic truck load test is conducted to determine specific information about the condition or behavior of a bridge, such as for investigating the transfer of live load stress between various bridge components. A test conducted for rating purposes seeks to objectively establish the load capacity of a bridge. Of course, only the liveload response is actually measured during a truckload test, but the other structural characteristics required for load rating such as material/sectional capacity and deadload response can be obtained from the design analysis. In this particular case, the deadload can also be obtained from the vibrating wire gages which were installed prior to segment erection and maintain a reliable reading throughout construction and into service.

Last but not least, the measured liveload response from the truckload tests can be compared directly with the predicted liveload response from the design analysis. In this manner, analytical assumptions used in the design process such as effective width and composite action can be assessed quantitatively and directly.

6.2 Analytical Liveload Response by Design

HNTB provided estimates for HS20 liveload moment, axial force, and shear response.

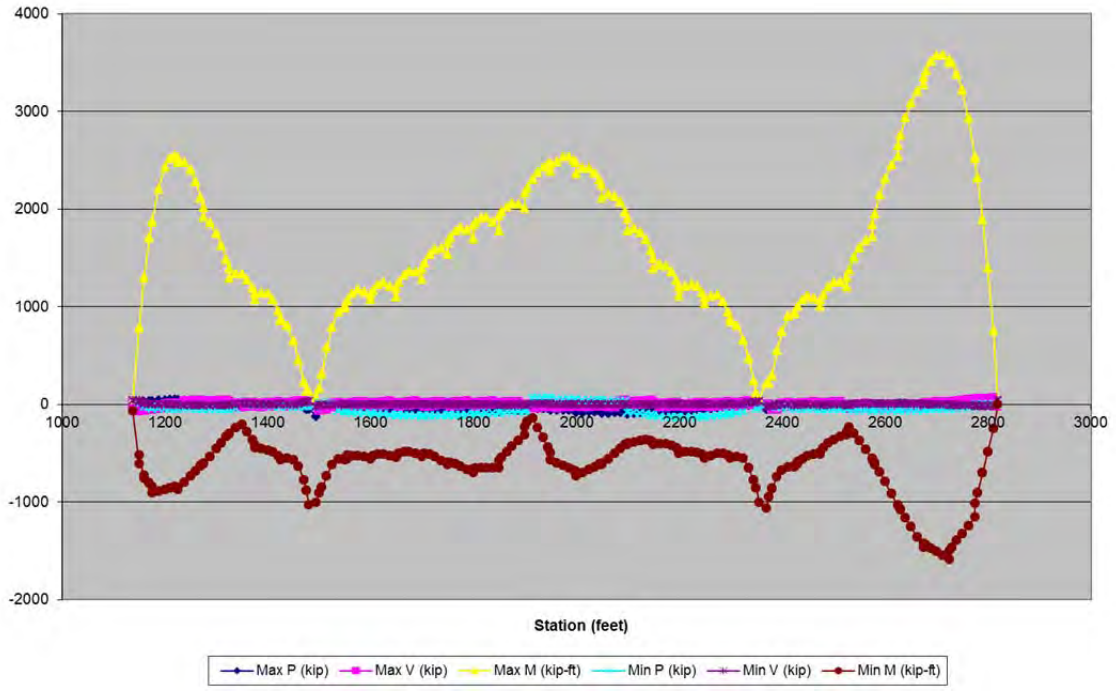

Figure 6.1: Design Envelope for Single HS20 Truck Load, U.S. Grant Bridge (HNTB, 2000)

Lane load was found to control, as is typical of large structures, and is the only liveload included in our rating spreadsheet and figures.

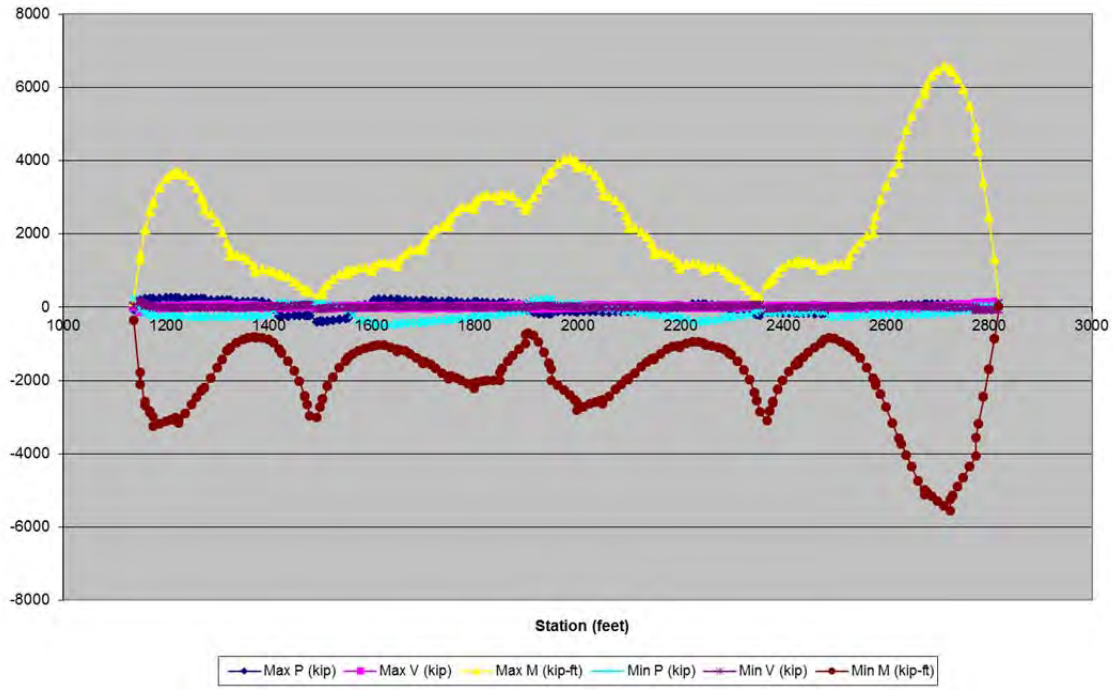

Figure 6.2: Design Envelope for Single HS20 Lane Load, U.S. Grant Bridge (HNTB, 2000)

The calculation of liveload stress for the composite and noncomposite (or cracked) section is discussed at length in Chapter 3. Here, composite action is assumed. Note that no adjustment for axial straining or other creep effects needs to be included in the calculation of liveload.

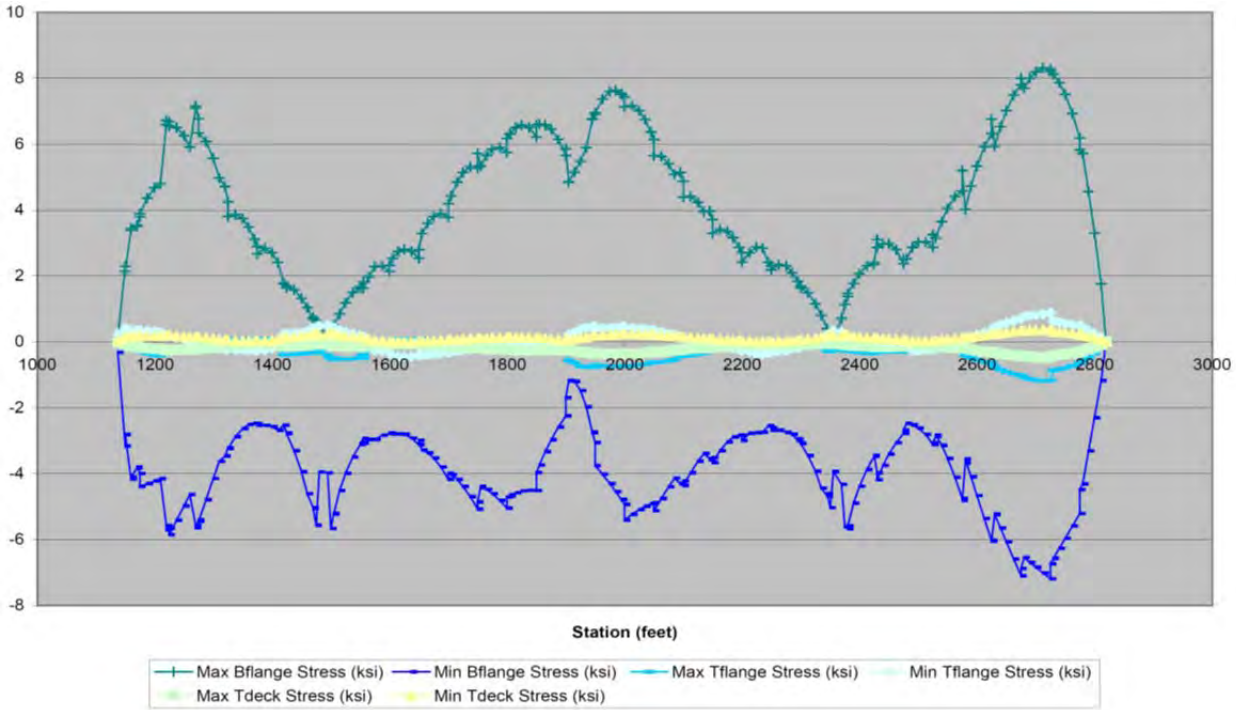

Figure 6.3: Stress Envelope for Single HS20 Lane Load, U.S. Grant Bridge (UCII, 2004)

For rating purposes, this liveload is later scaled by a variety of factors: the result is scaled by 1.25 to represent an HS25 liveload as intended by its design, scaled by a distribution factor of 1.74 to account for lateral effects not included in the two dimensional, finite element model used in the design, and scaled by an impact factor of 1.1 for the controlling lane load.

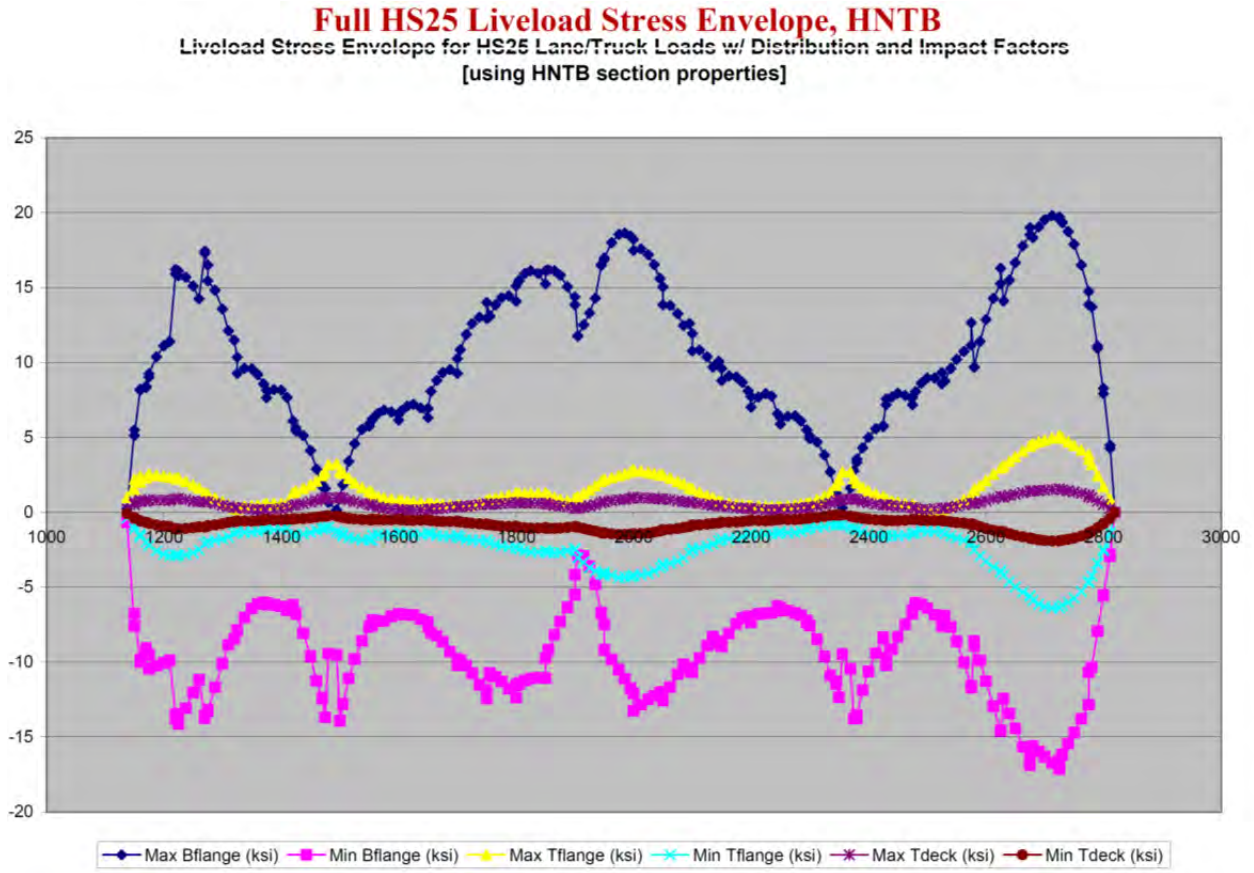

Figure 6.4: Stress Envelope for Four HS20 Lane Load, U.S. Grant Bridge (UCII, 2004)

Here, the stress envelope was calculated with both bending moment and axial force stresses added together; this allowed both effects to be considered simultaneously. Note, however, that the stress due to the axial force is significantly smaller than the stress due to bending moment.

Also, recall that there were significant discrepancies between HNTB and B&T in regards to various analytical assumptions such as effective width in bending (i.e., 96" and 201", respectively) and under axial force (they differ in areas of low axial force, at the ends and middle of the bridge). See Figures 3.4 and 3.5, respectively, for illustrations of these differences. These differences in basic assumptions would affect a variety of things including sectional properties such as centroid, inertia, and modulus, as well as other concepts such as the depth of the stress block for the compactness check in positive moment.

6.3 Baseline Testing, 2006, Prior to Service

The constructed-state baseline is an objective characterization of a structure's intrinsic properties and performance before it experiences sustained exposure to combinations of complex phenomena that instigate damage and deterioration. After construction is complete, a bridge is in the most undefiled or unspoiled condition possible. The structure was already exposed to numerous phenomena which influence its condition during construction; however, the overall condition of the bridge at this instant is likely better with respect to any subsequent point during its life-span.

The constructed-state baseline of a bridge is important for several reasons. First, the baseline may be used to calibrate analytical models of the structure. The reliability and usefulness of such models are substantially increased if they have been calibrated using the measured properties and responses of the structure. The baseline can also be used to generate objective condition indices that relate to the initial health and performance of the structure. Subsequent tests can identify changes in these indices and quantify the condition of the bridge relative to its baseline condition as the structure ages and deteriorates. Such indices are necessary to enable more rational and efficient maintenance management, and for identifying and mitigating causative effects.

Finally, the majority of structural identification testing that has been conducted thus far has been with bridges already in service or those that have deteriorated somewhat from their initial constructed condition. The sensitivity of the structural identification process to the age at which a bridge's baseline condition is established can be analyzed using a constructed-state baseline.

6.3.1 Baseline Test Design

The first step for the static truck load test was to design a set of truck positions or load cases for the bridge. Four standard salt trucks were used, as shown in Table 6.1. As illustrated in Table 6.2, a total of seventeen truck positions were selected. A number of objectives for the truck load test were used to select the positions, but primarily to locate the trucks side-by-side in the two marked traffic lanes and two shoulders, at each instrumented station. These load cases would be staggered with "no load" cases, where the trucks would be moved off the bridge.

Static Truckload Test of US Grant Bridge, October 10, 2006								
Truck#	Position	Lane#	Ft Axle (lbs)	Back Axle (lbs)	Total Wt (lbs)	Space (in, CL-t	Ft Tire Space (i	Back Tire Spac
827	DS, shoulder	1	9020	17640	26660	140	88	93
521	DS, lane	2	9140	21740	30880	140	88	93
528	US, lane	3	10960	23840	34800	178	91	93
602	US, shoulder	4	9240	20820	30060	140	88	93
Total			38360	84040	122400			
4 HS25			40000	320000	360000	2.941176471	34.00%	Ratio of Test Lo

Table 6.1: Truck Specifications Used in Static Test Plan, 2006

Test#	Time Start	Position	Time End	Notes
1	9:28	OH Apprch	9:34	No load condition
2	9:36	2N	9:44	Back axle located adjacent to stay where it exits the deck
3	9:48	OH Apprch	9:56	No load condition
4	9:58	4N	10:06	Back axle located adjacent to stay where it exits the deck
5	10:08	OH Apprch	10:16	No load condition
6	10:18	6N	10:24	Back axle located adjacent to stay where it exits the deck
7	10:34	OH Apprch	10:41	No load condition
8	10:44	16N	10:52	Back axle located adjacent to stay where it exits the deck
9	10:54	KY Apprch	11:05	No load condition, backhoe drove across bridge in DS lane
10	11:08	9S	11:16	Back axle located adjacent to stay where it exits the deck
11	11:18	KY Apprch	11:31	No load condition, backhoe drove across bridge in DS lane
12	11:34	6S	11:42	Back axle located adjacent to stay where it exits the deck
13	11:44	KY Apprch	11:58	No load condition
14	12:02	4S	12:10	Back axle located adjacent to stay where it exits the deck
15	12:12	KY Apprch	12:20	No load condition
16	12:22	2S	12:30	Back axle located adjacent to stay where it exits the deck
17	12:32	KY Apprch	12:36	No load condition

Table 6.2: Static Truckload Test Plan, 2006

The instrumentation scheme for the truck load test consisted of strain gages installed on the bridge during construction. Each location includes both a vibrating wire gage for slow-speed reading of long-term behavior without drift, and a traditional foil gage for high-speed reading of short liveload response. The stations of the sensors are listed on the right side of Figure 3.8.

6.3.2 Conduct of Testing

The Ohio Department of Transportation provided four tandem-axle dump trucks that were used to conduct the truck load test. Tandem-axle dump trucks were requested because, when fully loaded, they are typically much heavier than their single rear axle counterpart. The truck weight is important because it should be sufficient to cause sensor readings that are above noise levels.

Figure 6.5: Pictures of the Truckload Test, USG, 2006 (UCII, 2007)

Two data acquisition systems were used during the test because a combination of high speed and low speed (vibrating wire) sensors were used for the test. Several Campbell Scientific CR-10X data logger systems were used to power and read the vibrating wire based gages and two Optim MEGADAC data acquisition system was used to power and read the high-speed sensors.

The trucks were placed in one of the positions from the test plan and at least three readings were recorded from each sensor. It took about 10 minutes to test each position because the CR-10X loggers required about 2 minutes to scan the all of the vibrating wire gages and there was always some delay in positioning the trucks. A set of readings with no load on the bridge was recorded periodically during the test to cancel out any environmental effects in the results.

The moving truckload tests were conducted after the static tests, throughout the remainder of the afternoon. Truck #528 was selected and the other trucks were returned to the garage. One person with a walkie-talkie took the passenger seat of the truck. The truck driver was to start north of the bridge, accelerate to a speed of about 20mph, center the truck in the test lane, and maintain that speed (and lane) for the entire length of the bridge. Upon reaching the south abutment, the truck would immediately brake to stop short of the intersection just south of the bridge. Two high-speed data acquisition systems were deployed at the northern sensor station (i.e., 2N). Data collection at 200Hz was manually triggered to commence as the front tire reached the north expansion joint and concluded when the back tire reached the southern expansion joint. Data was collected as the truck ran each marked lane and shoulder; then, the data systems would be relocated to the next sensor station, and the entire set of tests run again.

6.3.3 Static Baseline Truckload Test Results

In Figure 6.6, an example set of sensor responses to the static truckload test plan is provided for both an upstream and downstream location (i.e., station 2N). Other sensor responses at other stations provided similar results and allowed verification of all the installed gages.

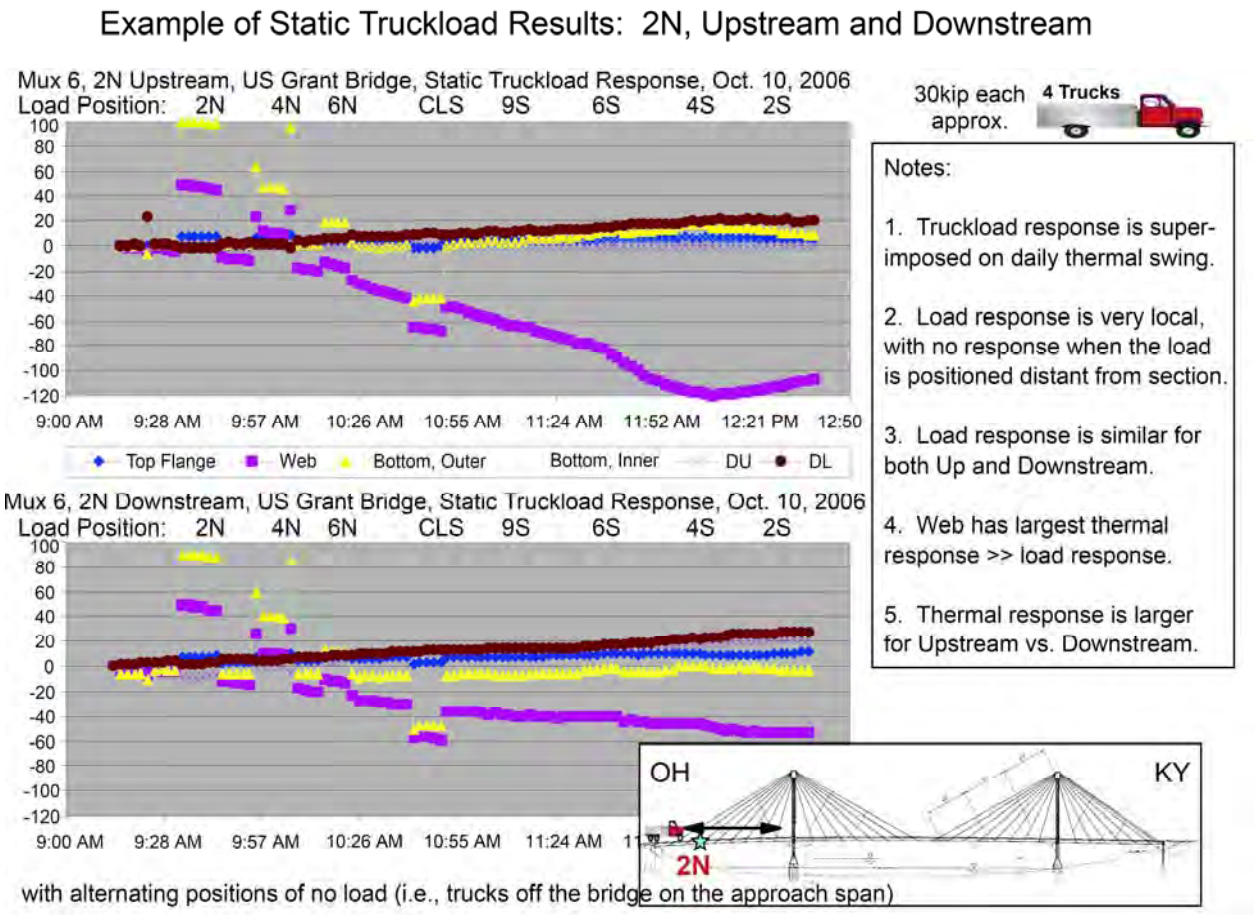

Figure 6.6: Static Truckload Results, Station 2N, USG, 2006 (UCII, 2007)

Some selected strain profiles are plotted in Figure 6.7 in order to illustrate how the structure is clearly acting as a composite section under truckload at all the instrumented stations. Further, you can note that the slope of the measured strain profile is larger than those assumed by the analysis of both the designer HNTB and the erection engineer B&T. If the axial force under truckload is small (as predicted above in Figure 6.1), then this larger slope translates into a larger effective deck width that contributes to sectional strength.

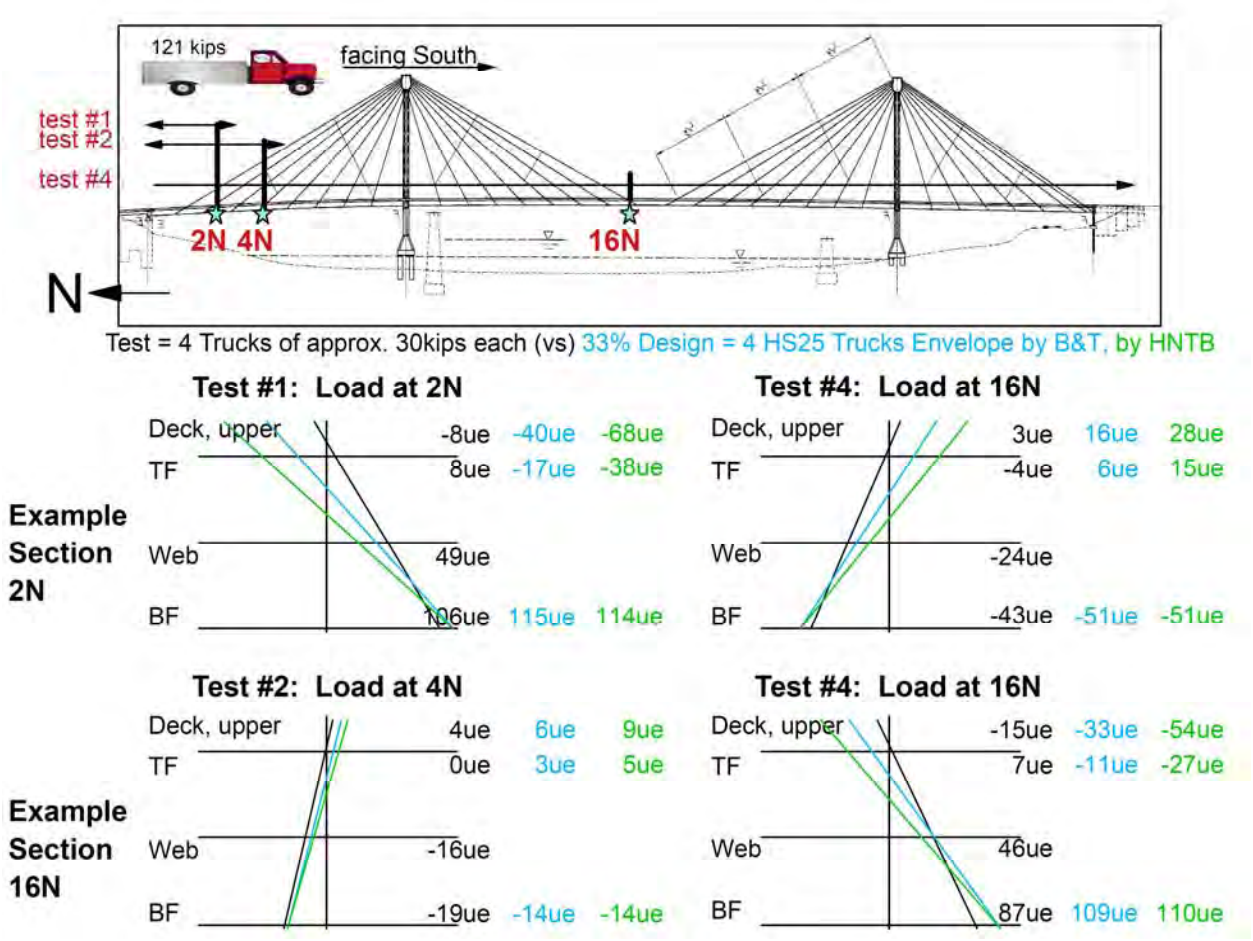

Figure 6.7: Selected Strain Profiles, Truckload Test, USG, 2006 (UCII, 2007)

Table 6.3 provides a summary of the static truckload test results for Upstream gaging, as compared to the results predicted using the liveload design envelope of HNTB and the sectional properties provided by B&T. The columns provide the change in response for the given vibrating wire strain gage between the indicated static truck load position and its subsequent “no load” condition; in this fashion, one removes the thermal effect seen in Figure 6.6. The min and max of these columns is compared to a similar load applied to the B&T section properties of the given instrumented station. Of course, there is some difference simply because the static load positions cannot represent a continuous load influence line to the same spatial resolution as the analysis; however, it provides a ballpark comparison. The moving test is a better comparison.

Upstream	Truckload (34% Design Load) Position										34% Design, No Impact	
Sensor/Segment	2N	4N	6N	16N	9S	6S	4S	2S	Min (ue)	Max (ue)	Min (ue)	Max (ue)
Segment 2N												
Deck Upper	0	0	0	0	0	0	0	0	0	0	-40.5657704	16.2016367
Deck Lower	-1.2	2.1	0.3	0.6	-1.2	-0.2	0.7	0.2	-1.2	2.1		
Top Flange	7.5	5.2	2.6	-4.3	-0.2	0.3	0.9	-0.4	-4.3	7.5	-17.2297581	6.12640932
Web	49.1	11.7	6.7	-23.5	-3.4	-0.9	-4.3	1.3	-23.5	49.1		
Bottom Flange, Outer	99.5	47.9	18.1	-43	-0.2	2.6	4.1	-0.4	-43	99.5	-50.9378865	114.710801
Bottom Flange, Inner	106.1	47.7	18	-41.1	-0.4	2.8	3.1	-0.8	-41.1	106.1		
Segment 4N												
Top Flange	1.8	6.8	4.1	-1.9	-0.1	-0.2	0.5	0.9	-1.9	6.8	-9.13867634	1.13285849
Bottom Flange, Inner	21.1	81.3	20.5	-28.1	-1.3	1.1	0.6	-1.6	-28.1	81.3	-30.3841633	88.2705988
Segment 16N												
Deck Upper	2.9	3.6	2.5	-6.4	0.3	0.3	0.2	-0.6	-6.4	3.6		
Deck Lower	2.2	1.5	0.7	-15.4	0	0.6	0.3	-0.8	-15.4	2.2	-32.863611	6.27612874
Top Flange	-0.4	-0.3	-0.1	7.3	-0.4	-0.7	-1.1	-1.2	-1.2	7.3		
Web	-9.9	-15.8	-6.5	46.1	-4.3	-3.7	-7	-0.5	-15.8	46.1	-11.0844412	3.20263165
Bottom Flange, Outer	-13.1	-16.6	-9.5	83.6	-1.5	-2.6	-3.5	-2.3	-16.6	83.6		
Bottom Flange, Inner	-13.9	-18.5	-10.4	86.7	-1.9	-3.4	-7.4	-4.6	-18.5	86.7	-13.5826766	108.663197
Segment 9S												
Deck Upper	2.4	3.7	1.2	-1.6	-3	-1.1	0.1	-0.4	-3	3.7		
Deck Lower	3.2	4	1.5	-1.3	-0.2	0	0.1	-0.8	-1.3	4	-8.4664065	10.4857035
Top Flange	2.4	2.8	1	-2.9	-2.8	-2.3	-0.8	-0.4	-2.9	2.8		
Web	-1.1	-5.4	0.3	-6.8	-11.3	-10.7	-5.7	-0.6	-11.3	0.3	-3.83878282	2.75014686
Bottom Flange, Outer	0.3	-1.6	1	-4.7	-7.3	-13.6	-4.2	-2.7	-13.6	1		
Bottom Flange, Inner	0.3	-2.5	1.6	-6.1	-12.2	-13.6	-5.6	-3.6	-13.6	1.6	-39.1752085	31.2228443
Segment 4S												
Deck Upper	2.4	3.2	0.4	0.1	0.3	-1.8	-4.8	-0.3	-4.8	3.2		
Deck Lower	1.2	2.2	0.8	-1.3	0.1	1.9	0.9	-0.5	-1.3	2.2	-27.794752	7.26563605
Top Flange	0.5	1	1	-2	-0.4	1.9	3.6	0	-2	3.6		
Web	-5.2	-7.4	0.6	-8.7	-3.5	10.6	23	3.9	-8.7	23	-7.79739883	1.30596658
Bottom Flange, Outer	-7.3	-6.5	2.6	-18.7	-1.2	29.2	71.8	9.1	-18.7	71.8		
Bottom Flange, Inner	-8.7	-8.7	3.4	-17.5	-2.5	28.7	70.7	8.2	-17.5	70.7	-31.6818635	102.639774
Segment 2S												
Deck Upper	4.5	5.4	0.8	0	0.4	3.3	3.8	2.9	0	5.4		
Deck Lower	4.1	5.5	0.5	0.4	0.3	2.2	1.5	0.5	0.3	5.5	-14.8481064	8.06925661
Top Flange	3	4.1	0.9	-1.2	0	0.1	2	0.9	-1.2	4.1		
Web	-10.2	-14	0.7	-6	-2.3	-8.1	-6	12.2	-14	12.2	-4.90049174	2.51295038
Bottom Flange, Outer	-10.9	-10.4	3.6	-7.4	0.9	-10	-0.4	12.3	-10.9	12.3		
Bottom Flange, Inner	-14.9	-14.1	3.6	-7.6	1.2	-11.8	-3.2	17.9	-14.9	17.9	-28.5360195	50.657403
= Bad Sensor												

Table 6.3: Static Truckload Test Results vs Predicted, Upstream, USG, 2006

6.3.4 Dynamic Baseline Truckload Test Results

In Figure 6.8, an example set of sensor responses to the moving truckload test is provided for upstream locations when the truck is driven in the adjacent lane 4 (i.e., the eastern shoulder). Other sensor responses at other stations provided similar results and allowed verification of all the installed gages. Note the balanced peak response of about +40ue ~ 1.16ksi in each span.

The strain profile measured during the moving truck test in the adjacent lane is shown for Station 4S. It clearly shows composite action between the decking and edge girder, as the profile is continuous throughout the section and the neutral axis is near the bottom of the deck. The other stations show similar levels of composite action.

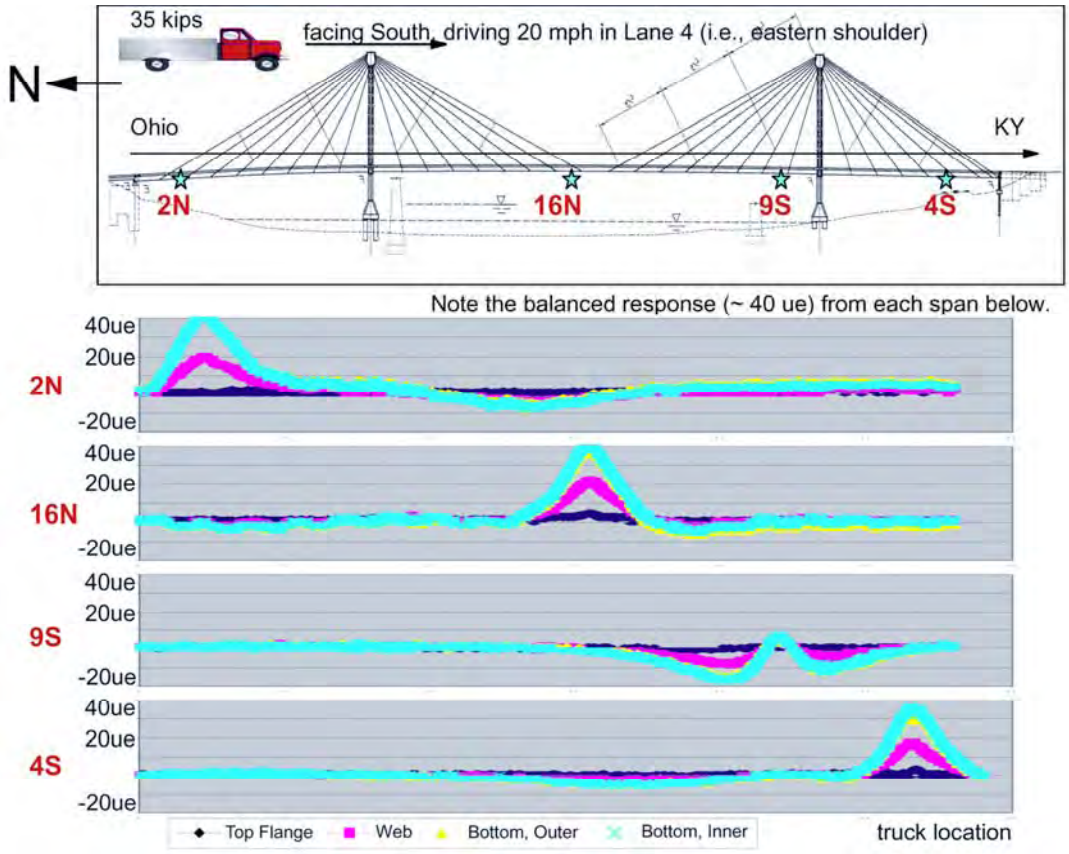

Figure 6.8: Selected Upstream Influence Lines, Truckload Test, USG, 2006 (UCII, 2007)

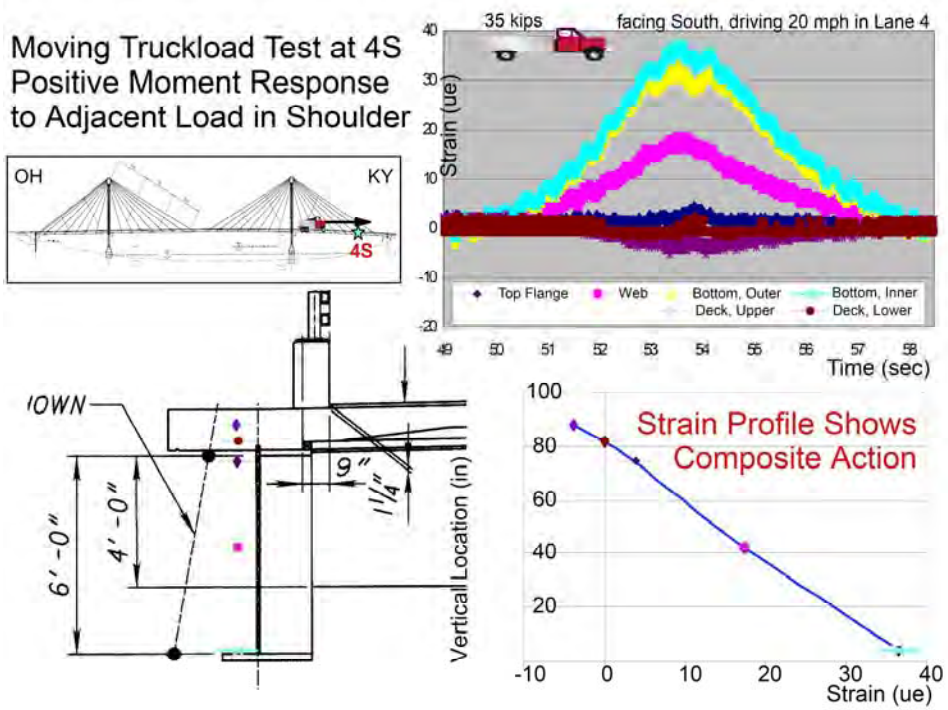

Figure 6.9: Truckload Test, Station 4S, USG, 2006 (UCII, 2007)

Note that, as mentioned earlier, only one truck is used for the moving tests, which obviously causes a much smaller response than if all four trucks are parked near the instrumented section as was done for the static test results. A better comparison to the static load test results would be found in Figure 6.10 which summarizes peak or envelope stress found when summing all four moving test results for a given station, corresponding to each of the marked lanes (and shoulders). This also allows comparison to the predicted liveload response from the design analysis, which is slightly larger than measured results.

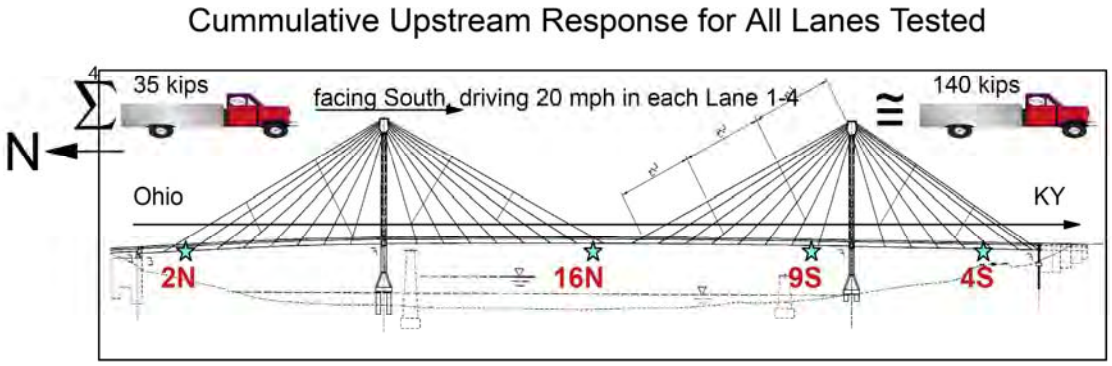

	Measured Test Envelope			39% Design Envelope, Comp.		
2N	TF	-6ue	+17ue	TF	-20ue	+7ue
	BF	-51ue	114ue = 3.3ksi	BF	-58ue	131ue = 3.8ksi
16N	TF	-5ue	+19ue	TF	-13ue	+4ue
	BF	-23ue	110ue = 3.2ksi	BF	-15ue	124ue = 3.6ksi
9S	TF	-10ue	+10ue	TF	-4ue	+3ue
	BF	-48ue	21ue = 0.6ksi	BF	-44ue	36ue = 1.0ksi
4S	TF	-5ue	+18ue	TF	-9ue	+2ue
	BF	-29ue	100ue = 2.9ksi	BF	-36ue	117ue = 3.4ksi

* No impact factor included.

Figure 6.10: Truckload Stress Envelope, Measured vs Design, USG, 2006 (UCII, 2007)

Table 6.4 provides a summary of the moving truckload test results for Upstream gaging, as compared to the results predicted using the liveload design envelope of HNTB and the sectional properties provided by B&T. The columns provide min or max response for the given foil strain gage and the indicated moving truck lane. The min and max of these columns is compared to a similar load applied to the B&T section properties of the given instrumented station. Measured results are slightly less than the conservative predictions of the design analysis. Of course, lane load results for such a monumental structure will control over moving truckload results.

Upstream	Minima (9.67% Design Load)				Maxima (9.67% Design Load)				Total			38.7% Design, No Impact	
Sensor/Segment	Lane 1	Lane 2	Lane 3	Lane 4	Lane 1	Lane 2	Lane 3	Lane 4	Min (ue)	Max (ue)		Min (ue)	Max (ue)
Segment 2N													
Top Flange	-1.79	-1.79	-1.79	-0.60	5.36	4.76	2.38	4.17	-5.95	16.67		-19.6115188	6.97329532
Web	-7.14	-6.55	-7.14	-5.36	10.72	12.50	17.86	20.84	-26.20	61.92			
Bottom Flange, Outer	-14.88	-14.29	-13.10	-8.93	16.07	20.24	33.34	42.27	-51.20	111.93		-57.9793003	130.567882
Bottom Flange, Inner	-13.69	-13.69	-13.10	-8.34	16.67	20.84	33.94	42.27	-48.82	113.71			
Segment 16N													
Top Flange	-1.19	-1.19	-2.38	-0.60	4.76	4.76	3.57	5.95	-5.36	19.05		-12.6167022	3.64534838
Web	-2.98	-2.98	-2.98	-2.98	8.93	11.91	18.46	22.62	-11.91	61.92			
Bottom Flange, Outer	-4.17	-4.76	-5.95	-7.74	13.69	17.86	32.74	39.29	-22.62	103.59		-15.4602819	123.684286
Bottom Flange, Inner	-5.36	-5.36	-5.95	-5.95	14.29	18.46	34.53	42.27	-22.62	109.55			
Segment 9S													
Top Flange	-3.57	-2.98	-1.19	-1.79	1.79	1.79	2.98	2.98	-9.53	9.53		-4.3694381	3.13031422
Web	-5.36	-4.17	-8.93	-9.53	1.79	3.57	3.57	5.95	-27.98	14.88			
Bottom Flange, Outer	-5.36	-8.34	-14.88	-16.67	2.98	2.98	4.17	5.36	-45.25	15.48		-44.590605	35.5389434
Bottom Flange, Inner	-5.36	-8.93	-16.07	-17.86	4.17	3.57	5.36	8.34	-48.22	21.43			
Segment 4S													
Deck Upper	-1.21	-1.21	-3.64	-4.86	3.64	3.64	3.03	3.64	-10.92	13.96		-31.6369678	8.27000338
Deck Lower	-1.21	-1.21	-1.21	-1.82	4.86	4.25	3.03	3.03	-5.46	15.17			
Top Flange	-1.19	-0.60	-1.79	-1.79	5.36	4.76	3.57	4.76	-5.36	18.46		-8.87527455	1.48649725
Web	-4.17	-2.98	-4.17	-3.57	8.93	10.72	15.48	18.46	-14.88	53.58			
Bottom Flange, Outer	-7.14	-6.55	-6.55	-6.55	12.50	16.67	27.98	33.34	-26.79	90.49		-36.0614153	116.828213
Bottom Flange, Inner	-8.34	-7.14	-7.14	-6.55	12.50	17.86	31.55	37.51	-29.17	99.42			
Segment 2S													
Deck Upper	-1.21	-1.82	-1.82	-3.03	3.03	2.43	3.64	3.64	-7.89	12.75		-16.9006388	9.18471267
Deck Lower	-1.82	-1.21	-1.82	-1.82	3.03	3.03	3.03	3.03	-6.68	12.14			
Top Flange	-1.19	-2.98	-1.19	-1.19	3.57	2.98	2.38	2.98	-6.55	11.91		-5.57791265	2.86032881
Web	-2.38	-2.38	-4.76	-5.95	2.98	4.17	6.55	6.55	-15.48	20.24			
Bottom Flange, Outer	-2.38	-3.57	-7.74	-10.12	4.76	5.36	8.93	10.12	-23.81	29.17		-32.4807046	57.6600441
Bottom Flange, Inner	-2.38	-4.17	-7.74	-10.72	4.76	5.36	9.53	11.31	-25.00	30.96			

Table 6.4: Moving Truckload Test Results vs Predicted, Upstream, USG, 2006

For the HS25-44 specification, the laneload is 0.8 kips per linear foot in each marked lane and at least one point load of 22.5 kips is positioned in each lane. The laneload is not necessarily continuous over the length of the structure or even within the length of any given span; the laneload is distributed in order to cause the greatest response for the simulated train of vehicles. For simple span (i.e., noncontinuous) bridges and for positive moment considerations, a single point load is used to determine the maximum liveload response; however, for negative moment evaluation of a continuous bridge design, a second point load (equal in weight to the first point load) is placed in the adjoining span to determine the maximum liveload response.

The HS25 laneload is virtually simulated in each marked traffic lane by linear superposition of the measured truckload influence lines, scaled by each truck's gross weight and normalized to the desired weights mentioned above. For example, the uniform load is calculated by integration over that portion of the truckload response that would actually magnify the moment for the section (i.e., bottom flange stress should be the same sign as the moment for the section). This uniform load is divided by the gross truck weight and then multiplied by 0.8 kips. To this, you would add the effect of at least one point load at the maximum or peak response of the truckload response, again divided by the gross weight and multiplied by 22.5 kips. This would be repeated for all marked lanes for a given station and the results summed together. This process is illustrated in Figure 6.11.

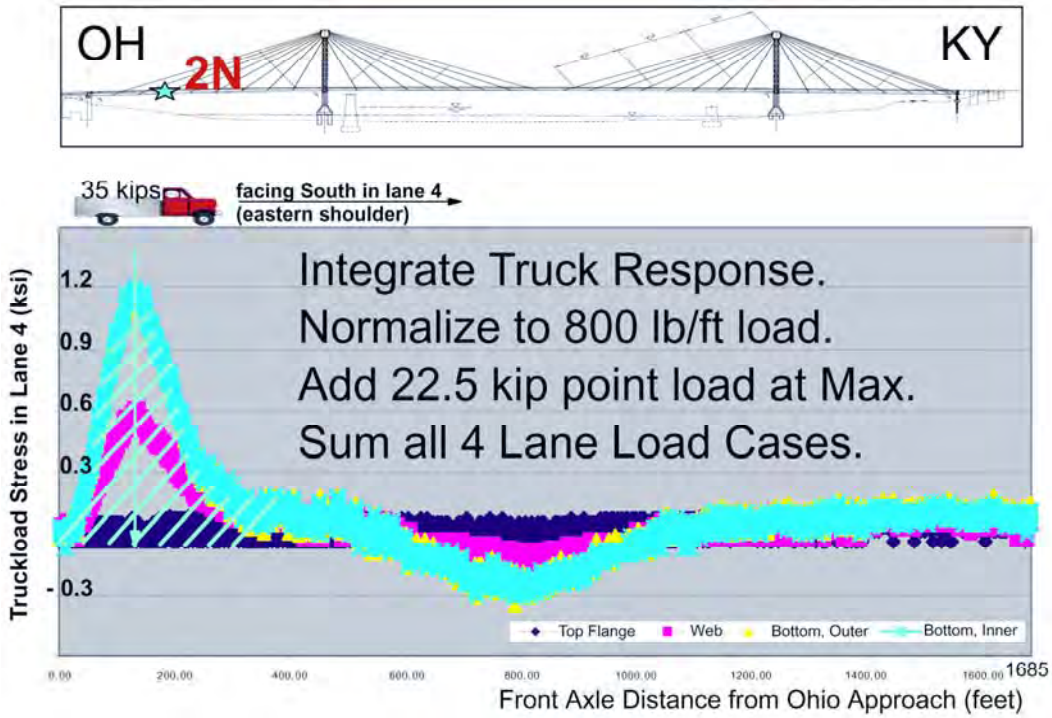

Figure 6.11: How To Calculate Laneload from Moving Test (UCII, 2007)

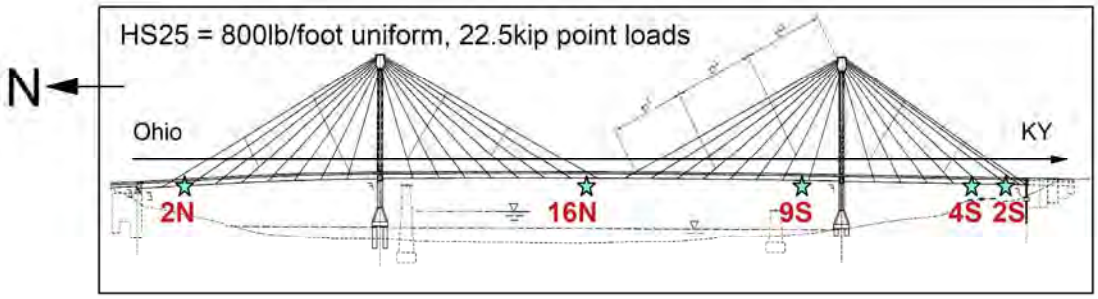

	Envelope from Truck Tests			Design Envelope, Composite		
2N	TF	-0.1ksi	+1.2ksi	TF	-2.6ksi	+1.8ksi
	BF	-9.7ksi	15.8ksi	BF	-15.3ksi	18.1ksi
16N	TF	-0.1ksi	+1.5ksi	TF	-1.7ksi	+0.9ksi
	BF	-2.5ksi	13.6ksi ← 6% larger	BF	-4.3ksi	12.8ksi
9S	TF	-0.4ksi	+0.3ksi	TF	-1.4ksi	+1.0ksi
	BF	-8.3ksi	1.2ksi	BF	-10.8ksi	2.0ksi
4S	TF	-0.1ksi	+1.6ksi	TF	-0.5ksi	+0.3ksi
	BF	-4.8ksi	10.4ksi	BF	-10.1ksi	12.9ksi
2S	TF	-0.1ksi	+0.7ksi	TF	-0.2ksi	+0.5ksi
	BF	-1.9ksi	1.8ksi ← much smaller	BF	-8.9ksi	7.4ksi

* No impact factor included.

Figure 6.12: Laneload Stress Envelope, Measured vs Design, USG, 2006 (UCII, 2007)

Table 6.5 provides a summary of the laneload results for Upstream gaging, as compared to the results predicted using the liveload design envelope of HNTB and the sectional properties provided by B&T. The columns provide the change in response for the given foil strain gage and the indicated truck lane. The min and max of these columns is compared to a similar load applied to the B&T section properties of the given instrumented station. Measured results are slightly less than the conservative predictions of the design analysis with two exceptions.

Compared to design values, the measured results for the middle span (16N) are larger and near the southern abutment (2S) are smaller; the reason for this anomaly (i.e., low rotational stiffness at the Kentucky abutment due to improper installation of the pulldowns) would not become apparent until the bridge was put into service and the Kentucky abutment began to crack; however, this deviation from design is readily apparent from these laneload results.

Upstream	**Minima (Design Load)**				**Maxima (Design Load)**				**Total**			**100% Design, No Impact**	
Sensor/Segment	Lane 1	Lane 2	Lane 3	Lane 4	Lane 1	Lane 2	Lane 3	Lane 4	Min (ue)	Max (ue)		**Min (ue)**	**Max (ue)**
Segment 2N													
Top Flange	-0.03	-0.03	-0.03	-0.01	0.51	0.32	0.06	0.35	-0.11	1.23		-2.56408329	1.83309144
Web	-1.08	-1.03	-0.97	-0.69	1.95	1.90	2.14	2.80	-3.77	8.79			
Bottom Flange, Outer	-2.81	-2.71	-2.53	-1.69	2.68	2.99	4.06	5.86	-9.73	15.60		-15.2631463	18.0821828
Bottom Flange, Inner	-2.66	-2.62	-2.28	-1.81	2.77	3.17	4.12	5.76	-9.37	15.83			
Segment 16N													
Top Flange	-0.02	-0.02	-0.04	-0.01	0.44	0.44	0.20	0.38	-0.10	1.46		-1.67589532	0.93887856
Web	-0.06	-0.06	-0.07	-0.11	1.64	1.42	2.32	2.23	-0.30	7.61			
Bottom Flange, Outer	-0.52	-0.39	-0.51	-1.06	2.33	2.33	3.72	3.84	-2.48	12.23		-4.29600007	12.8147421
Bottom Flange, Inner	-0.39	-0.50	-0.37	-0.99	2.56	2.73	4.30	4.02	-2.25	13.61			
Segment 9S													
Top Flange	-0.17	-0.09	-0.03	-0.06	0.04	0.04	0.06	0.16	-0.35	0.30		-1.40975437	1.00726114
Web	-0.50	-0.29	-1.36	-1.45	0.04	0.48	0.17	0.22	-3.60	0.91			
Bottom Flange, Outer	-0.43	-0.88	-3.24	-3.50	0.09	0.23	0.08	0.18	-8.05	0.58		-9.81845958	1.84013672
Bottom Flange, Inner	-0.40	-1.04	-3.34	-3.53	0.33	0.29	0.17	0.37	-8.31	1.17			
Segment 4S													
Deck Upper	0.07	0.05	0.05	0.05	-0.01	-0.01	-0.09	-0.21	0.23	-0.33		-0.47919301	0.32448698
Deck Lower	0.13	0.11	0.05	0.10	-0.01	-0.01	-0.02	-0.02	0.40	-0.07			
Top Flange	-0.02	-0.01	-0.03	-0.03	0.32	0.49	0.26	0.58	-0.10	1.64		-0.50022692	0.13276775
Web	-0.44	-0.40	-0.28	-0.24	0.87	0.86	1.43	1.62	-1.36	4.78			
Bottom Flange, Outer	-1.35	-1.05	-1.08	-0.89	1.37	1.93	2.72	3.44	-4.38	9.46		-10.0719162	12.8588484
Bottom Flange, Inner	-1.41	-1.26	-1.18	-0.93	1.53	1.95	3.09	3.85	-4.78	10.42			
Segment 2S													
Deck Upper	0.15	0.13	0.10	0.26	-0.02	-0.03	-0.03	-0.05	0.65	-0.12		-0.26421137	0.35696803
Deck Lower	0.10	0.06	0.14	0.14	-0.03	-0.02	-0.03	-0.03	0.44	-0.10			
Top Flange	-0.02	-0.06	-0.02	-0.02	0.08	0.33	0.16	0.08	-0.13	0.66		-0.2436984	0.49045895
Web	-0.04	-0.05	-0.29	-0.46	0.09	0.16	0.35	0.29	-0.84	0.89			
Bottom Flange, Outer	-0.05	-0.11	-0.56	-0.90	0.27	0.36	0.57	0.61	-1.61	1.81		-8.91638885	7.39850258
Bottom Flange, Inner	-0.06	-0.17	-0.64	-1.04	0.25	0.26	0.62	0.57	-1.90	1.71			

Table 6.5: Laneload Test Results vs Predicted, Upstream, USG, 2006

6.3.5 Baseline Test Conclusions and Recommendations

Upstream and downstream edge girders have comparable response to truckload; however, the thermal response for some gages (e.g., web) dwarfs the liveload response. Composite action is clearly evident in all test results, with a greater slope in the strain profile and hence large effective deck width than predicted by analysis. Laneload results control over the truckload results and are used as the liveload response in the rating analysis of the structure. Measured results are slightly less than the conservative predictions of the design analysis, with two exceptions at the middle span and Kentucky abutment. These locations should be especially observed during inspection for unexpected signs of distress.

6.4 Service Testing, 2009, After Initial Repairs, Prior to Pulldowns

After the bridge was opened to service in 2006, the Kentucky abutment and backwall began to exhibit cracking that started near the beam seat (see Figure 6.13) but became pervasive with increasing length and width over each subsequent inspection. It was believed that the source of this degradation was field modification to the location and installation of the steel pulldowns internal to the abutment. ODOT provided for immediate field rehabilitation of this installation, including the use of additional welding at the beam seat to resist further movement, which seemed to abate further cracking at the abutment. UCII then subsequently conducted another truckload test in order to observe/validate the effectiveness of the rehab and compare with expected design values.

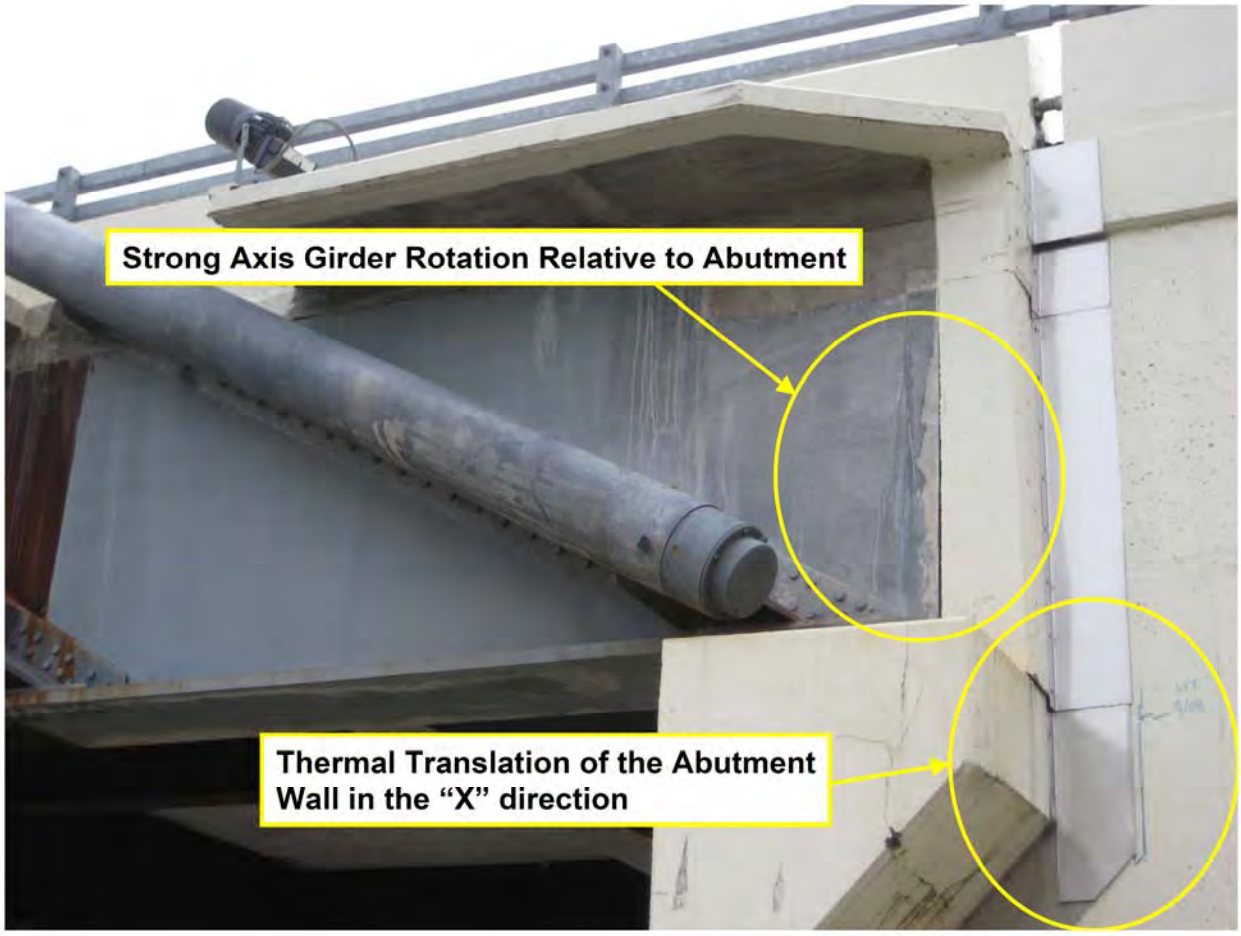

Figure 6.13 Deterioration of the Kentucky Abutment in Service

6.4.1 Baseline Test Design

The first step for the static truck load test was to design a set of truck positions or load cases for the bridge. Four standard salt trucks were again used, as shown in Table 6.6. As illustrated in Table 6.7, a total of thirteen truck positions were selected. A number of objectives for the truck load test were used to select the positions, but primarily to locate the trucks side-by-side in the two marked traffic lanes and two shoulders, at each instrumented station. These load cases would be staggered with "no load" cases, where the trucks would be moved off the bridge.

Static Truckload Test of US Grant Bridge, March 27, 2009								
Truck#	Position	Lane#	Ft Axle (lbs)	Back Axle (lbs)	Total Wt (lbs)	Tire, Axle Spaces, Axle Space (f		Back Tire Space
569	DS, shoulder	1	14400	31900	49800	178	53	73
671	DS, lane	2	11500	25600	39800	178	53	73
695	US, lane	3	14700	31700	49200	178	53	73
742	US, shoulder	4	15700	32000	49100	178	53	73
Total			56300	121200	187900			
4 HS25			40000	320000	360000	1.91591272	52.19%	Ratio of Test Lo

Table 6.6: Truck Specifications Used in Static Test Plan, 2009

Test#	Time Start	Position	Time End	Notes
1	10:47	OH Apprch	10:55	No load condition
2	10:56	2N	11:04	Back axle located adjacent to stay where it exits the deck
3	11:05	OH Apprch	11:11	No load condition
4	11:13	4N	11:21	Back axle located adjacent to stay where it exits the deck
5	11:22	OH Apprch	11:28	No load condition
6	11:31	16N	11:39	Back axle located adjacent to stay where it exits the deck
7	11:43	OH Apprch	11:49	No load condition, backhoe drove across bridge in DS lane
8	11:51	9S	12:00	Back axle located adjacent to stay where it exits the deck
9	12:01	KY Apprch	12:08	No load condition, backhoe drove across bridge in DS lane
10	12:10	4S	12:18	Back axle located adjacent to stay where it exits the deck
11	12:19	KY Apprch	12:25	No load condition
12	12:28	2S	12:36	Back axle located adjacent to stay where it exits the deck
13	12:44	OH Apprch		No load condition

Table 6.7: Static Truckload Test Plan, 2009

The instrumentation scheme for the truck load test consisted of strain gages installed on the bridge during construction. Each location includes both a vibrating wire gage for slow-speed reading of long-term behavior without drift, and a traditional foil gage for high-speed reading of short liveload response. The stations of the sensors are listed on the right side of Figure 3.8.

6.4.2 Conduct of Testing

The Ohio Department of Transportation provided four tandem-axle dump trucks that were used to conduct the truck load test. Tandem-axle dump trucks were requested because, when fully loaded, they are typically much heavier than their single rear axle counterpart. The truck weight is important because it should be sufficient to cause sensor readings that are above noise levels.

Two data acquisition systems were used during the test because a combination of high speed and low speed (vibrating wire) sensors were used for the test. Several Campbell Scientific CR-10X data logger systems were used to power and read the vibrating wire based gages and two Optim MEGADAC data acquisition system was used to power and read the high-speed sensors.

The moving truckload tests were conducted after the static tests, throughout the remainder of the afternoon. Truck #569 was selected and the other trucks were returned to the garage. One person with a walkie-talkie took the passenger seat of the truck. The truck driver was to start north of the bridge, accelerate to a speed of about 20mph, center the truck in the test lane, and maintain that speed (and lane) for the entire length of the bridge. Upon reaching the south abutment, the truck would immediately brake to stop short of the intersection just south of the bridge. Two high-speed data acquisition systems were deployed at the northern sensor station (i.e., 2N). Data collection at 200Hz was manually triggered to commence as the front tire reached the north expansion joint and concluded when the back tire reached the southern expansion joint. Data was collected as the truck ran each marked lane and shoulder; then, the data systems would be relocated to the next sensor station, and the entire set of tests run again.

6.4.3 Dynamic Truckload Test Results, 2009, Prior to Pulldowns

In Figure 6.15, an example set of sensor responses to the moving truckload test is provided for upstream locations when the truck is driven in the adjacent lane 4 (i.e., the eastern shoulder). The blue lines represent the measured results from 2006, while the green lines are the scaled results from 2009 to account for the lighter trucks used in 2006. Other sensor responses at other stations provided similar results and allowed verification of all the installed gages, as well as verification of structural behavior consistent with the 2006 baseline. Any deviation observed in these plots on the X axis (i.e., distance of the front axle of the truck from the Ohio abutment) is due to variation in the truck speed and not from a change in structural behavior.

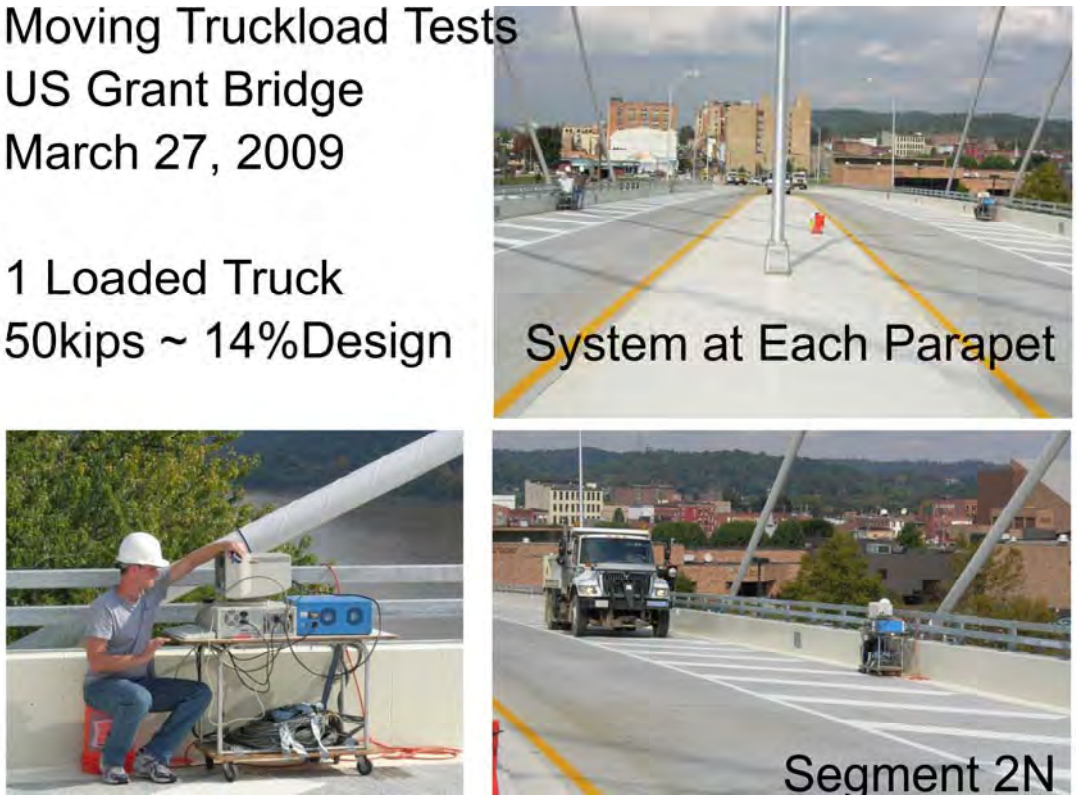

Figure 6.14: Pictures of the Truckload Test, USG, 2009 (UCII, 2009)

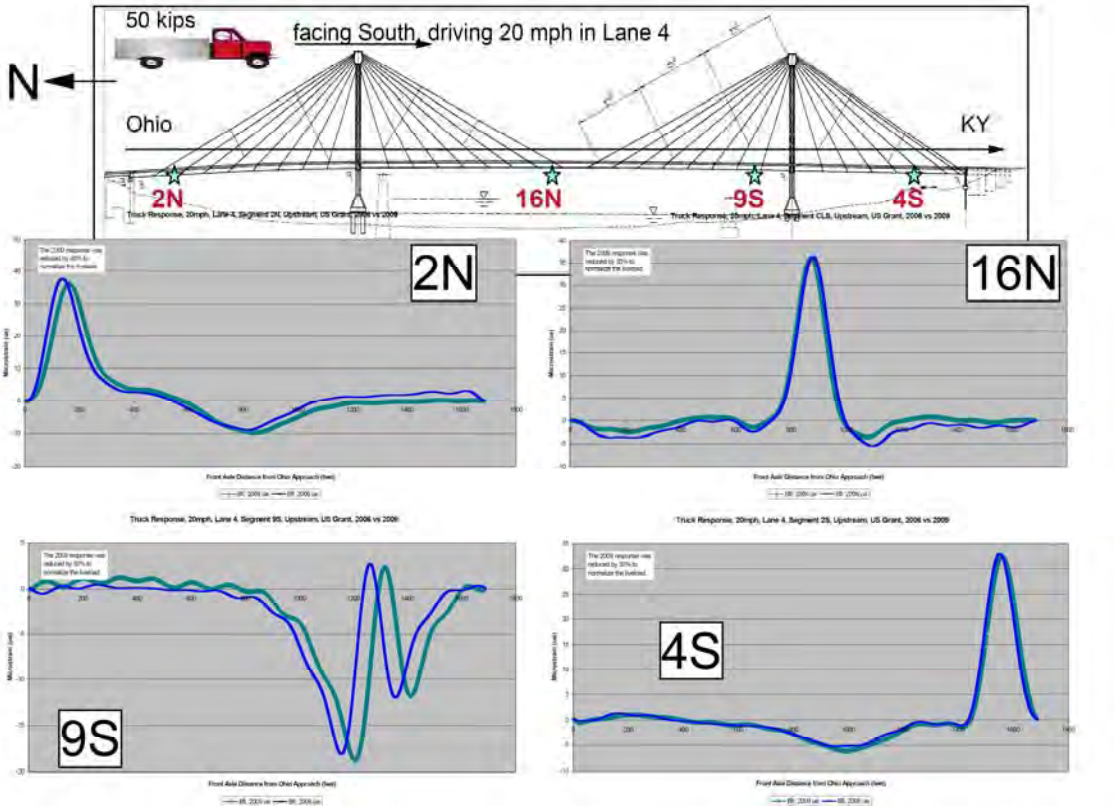

Figure 6.15: Upstream Influence Lines, Truckload Test, USG, 2006 vs 2009 (UCII, 2009)

A significant change in the truck response was observed near the Kentucky abutment (see Figure 6.16). The post-rehab influence line exhibits a more pronounced middle span response and an increased tensile bias in the Kentucky endspan, as compared to the baseline results.

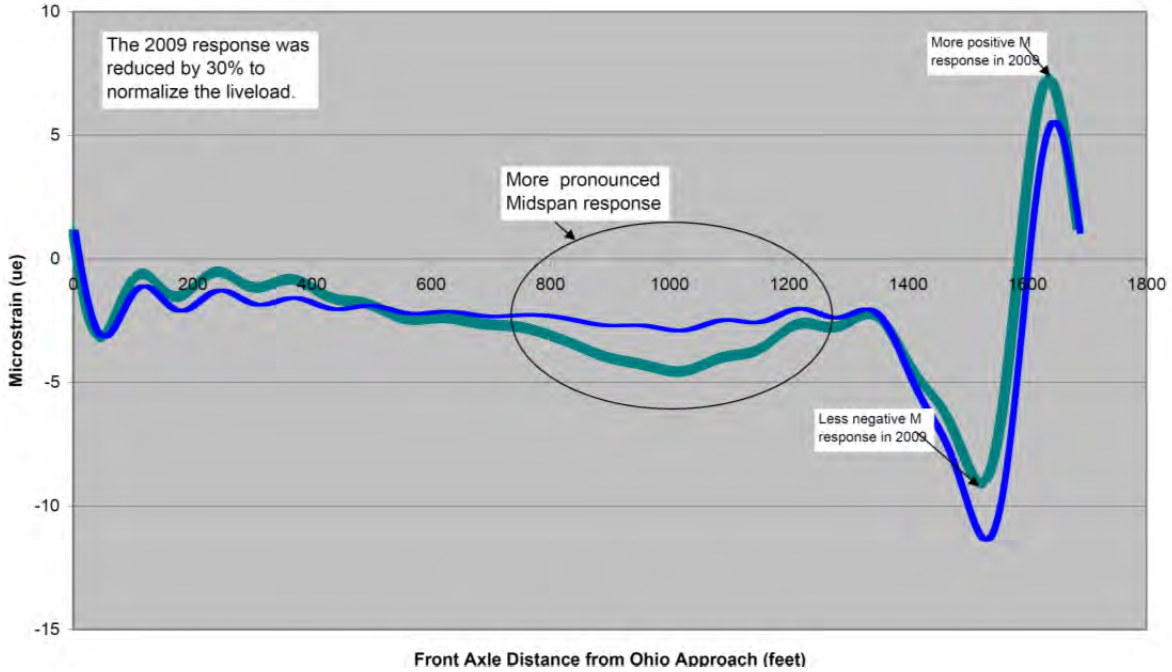

Figure 6.16: Abutment Influence Lines, Truckload Test, USG, 2006 vs 2009 (UCII, 2009)

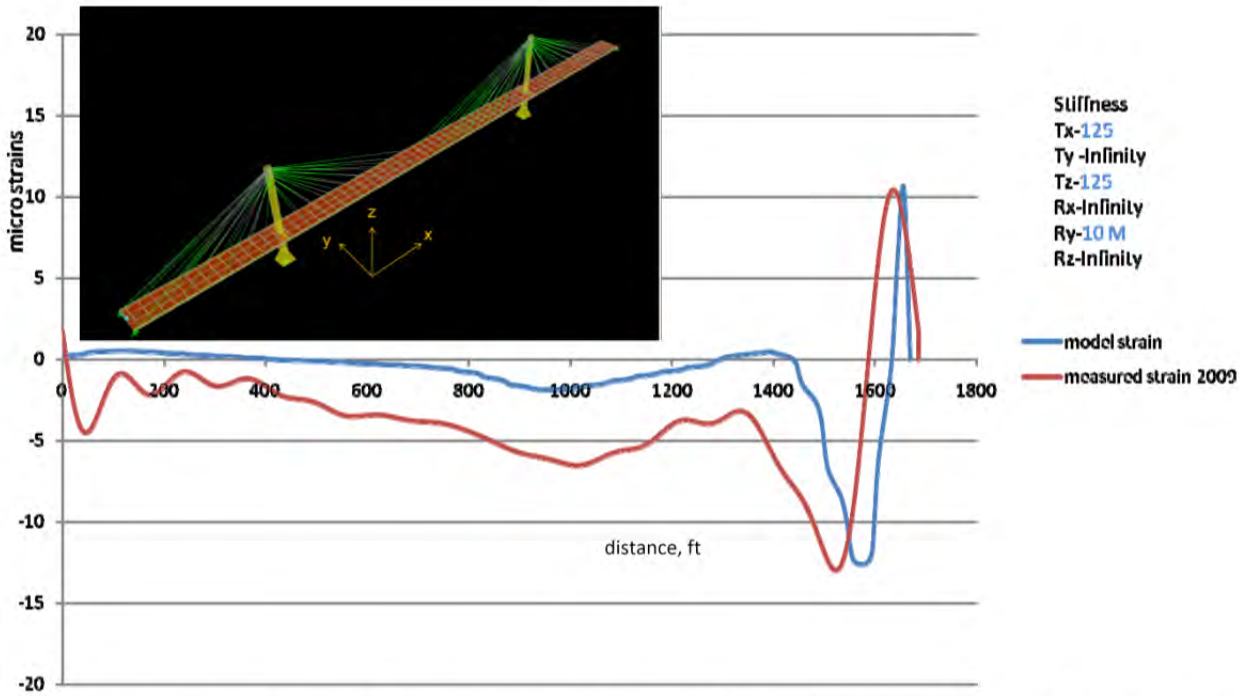

Note: Notice the value of Ry, supports are 10 times more stiff than previously.

Figure 6.17: Rotational Stiffness, Kentucky Abutment, USG, 2006 vs 2009, (UCII, 2009)

This change to the influence line was considered further using a series of calibrations to our finite element model. Compared to baseline test results, the measured results for the middle span (16N) have been reduced and the southern abutment (2S) results are larger; the reason for this change is the rehabilitation of the pulldowns done by ODOT (i.e., x10 increased rotational stiffness at the Kentucky abutment, as determined by UCII finite element model calibrated to the measured truckload influence lines in 2006 and 2009, see Figure 6.17).

The strain profile measured during the moving truck test in the adjacent lane is shown for several selected Upstream stations in Figure 6.18. It clearly shows composite action between the decking and edge girder, as the profile is continuous throughout the section and the neutral axis is near the bottom of the deck. The other stations show similar levels of composite action.

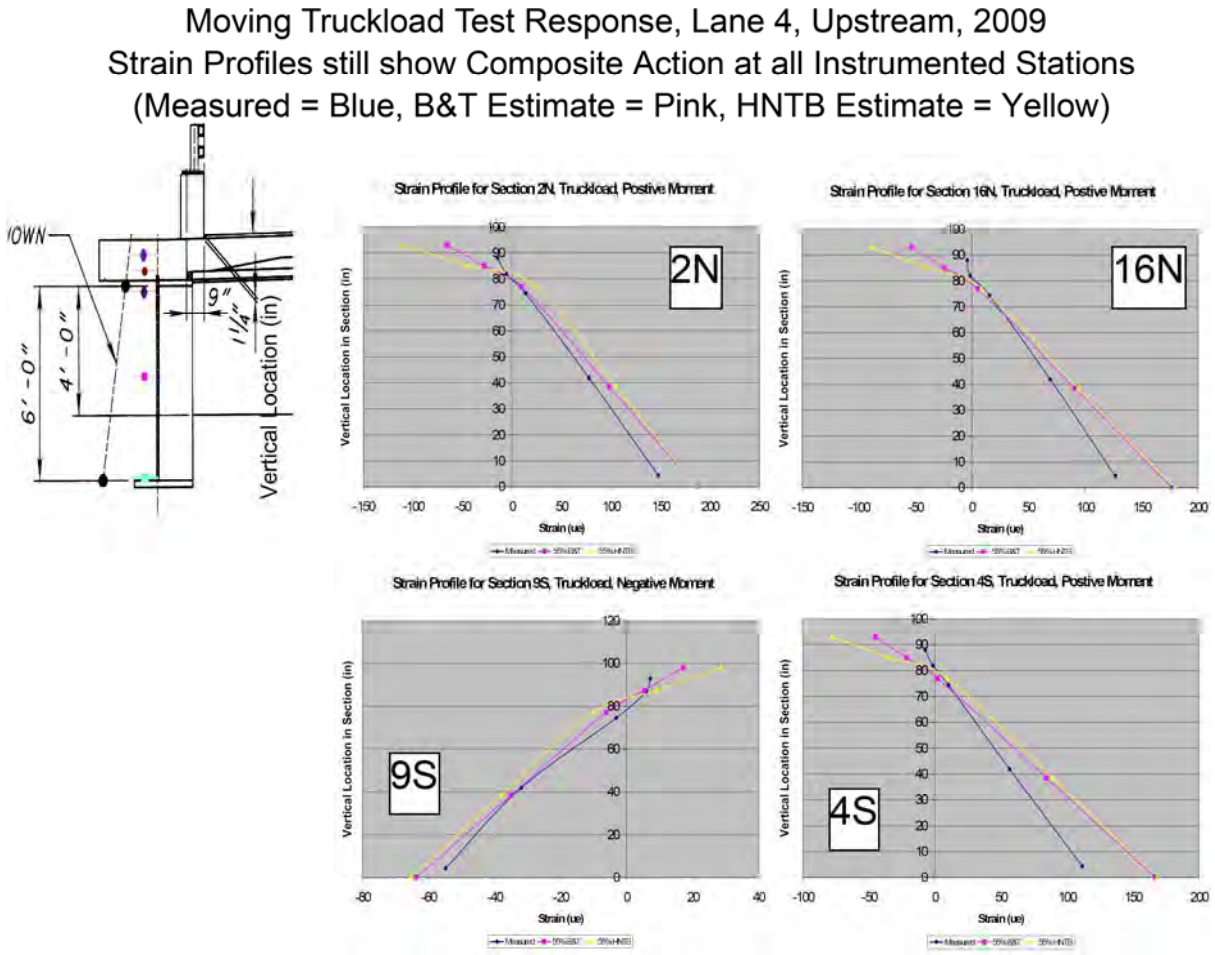

Figure 6.18: Selected Strain Profiles, Truckload Test, USG, 2009 (UCII, 2009)

Note that, as mentioned earlier, only one truck is used for the moving tests, which obviously causes a much smaller response than if all four trucks are parked near the instrumented section as was done for the static test results. A better comparison to the design predictions would be found in Figure 6.19 which summarizes peak or envelope stress found when summing all four moving test results for a given station, corresponding to each of the marked lanes (and shoulders). Measured results are equal to or slightly less than the conservative predictions of the design analysis.

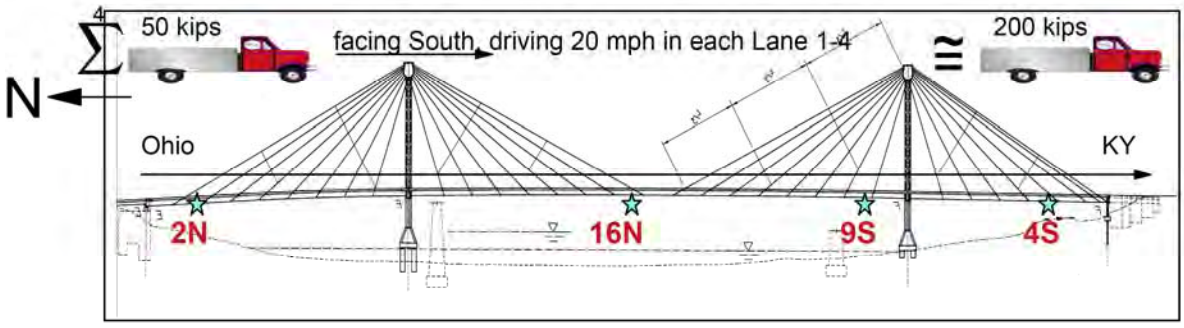

	Measured Test Envelope			55% B&T Design Envelope, Comp.		
2N	TF	-3ue	+15ue	TF	-28ue	+10ue
	BF	-62ue	149ue = 4.3ksi	BF	-83ue	187ue = 5.4ksi
16N	TF	-2ue	+17ue	TF	-18ue	+5ue
	BF	-21ue	132ue = 3.8ksi	BF	-22ue	177ue = 5.1ksi
9S	TF	-4ue	+3ue	TF	-6ue	+4ue
	BF	-64ue	10ue -1.9ksi	BF	-64ue	51ue -1.9ksi
4S	TF	-4ue	+11ue	TF	-12ue	+2ue
	BF	-40ue	122ue = 3.5ksi	BF	-52ue	167ue = 4.8ksi

* No impact factor included.

Figure 6.19: Truckload Stress Envelope, Measured vs Design, USG, 2009 (UCII, 2009)

Table 6.8 provides a summary of the moving truckload test results for Upstream gaging, as compared to the results predicted using the liveload design envelope of HNTB and the sectional properties provided by B&T. The columns provide min or max response for the given foil strain gage and the indicated moving truck lane. The min and max of these columns is compared to a similar load applied to the B&T section properties of the given instrumented station. Measured results are slightly less than the conservative predictions of the design analysis. Of course, lane load results for such a monumental structure will control over moving truckload results.

Upstream	**Minima (13.8% Design Load)**				**Maxima (13.8% Design Load)**				**Total**			**55.32% Design, No Impact**	
Sensor/Segment	Lane 1	Lane 2	Lane 3	Lane 4	Lane 1	Lane 2	Lane 3	Lane 4	Min (ue)	Max (ue)		**Min (ue)**	**Max (ue)**
Segment 2N													
Deck Upper	-0.34	-0.34	-6.36	-8.36	2.43	1.97	1.73	1.40	-15.40	7.53		-66.0028947	26.3610159
Deck Lower	-0.53	-0.38	-2.17	-3.47	2.62	1.93	0.43	0.16	-6.55	5.14			
Top Flange	-0.89	-0.86	-0.24	-0.60	5.29	4.46	2.51	2.38	-2.59	14.65		-28.03383	9.96802834
Web	-9.68	-8.31	-7.72	-7.32	13.15	16.48	23.75	25.40	-33.03	78.78			
Bottom Flange, Outer	-18.05	-15.33	-14.20	-13.91	21.22	27.83	47.52	52.22	-61.49	148.80		-82.8789378	186.641221
Bottom Flange, Inner	-18.46	-15.50	-14.33	-13.98	21.25	28.35	47.28	51.65	-62.27	148.53			
Segment 16N													
Deck Upper	-0.46	-0.67	-1.53	-2.48	2.01	1.22	0.43	0.78	-5.13	4.45		-53.4710283	10.2116306
Deck Lower	-0.69	-0.42	-0.45	-0.83	3.30	3.38	2.79	1.90	-2.39	11.36			
Top Flange	-0.71	-0.37	-0.22	-0.80	4.13	4.35	4.27	3.85	-2.10	16.60		-18.0350378	5.21087008
Web	-1.93	-1.80	-2.66	-1.59	9.45	12.99	21.82	25.96	-7.98	70.23			
Bottom Flange, Outer	-4.69	-5.01	-5.02	-5.17	13.68	21.48	42.38	50.33	-19.88	127.86		-22.0998139	176.801413
Bottom Flange, Inner	-4.85	-5.21	-5.43	-5.20	15.17	22.47	43.25	51.53	-20.69	132.42			
Segment 9S													
Deck Upper	-0.85	-0.52	-0.62	-0.29	1.14	1.11	2.56	3.38	-2.28	8.19		-13.7753414	17.0608563
Deck Lower	-1.54	-1.89	-0.75	-0.63	1.20	0.90	2.34	2.47	-4.81	6.91			
Top Flange	-1.02	-1.23	-1.22	-0.68	1.33	0.31	0.13	0.83	-4.15	2.60		-6.24592546	4.47465072
Web	-3.18	-5.38	-11.15	-13.21	1.56	1.64	1.45	2.19	-32.91	6.84			
Bottom Flange, Outer	-3.34	-7.92	-20.43	-24.13	2.00	1.59	0.96	2.26	-55.83	6.80		-63.7403687	50.8014043
Bottom Flange, Inner	-4.51	-9.58	-22.88	-26.76	2.66	1.77	1.74	3.46	-63.73	9.65			
Segment 4S													
Deck Upper	-0.21	-0.14	-3.33	-4.65	2.31	0.43	0.83	0.94	-8.33	4.50		-45.2236966	11.8216172
Deck Lower	-1.61	-0.36	-0.35	-0.33	2.81	2.89	0.22	1.56	-2.65	7.48			
Top Flange	-1.57	-0.77	-1.34	-0.24	3.75	3.73	2.05	1.72	-3.92	11.25		-12.6868266	2.12488445
Web	-5.02	-4.29	-4.59	-3.81	8.12	11.05	17.90	20.46	-17.71	57.52			
Bottom Flange, Outer	-9.33	-9.70	-9.51	-8.62	14.31	19.14	36.70	42.43	-37.16	112.58		-51.5482556	167.00095
Bottom Flange, Inner	-10.12	-10.19	-10.20	-9.28	15.60	21.20	39.74	45.76	-39.80	122.29			
Segment 2S													
Deck Upper	-0.63	-0.40	-0.79	-1.41	1.28	0.41	1.96	2.71	-3.23	6.36		-24.1587426	13.1291552
Deck Lower	-0.86	-0.35	-0.07	-0.59	1.34	0.48	0.57	1.90	-1.89	4.29			
Top Flange	-0.75	-1.77	-0.17	-0.58	2.03	0.85	0.29	0.92	-3.26	4.09		-7.97338832	4.08871809
Web	-2.36	-2.42	-6.38	-7.95	1.74	1.91	2.76	3.63	-19.12	10.04			
Bottom Flange, Outer	-3.37	-4.59	-10.66	-12.98	3.86	3.16	6.78	8.98	-31.59	22.78		-46.4297824	82.4225746
Bottom Flange, Inner	-3.83	-4.63	-11.75	-14.48	3.58	3.35	6.58	8.88	-34.70	22.38			

Table 6.8: Moving Truckload Test Results vs Predicted, Upstream, USG, 2009

Table 6.9 and Figure 6.20 provide a summary of the laneload results for Upstream gaging, as compared to the results predicted using the liveload design envelope of HNTB and the sectional properties provided by B&T. The columns provide the change in response for the given foil strain gage and the indicated truck lane. The min and max of these columns is compared to a similar load applied to the B&T section properties of the given instrumented station. Measured results are slightly less than the conservative predictions of the design analysis.

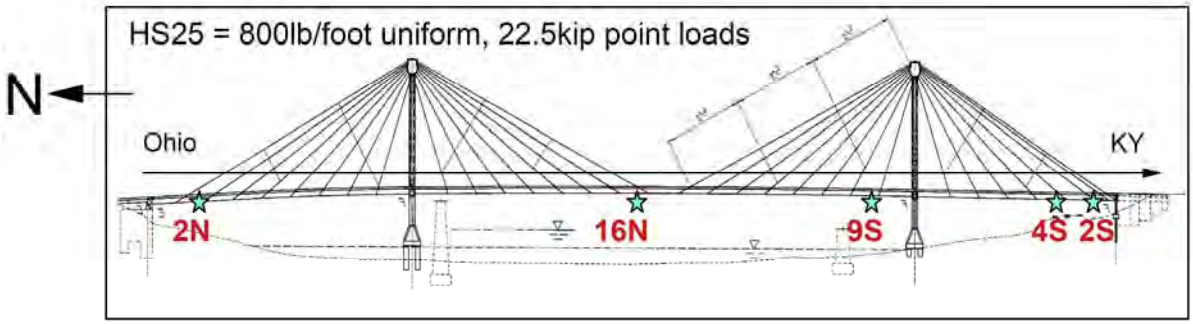

	Envelope from Truck Tests			Design Envelope, Composite		
2N	TF	-0.2ksi	+1.8ksi	TF	-2.6ksi	+1.8ksi
	BF	-10.6ksi	15.7ksi	BF	-15.3ksi	18.1ksi
16N	TF	-0.1ksi	+1.3ksi	TF	-1.7ksi	+0.9ksi
	BF	-3.6ksi	10.4ksi	BF	-4.3ksi	12.8ksi
9S	TF	-0.2ksi	+0.2ksi	TF	-1.4ksi	+1.0ksi
	BF	-8.9ksi	1.3ksi	BF	-10.8ksi	2.0ksi
4S	TF	-0.4ksi	+0.9ksi	TF	-0.5ksi	+0.3ksi
	BF	-7.6ksi	9.6ksi	BF	-10.1ksi	12.9ksi
2S	TF	-0.4ksi	+0.1ksi	TF	-0.2ksi	+0.5ksi
	BF	-8.8ksi	1.3ksi ← large change from 2006	BF	-8.9ksi	7.4ksi

* No impact factor included.

Figure 6.20: Laneload Stress Envelope, Measured vs Design, USG, 2009 (UCII, 2009)

Upstream	Minima (Design Load)				Maxima (Design Load)				Total			100% Design, No Impact	
Sensor/Segment	Lane 1	Lane 2	Lane 3	Lane 4	Lane 1	Lane 2	Lane 3	Lane 4	Min (ue)	Max (ue)		Min (ue)	Max (ue)
Segment 2N													
Deck Upper	0.17	0.15	0.12	0.08	0.00	0.00	-0.25	-0.33	0.52	-0.58		-1.02209353	0.79799772
Deck Lower	0.10	0.05	0.00	0.00	0.00	0.00	-0.07	-0.11	0.15	-0.19			
Top Flange	-0.21	-0.01	0.00	-0.01	0.56	0.53	0.39	0.28	-0.23	1.77		-2.56408329	1.83309144
Web	-1.43	-1.41	-1.27	-1.16	1.75	1.85	2.24	2.44	-5.26	8.28			
Bottom Flange, Outer	-2.90	-2.58	-2.35	-2.33	3.05	3.27	4.62	4.94	-10.16	15.89		-15.2631463	18.0821828
Bottom Flange, Inner	-3.04	-2.79	-2.45	-2.34	3.04	3.25	4.53	4.85	-10.63	15.67			
Segment 16N													
Deck Upper	0.07	0.05	0.00	0.01	0.00	0.00	-0.04	-0.08	0.13	-0.13		-0.7098797	0.30941724
Deck Lower	0.13	0.14	0.13	0.07	0.00	0.00	0.00	-0.01	0.47	-0.02			
Top Flange	-0.01	-0.01	-0.01	-0.01	0.28	0.32	0.34	0.31	-0.04	1.25		-1.67589532	0.93887856
Web	-0.35	-0.17	-0.55	-0.12	0.89	1.17	1.58	1.85	-1.20	5.50			
Bottom Flange, Outer	-0.79	-0.82	-1.22	-0.76	1.45	2.02	3.11	3.49	-3.58	10.07		-4.29600007	12.8147421
Bottom Flange, Inner	-0.71	-0.87	-1.26	-0.79	1.61	2.09	3.14	3.59	-3.63	10.44			
Segment 9S													
Deck Upper	0.05	0.03	0.16	0.20	-0.01	0.00	0.00	0.00	0.44	-0.02		-0.28157575	0.45244545
Deck Lower	0.09	0.01	0.07	0.07	-0.20	-0.23	-0.01	0.00	0.23	-0.45			
Top Flange	-0.04	-0.07	-0.09	-0.02	0.17	0.00	0.00	0.01	-0.22	0.19		-1.40975437	1.00726114
Web	-0.43	-0.75	-1.45	-1.84	0.28	0.30	0.04	0.12	-4.47	0.74			
Bottom Flange, Outer	-0.37	-1.06	-3.02	-3.61	0.24	0.14	0.01	0.17	-8.07	0.57		-9.81845958	1.84013672
Bottom Flange, Inner	-0.50	-1.36	-3.22	-3.84	0.50	0.29	0.13	0.33	-8.91	1.25			
Segment 4S													
Deck Upper	0.07	0.00	0.01	0.01	0.00	0.00	-0.11	-0.15	0.09	-0.27		-0.47919301	0.32448698
Deck Lower	0.10	0.11	0.00	0.05	-0.10	0.00	0.00	0.00	0.27	-0.11			
Top Flange	-0.25	-0.01	-0.11	0.00	0.30	0.29	0.20	0.13	-0.38	0.92		-0.50022692	0.13276775
Web	-1.00	-0.62	-0.84	-0.56	0.72	0.96	1.25	1.46	-3.03	4.39			
Bottom Flange, Outer	-1.59	-1.70	-1.83	-1.59	1.58	1.75	2.62	3.23	-6.71	9.19		-10.0719162	12.8588484
Bottom Flange, Inner	-1.90	-1.84	-2.05	-1.77	1.55	1.93	2.83	3.34	-7.55	9.64			
Segment 2S													
Deck Upper	0.03	0.00	0.05	0.09	0.00	0.00	-0.01	-0.03	0.18	-0.04		-0.26421137	0.35696803
Deck Lower	0.03	0.00	0.00	0.06	-0.01	0.00	0.00	0.00	0.10	-0.01			
Top Flange	-0.02	-0.37	0.00	-0.01	0.11	0.01	0.00	0.01	-0.40	0.14		-0.2436984	0.49045895
Web	-0.74	-0.90	-1.78	-2.24	0.08	0.09	0.13	0.17	-5.67	0.47			
Bottom Flange, Outer	-0.50	-1.34	-2.57	-2.86	0.35	0.16	0.34	0.44	-7.26	1.29		-8.91638885	7.39850258
Bottom Flange, Inner	-0.80	-1.36	-3.18	-3.48	0.33	0.17	0.32	0.43	-8.83	1.25			

Table 6.9: Laneload Test Results vs Predicted, Upstream, USG, 2009

6.4.4 Service Test, 2009, Prior to Pulldowns, Conclusions and Recommendations

Upstream and downstream edge girders have comparable response to truckload; however, the thermal response for some gages (e.g., web) dwarfs the liveload response. Composite action is clearly evident in all test results, with a greater slope in the strain profile and hence large effective deck width than predicted by analysis. Laneload results control over the truckload results and are used as the liveload response in the rating analysis of the structure. After rehab of the Kentucky abutment, measured results are now equal to or slightly less than the conservative predictions of the design analysis.

6.5 Service Testing, 2012, After Pulldown and Rehabilitation

A major rehabilitation of the Kentucky abutment pulldowns was conducted in 2011 in order to further examine, stiffen, and provide redundancy in the form of structural strands exterior to the abutment affixed to the edge girders and secured with rock anchors (see Figure 6.21). HNTB designed the rehab and Brayman contracted the work. UCII installed additional instrumentation which are detailed in Chapter 7, along with any monitoring and truckload test results of same. A follow-up truckload test was conducted for comparison with previous test results, for verification of the continued performance of the structure and its new pulldowns, as well as to document the new baseline liveload response of the bridge.

Figure 6.21: Pulldown Rehab at Kentucky Abutment, USG, 2011

6.5.1 Baseline Test Design

The first step for the static truck load test was to design a set of truck positions or load cases for the bridge. Four standard salt trucks were used, as shown in Table 6.10. As illustrated in Table 6.11, a total of seventeen truck positions were selected. A number of objectives for the truck load test were used to select the positions, but primarily to locate the trucks side-by-side in the two marked traffic lanes and two shoulders, at each instrumented station. These load cases would be staggered with “no load” cases, where the trucks would be moved off the bridge.

Static Truckload Test of US Grant Bridge, October 16, 2012								
Truck#	Position	Lane#	Ft Axle (lbs)	Back Axle (lbs)	Total Wt (lbs)	Tire, Axle Spaces, Axle Space (		Back Tire Space
802	DS, shoulder	1	13840	38080	52400	178	53	73
856	DS, lane	2	13540	38420	52540	178	53	73
695	US, lane	3	19940	36960	52480	178	53	73
778	US, shoulder	4	13920	39680	54360	178	53	73
Total			61240	153140	211780			
4 HS25			40000	320000	360000	1.699877231	58.83%	Ratio of Test Lo
4 HS20			32000	256000	288000	1.359901785	73.53%	Ratio of Test Lo

Table 6.10: Truck Specifications Used in Static Test Plan, 2012

Test#	Time Start	Position	Time End	Notes
1	10:15	OH Apprch	10:25	No load condition
2	10:27	2N	10:37	Back axle located adjacent to stay where it exits the deck
3	10:40	OH Apprch	10:42	No load condition
4	10:56	4N	11:04	Back axle located adjacent to stay where it exits the deck
5	11:05	OH Apprch	11:13	No load condition
6	11:14	16N	11:26	Back axle located adjacent to stay where it exits the deck
7	11:27	KY Apprch	11:36	No load condition
8	11:37	9S	11:47	Back axle located adjacent to stay where it exits the deck
9	11:48	KY Apprch	11:55	No load condition
10	11:56	4S	12:05	Back axle located adjacent to stay where it exits the deck
11	12:06	KY Apprch	12:14	No load condition
12	12:15	2S	12:24	Back axle located adjacent to stay where it exits the deck
13	12:25	KY Apprch	12:33	No load condition
14	12:34	KY CL	12:44	Back axle located just north of the KY expansion plates
15	12:45	KY Apprch	1:00	No load condition

Table 6.11: Static Truckload Test Plan, 2012

The instrumentation scheme for the truck load test consisted of strain gages installed on the bridge during construction. Each location includes both a vibrating wire gage for slow-speed reading of long-term behavior without drift, and a traditional foil gage for high-speed reading of short liveload response. The stations of the sensors are listed on the right side of Figure 3.8.

6.5.2 Conduct of Testing

The Ohio Department of Transportation provided four tandem-axle dump trucks that were used to conduct the truck load test. Tandem-axle dump trucks were requested because, when fully loaded, they are typically much heavier than their single rear axle counterpart. The truck weight is important because it should be sufficient to cause sensor readings that are above noise levels.

Two data acquisition systems were used during the test because a combination of high speed and low speed (vibrating wire) sensors were used for the test. Several Campbell Scientific CR-10X data logger systems were used to power and read the vibrating wire based gages and two Optim MEGADAC data acquisition system was used to power and read the high-speed sensors.

The trucks were placed in one of the positions from the test plan and at least three readings were recorded from each sensor. It took about 10 minutes to test each position because the CR-10X loggers required about 2 minutes to scan the all of the vibrating wire gages and there was always some delay in positioning the trucks. A set of readings with no load on the bridge was recorded periodically during the test to cancel out any environmental effects in the results.

The moving truckload tests were conducted after the static tests, throughout the remainder of the afternoon. Truck #802 was selected and the other trucks were returned to the garage. One person with a walkie-talkie took the passenger seat of the truck. The truck driver was to start north of the bridge, accelerate to a speed of about 20mph, center the truck in the test lane, and maintain that speed (and lane) for the entire length of the bridge. Upon reaching the south abutment, the truck would immediately brake to stop short of the intersection just south of the bridge. Two high-speed data acquisition systems were deployed at the northern sensor station (i.e., 2N). Data collection at 200Hz was manually triggered to commence as the front tire reached the north expansion joint and concluded when the back tire reached the southern expansion joint. Data was collected as the truck ran each marked lane and shoulder; then, the data systems would be relocated to the next sensor station, and the entire set of tests run again.

6.5.3 Static Baseline Truckload Test Results, 2012, After Pulldowns

Table 6.12 provides a summary of the static truckload test results for Upstream gaging, as compared to the results predicted using the liveload design envelope of HNTB and the sectional properties provided by B&T. The columns provide the change in response for the given vibrating wire strain gage between the indicated static truck load position and its subsequent “no load” condition; in this fashion, one removes the thermal effect seen in Figure 6.6. The min and max of these columns is compared to a similar load applied to the B&T section properties of the given instrumented station. Of course, there is some difference simply because the static load positions cannot represent a continuous load influence line to the same spatial resolution as the analysis; however, it provides a ballpark comparison. The moving test is a better comparison.

Upstream	Truckload (59% Design Load) Position								59% Design, No Impact	
Sensor/Segment	2N	4N	16N	9S	4S	2S	Min (ue)	Max (ue)	Min (ue)	Max (ue)
Segment 2N										
Deck Upper	0	0	0	0	0	0	0	0	-70.3935428	28.1146048
Deck Lower	-1	0.1	0.5	0.7	0.7	0.6	-1	0.7		
Top Flange	15.5	11.9	-6.1	0.7	-0.4	-0.2	-6.1	15.5	-29.8986979	10.6311221
Web	86.7	29.7	-53.7	-5.4	-0.2	5.3	-53.7	86.7		
Bottom Flange, Outer	175.9	86.8	-70.5	0.5	2.7	-2.9	-70.5	175.9	-88.3922149	199.056978
Bottom Flange, Inner	175.8	84.2	-69.7	-1.4	4.5	-2.6	-69.7	175.8		
Segment 4N										
Top Flange	-17.7	62	9.8	30.2	12	-2.8	-17.7	62	-15.8582913	1.96584267
Bottom Flange, Outer	38	141	-51.6	-3.9	-0.6	-2.5	-51.6	141	-52.7254598	153.175451
Bottom Flange, Inner	40.1	136.9	-49.8	-2.6	1.4	-1.2	-49.8	136.9		
Segment 16N										
Deck Upper	2.6	3.5	-7.5	0.6	0.7	0.3	-7.5	3.5	-57.0280309	10.8909293
Deck Lower	1	1.2	7.8	0.7	0.6	0.1	0.1	7.8		
Top Flange	-0.6	-0.5	13.3	-0.9	-0.7	-0.2	-0.9	13.3	-19.2347656	5.55750786
Web	-11.7	-16.4	67.5	107.6	-4.1	1.9	-16.4	107.6		
Bottom Flange, Outer	-18.9	-23.1	143.5	-0.7	-2.2	-4.1	-23.1	143.5	-23.5699389	188.562606
Bottom Flange, Inner	-22.6	-25.4	149.4	-4.7	-13	-5.6	-25.4	149.4		
Segment 9S										
Deck Upper	2.4	3	-2.1	-4.2	-0.1	0.8	-4.2	3	-14.6917054	18.1957795
Deck Lower	1.9	3.2	-1.7	1.2	-1.3	0.4	-1.7	3.2		
Top Flange	2.4	3.2	-3.9	-5.3	-0.8	0.2	-5.3	3.2	-6.66141725	4.77231367
Web	-0.1	1.2	-14.8	-23.7	-7.4	0.9	-23.7	1.2		
Bottom Flange, Outer	0.7	2.2	-5.5	-13.9	-4.4	-2.8	-13.9	2.2	-67.9805089	54.180818
Bottom Flange, Inner	2.4	3	-11.1	-22.3	-5.4	-4.4	-22.3	3		
Segment 4S										
Deck Upper	0	0	0	0	0	0	0	0	-48.2320697	12.6080155
Deck Lower	2	2.3	-0.2	1.1	2.7	0.7	-0.2	2.7		
Top Flange	2	2	-6.8	-3.4	9.4	1.5	-6.8	9.4	-13.5307803	2.26623612
Web	3.5	0.8	-20.9	-6.6	36.2	8.7	-20.9	36.2		
Bottom Flange, Outer	5.8	10.1	-28.6	-6	113.1	13.8	-28.6	113.1	-54.9773515	178.110196
Bottom Flange, Inner	8.4	8.6	-31.4	-7.2	113.4	13.4	-31.4	113.4		
Segment 2S										
Deck Upper	2.1	2.4	0.5	1.1	5.7	6.4	0.5	6.4	-25.7658317	14.0025335
Deck Lower	1.8	2.8	1.9	1.3	2	3	1.3	3		
Top Flange	2.4	2.3	-2.5	-0.5	5	3.5	-2.5	5	-8.50379448	4.36070801
Web	0.7	0	-17.1	-5.9	-3.4	16.9	-17.1	16.9		
Bottom Flange, Outer	2.5	2.6	-2.3	-0.1	2.6	4.9	-2.3	4.9	-49.5183868	87.9054935
Bottom Flange, Inner	4.8	7.9	-11.2	-0.4	-1.5	25.9	-11.2	25.9		
= Bad Sensor										

Table 6.12: Static Truckload Test Results vs Predicted, Upstream, USG, 2012

Table 6.13 provides a summary of the static truckload test results for Upstream gaging, as compared to the results from the 2006 static truckload test, scaled up to account for the lighter trucks used in the baseline test. The min and max of these columns are rather comparable; however, it is of note that the maximum (or positive moment response) at segments 2N, 4S, and 2S are smaller in 2012 compared to 2006. The latter two are related to the pulldown rehab and repairs, as the increased rotational stiffness (found in our finite element analysis, Figure 6.X) and the additional pulldown in segment 1S reduces the liveload moment in adjacent segments. In addition, the minimum (or negative moment response) at segment 2S is also smaller in 2012 compared to 2006, and also related to the pulldown rehab and repairs.

Upstream	Truckload (59% Design Load) Position								2006 Test, Scaled Up	
Sensor/Segment	2N	4N	16N	9S	4S	2S	Min (ue)	Max (ue)	Min (ue)	Max (ue)
Segment 2N										
Deck Upper	0	0	0	0	0	0	0	0	0.00	0.00
Deck Lower	-1	0.1	0.5	0.7	0.7	0.6	-1	0.7	-2.08	3.64
Top Flange	15.5	11.9	-6.1	0.7	-0.4	-0.2	-6.1	15.5	-7.46	13.01
Web	86.7	29.7	-53.7	-5.4	-0.2	5.3	-53.7	86.7	-40.78	85.20
Bottom Flange, Outer	175.9	86.8	-70.5	0.5	2.7	-2.9	-70.5	175.9	-74.62	172.66
Bottom Flange, Inner	175.8	84.2	-69.7	-1.4	4.5	-2.6	-69.7	175.8	-71.32	184.11
Segment 4N										
Top Flange	-17.7	62	9.8	30.2	12	-2.8	-17.7	62	-3.30	11.80
Bottom Flange, Outer	38	141	-51.6	-3.9	-0.6	-2.5	-51.6	141	0.00	0.00
Bottom Flange, Inner	40.1	136.9	-49.8	-2.6	1.4	-1.2	-49.8	136.9	-48.76	141.08
Segment 16N										
Deck Upper	2.6	3.5	-7.5	0.6	0.7	0.3	-7.5	3.5	-11.11	6.25
Deck Lower	1	1.2	7.8	0.7	0.6	0.1	0.1	7.8	-26.72	3.82
Top Flange	-0.6	-0.5	13.3	-0.9	-0.7	-0.2	-0.9	13.3	-2.08	12.67
Web	-11.7	-16.4	67.5	107.6	-4.1	1.9	-16.4	107.6	-27.42	80.00
Bottom Flange, Outer	-18.9	-23.1	143.5	-0.7	-2.2	-4.1	-23.1	143.5	-28.81	145.07
Bottom Flange, Inner	-22.6	-25.4	149.4	-4.7	-13	-5.6	-25.4	149.4	-32.10	150.45
Segment 9S										
Deck Upper	2.4	3	-2.1	-4.2	-0.1	0.8	-4.2	3	-5.21	6.42
Deck Lower	1.9	3.2	-1.7	1.2	-1.3	0.4	-1.7	3.2	-2.26	6.94
Top Flange	2.4	3.2	-3.9	-5.3	-0.8	0.2	-5.3	3.2	-5.03	4.86
Web	-0.1	1.2	-14.8	-23.7	-7.4	0.9	-23.7	1.2	-19.61	0.52
Bottom Flange, Outer	0.7	2.2	-5.5	-13.9	-4.4	-2.8	-13.9	2.2	-23.60	1.74
Bottom Flange, Inner	2.4	3	-11.1	-22.3	-5.4	-4.4	-22.3	3	-23.60	2.78
Segment 4S										
Deck Upper	0	0	0	0	0	0	0	0	-8.33	5.55
Deck Lower	2	2.3	-0.2	1.1	2.7	0.7	-0.2	2.7	-2.26	3.82
Top Flange	2	2	-6.8	-3.4	9.4	1.5	-6.8	9.4	-3.47	6.25
Web	3.5	0.8	-20.9	-6.6	36.2	8.7	-20.9	36.2	-15.10	39.91
Bottom Flange, Outer	5.8	10.1	-28.6	-6	113.1	13.8	-28.6	113.1	-32.45	124.59
Bottom Flange, Inner	8.4	8.6	-31.4	-7.2	113.4	13.4	-31.4	113.4	-30.37	122.69
Segment 2S										
Deck Upper	2.1	2.4	0.5	1.1	5.7	6.4	0.5	6.4	0.00	9.37
Deck Lower	1.8	2.8	1.9	1.3	2	3	1.3	3	0.52	9.54
Top Flange	2.4	2.3	-2.5	-0.5	5	3.5	-2.5	5	-2.08	7.11
Web	0.7	0	-17.1	-5.9	-3.4	16.9	-17.1	16.9	-24.29	21.17
Bottom Flange, Outer	2.5	2.6	-2.3	-0.1	2.6	4.9	-2.3	4.9	-18.91	21.34
Bottom Flange, Inner	4.8	7.9	-11.2	-0.4	-1.5	25.9	-11.2	25.9	-25.86	31.06
= Bad Sensor										

Table 6.13: Static Truckload Test Results, 2006 vs 2012, Upstream, USG, 2012

6.5.4 Dynamic Baseline Truckload Test Results, 2012, After Pulldowns

In Figures 6.22 – 6.26, an example set of sensor responses to the moving truckload test is provided for upstream locations when the truck is driven in the adjacent lane 4 (i.e., the eastern shoulder). The blue lines represent the measured results from 2006, while the red and green lines are the scaled results from 2012 and 2009, respectively, to account for the lighter trucks used in 2006. Other sensor responses at other stations provided similar results and allowed verification of all the installed gages, as well as verification of structural behavior consistent with the 2006 baseline. The X axis (i.e., distance of the front axle of the truck from the Ohio abutment) for these responses has been somewhat modified to account for variation in the truck speed.

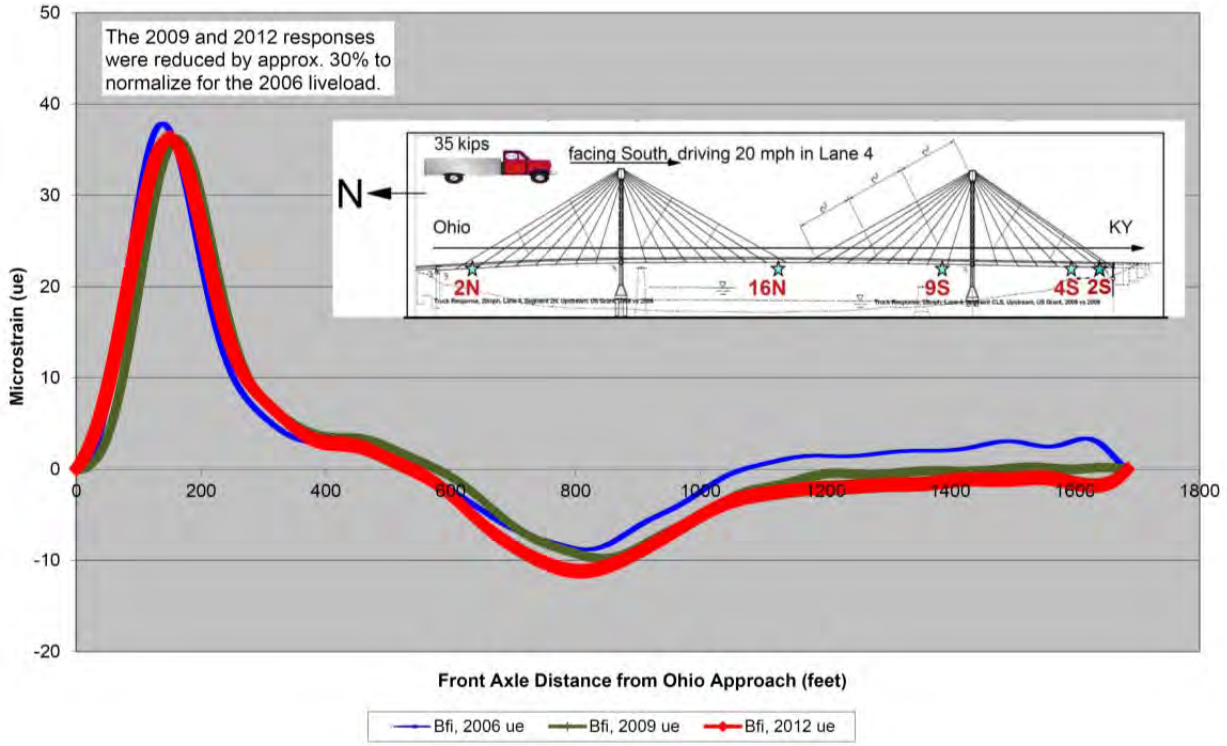

Figure 6.22: History of Upstream Influence Lines, Bottom Flange, Station 2N, USG

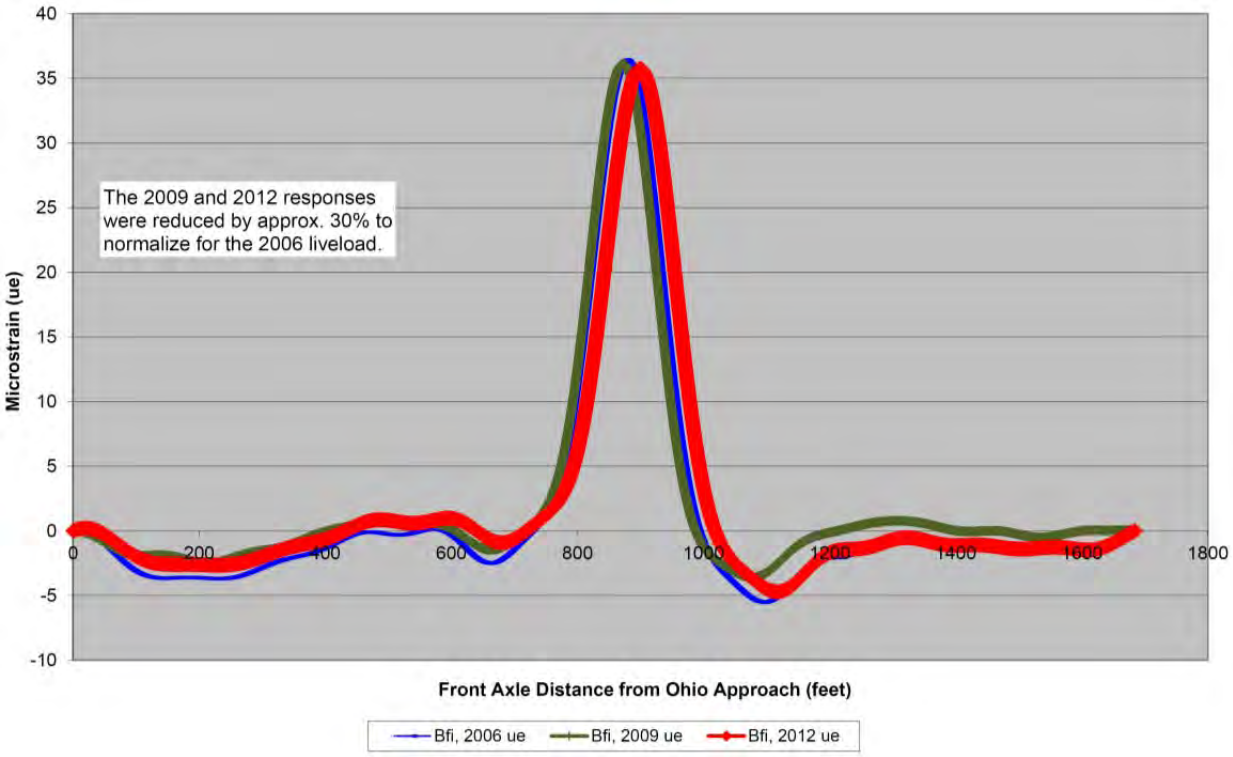

Figure 6.23: History of Upstream Influence Lines, Bottom Flange, Station 16N, USG

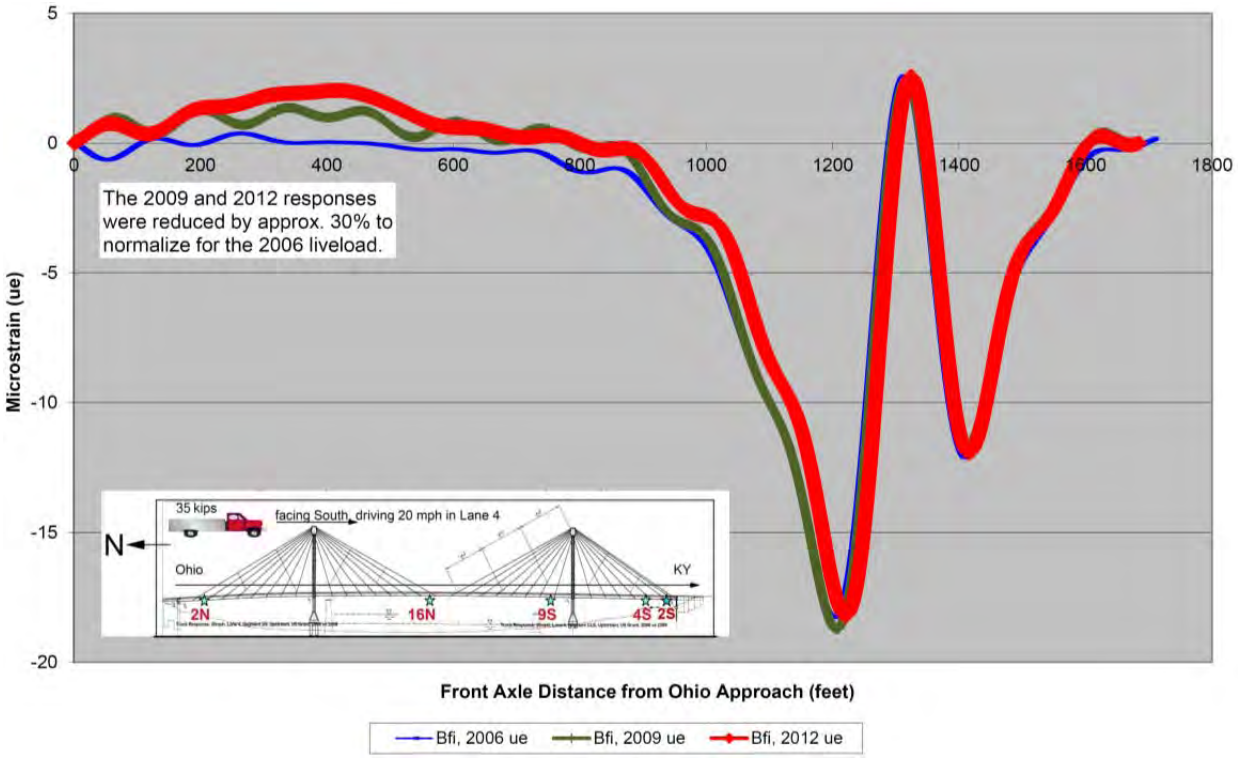

Figure 6.24: History of Upstream Influence Lines, Bottom Flange, Station 9S, USG

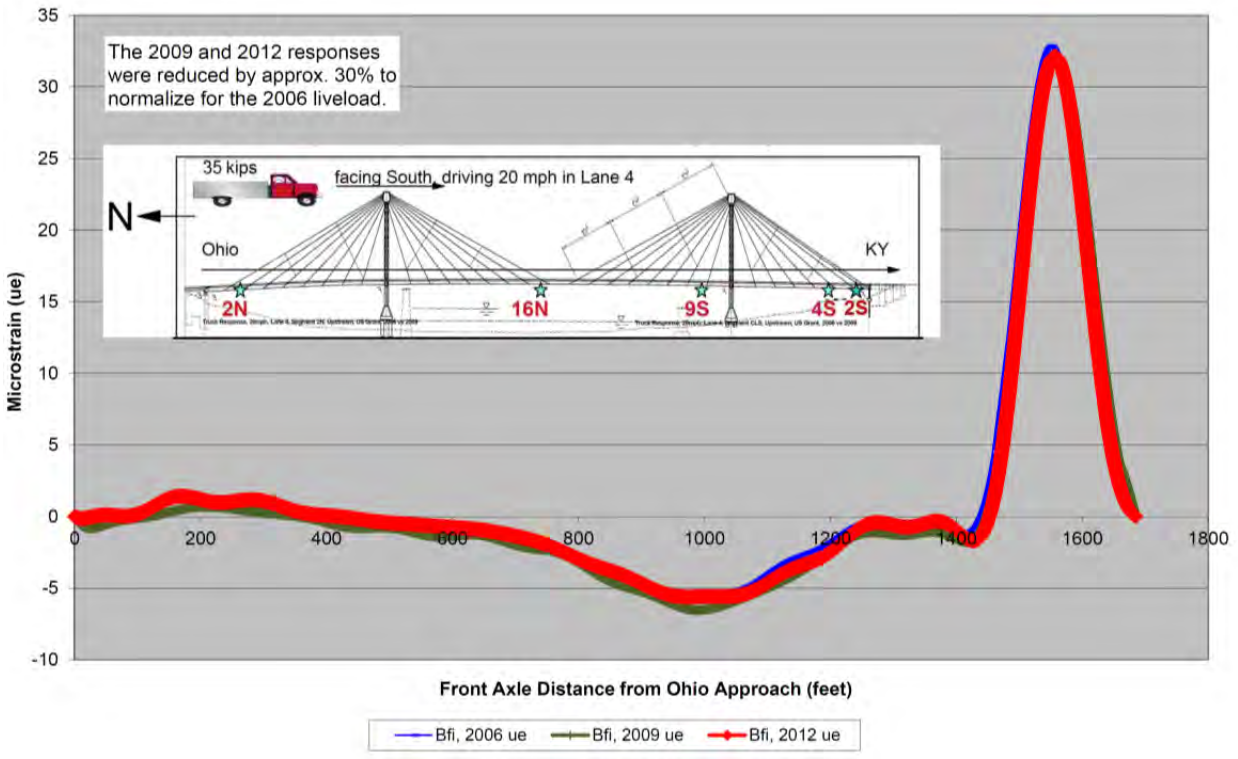

Figure 6.25: History of Upstream Influence Lines, Bottom Flange, Station 4S, USG

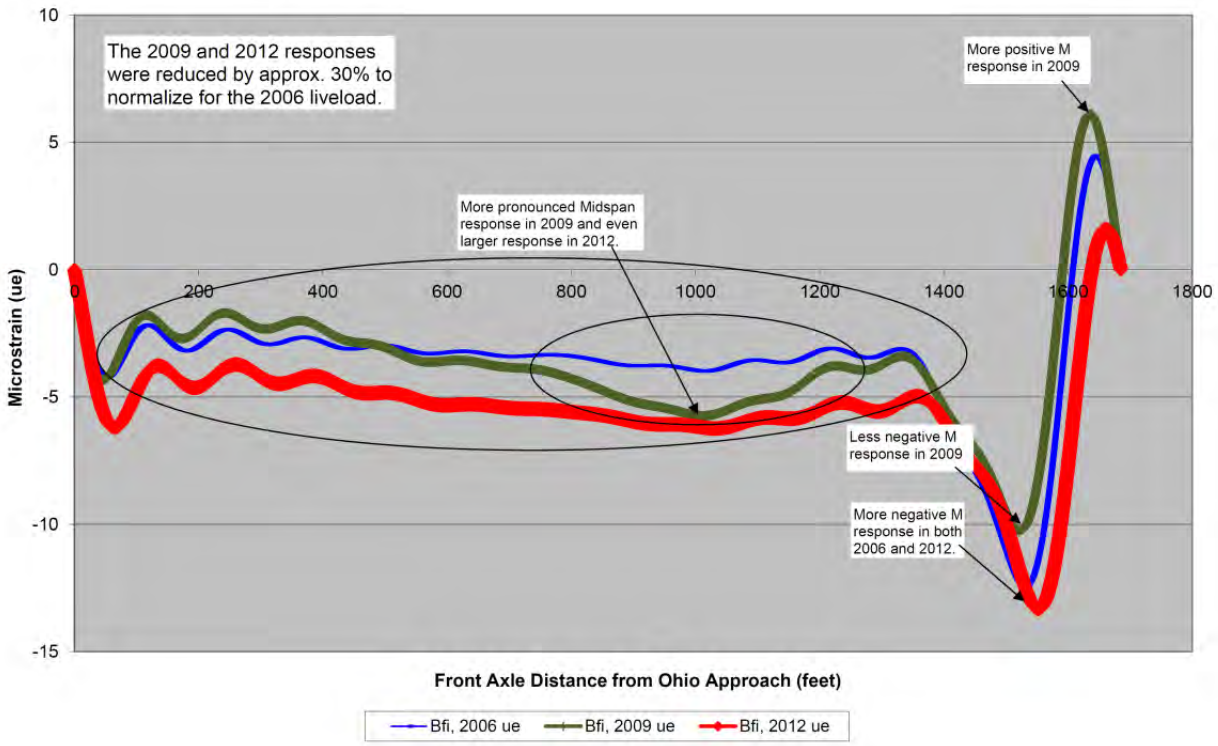

Figure 6.26: History of Upstream Influence Lines, Bottom Flange, Station 2S, USG

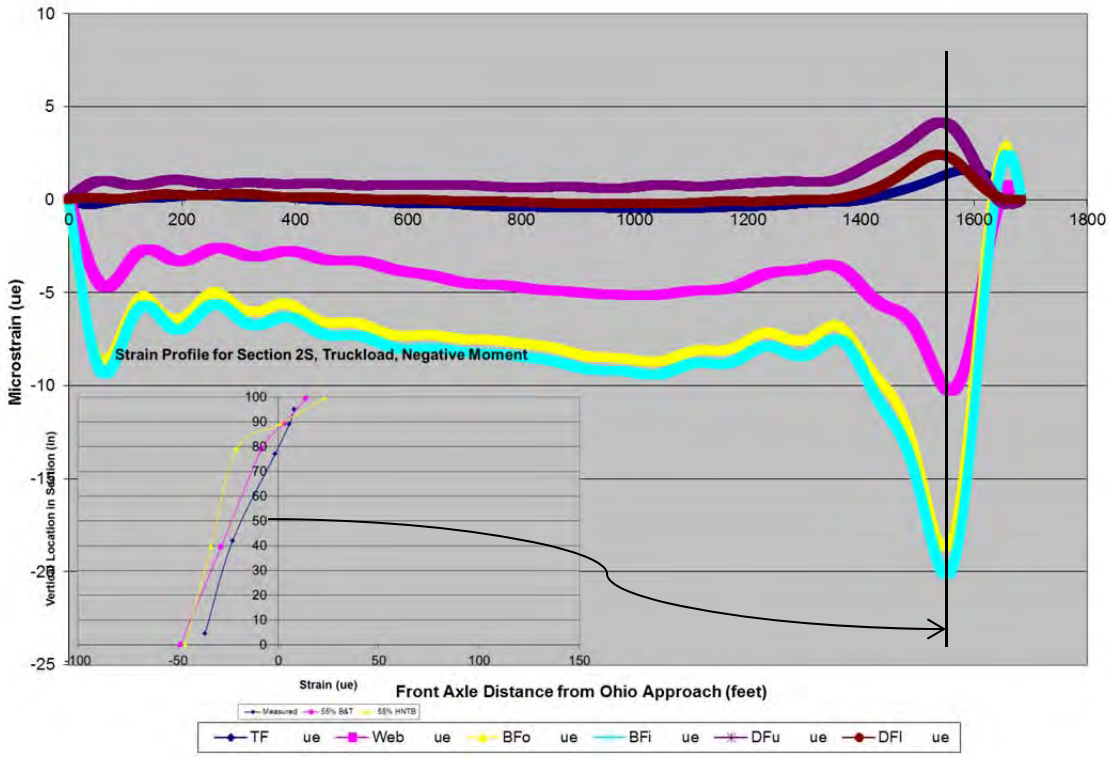

Figure 6.27: Upstream Influence Lines, Station 2S, USG, 2012

In Figure 6.27, the influence lines and strain profile measured during the moving truck test in the adjacent lane is shown for Station 2S. It clearly shows composite action between the decking and edge girder, as the profile is continuous throughout the section and the neutral axis is near the bottom of the deck. The other stations show similar levels of composite action.

Note that, as mentioned earlier, only one truck is used for the moving tests, which obviously causes a much smaller response than if all four trucks are parked near the instrumented section as was done for the static test results. A better comparison to the static load test results would be found in Figure 6.28 which summarizes peak or envelope stress found when summing all four moving test results for a given station, corresponding to each of the marked lanes (and shoulders). Here, the design envelope is scaled to the actual truckload weight employed in the tests. This also allows comparison to the predicted liveload response from the design analysis, which is slightly larger than measured results.

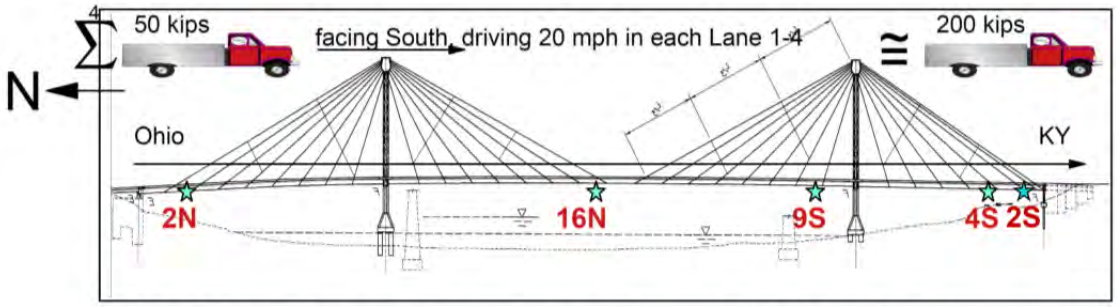

Table of Min/Max Controlling Envelope Stress (ksi) Values for Bottom Flange

Segment	Design Min	Design Max	2009 Min	2009 Max	2012 Min Dn	2012 Max Dn	2012 Min Up	2012 Max Up
2N	-2.4	5.4	-1.8	4.3	n/a	n/a	-2.0 ✔	4.6 ✔
16N		5.1		3.8		3.9 ✔		4.0 ✔
9S	-1.9		-1.9		-1.9 ✔		-1.9 ✔	
4S		4.8		3.5		3.7 ✔		3.6 ✔
2S	-1.3		-0.9		-1.1 ↑		**-1.3** ↑	

n/a = gage needs replacement ✔ = 2009 and 2012 results similar

Figure 6.28: Truckload Stress Envelope, Design vs 2009 vs 2012, USG

Table 6.14 provides a summary of the moving truckload test results for Upstream gaging, as compared to the results predicted using the liveload design envelope of HNTB and the sectional properties provided by B&T. The columns provide min or max response for the given foil strain gage and the indicated moving truck lane. The min and max of these columns is compared to a similar load applied to the B&T section properties of the given instrumented station. Measured results are less than the conservative predictions of the design analysis. Of course, lane load results for such a monumental structure will control over moving truckload results.

Upstream	**Minima (14.6% Design Load)**				**Maxima (14.6% Design Load)**				**Total**			**58.24% Design, No Impact**	
Sensor/Segment	Lane 1	Lane 2	Lane 3	Lane 4	Lane 1	Lane 2	Lane 3	Lane 4	Min (ue)	Max (ue)		**Min (ue)**	**Max (ue)**
Segment 2N													
Deck Upper	-1.38	-0.49	-7.19	-8.28	2.04	2.14	1.31	0.39	-17.34	5.89		-69.4867786	27.7524506
Deck Lower	-0.30	-0.35	-2.30	-2.22	2.84	1.40	0.18	0.15	-5.17	4.57			
Top Flange	-1.80	-1.72	-1.20	-1.12	5.35	4.24	2.20	2.87	-5.85	14.66		-29.5135621	10.4941788
Web	-8.75	-11.67	-8.78	-9.48	14.55	14.84	24.37	27.39	-38.68	81.15			
Bottom Flange, Outer	-16.06	-22.06	-16.25	-16.21	23.65	24.33	48.56	54.51	-70.58	151.05		-87.2536033	196.492854
Bottom Flange, Inner	-29.85	-21.38	-17.38	-17.05	27.58	25.92	48.98	54.89	-85.67	157.36			
Segment 16N													
Deck Upper	-0.27	-0.55	-1.63	-2.86	1.42	0.87	0.88	0.40	-5.31	3.58		-56.2934325	10.7506394
Deck Lower	-1.01	-0.45	-0.87	-1.10	3.56	3.62	2.78	1.32	-3.44	11.28			
Top Flange	-0.33	-0.67	-0.71	-0.20	4.69	4.41	4.04	3.94	-1.91	17.09		-18.9869957	5.48591963
Web	-2.75	-2.11	-2.47	-3.30	9.35	13.43	23.44	26.97	-10.63	73.19			
Bottom Flange, Outer	-4.65	-5.02	-5.44	-6.61	15.15	21.96	44.74	53.37	-21.72	135.22		-23.2663261	186.133664
Bottom Flange, Inner	-4.64	-5.38	-5.59	-7.16	15.66	22.34	45.98	54.12	-22.76	138.10			
Segment 9S													
Deck Upper	-1.05	-1.58	-0.28	-0.28	1.39	0.96	2.48	3.86	-3.18	8.70		-14.5024563	17.9613932
Deck Lower	-0.65	-1.62	-1.47	-0.35	1.76	0.84	1.88	2.79	-4.08	7.27			
Top Flange	-1.36	-1.70	-1.07	-0.43	1.27	1.06	0.70	0.75	-4.56	3.78		-6.57560916	4.7108398
Web	-3.14	-6.06	-11.69	-13.27	1.99	0.64	1.55	2.80	-34.15	6.99			
Bottom Flange, Outer	-3.32	-8.26	-20.65	-24.73	2.40	1.08	1.26	2.50	-56.95	7.24		-67.1048278	53.4828956
Bottom Flange, Inner	-6.18	-8.73	-23.79	-27.58	1.57	7.00	1.69	3.86	-66.28	14.12			
Segment 4S													
Deck Upper	-0.19	-0.19	-3.79	-5.06	2.38	0.16	0.39	1.17	-9.24	4.11		-47.6107753	12.4456072
Deck Lower	-0.59	-0.51	-0.32	-0.65	3.50	2.31	0.30	1.17	-2.06	7.28			
Top Flange	-0.42	-0.41	-0.27	-0.11	4.44	4.13	1.82	1.68	-1.19	12.07		-13.3564855	2.23704393
Web	-4.04	-4.37	-5.15	-3.75	8.79	11.21	18.55	21.63	-17.31	60.18			
Bottom Flange, Outer	-9.22	-9.23	-8.73	-7.95	13.10	19.30	38.74	45.43	-35.13	116.58		-54.2691686	175.815895
Bottom Flange, Inner	-10.06	-9.67	-10.27	-8.48	14.04	21.06	40.60	48.72	-38.48	124.42			
Segment 2S													
Deck Upper	-1.21	-0.64	-0.66	-0.28	1.99	0.59	2.28	4.12	-2.78	8.98		-25.4339329	13.8221619
Deck Lower	-1.12	-0.77	-0.16	-0.24	2.10	0.90	1.01	2.39	-2.29	6.40			
Top Flange	-0.84	-1.06	-0.26	-0.47	2.08	1.28	0.86	1.59	-2.64	5.81		-8.39425408	4.30453618
Web	-1.83	-3.50	-8.23	-10.26	2.85	0.92	1.59	0.81	-23.82	6.17			
Bottom Flange, Outer	-1.90	-4.15	-13.02	-18.51	3.74	2.56	4.80	3.02	-37.58	14.12		-48.8805229	86.7731516
Bottom Flange, Inner	-2.13	-6.18	-15.39	-20.06	1.63	0.58	3.73	2.53	-43.76	8.47			
= Bad Sensor													

Table 6.14: Moving Truckload Test Results vs Predicted, Upstream, USG, 2012

Table 6.15 provides a summary of the moving truckload test results for Upstream gaging, as compared to the results from the 2009 moving truckload test. The min and max of these columns are very comparable, with the exception of the change in influence line at station 2S (see Figure 6.26). It is our hypothesis that this change between 2009 and 2012 is entirely due to the new exterior pulldowns installed at station 1S, which slightly alter the influence line for adjacent station 2S. This leads to a reduced minimum and maximum in the 2012 results as compared to the 2009 results.

Upstream	**Minima (14.6% Design Load)**				**Maxima (14.6% Design Load)**				**Total**			**Upstream 2009**	
Sensor/Segment	Lane 1	Lane 2	Lane 3	Lane 4	Lane 1	Lane 2	Lane 3	Lane 4	Min (ue)	Max (ue)		Min (ue)	Max (ue)
Segment 2N													
Deck Upper	-1.38	-0.49	-7.19	-8.28	2.04	2.14	1.31	0.39	-17.34	5.89		-15.40	7.53
Deck Lower	-0.30	-0.35	-2.30	-2.22	2.84	1.40	0.18	0.15	-5.17	4.57		-6.55	5.14
Top Flange	-1.80	-1.72	-1.20	-1.12	5.35	4.24	2.20	2.87	-5.85	14.66		-2.59	14.65
Web	-8.75	-11.67	-8.78	-9.48	14.55	14.84	24.37	27.39	-38.68	81.15		-33.03	78.78
Bottom Flange, Outer	-16.06	-22.06	-16.25	-16.21	23.65	24.33	48.56	54.51	-70.58	151.05		-61.49	148.80
Bottom Flange, Inner	-29.85	-21.38	-17.38	-17.05	27.58	25.92	48.98	54.89	-85.67	157.36		-62.27	148.53
Segment 16N													
Deck Upper	-0.27	-0.55	-1.63	-2.86	1.42	0.87	0.88	0.40	-5.31	3.58		-5.13	4.45
Deck Lower	-1.01	-0.45	-0.87	-1.10	3.56	3.62	2.78	1.32	-3.44	11.28		-2.39	11.36
Top Flange	-0.33	-0.67	-0.71	-0.20	4.69	4.41	4.04	3.94	-1.91	17.09		-2.10	16.60
Web	-2.75	-2.11	-2.47	-3.30	9.35	13.43	23.44	26.97	-10.63	73.19		-7.98	70.23
Bottom Flange, Outer	-4.65	-5.02	-5.44	-6.61	15.15	21.96	44.74	53.37	-21.72	135.22		-19.88	127.86
Bottom Flange, Inner	-4.64	-5.38	-5.59	-7.16	15.66	22.34	45.98	54.12	-22.76	138.10		-20.69	132.42
Segment 9S													
Deck Upper	-1.05	-1.58	-0.28	-0.28	1.39	0.96	2.48	3.86	-3.18	8.70		-2.28	8.19
Deck Lower	-0.65	-1.62	-1.47	-0.35	1.76	0.84	1.88	2.79	-4.08	7.27		-4.81	6.91
Top Flange	-1.36	-1.70	-1.07	-0.43	1.27	1.06	0.70	0.75	-4.56	3.78		-4.15	2.60
Web	-3.14	-6.06	-11.69	-13.27	1.99	0.64	1.55	2.80	-34.15	6.99		-32.91	6.84
Bottom Flange, Outer	-3.32	-8.26	-20.65	-24.73	2.40	1.08	1.26	2.50	-56.95	7.24		-55.83	6.80
Bottom Flange, Inner	-6.18	-8.73	-23.79	-27.58	1.57	7.00	1.69	3.86	-66.28	14.12		-63.73	9.65
Segment 4S													
Deck Upper	-0.19	-0.19	-3.79	-5.06	2.38	0.16	0.39	1.17	-9.24	4.11		-8.33	4.50
Deck Lower	-0.59	-0.51	-0.32	-0.65	3.50	2.31	0.30	1.17	-2.06	7.28		-2.65	7.48
Top Flange	-0.42	-0.41	-0.27	-0.11	4.44	4.13	1.82	1.68	-1.19	12.07		-3.92	11.25
Web	-4.04	-4.37	-5.15	-3.75	8.79	11.21	18.55	21.63	-17.31	60.18		-17.71	57.52
Bottom Flange, Outer	-9.22	-9.23	-8.73	-7.95	13.10	19.30	38.74	45.43	-35.13	116.58		-37.16	112.58
Bottom Flange, Inner	-10.06	-9.67	-10.27	-8.48	14.04	21.06	40.60	48.72	-38.48	124.42		-39.80	122.29
Segment 2S													
Deck Upper	-1.21	-0.64	-0.66	-0.28	1.99	0.59	2.28	4.12	-2.78	8.98		-3.23	6.36
Deck Lower	-1.12	-0.77	-0.16	-0.24	2.10	0.90	1.01	2.39	-2.29	6.40		-1.89	4.29
Top Flange	-0.84	-1.06	-0.26	-0.47	2.08	1.28	0.86	1.59	-2.64	5.81		-3.26	4.09
Web	-1.83	-3.50	-8.23	-10.26	2.85	0.92	1.59	0.81	-23.82	6.17		-19.12	10.04
Bottom Flange, Outer	-1.90	-4.15	-13.02	-18.51	3.74	2.56	4.80	3.02	-37.58	14.12		-31.59	22.78
Bottom Flange, Inner	-2.13	-6.18	-15.39	-20.06	1.63	0.58	3.73	2.53	-43.76	8.47		-34.70	22.38
= Bad Sensor													

Table 6.15: Moving Truckload Test Results vs Predicted, Upstream, USG, 2009 vs 2012

Figure 6.29 and Table 6.16 provide a summary of the laneload results for Upstream gaging, as compared to the results predicted using the liveload design envelope of HNTB and the sectional properties provided by B&T. The columns provide the change in response for the given foil strain gage and the indicated truck lane. The min and max of these columns is compared to a similar load applied to the B&T section properties of the given instrumented station. Measured results are slightly less than the conservative predictions of the design analysis with the exception of station 2S, due to the installation of the exterior pulldowns in 1S. Note that the increase in laneload stress at 2S is not due to the peak liveload response (as shown in Figure 6.28 and Table 6.14) but due to the overall shape of the influence line (like the changes observed in Figure 6.26). This change is exhibited over all four lanes, and is hypothesized to have occurred due to the transverse bracing added above the new pulldowns.

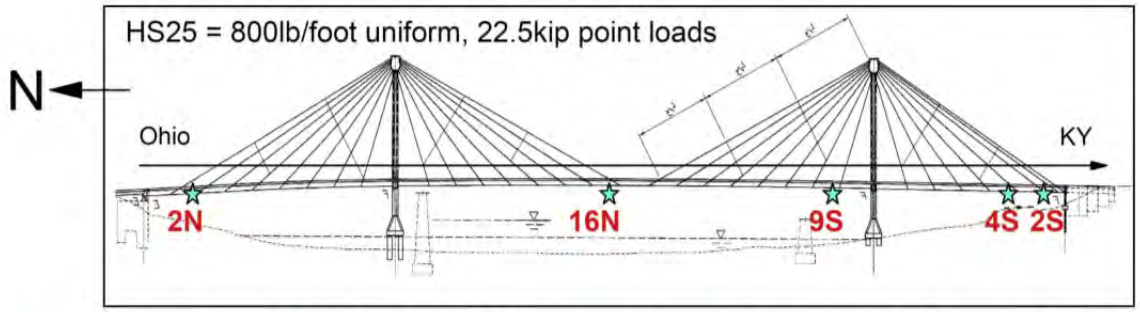

Table of Min/Max Controlling Envelope Stress (ksi) Values for Bottom Flange

Segment	Design Min	Design Max	2009 Min	2009 Max	2012 Min Dn	2012 Max Dn	2012 Min Up	2012 Max Up
2N	-15.3	18.1	-10.6	15.7	n/a	n/a	-13.3 ↑	13.5 ↓
16N		12.8		10.4		10.4 ✔		10.3 ✔
9S	-10.8		-8.9		-8.0 ↓		-7.6 ↓	
4S		12.9		9.6		9.3 ✔		8.6
2S	-8.9		-8.8		-9.3 ↑		**-10.5** ↑	

n/a = gage needs replacement ✔ = 2009 and 2012 results similar

Figure 6.29: Laneload Stress Envelope, Measured vs Design, USG, 2012

Figure 6.29 and Table 6.17 provide a summary of the laneload results for Upstream gaging, as compared to the results from the 2009 laneload results. The min and max of these columns are rather comparable, with the exception of station 2S as noted above and 2N. The minimum has been increased but the maximum laneload stress has been decreased at Station 2N, relative to 2009 test results. This compressive change occurs primarily due to the response of distant lanes for a given edge girder, much like that observed at station 2S; however, there has been no rehab work done nor signs of visible deterioration occurring at the Ohio abutment to explain this change. We recommend continued inspection at this location.

Upstream	**Minima (Design Load)**				**Maxima (Design Load)**				**Total**			**100% Design, No Impact**	
Sensor/Segment	Lane 1	Lane 2	Lane 3	Lane 4	Lane 1	Lane 2	Lane 3	Lane 4	Min (ksi)	Max (ksi)		Min (ksi)	Max (ksi)
Segment 2N													
Deck Upper	0.03	0.11	0.01	0.00	-0.01	0.00	-0.26	-0.30	0.15	-0.58		-1.02209353	0.79799772
Deck Lower	0.07	0.01	0.00	0.00	0.00	0.00	-0.06	-0.04	0.09	-0.10			
Top Flange	-0.02	-0.12	-0.01	-0.02	0.41	0.26	0.13	0.19	-0.17	0.98		-2.56408329	1.83309144
Web	-1.40	-3.71	-1.50	-1.78	1.59	1.10	2.00	2.34	-8.39	7.02			
Bottom Flange, Outer	-2.70	-4.71	-2.95	-2.95	2.79	1.85	4.12	4.69	-13.31	13.46		-15.2631463	18.0821828
Bottom Flange, Inner	-4.35	-4.56	-3.46	-3.92	4.94	2.00	4.09	4.77	-16.28	15.81			
Segment 16N													
Deck Upper	0.01	0.01	0.01	0.00	0.00	0.00	-0.01	-0.07	0.02	-0.09		-0.7098797	0.30941724
Deck Lower	0.09	0.11	0.09	0.01	-0.01	0.00	-0.01	-0.01	0.30	-0.02			
Top Flange	-0.01	-0.01	-0.01	0.00	0.29	0.27	0.29	0.22	-0.03	1.06		-1.67589532	0.93887856
Web	-0.33	-0.07	-0.20	-0.19	0.74	1.10	1.67	1.86	-0.79	5.37			
Bottom Flange, Outer	-0.53	-0.58	-0.91	-0.89	1.54	1.92	3.16	3.70	-2.90	10.32		-4.29600007	12.8147421
Bottom Flange, Inner	-0.69	-1.07	-0.84	-1.18	1.46	1.76	3.17	3.70	-3.78	10.09			
Segment 9S													
Deck Upper	0.01	0.01	0.05	0.17	-0.01	-0.01	0.00	0.00	0.24	-0.02		-0.28157575	0.45244545
Deck Lower	0.01	0.01	0.01	0.06	0.00	-0.01	-0.01	0.00	0.09	-0.03			
Top Flange	-0.02	-0.04	-0.03	-0.01	0.02	0.01	0.01	0.01	-0.10	0.05		-1.40975437	1.00726114
Web	-0.21	-0.85	-1.46	-1.58	0.06	0.01	0.02	0.07	-4.09	0.15			
Bottom Flange, Outer	-0.21	-1.04	-2.91	-3.41	0.13	0.01	0.02	0.14	-7.57	0.29		-9.81845958	1.84013672
Bottom Flange, Inner	-0.83	-2.31	-3.35	-3.66	0.02	0.76	0.02	0.39	-10.14	1.20			
Segment 4S													
Deck Upper	0.05	0.00	0.00	0.01	0.00	0.00	-0.10	-0.14	0.06	-0.24		-0.47919301	0.32448698
Deck Lower	0.11	0.04	0.00	0.01	0.00	0.00	0.00	0.00	0.16	-0.01			
Top Flange	-0.01	-0.01	0.00	0.00	0.30	0.22	0.02	0.02	-0.02	0.56		-0.50022692	0.13276775
Web	-0.53	-0.62	-0.92	-0.50	0.69	0.69	1.18	1.38	-2.57	3.93			
Bottom Flange, Outer	-1.57	-1.53	-1.54	-1.31	1.14	1.42	2.74	2.95	-5.95	8.24		-10.0719162	12.8588484
Bottom Flange, Inner	-1.81	-1.66	-2.17	-1.51	1.10	1.66	2.73	3.10	-7.16	8.58			
Segment 2S													
Deck Upper	0.04	0.00	0.04	0.15	-0.01	0.00	0.00	0.00	0.23	-0.02		-0.26421137	0.35696803
Deck Lower	0.04	0.01	0.01	0.05	-0.01	-0.01	0.00	0.00	0.11	-0.02			
Top Flange	-0.02	-0.03	-0.01	-0.01	0.07	0.02	0.01	0.02	-0.06	0.11		-0.2436984	0.49045895
Web	-0.04	-0.27	-1.50	-2.97	0.11	0.01	0.04	0.01	-4.78	0.16			
Bottom Flange, Outer	-0.04	-0.50	-2.30	-5.09	0.16	0.07	0.19	0.04	-7.92	0.46		-8.91638885	7.39850258
Bottom Flange, Inner	-0.11	-1.30	-3.33	-5.71	0.02	0.01	0.14	0.03	-10.46	0.20			
= Bad Sensor													

Table 6.16: Laneload Test Results vs Predicted, Upstream, USG, 2012

Upstream	Minima (Design Load)				Maxima (Design Load)				Total			Upstream 2009	
Sensor/Segment	Lane 1	Lane 2	Lane 3	Lane 4	Lane 1	Lane 2	Lane 3	Lane 4	Min (ksi)	Max (ksi)		Min (ksi)	Max (ksi)
Segment 2N													
Deck Upper	0.03	0.11	0.01	0.00	-0.01	0.00	-0.26	-0.30	0.15	-0.58		0.52	-0.58
Deck Lower	0.07	0.01	0.00	0.00	0.00	0.00	-0.06	-0.04	0.09	-0.10		0.15	-0.19
Top Flange	-0.02	-0.12	-0.01	-0.02	0.41	0.26	0.13	0.19	-0.17	0.98		-0.23	1.77
Web	-1.40	-3.71	-1.50	-1.78	1.59	1.10	2.00	2.34	-8.39	7.02		-5.26	8.28
Bottom Flange, Outer	-2.70	-4.71	-2.95	-2.95	2.79	1.85	4.12	4.69	-13.31	13.46		-10.16	15.89
Bottom Flange, Inner	-4.35	-4.56	-3.46	-3.92	4.94	2.00	4.09	4.77	-16.28	15.81		-10.63	15.67
Segment 16N													
Deck Upper	0.01	0.01	0.01	0.00	0.00	0.00	-0.01	-0.07	0.02	-0.09		0.13	-0.13
Deck Lower	0.09	0.11	0.09	0.01	-0.01	0.00	-0.01	-0.01	0.30	-0.02		0.47	-0.02
Top Flange	-0.01	-0.01	-0.01	0.00	0.29	0.27	0.29	0.22	-0.03	1.06		-0.04	1.25
Web	-0.33	-0.07	-0.20	-0.19	0.74	1.10	1.67	1.86	-0.79	5.37		-1.20	5.50
Bottom Flange, Outer	-0.53	-0.58	-0.91	-0.89	1.54	1.92	3.16	3.70	-2.90	10.32		-3.58	10.07
Bottom Flange, Inner	-0.69	-1.07	-0.84	-1.18	1.46	1.76	3.17	3.70	-3.78	10.09		-3.63	10.44
Segment 9S													
Deck Upper	0.01	0.01	0.05	0.17	-0.01	-0.01	0.00	0.00	0.24	-0.02		0.44	-0.02
Deck Lower	0.01	0.01	0.01	0.06	0.00	-0.01	-0.01	0.00	0.09	-0.03		0.23	-0.45
Top Flange	-0.02	-0.04	-0.03	-0.01	0.02	0.01	0.01	0.01	-0.10	0.05		-0.22	0.19
Web	-0.21	-0.85	-1.46	-1.58	0.06	0.01	0.02	0.07	-4.09	0.15		-4.47	0.74
Bottom Flange, Outer	-0.21	-1.04	-2.91	-3.41	0.13	0.01	0.02	0.14	-7.57	0.29		-8.07	0.57
Bottom Flange, Inner	-0.83	-2.31	-3.35	-3.66	0.02	0.76	0.02	0.39	-10.14	1.20		-8.91	1.25
Segment 4S													
Deck Upper	0.05	0.00	0.00	0.01	0.00	0.00	-0.10	-0.14	0.06	-0.24		0.09	-0.27
Deck Lower	0.11	0.04	0.00	0.01	0.00	0.00	0.00	0.00	0.16	-0.01		0.27	-0.11
Top Flange	-0.01	-0.01	0.00	0.00	0.30	0.22	0.02	0.02	-0.02	0.56		-0.38	0.92
Web	-0.53	-0.62	-0.92	-0.50	0.69	0.69	1.18	1.38	-2.57	3.93		-3.03	4.39
Bottom Flange, Outer	-1.57	-1.53	-1.54	-1.31	1.14	1.42	2.74	2.95	-5.95	8.24		-6.71	9.19
Bottom Flange, Inner	-1.81	-1.66	-2.17	-1.51	1.10	1.66	2.73	3.10	-7.16	8.58		-7.55	9.64
Segment 2S													
Deck Upper	0.04	0.00	0.04	0.15	-0.01	0.00	0.00	0.00	0.23	-0.02		0.18	-0.04
Deck Lower	0.04	0.01	0.01	0.05	-0.01	-0.01	0.00	0.00	0.11	-0.02		0.10	-0.01
Top Flange	-0.02	-0.03	-0.01	-0.01	0.07	0.02	0.01	0.02	-0.06	0.11		-0.40	0.14
Web	-0.04	-0.27	-1.50	-2.97	0.11	0.01	0.04	0.01	-4.78	0.16		-5.67	0.47
Bottom Flange, Outer	-0.04	-0.50	-2.30	-5.09	0.16	0.07	0.19	0.04	-7.92	0.46		-7.26	1.29
Bottom Flange, Inner	-0.11	-1.30	-3.33	-5.71	0.02	0.01	0.14	0.03	-10.46	0.20		-8.83	1.25
= Bad Sensor													

Table 6.17: Laneload Test Results vs Predicted, Upstream, USG, 2009 vs 2012

6.5.5 Service Test, 2012, After to Pulldowns, Conclusions and Recommendations

Upstream and downstream edge girders have comparable response to truckload; however, the thermal response for some gages (e.g., web) dwarfs the liveload response. Composite action is clearly evident in all test results, with a greater slope in the strain profile and hence large effective deck width than predicted by analysis. Laneload results control over the truckload results and are used as the liveload response in the rating analysis of the structure. Measured results are slightly less than the conservative predictions of the design analysis, with the exception of the Kentucky abutment due to the addition of the exterior pulldowns and transverse bracing at Station 1S. In addition, there was a slight, unexplained change in influence line at Station 2S in 2012 as compared to the 2009 test results. These locations should be especially observed during inspection for unexpected signs of distress.

REFERENCES

1. Howard, Needles, Tammen, and Bergendoff (HNTB), Design Calculations for the U.S. Grant Bridge, 2000.
2. Buckland & Taylor (B&T), Superstructure Erection Submission for U.S. Grant Bridge, Rev. 3, 2004.
3. A. Helmicki, and V. Hunt, “Instrumentation of the US Grant Bridge for Monitoring of Fabrication, Erection, In-service Behavior, and to Support Management, Maintenance, and Inspection,” Project Review, ODOT Central Office, 2004.
4. C.S. Cai, J. Nie, and Y. Zhang, “Composite Girder Design of Cable-Stayed Bridges.” Structural Design and Construction, ASCE, Vol. 3, No. 4, November 1998: 158-163.
5. A. Helmicki, and V. Hunt, “Instrumentation of the US Grant Bridge for Monitoring of Fabrication, Erection, In-service Behavior, and to Support Management, Maintenance, and Inspection,” Project Review, ODOT Central Office, 2007.
6. J.S. Saini, “Effects of Nonlinearities due to Geometry, Cables and Tuned Mass Dampers on the Analysis of Cable-stayed Bridges,” MS Thesis, Department of Civil and Environmental Engineering, University of Cincinnati, Cincinnati, OH, 2007.
7. A. Helmicki, and V. Hunt, “Instrumentation of the US Grant Bridge for Monitoring of Fabrication, Erection, In-service Behavior, and to Support Management, Maintenance, and Inspection,” Project Review, ODOT Central Office, 2009.
8. A. Helmicki, and V. Hunt, “Instrumentation of the US Grant Bridge for Monitoring of Fabrication, Erection, In-service Behavior, and to Support Management, Maintenance, and Inspection,” Project Review, ODOT Central Office, 2013.

Chapter 7 Analytical and Experimental Result for Pulldown Installation

7.1 Introduction

After the bridge was opened to service in 2006, the Kentucky abutment and backwall began to exhibit cracking that started near the beam seat (see Figure 6.13) but became pervasive with increasing length and width over each subsequent inspection. It was believed that the source of this degradation was field modification to the location and installation of the steel pulldowns internal to the abutment. ODOT provided for immediate field rehabilitation of this installation, including the use of additional welding at the beam seat to resist further movement, which seemed to abate further cracking at the abutment. UCII then subsequently conducted another truckload test in order to observe/validate the effectiveness of the rehab and compare with expected design values.

A major rehabilitation of the Kentucky abutment pulldowns was conducted in 2011 in order to further examine, stiffen, and provide redundancy in the form of structural strands exterior to the abutment affixed to the edge girders and secured with rock anchors.

The goal of this part of the project was to install additional instrumentation at KYA on the US Grant bridge to monitor that location and track changes in its state of stress during and beyond the pending retrofit at that location. Vibrating wire gages were to be installed on both of the new upstream and downstream pull downs and at the abutment wall near KYA. The low speed, VW, gages would be interfaced into the existing monitor with data being collected, archived every 15-30 minutes into an upgraded US Grant database, and incorporated into the operation of the existing monitor website. These gages would provide information about the magnitude of the changes occurring at this location and will augment the findings of visual inspections. This task included the help and support of the contractor and ODOT in the form of access, conduit installation and traffic control.

A full truckload test of the bridge would be conducted to measure its new liveload response and to compare against the previous benchmark and to the originally intended design. The goal of this task was to conduct a truckload test duplicating those conducted previously and to also incorporate the new gaging package on the retrofit.

Once connection was achieved with the existing system, the web-based interface for the US Grant monitor would be upgraded to incorporate the new retrofit sensor package. The interface would automatically manage download and display of the gage and temperature data. This task would enable easy, user-friendly access for the ODOT D09 personnel in order to track the performance of this structure.

7.2 Instrumentation and Data Acquisition during Construction

An instrumentation scheme was developed for the pulldown system during the initial planning stages of the retrofit. This instrumentation design was guided by the stated objectives for the project: observing and documenting behavior and corresponding causative effects for a stay bridge during construction, observing and documenting the behavior and corresponding causative effects for the same bridge during service, and laying the groundwork for further development of intelligent bridge monitoring applications. To fulfill these objectives, vibrating wire gages (i.e., slow speed, long term reliability) were proposed to monitor global changes in the structure, such as magnitudes of displacement in the pulldowns themselves and rotation/tilt at the abutment induced by construction or environmental effects.

There were several redesigns of the KYA retrofit for the US Grant bridge and, subsequently, redesigns of the sensor package and envisioned future work for the UCII team. The initial plan (see Figure 7.1) would be to instrument both pairs of the back-up W12 pull downs at mid-height with five vibrating wire strain gages per W12 (one on each flange and one redundant gage at center of web) in order to be able to measure axial force and bending in both directions for each pull down. In addition to the pull down sensors, we proposed instrumenting both ends of the new cross girder, midway between the edge girder and the splice plate with again five vibrating wire gages (one on each flange and one redundant gage at center of web) to monitor its response. This plan would total 5 x 4 pulldowns + 5 x 2 cross girder ends = 30 gages.

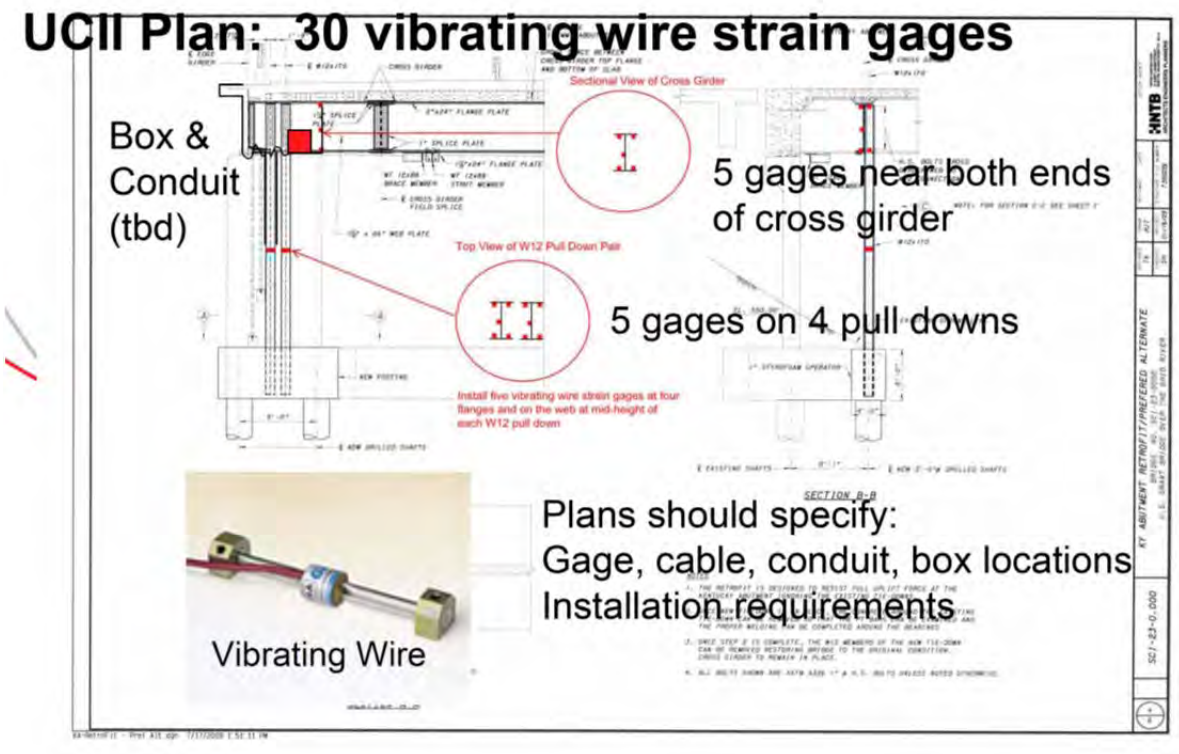

Figure 7.1: Initial Design of the Pulldown Instrumentation (UCII, 2009)

A major redesign of the retrofit now incorporates structural strand pull downs (as opposed to W12 beams) with rock anchors. Now, the sensor plan includes strand meters on each pulldown and tilt meters at the abutment wall, although there was some consideration given to adding load cells on some the rock anchors. Specifications for these sensors and their installation and protection were discussed and disseminated with both ODOT and HNTB, who was designing the retrofit. These details were then included within the design plans and notes (see Figure 5.2) so that the contractor Brayman would be able to facilitate their installation and connection to the existing wireway in the parapet. Specifications were included in a special provision to the plans.

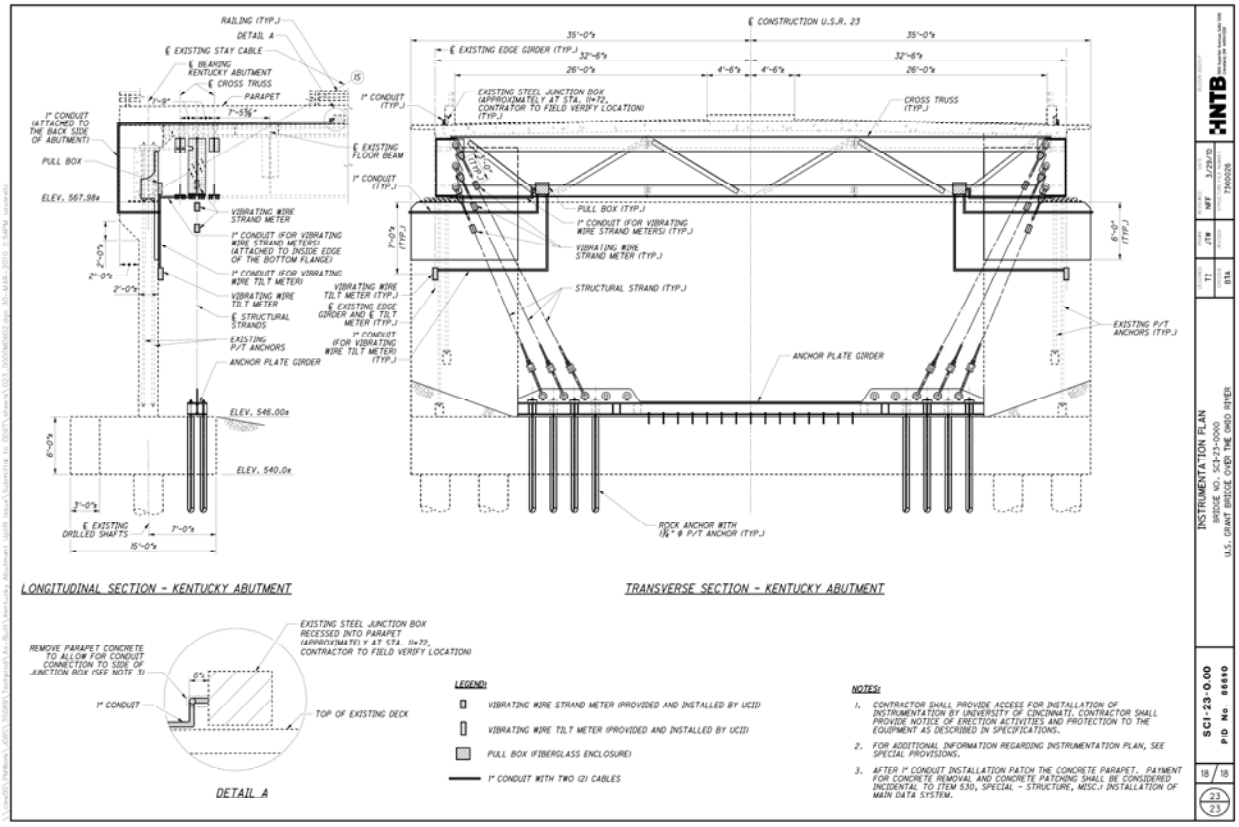

Figure 7.2: Final Design of the Pulldown Instrumentation (HNTB, 2010)

In January, 2011, tiltmeters were installed upon the abutment wall so as to document its pre-retrofit behavior to long-term effects such as daily temperature swings. We used vibrating wire based sensors so as to facilitate its connection with the existing and future electronics used by the other vibrating wire gages. The Geokon 6350 tilt meter has a range of +/- 15 degrees and a resolution of 8 arc seconds. The tiltmeters are shown in Figure 7.2 as installed upon the exterior face of the abutment wall; however, the final location was on the inside face, within the abutment cell accessed by a manhole within the Kentucky approach slab. This provided significant protection from both the environment as well as the pending construction effort.

Figure 7.4: Tilt Meter on Abutment Wall, USG Bridge (UCII, 2012)

In June, 2011, strand meters were installed immediately after the installation of the exterior pulldowns for the bridge. Strand meters are specifically designed to measure the axial displacement within a steel strand for a variety of applications. The Geokon 4410 strand meter has a range of 3mm (118 mils) and an accuracy of +/-0.1%FS or +/-0.003mm (0.118 mils). In addition to the strand meter, a Geokon 4000 strain gage was also installed on each pulldown for redundancy and in an effort to improve upon the accuracy. Both required special mounting collars to be fabricated from stainless steel (see Figure 7.3). Some tweaking of the proposed sensor locations was required to avoid pulldown and floorbeam details and other construction concerns.

The Campbell Scientific CR-10X data acquisition system was used for monitoring the vibrating wire strain gages throughout construction. These loggers were housed in white fiberglass enclosures and literally tethered to the gages by their own sensor cables. This allowed some flexibility in the exact location of the enclosure so as to avoid construction efforts, but also some level of protection from the very same concern. The data acquisition system was set to scan each gage in half-hour increments during most of the construction. Regular visits to the bridge allowed us to download the collected data into our laptop and to change the 12V battery powering the system.

Figure 7.3: Strand Meter and Strain Gage on Pulldown, USG Bridge (UCII, 2012)

Near the end of construction, a conduit spine was installed by the contractor down the length of both parapets and connected to a main cabinet located in the Ohio tower at roadway level. The batteries were then connected to and continuously charged by standard 120VAC power and the loggers were networked to the UCII labs by various communication services (i.e., initially by analog phone modem, then by digital ADSL router).

7.3 Thermal Response of the Sensor and Structure

An important characteristic of the vibrating wire strain gages is temperature compensation. For example, the vibrating wire strand meter is made of the very same material (i.e., steel) as the pulldowns upon which they are installed; hence, they have the very same temperature coefficient (i.e., response to temperature). So, when the gage and the steel host are at the same temperature, and both are completely free to move, the gage will indicate no change in strain reading. The result is that a temperature compensated gage will not exhibit any response not related to displacement/stress; or, in other words, a change in reading by a compensated strain gage infers that there is displacement/stress in the member upon which it is installed.

While monitoring the steel pulldown system during construction, the displacement/strain responses of all strand gages regularly indicated increased compressive displacement/strain behavior during the middle of the day, and tensile response at night. There is a slightly delayed relationship between increasing temperature and increasing compressive displacement/strain, and vice versa, at these locations. This behavior was repeated daily and an example of this behavior is illustrated in Figure 7.4. Note that this matches the strain gage response with temperature on the bottom flange of the exterior girders (see Figure 5.8).

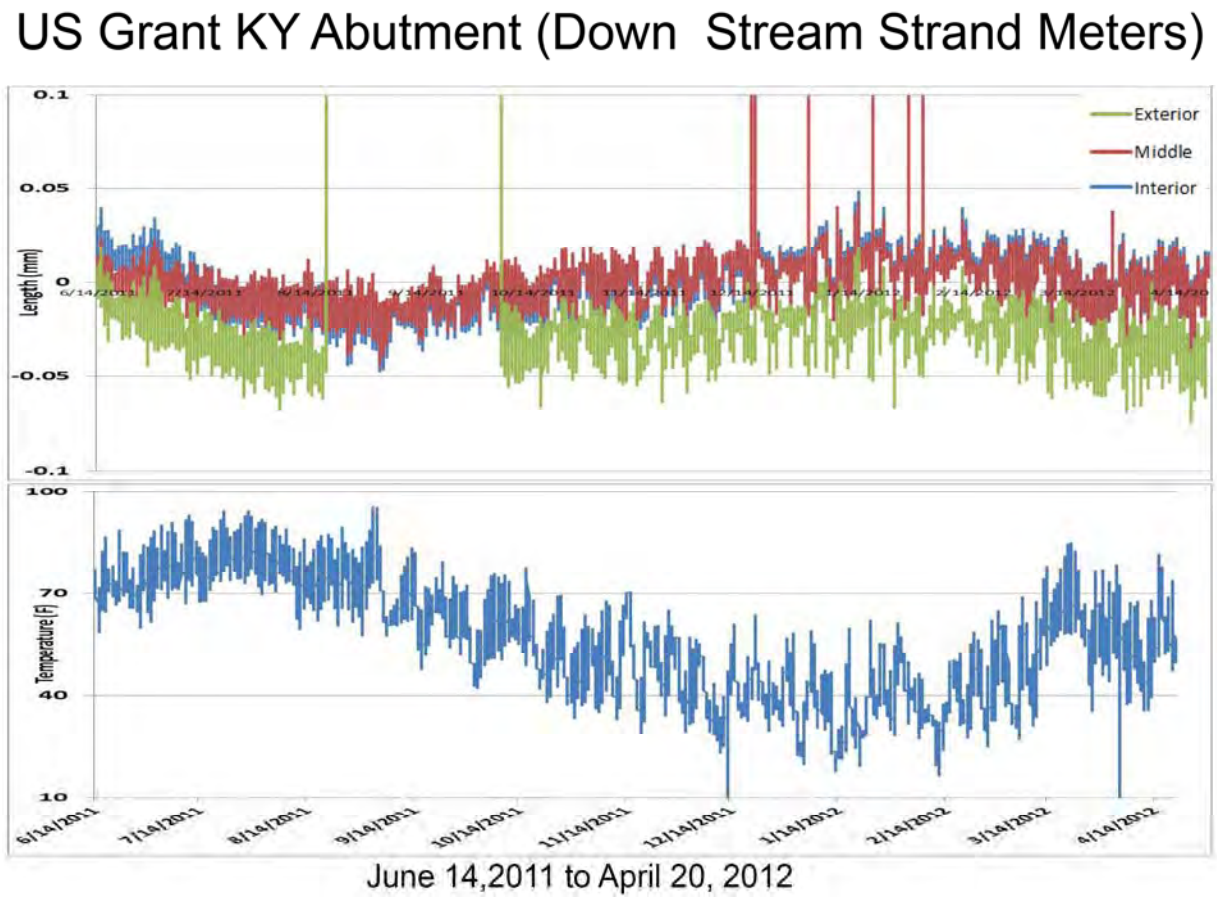

Figure 7.4: Strand Meter Response with Temperature, USG Bridge (UCII, 2012)

This also demonstrates what is believed to be apparent displacement/strain response from the sensors. If the temperature is similar for both the strand and gage (e.g., at night, when the sun is not a factor), the gage will experience tensile displacement/strains with a decrease in temperature, because its free compression is resisted by a strand that is somehow not completely free to move. Similarly, during the day, a gage will experience compressive displacement/strains with an increase in temperature, because its free extension is resisted again by a strand not completely free to move. So, it is not entirely clear if this displacement is actually occurring with temperature or if it is the response of the sensor from not being allowed to move freely with temperature; however, the important observation is that it is a small but rather consistent response with temperature and can hence be predicted and used by the monitor.

This daily relationship between strand meter and temperature is captured in Figure 7.5 as well for nearly a full year of service. Note that its slope varied during some initial burn-in period of a few months, but then became consistent thereafter.

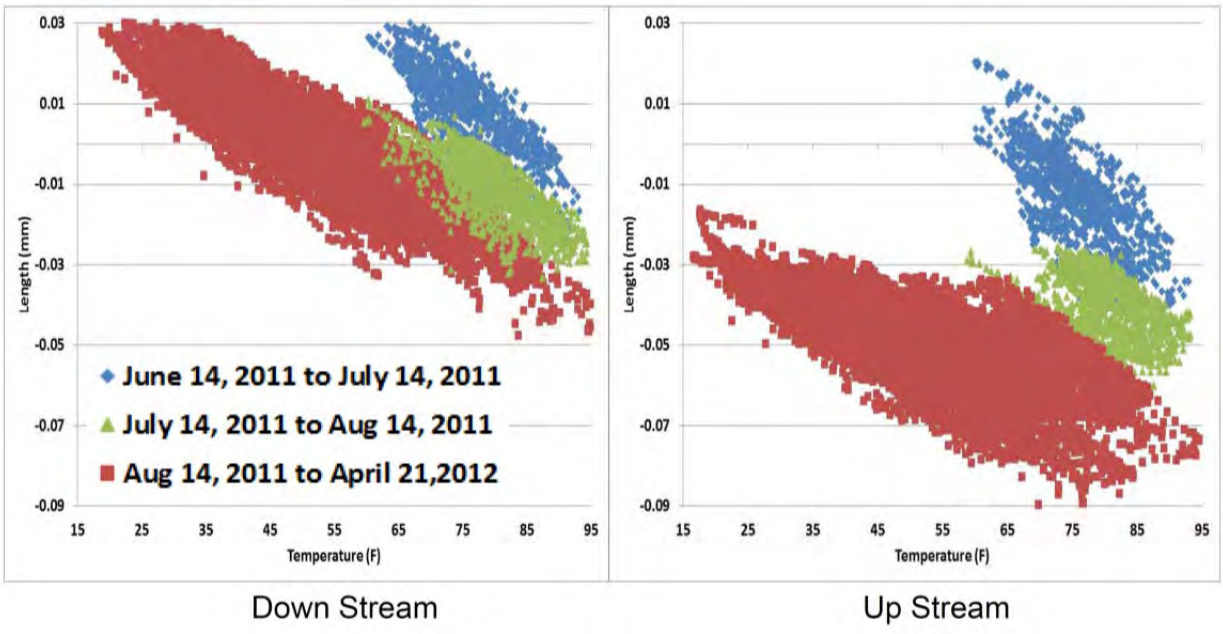

Figure 7.5: Strand Meter Displacement versus Temperature, USG Bridge (UCII, 2012)

Similar to the above, the tilt meters have a small but consistent response to temperature that can also be used by the monitor. The temperature compensation method advised by the Geokon manual has been used to alleviate the effect of it upon the long-term data. In addition, it should be pointed out that the temperature does not change as much in the abutment cell as it does external to the cell; hence, the effect of temperature upon the tilt meter itself is minimized by its installation within the cell. Further, the response with temperature was consistent before and after the pulldown installation. All that being said, it is again uncertain whether the response from the tilt meter is due to the actual rotation/tilt of the abutment wall or from the thermal response of the sensor itself (or both). If this exact measurement was required in future work, it is advised to install a second tiltmeter adjacent to each existing tiltmeter but in reverse angular orientation so that one may average their readings to completely remove any thermal (or other non-structural) effects. However, for the purposes of monitoring the wall for changes in rotational behavior, the existing plan provides a consistent benchmark.

Just as there was consistent behavior for the strain gages on the exterior girders over time, the strand and tilt meters show daily and seasonal cycles with very little drift over their deployment.

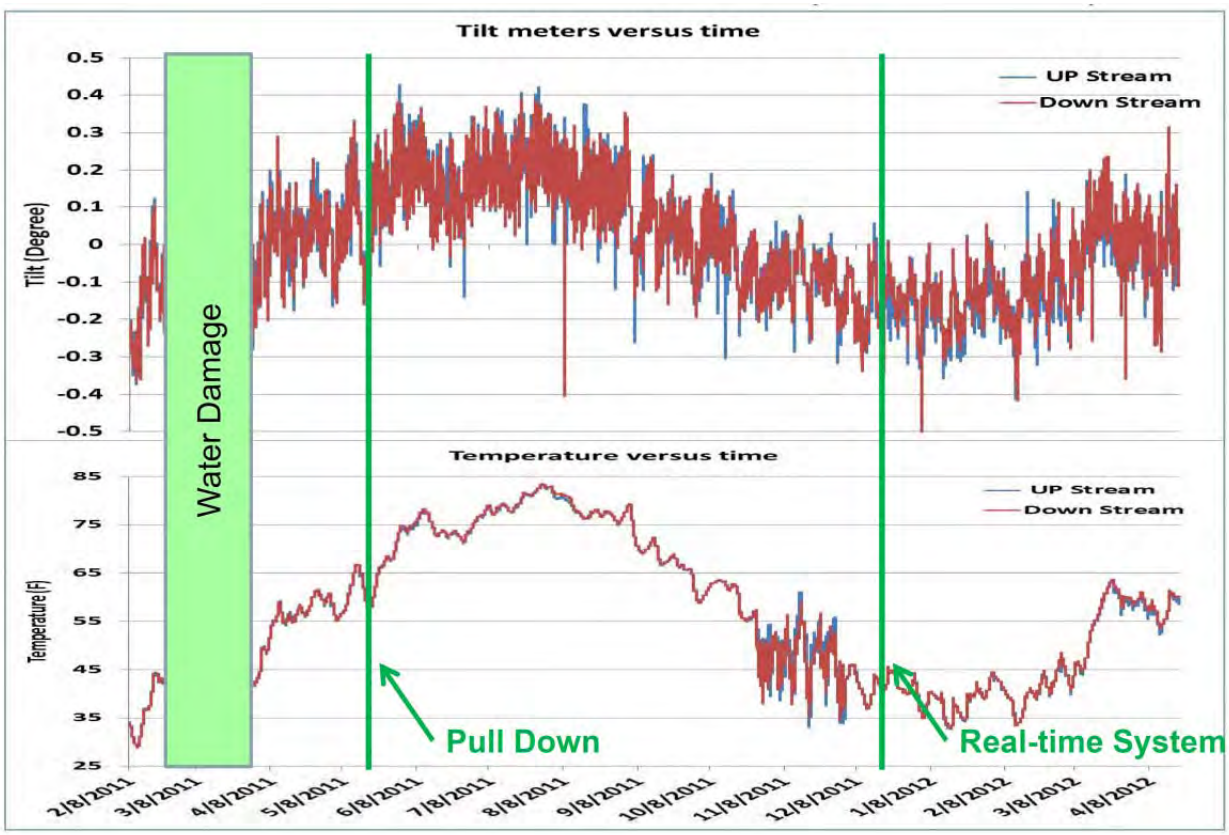

Figure 7.6: Tilt Meter Response with Temperature, USG Bridge (UCII, 2012)

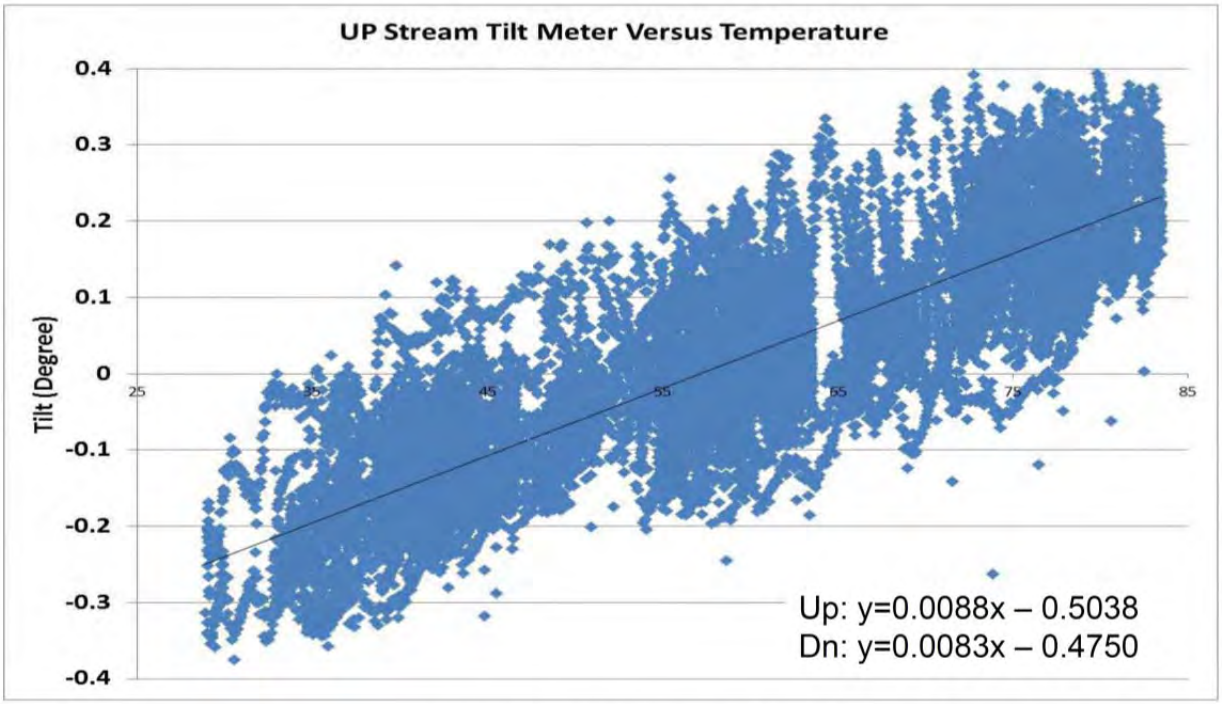

Figure 7.7: Tilt Meter Angle versus Temperature, USG Bridge (UCII, 2012)

7.4 Truckload Test Results

The first step for the static truck load test was to design a set of truck positions or load cases for the bridge. Four standard salt trucks were used, as shown in Table 6.10. As illustrated in Table 6.11, a total of seventeen truck positions were selected. A number of objectives for the truck load test were used to select the positions, but primarily to locate the trucks side-by-side in the two marked traffic lanes and two shoulders, at each instrumented station. These load cases would be staggered with “no load” cases, where the trucks would be moved off the bridge.

As a reminder, the other locations on USG also include welded foil gages which are used during moving load tests in order to measure the entire influence line as the truck crosses the bridge. The strand and tilt meters are vibrating wire based sensors and, hence, can only utilize static truckload tests to benchmark their liveload response. An additional static position was added to the test plan where the back tires of the trucks were located on the bridge but immediately adjacent to the abutment expansion joint.

The trucks were placed in one of the positions from the test plan and at least three readings were recorded from each sensor. It took about 10 minutes to test each position because the CR-10X loggers required about 2 minutes to scan the all of the vibrating wire gages and there was always some delay in positioning the trucks. A set of readings with no load on the bridge was recorded periodically during the test to cancel out any environmental effects in the results.

Figure 7.8 illustrates the measured results of the downstream (right) strand meters over the course of the static truckload tests. The upstream sensor responses had similar results and allowed verification of all the installed gages. Note that this figure appears to yield similar conclusions as that found for the strain gages upon the exterior girders (see Figure 6.6) under static truckload. For example, the gage responses are clearly superimposed upon the daily thermal swing (i.e., the slow decreasing response over the course of the morning). Second, the response is clearly local, as there is very little change for truck positions distant (e.g., 2N and 4N) and get larger as the trucks approach the location of the sensors (i.e., 1S). Last, the three downstream (right) strand meters have very similar responses to most of the truckload positions; any difference between them is hypothesized to be attributed to the difference in the locations of their connection to the edge girders. For example, the exterior strand exhibits a much larger response than the other sensors when the trucks are positioned in the middle of the end span (i.e., 4S); this may be due to it’s lowest connection to the beam and out-of-plane bending of the beam, which is resisted by the upper part of the beam which is embedded in the concrete decking and hence causes less response for the middle and interior strand meters.

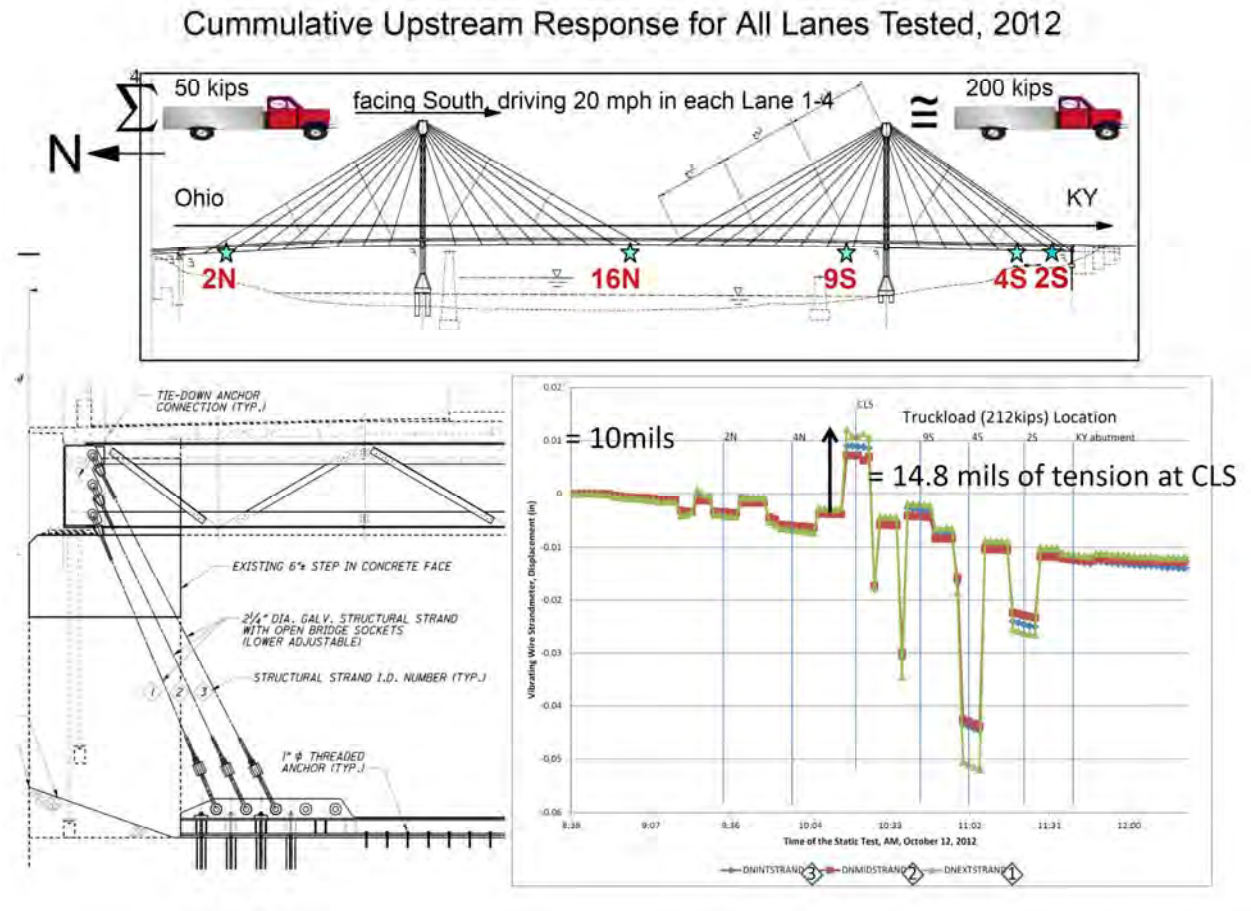

Figure 7.8: Strand Meter Response to Truckload Test, USG Bridge, 2012

These results provide a liveload benchmark of the pulldown sensor package for future reference, and allow some rating analysis for the pulldowns themselves (see next section); however, to our knowledge, there is no design or predicted analytical value with which to make a comparison. Note that the response is compressive when the trucks are located in the span coincident with the sensors and tensile when the trucks are located in the adjacent or middle span of the bridge. Since the strands were pre-tensioned to act as pulldowns, compressive effects are not a concern in damaging the strands and only the tensile response that occurs for trucks located in the middle span needs to be analyzed.

7.5 Rating Analysis and Results

Figure 7.9 provides a rating analysis for the pulldown strands using the largest tensile liveload response of 14.8 mils, which was observed on the exterior strand as a response to the static truckload test of 212 kips. This is of course scaled up to the equivalent linear response of the strand to the full AASHTO HS25 design load of 360 kips.

Rating of the Pulldown Strands using Truckload Test Results

ASTM A586, Grade 1, 2.25" Diameter:

E = 24,000 ksi Modulus
Pult = 620 kips Capacity
Area = 3.0 in^2 Effective

Strandmeter Gage Length = 8"

Measured Truckload = 212 kips
Four HS25 Design Truckload = 360 kips
Liveload = 14.8 mils / 8000" x 24,000ksi / 3in^2 x 360/212 = 25.1 kips

Deadload = 384 kips (interior strand, as per plan sheet 9/18)

Impact Factor = 50'(Span Length + 125') = 0.105

Rating Factor = (Ultimate Capacity – 1.3 x Deadload) / (2.17x(1+IF)xLiveload)
= (620 – 1.3 x 384) / (2.17 x 1.105 x 25.1)
= 2.0

Notes: Truckload used here, but Laneload will control.
This does not include any measured long term environmental response.
If nothing else, these results form a benchmark for future tests.

Figure 7.9: Rating Analysis for Pulldown Strands, USG Bridge, 2012

Note that several assumptions are made here, including the strand specifications tabulated for ASTM standard A586, Grade 1, 2.25" Diameter strand (which provide the material properties shown in the dark blue box in Figure 7.9). Given these properties, the strand would experience 25.1 kips under the full AASHTO HS25 truckload. In addition, we used the pre-tensioning specifications for the pulldown strands listed in the retrofit plans by HNTB for the largest deadload of 384 kips. Last, an impact factor is calculated as per AASHTO for the end span. The load factor rating of the strands was then found to be 2.0 under static truckload; however, we know that laneload will be a larger response and hence control for ratings purposes. Unfortunately, this cannot be estimated directly from the static truckload test results; however, if an analytical version of the laneload were provided for the strands, it could be easily scaled according to these test results and then used for ratings purposes. In any case, we will find that these rating results are comparable to those found using the strain gages on the exterior girders and, hence, the pulldowns are of similar condition to that of the superstructure itself.

7.6 Conclusions and Recommendations

The goal of this part of the project was to install additional instrumentation at KYA on the US Grant bridge to monitor that location and track changes in its state of stress during and beyond the pending retrofit at that location. Vibrating wire gages were to be installed on both of the new upstream and downstream pull downs and at the abutment wall near KYA. Just as there was consistent behavior for the strain gages on the exterior girders over time, the strand and tilt meters show daily and seasonal cycles with very little drift over their deployment.

Figure 7.8 illustrates the measured results of the downstream (right) strand meters over the course of the static truckload tests. Note that this figure appears to yield similar conclusions as that found for the strain gages upon the exterior girders (see Figure 6.6) under static truckload. These results provide a liveload benchmark of the pulldown sensor package for future reference, and allow some rating analysis for the pulldowns themselves. Note that the response is compressive when the trucks are located in the span coincident with the sensors and tensile when the trucks are located in the adjacent or middle span of the bridge. Since the strands were pre-tensioned to act as pulldowns, compressive effects are not a concern in damaging the strands and only the tensile response that occurs for trucks located in the middle span needs to be analyzed.

The load factor rating of the strands was then found to be 2.0 under static truckload; however, we know that laneload will be a larger response and hence control for ratings purposes. Unfortunately, this cannot be estimated directly from the static truckload test results; however, if an analytical version of the laneload were provided for the strands, it could be easily scaled according to these test results and then used for ratings purposes. In any case, we will find that these rating results are comparable to those found using the strain gages on the exterior girders and, hence, the pulldowns are of similar condition to that of the superstructure itself.

REFERENCES

1. A. Helmicki, and V. Hunt, “Proposal for Continued/Enhanced Monitoring and Evaluation of US Grant Bridge During and After Abutment Retrofit,” University of Cincinnati Infrastructure Institute, Cincinnati, OH, 2009.
2. Howard, Needles, Tammen, and Bergendoff (HNTB), Retrofit Design Plans for the U.S. Grant Bridge, 2010.
3. A. Helmicki, and V. Hunt, “Instrumentation of the US Grant Bridge for Monitoring of Fabrication, Erection, In-service Behavior, and to Support Management, Maintenance, and Inspection,” Project Review, ODOT Central Office, 2012.

Chapter 8 Experimental Load Rating using Bridge Long-Term Response

8.1 Introduction

The AASHTO Manual for Condition Evaluation of Bridges suggests “load testing as an effective means of evaluating the structural performance of a bridge or its selected components. This applies particularly to those bridges which cannot be accurately modeled by analysis, or to those whose structural response to live load is in question. Load evaluation tests are made to determine the magnitude and variation of loads and load effects such as those due to traffic, temperature changes and wind. Diagnostic load tests are performed to determine the effect on various components of a known load on the structure. Proof load testing is designed to directly determine the maximum live load that the bridge can support safely.”

The NCHRP Manual for Bridge Rating Through Load Testing [Lichtenstein, 1998] simply suggests that the design rating for the bridge could be scaled by the $K_a = \varepsilon_c/\varepsilon_m$, where ε_t is the maximum strain/stress during the load test and ε_c is its corresponding theoretical strain/stress due to the test vehicle and its position which produced ε_m. If the measured stress is less than expected ($\varepsilon_m < \varepsilon_c$, which is quite often the case due to the many inherent but unconsidered mechanisms for load distribution), then the bridge rating is increased.

The design of a structure is based upon a set of loading conditions which the component or element must withstand. In order to form a consistent national basis for design, organizations such as AASHTO have developed methods for defining component and element capacities and a standard set of loading conditions to be considered against such capacities. In bridge engineering, there are two principal methods for design in use today: working stress and limit states. The intent for both methods is for the entire structure to operate well within the elastic or linear range of the constructed material. The point where a material ceases to behave elastically is defined as the proportional or yield limit. Once stress and strain are no longer proportional, the material enters the plastic range and a permanent deformation will occur to the member.

8.1.1. Working or Allowable Stress Method

For most of the century, the working stress approach was the standard by which bridges and other structural engineering projects were designed. An allowable stress is defined for each structural member to allow a safe margin below the controlling criterion under normal working conditions. Typically, the allowable stress is a fraction of some failure stress for the given material (e.g., yield or buckling stress for steel, compressive strength of concrete, etc.). For steel-stringer bridges, the allowable stress is the yield stress at the bottom flange of the girder (fy as per the design plans or per Table 6.6.2.1-1 of the AASHTO Manual for Condition Evaluation) multiplied by a safety factor (SF, defined below).

8.1.2. Limit States or Load Factor Method

By the 1970's, the limit states approach began to gain acceptance by the general engineering community and especially in the design of concrete structures. Concrete behaves linearly only over about half of its total compressive strength; hence, concrete elements designed under the working stress approach utilize much less than half of their capacity. The limit state approach makes use of the entire plastic range for the design of structural members and incorporates unique safety or load factors (LF, defined below) to account for the inherent variability of each loading configuration. Typically, the ultimate moment is defined to be equal to some failure stress for the given section (e.g., shear or plastic moment) which will vary depending upon the level of composite action between the steel girder and the concrete decking.

A belief that is fairly widespread in the transportation community is that the working stress method is overly conservative in the analysis of bridges. The AASHTO Guide states that the load factor method is intended to recognize "the large safety margins present" in the more conventional working stress method. In general, a well maintained bridge with redundant load paths will have a higher rating by the load factor method than with the working stress method. However, the AASHTO Guide emphasizes the use of site specific data and performance histories in the evaluation of the appropriate load factors for the structure; hence, a deteriorated bridge or a design susceptible to certain failure modes can actually be rated lower by the limit states method as opposed to the rote approach of the allowable stress method. The subjectivity of the limit states approach, therefore, places a great deal of responsibility on the design/test engineer and upon the transportation department as a whole.

8.1.3. Inventory and Operating Load Ratings

A quantitative benchmark of the performance of any highway bridge has been standardized by AASHTO. It is not a magic bullet and its assumptions and limits are well known by the transportation field. The load rating, like inspection data, is only a gauge of bridge condition and a component in an overall profile of the structure. Unlike the inspection data, however, the load rating is calculated using analytical rather than subjective methods. One immediate use for the load rating is in the posting of a bridge (i.e., limiting the type and/or weights of vehicles which may pass over the structure). The load rating may also impact any decisions by the transportation department regarding maintenance, rehabilitation, or replacement of the bridge to meet the local, state, and federal requirements for the highway system.

AASHTO differentiates between lower and upper ranges of bridge performance. The lower or inventory range of performance is meant to imply safe use of the highway bridge on a day-to-day basis "for an indefinite period of time". There are instances, however, when a vehicle has to carry an abnormally large load over the structure. While a structure can withstand these loads on occasion, it is not desirable to have them repeatedly pass over the structure. An upper or operating range of performance is meant to represent the "absolute maximum permissible load level to which the structure may be subjected."

The inventory and operating rating factors (RF) can be calculated using either the allowable stress or the load factor method and are represented by the ratio of the remaining capacity-to-liveload for the specified design load. For allowable stress method, the remaining capacity is considered as the factored yield stress reduced by any permanent loads (i.e., deadload, D, as defined below) upon the structure. For limit states method, the remaining capacity is considered as the ultimate moment reduced by the factored permanent load upon the structure. In the denominator, the liveload (L) is increased by the impact factor and, if appropriate, its load factor. A safe structure necessitates that its rating factor is greater than one.

$$RF = \frac{C - LF_1 \cdot D}{LF_2 \cdot L \cdot (1 + IF)}$$

For the evaluation of rating factor for steel-stringer bridges, the following will be utilized by this research:

For Allowable Stress Method: $LF_1 = LF_2 = 1$
- Inventory Rating: $C = 0.55\ f_y$ (stress), $C = 0.55\ f_y\ S_{LL}$ (moment, M_{ASinv})
- Operating Rating: $C = 0.75\ f_y$ (stress), $C = 0.75\ f_y\ S_{LL}$ (moment, M_{ASopr})

For Load Factor Method: C = ultimate moment, M_{ult}
- Inventory Rating: $LF_1 = 1.3$, $LF_2 = 2.17$
- Operating Rating: $LF_1 = 1.3$, $LF_2 = 1.3$

where S_{LL} = sectional modulus as defined by the appropriate analytical method.

8.1.4. Capacity Assumptions Used to Date

Many of the sections have a bottom flange whose dimensions are such that the section will fail the compression flange check for compact and even braced sections. Many of the sections have lateral bracing (e.g., floorbeams) which does not meet the specification for the compression flange of a compact nor even a braced section. Both of these concerns are with regards to negative moment case. The above was noted at various presentations and discussions with ODOT. See the appendix to Chapter 3 and Section 8.5 for further details.

Negative Ultimate Moment for the unbraced section (see above) was then assumed to be equal to that of the Yield Moment of the steel alone (i.e., girder and reinforcement), irregardless of the status of the composite action for the section. For sensor locations, this assumption would suffice since most of the structure was controlled by positive moment.

Positive Ultimate Moment for a composite section was calculated according to stress block concept (i.e., AASHTO Specification 10.50.1 where the compactness check is found in Eq. 10-129b). Based upon the effective width by B&T, all the composite sections pass and the ultimate moment is set to the plastic limit (Mu = Mp).

8.1.5. Rating Assumptions Used to Date

An inventory HS25 rating using both the allowable stress (see Figures 3.2 and 3.3) and load factor (see Figures 3.6 and 3.7) methods was formulated for both the composite and noncomposite or cracked case for each section as defined by the stations used by both HNTB and B&T. Note that the bridge was designed by load factor design (LFD) method; however, assessment by allowable stress design (ASD) methods will allow consideration of material capacity limits (e.g., cracking of the concrete deck). Those sections where the concrete experiences a state of stress that approaches its allowable limit should not be considered composite but instead as noncomposite or "cracked". For more info, see Chapter 3.

Each section was analyzed by each method at the bottom flange, top flange, cast-in-place (CIP) decking immediately above the edge girder, and for the deck panel adjacent to the edge girder which is to include the effect of the post tensioning (PT) force reported by B&T. Note that the deck and panel ratings are not calculated for the noncomposite or cracked section.

In addition, each of these members was analyzed under both the positive and negative liveload moment reported by HNTB (see Figures 6.1 and 6.2).

Note that all rating formulations were conducted in terms of stresses for consistency. For example, the equations used to convert the deadload moments and axial forces into stresses can be found in the Appendix for Chapter 3.

Initially, the rating formulations were conducted with both bending moment and axial force stresses added together; this allowed both effects to be considered simultaneously. In addition, the axial force is greatly diminished near the abutments and centerline of the structure, which also happens to be the locations of the lowest rated sections of the bridge; so, axial force was only somewhat reducing the controlling rating values.

However, load factor design has commonly separated bending moment and axial force effects in the standard rating calculation. Upon review of the design manuals by HNTB, it seemed that this convention was also intended in the design of this bridge. Given that the axial force was only somewhat affecting the controlling rating values, it was decided to follow this convention.

8.1.6. Inventory and Operating Interaction or Combined Ratings

An interaction or combined rating was also formulated (AASHTO Specification 10.54.2) for compression members with a reduced capacity for buckling concerns. This particular rating was intended for analyzing columns under compression; however, the superstructure of a stay bridge can be considered as such given the axial forces that occur during construction. Again, the buckling stress was assumed to be the yield stress, as above. Interaction ratings were calculated for both top and bottom flange for a composite section and found not to control (see Figure 8.1).

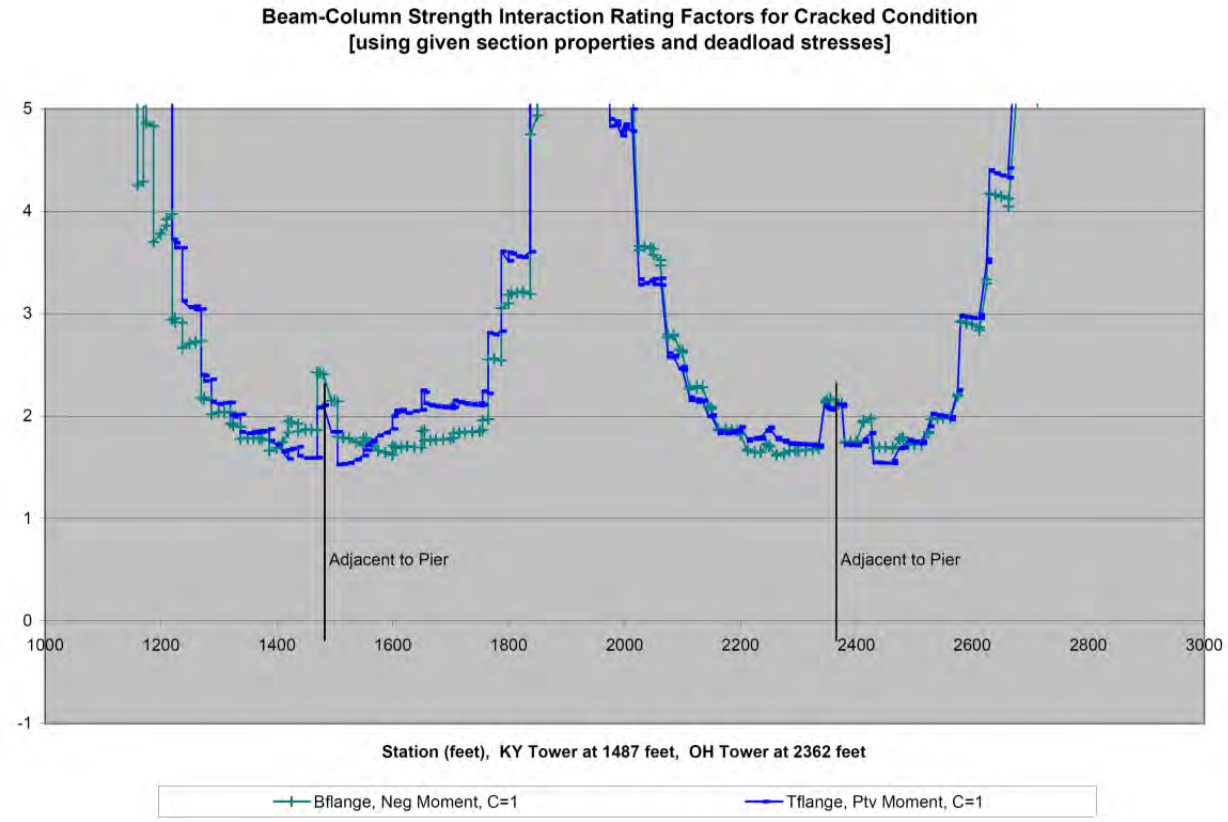

Figure 8.1: Interaction or Combined Rating, USG Bridge (UCII, 2005)

8.1.7. Inventory and Operating Overload Ratings

Note that the Overload case used by the Load Factor Design method (AASHTO Specification 10.57) is not considered in this analysis. It quite often will control rating for structures in the negative moment region, but was not considered here in determining sensor locations (or any subsequent ratings based upon sensor data) in order to maintain consistency in the method.

8.1.8. Multiple Presence Factor

In the AASHTO Specifications, there is the allowance for a reduction in load intensity (Section 3.12), also known as the Multiple Presence Factor (MPF). There is no mention of MPF in the AASHTO Manual for Condition Evaluation of Bridges; only that "when conditions of traffic ... would warrant it, fewer traffic lanes than specified by AASHTO may be considered." For this analysis, we will be conservative and not use MPF.

8.2 Load Factor Inventory Rating at End of Construction (EOC)

Figure 8.2 tabulates both the measured and designed load factor rating at the instrumented sections of the US Grant bridge. Based upon the above assumptions and conventions, an inventory rating of the bridge was formulated using the measured deadload and superimposed deadload (DL) from the vibrating wire strain gages (see Chapter 5), both with and without the measured liveload (LL) response from the moving truckload tests (see Chapter 6), for the instrumented sections at the End of Construction (EOC) in October, 2006. Note that for the column/case marked "DL only", the design liveload was used for the formulation. For the same stations, an inventory rating (shown in blue) was formulated using the analytical estimates of the erected deadload by B&T (version 3) and the design liveload by HNTB for comparison.

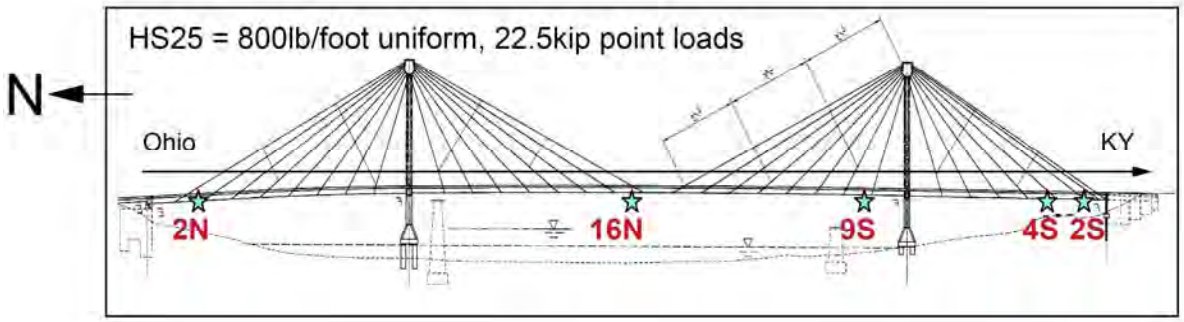

	Rating from Measurements			from Design/Erection Plans	
		DL only	DL & LL	DL from B&T, ver3; LL from HNTB	
2N	+M	1.39	1.56	+M	1.36
	-M	1.11	1.89	-M	1.20
16N	+M	1.14	1.11 ← much smaller due to DL change	+M	1.49
9S	-M	1.99	3.05 ← much larger due to LL change	-M	1.95
4S	+M	1.67	2.18	+M	1.66
2S	-M	1.45	6.93	-M	1.13

* +M = Pos. LL Moment, Composite Section, -M = Neg. LL Moment, Cracked Section

* No axial forces included.

Figure 8.2: Inventory HS25 Load Factor Rating, P=0, EOC, US Grant Bridge (UCII, 2007)

In Figure 8.2, note how similar the measured and design/erection ratings are for the case of "DL only", except at locations 2S and 16N. This indicates that the deadloads were close to that expected by the erection plan, as discussed in Chapter 5 (see Table 5.1); however, the one outlier (with Table 5.1) is location 9S, which has comparable measured and predicted deadload only when you remove the axial force effect (as is done here). When you include the liveloads, the measured and designed ratings diverge considerably, which causes the measured ratings to be considerably higher in comparison, except at 16N. As discussed in Chapters 6 and 7, these differences will moderate significantly with the future repairs/retrofit at the Kentucky abutment.

A point of interest to note for Figure 8.1 is that no seasonal (i.e., long-term thermal, and other) effects are included in this EOC rating of the bridge. At EOC, the daily thermal cycle is rather small and averaged into the deadload with little effect; however, there has not been enough long-term data collected to sufficiently characterize any long-term effects.

As discussed above, an effort has been made to remove the effect of axial force from these load factor ratings. This involved subtracting the deadload stress caused by the estimated axial force at EOC by B&T (see Figure 5.2) from the measured stresses by the vibrating wire strain gages, as their reading cannot distinguish between moment and axial force. This requires using their assumption of effective width/area applied to axial force effects (see Figure 3.5), as no controlled experiments to determine such were possible during the construction process. It should be noted here that we could have alternatively calculated the axial force effects by using this or another assumed effective area and the geometry employed by the gages in the section; however, since the measured and predicted deadloads were mostly in agreement, we simply used the predicted values for axial force. In Figure 5.2, note that axial force during construction is small near both abutments and midspan (i.e., 2S, 2N, 16N) and relatively small compared to the moment at 9S; hence, the correction for axial force effect will be relatively small at most locations except 4S. As axial force during construction causes compression throughout the section, the result of subtracting its effects upon positive liveload moment regions is to increase or improve the rating (and vice versa, see Table 8.1). Also, note that there is little to no axial force effect assumed within liveload response (see Figure 6.1 and 6.2); hence, no correction of the measured liveload values for axial force effect is conducted here.

Table 8.1 provides the inventory ratings at the instrumented sections if no adjustment is done to the deadload for axial force effects.

No P	DL only	DL & LL		No adjust	DL only	DL & LL
2N +M	1.39	1.56		2N +M	1.50	1.70
2N –M	1.11	1.89		2N –M	1.01	1.87
16N +M	1.14	1.11		16N +M	1.24	1.17
9S –M	1.99	3.05		9S –M	2.00	2.85
4S +M	1.67	2.18		4S +M	1.85	2.52
2S –M	1.45	6.93		2S –M	1.16	6.65

Table 8.1: Inventory HS25 Load Factor Rating, With and Without P, EOC, US Grant Bridge

Note that all of the above ratings were controlled by the bottom flange analysis. Since the section remains composite under liveload (see Figures 6.7, 6.9, 6.18, 6.27, etc.), the measured response for the deck and at the top flange is near zero because it is near the neutral axis of the composite section; hence, its associated ratings will be very large compared to those for the bottom flange. As a reminder, the "Cracked" non-composite limit state was examined in Chapter 3 and the bottom flange was found to still control the rating because it is assumed the deck reinforcement would absorb some of the stress at the top of the section (see Figure 3.7).

8.3 Load Factor Inventory Rating after Initial Service, before Retrofit

Figure 8.3 tabulates both the measured and designed load factor rating at the instrumented sections of the US Grant bridge. Based upon the above assumptions and conventions, an inventory rating of the bridge was formulated using the measured deadload and superimposed deadload (DL) from the vibrating wire strain gages (see Chapter 5), both with and without the measured liveload (LL) response from the moving truckload tests (see Chapter 6), for the instrumented sections in March, 2009 (i.e., after initial repairs at the Kentucky abutment, but before installation of exterior pulldowns). Note that for the column/case marked "DL only", the design liveload was used for the formulation. For the same stations, an inventory rating (shown in blue) was formulated using the analytical estimates of the erected deadload by B&T (version 3) and the design liveload by HNTB for comparison. Note that the blue design ratings are the same as shown previously in Figure 8.2, but the black ratings based upon measurements are updated for this table.

In Figure 8.3, note how similar the measured and design/erection ratings are for the case of "DL only", except at location 9S. This indicates that the deadloads were close to that expected by the erection plan, as discussed in Chapter 5 (see Table 5.2); however, the one outlier (with Table 5.2) is location 9S, which has comparable measured and predicted deadload only when you retain the axial force and composite action effect (as is done in Table 5.2). To be conservative in rating analysis, we assume here the "Cracked" noncomposite case in regions of negative liveload moment (as is indicated at the bottom of Figures 8.2 and 8.3). For locations 2S and 2N, the predicted bottom flange stress is similar for either composite or noncomposite cases when the axial force effect is removed (i.e., P=0); however, for location 9S, the predicted bottom flange stress assumed by design is quite different for composite (i.e., -1.4ksi for P=P, from Table 5.2) and noncomposite cases (i.e., +6.1ksi, where P=0). The measured deadload at location 9S was closer to the noncomposite case in 2006 and closer to the composite case in 2009. This explains why the rating for location 9S for the "DL only" case was close to design in Figure 8.2 and not in Figure 8.3.

When comparing the "DL only" case with Figure 8.2, note that locations 16N, 9S, and 2S have changed significantly; 16N and 2S are now more comparable with the design rating, while 9S is now quite lower than the predicted design rating. With regards to 16N, the rating increased compared to past results as it was finally determined that the sensor upon which this deadload

was based (i.e., 1934CLSBI) was suspicious since the parapet construction. With regards to all other locations, this decrease in 2009 from 2006 ratings is attributed to several long-term effects and events that were not included within the EOC data: seasonal cycle upon the bridge (e.g., thermal, boundary conditions), creep and shrinkage effects on the concrete CIP joint, the initial repairs at the Kentucky abutment, etc. Of these, the main effect was the seasonal cycle.

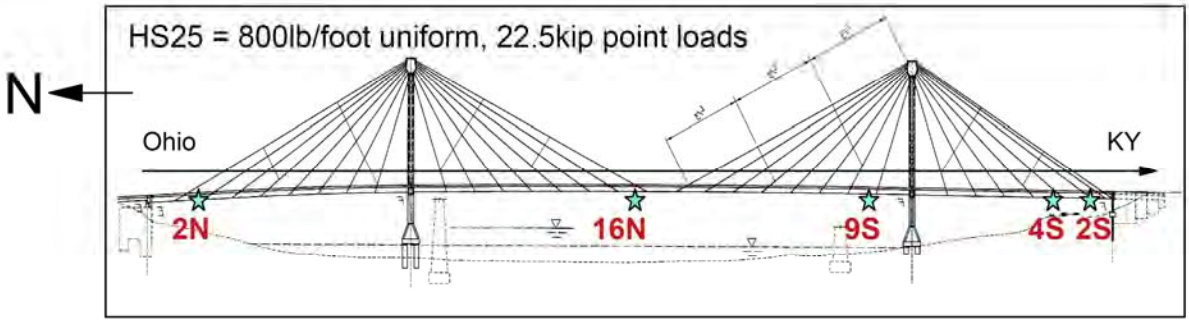

	Rating from Measurements			from Design/Erection Plans	
		DL only	DL & LL	DL from B&T, ver3; LL from HNTB	
2N	+M	1.23	1.40	+M	1.36
	-M	1.03	1.60	-M	1.20
16N	+M	1.39	1.74	+M	1.49
9S	-M	1.32	1.92	-M	1.95
4S	+M	1.62	2.24	+M	1.66
2S	-M	1.15	1.18	-M	1.13

* +M = Pos. LL Moment, Composite Section, -M = Neg. LL Moment, Cracked Section

* No axial forces included.

Figure 8.3: Inventory HS25 Load Factor Rating, P=0, 2009, US Grant Bridge (UCII, 2009)

As documented in Chapter 6, the measured liveload response in 2009 was considerably less than predicted by design, except at location 2S where it is similar to design. Recall that the measured liveload response in 2006 was considerably less than predicted by design, except at location 16N where it was a bit more than design. So, the effect of liveload (e.g., when comparing the “DL only” case versus the “DL & LL” case for measurements) was flipped for 2S and 16N compared to design between these two cases and as shown in Figures 8.2 and 8.3. The reason for this result is attributed to the initial repairs to the Kentucky abutment. See Chapter 6 for additional details.

When you include the liveloads (i.e., “DL & LL” case in Figure 8.3), the measured ratings are slightly higher than the designed ratings, except at 9S and 2S where they are similar to design. As noted above, the reasons for each are different: measurements at location 9S suggest a higher deadload and lower liveload compared to the noncomposite design which offset each other in the ratings analysis; whereas location 2S has both similar deadload and liveload compared to design.

As discussed in Section 8.2, an effort has been made to remove the effect of axial force from these load factor ratings. This involved subtracting the deadload stress caused by the estimated axial force at EOC by B&T (see Figure 5.2) from the measured stresses by the vibrating wire strain gages, as their reading cannot distinguish between moment and axial force. Table 8.2 provides the inventory ratings at the instrumented sections for 2009 if no adjustment is done to the deadload for axial force effects.

No P	DL only	DL & LL		No adjust	DL only	DL & LL
2N +M	1.23	1.40		2N +M	1.36	1.52
2N –M	1.03	1.64		2N –M	0.94	1.58
16N +M	1.39	1.74		16N +M	1.49	1.80
9S –M	1.32	1.94		9S –M	1.28	1.73
4S +M	1.62	2.24		4S +M	1.66	2.61
2S –M	1.15	1.18		2S –M	0.91	1.12

Table 8.2: Inventory HS25 Load Factor Rating, With and Without P, 2009, US Grant Bridge

Note that all of the above ratings were controlled by the bottom flange analysis. Since the section remains composite under liveload (see Figures 6.7, 6.9, 6.18, 6.27, etc.), the measured response for the deck and at the top flange is near zero because it is near the neutral axis of the composite section; hence, its associated ratings will be very large compared to those for the bottom flange. As a reminder, the “Cracked” non-composite limit state was examined in Chapter 3 and the bottom flange was found to still control the rating because it is assumed the deck reinforcement would absorb some of the stress at the top of the section (see Figure 3.7).

8.4 Load Factor Inventory Rating after Retrofit

During our Project Review with ODOT in 2009, we were asked to report ratings in two distinct fashions: 1) deadload based only upon EOC structural condition, and 2) deadload which incorporates both EOC structural condition and any/all other long-term effects and events that were not included within the EOC data: seasonal cycle upon the bridge (e.g., thermal, boundary conditions), creep and shrinkage effects on the concrete CIP joint, the initial repairs at the Kentucky abutment, etc. Of these, the main effect is the seasonal cycle; however, all are actual measured stresses that would constitute a reduction in capacity and lead to the most conservative estimate of the load rating. Each is given its own subsection below.

8.4.1. Analysis using only Structural Deadloads at EOC

Figure 8.4 tabulates both the measured and designed load factor rating at the instrumented sections of the US Grant bridge. Based upon the above assumptions and conventions, an inventory rating of the bridge was formulated using the measured deadload and superimposed deadload (DL) from the vibrating wire strain gages at the end of construction (see Table 5.1), with the measured liveload (LL) response from the moving truckload tests in March, 2009 (ratings shown in columns 4 and 5 for negative and positive liveload moment cases, respectively) and October, 2012 (ratings shown in columns 6 and 7 for negative and positive liveload moment cases, respectively). For the same stations, a design rating was formulated using the analytical estimates of the erected deadload by B&T (version 3) and the design liveload by HNTB for comparison. Note that the design ratings are the same as shown previously in Figures 8.2 and 8.3.

Note that the "DL only" case used in Figures 8.2 and 8.3 is removed from this tabulation for simplicity. Further, the goal of this subsection is to fix the deadload to EOC condition and only examine the effect of changes in liveload response upon the ratings.

Load Factor Inventory Rating, US Grant Bridge, 2012
(Deadload considers only Structural EOC)

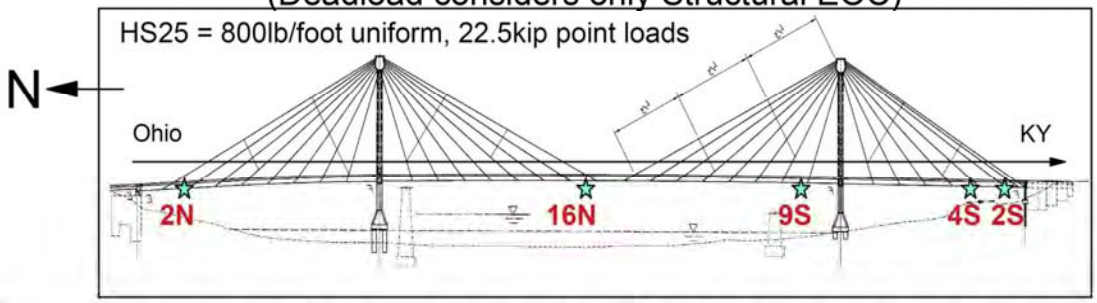

Table of Rating Factors, Composite Section for +M, Cracked Section for –M, No Axial Forces

Segment	Design –M LL	Design +M LL	2009 –M LL	2009 +M LL	2012 –M LL	2012 +M LL
2N	1.20	1.36	1.73	1.55	1.38 ↓	1.83 ↑
16N		1.49		1.44		1.47
9S	1.95		2.91		3.23	
4S		1.66		2.31		2.45
2S	1.13 DL from B&T, ver3; LL from HNTB.		1.49 DL measured at EOC; LL measured as listed.		1.26 ↓	Controls

Figure 8.4: Inventory HS25 Load Factor Rating, Structural DL Only, P=0, US Grant Bridge

In Figure 8.4, note that the measured ratings are higher than the design/erection ratings, except at location 16N. In general, the deadloads are similar between measurements and design, but the measured liveload is significantly lower than expected by design. For location 16N, these lower liveloads are offset by a higher measured deadload in 2006 as compared to design such that the rating between design and measurement are similar. Note that this deadload at 16N was later discounted in 2009 when the sensor upon which this deadload was based (i.e., 1934CLSBI) was finally determined to be suspicious since the parapet construction. If one were to use the discounted deadload at 16N, then all ratings based upon measurements would be higher than those by design.

As documented in Chapter 6, the measured liveload response in 2012 was similar to the 2009 results, except at locations 2N, 9S, and 2S. For location 2S, the increase in laneload stress is due to the change in the overall shape of the influence line (like the changes observed in Figure 6.26). This change is exhibited over all four lanes, and is hypothesized to have occurred due to the transverse bracing added above the new pulldowns. For location 2N, a compressive change in the influence line occurs primarily due to the response of distant lanes for a given edge girder, much like that observed at station 2S; however, there has been no rehab work done nor signs of visible deterioration occurring at the Ohio abutment to explain this change. For location 9S, the laneload response has been slowly decreasing over the years again due to slight changes in the influence response of distant lanes for a given edge girder. We recommend continued inspection at these locations. See Chapter 6 for additional details.

As discussed in Section 8.2, an effort has been made to remove the effect of axial force from these load factor ratings. This involved subtracting the deadload stress caused by the estimated axial force at EOC by B&T (see Figure 5.2) from the measured stresses by the vibrating wire strain gages, as their reading cannot distinguish between moment and axial force. Table 8.3 provides the inventory ratings at the instrumented sections for 2012 if no adjustment is done to the deadload for axial force effects.

No P	2009	2012		No adjust	2009	2012
2N +M	1.55	1.83		2N +M	1.69	2.00
2N –M	1.73	1.38		2N –M	1.71	1.37
16N +M	1.44	1.47		16N +M	1.51	1.53
9S –M	2.91	3.23		9S –M	2.71	3.01
4S +M	2.31	2.45		4S +M	2.67	2.84
2S –M	1.49	1.26		2S –M	1.43	1.21

Table 8.3: Inventory HS25 Load Factor Rating, EOC DL Only, Both P, 2012, US Grant Bridge

8.4.2. Analysis using both Structural and Long-Term Environmental Deadloads to Date

Figure 8.5 tabulates both the measured and designed load factor rating at the instrumented sections of the US Grant bridge. Based upon the above assumptions and conventions, an inventory rating of the bridge was formulated using the measured deadload and superimposed deadload (DL) from the vibrating wire strain gages before and after the retrofit (see Tables 5.2 and 5.3), with the measured liveload (LL) response from the moving truckload tests in March, 2009 (ratings shown in columns 4 and 5 for negative and positive liveload moment cases, respectively) and October, 2012 (ratings shown in columns 6 and 7 for negative and positive liveload moment cases, respectively). For the same stations, a design rating was formulated using the analytical estimates of the erected deadload by B&T (version 3) and the design liveload by HNTB for comparison. The design ratings are the same as shown previously.

Note that the "DL only" case used in Figures 8.2 and 8.3 is removed from this tabulation for simplicity. The changes in deadload and their effect upon the rating between 2006 and 2009 are discussed above. The deadloads remain relatively similar between 2009 and 2012 (as shown in Table 5.3) with the exception at location 2S due to the installation of the exterior pulldowns. Hence, the goal of this subsection is to examine the effect of changes in both measured deadload and liveload over time as compared to design ratings.

Load Factor Inventory Rating, US Grant Bridge, 2012
(Deadload considers Net Structural + Environmental)

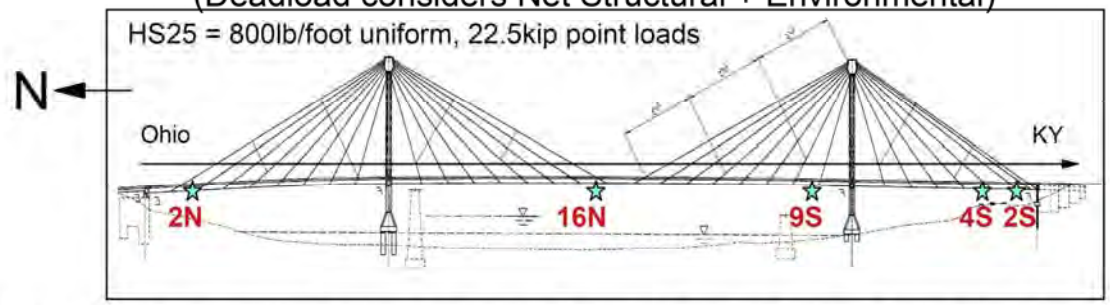

Table of Rating Factors, Composite Section for +M, Cracked Section for –M, No Axial Forces

Segment	Design –M LL	Design +M LL	2009 –M LL	2009 +M LL	2012 –M LL	2012 +M LL
2N	1.20	1.36	1.60	1.38	1.28 ↓	1.93 ↑
16N		1.49		1.74		1.73
9S	1.95		1.93		2.68	
4S		1.66		2.24		2.38
2S	1.13		1.18		1.15 ↓	Controls

DL from B&T, ver3; LL from HNTB.

DL measured thru date listed; LL measured as listed.

Figure 8.5: Inventory HS25 Load Factor Rating, Structural +LT DL, P=0, US Grant Bridge

In Figure 8.5, note that the measured ratings are slightly higher than the design/erection ratings at all locations. This is because all of the long-term effects are now included within the analysis for the measured results, whereas the design does not include them; however, it must again be noted that these long-term stresses are actually measured and a truly conservative rating should include them in its assessment. Hence, the controlling ratings are all lower than those found in Figure 8.6.

As documented in Chapter 6, the measured liveload response in 2012 was similar to the 2009 results, except at locations 2N, 9S, and 2S. For location 2S, the increase in laneload stress is due to the change in the overall shape of the influence line (like the changes observed in Figure 6.26). This change is exhibited over all four lanes, and is hypothesized to have occurred due to the transverse bracing added above the new pulldowns. For location 2N, a compressive change in the influence line occurs primarily due to the response of distant lanes for a given edge girder, much like that observed at station 2S; however, there has been no rehab work done nor signs of visible deterioration occurring at the Ohio abutment to explain this change. For location 9S, the laneload response has been slowly decreasing over the years again due to slight changes in the influence response of distant lanes for a given edge girder. We recommend continued inspection at these locations. See Chapter 6 for additional details.

As discussed in Section 8.2, an effort has been made to remove the effect of axial force from these load factor ratings. This involved subtracting the deadload stress caused by the estimated axial force at EOC by B&T (see Figure 5.2) from the measured stresses by the vibrating wire strain gages, as their reading cannot distinguish between moment and axial force. Table 8.4 provides the inventory ratings at the instrumented sections for 2012 if no adjustment is done to the deadload for axial force effects.

No P	2009	2012		No adjust	2009	2012
2N +M	1.38	1.93		2N +M	1.52	2.10
2N –M	1.60	1.28		2N –M	1.58	1.27
16N +M	1.74	1.73		16N +M	1.80	1.79
9S –M	1.93	2.68		9S –M	1.73	2.46
4S +M	2.24	2.38		4S +M	2.61	2.77
2S –M	1.18	1.15		2S –M	1.12	1.10

Table 8.4: Inventory HS25 Load Factor Rating, EOC +LT DL, Both P, 2012, US Grant Bridge

Note that all of the above ratings were controlled by the bottom flange analysis. Since the section remains composite under liveload (see Figures 6.7, 6.9, 6.18, 6.27, etc.), the measured response for the deck and at the top flange is near zero because it is near the neutral axis of the composite section; hence, its associated ratings will be very large compared to those for the bottom flange. As a reminder, the “Cracked” non-composite limit state was examined in Chapter 3 and the bottom flange was found to still control the rating because it is assumed the deck reinforcement would absorb some of the stress at the top of the section (see Figure 3.7).

8.5 Load Factor Inventory Rating after Retrofit using Reduced Capacity

In 2010, the designer HNTB provided a draft of their Bridge Analysis and Rating Report for the U.S. Grant Bridge to ODOT. A global model of the entire structure was used to calculate the internal demand forces for various structural components of the bridge, including the edge girders, cable stays, deck panels, floor and strut beams. The deadloads were taken from the final erection analysis (2010) by B&T, based upon the as-built conditions, as compared to their earlier estimates which we have used in the above sections of this report (see Figure 8.6). In addition, HNTB simulated the deadload effect from the installed pulldowns near the Kentucky abutment. The liveload for the structure was refined by HNTB over their earlier estimates, which we have used in the above sections of this report (see Figure 8.7).

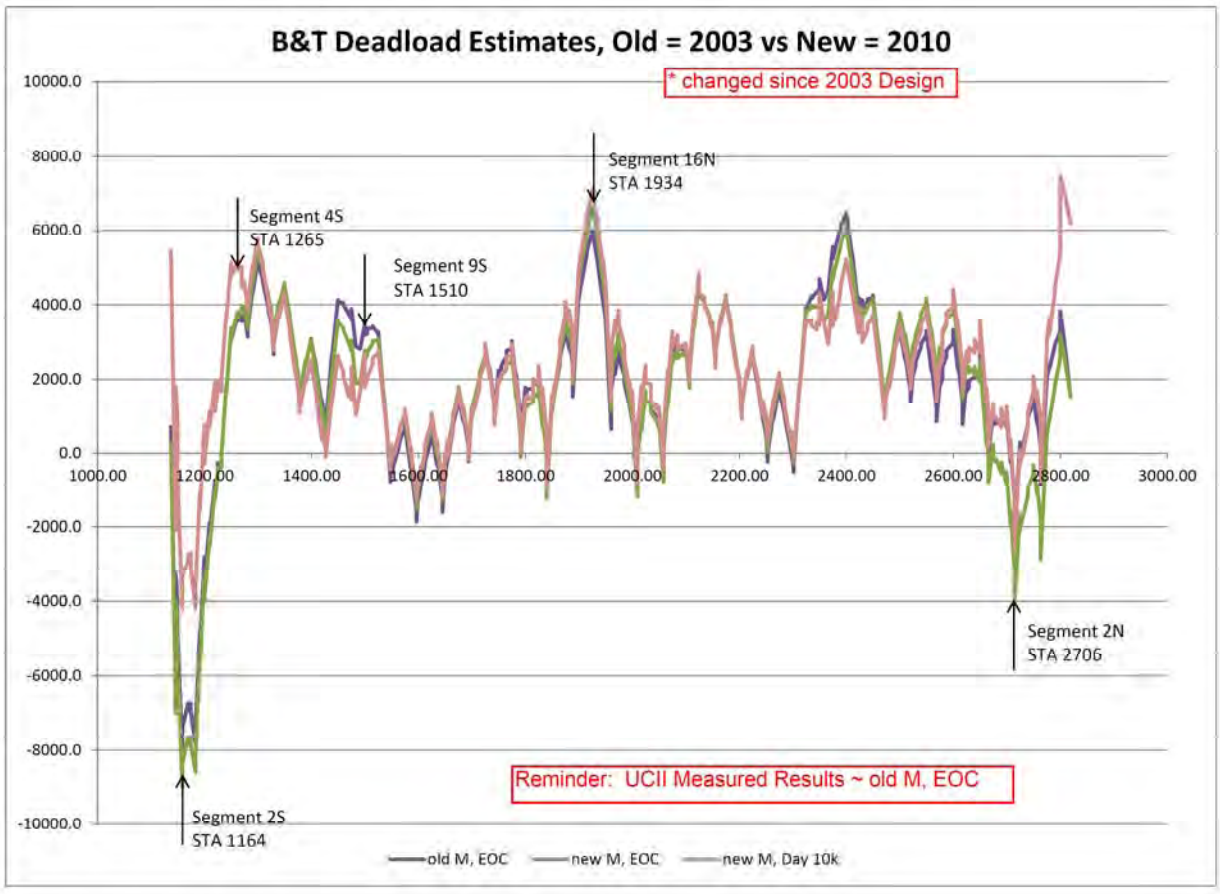

Figure 8.6: Initial, As-Built, and Day 10K Estimates of Deadload Moment, US Grant Bridge (B&T)

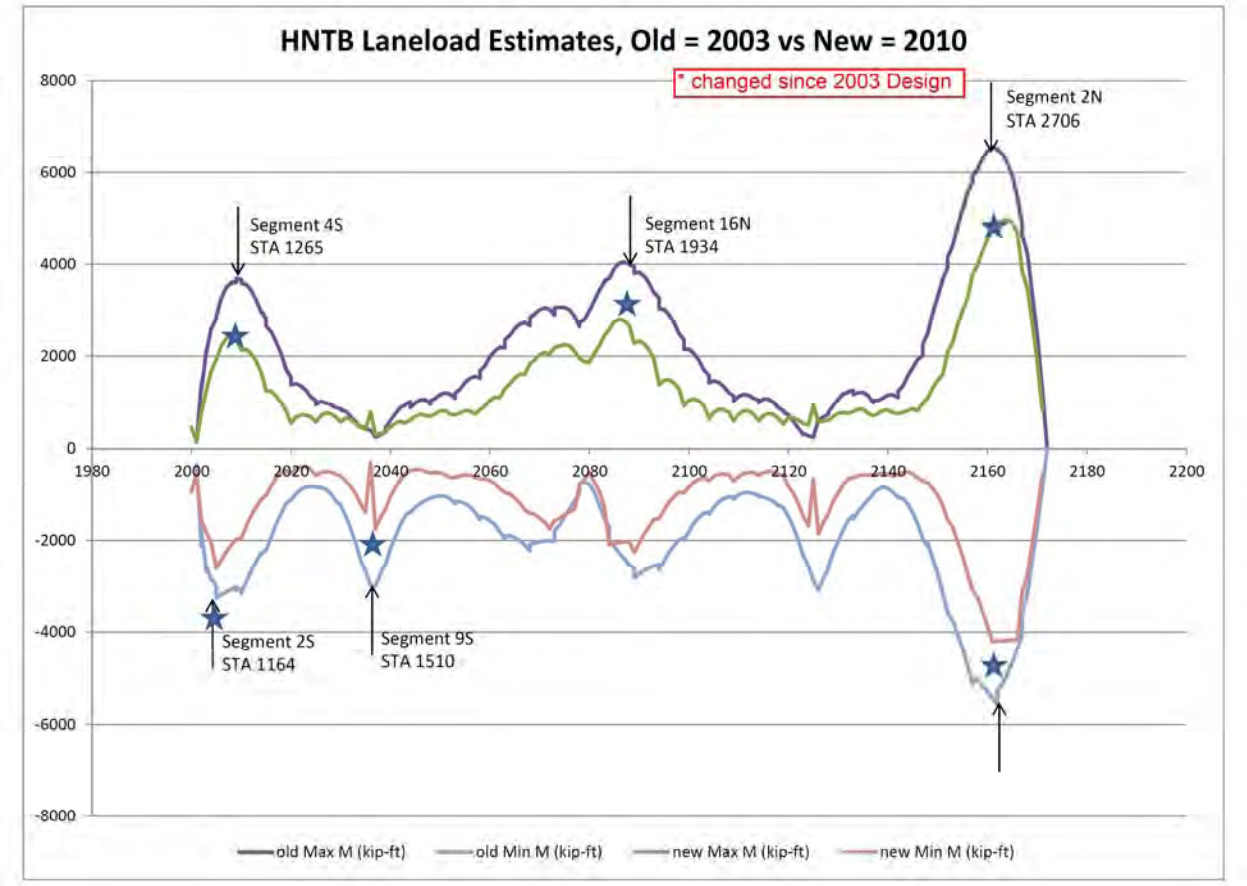

Figure 8.7: Initial and As-Built Estimates of Liveload Moment, US Grant Bridge (HNTB)

In their rating report, HNTB reported that the bridge just barely reached an HS20 inventory rating using Load Factor Method, with the most critical location identified as the West Girder of Segment 15N. This included a distribution factor (DF) of 1.74, an impact factor (IF) for the laneload of 1.1, and a multiple presence factor (MPF) of 0.9 for 4 lanes of traffic. Please note that the MPF is already included within their DF. Segment 15N is adjacent to one of our instrumented sections (16N), as it was identified by our earlier analysis that the very middle of the structure would indeed be the most critical area of the bridge for positive moment; however, our analytical ratings above were much larger than this result. Given that our deadloads and liveloads are not sufficiently different to cause such a reduction in our ratings, the reduction must come from capacity (see Appendix to Chapter 3 for more details).

In 2011, HNTB provided a written a draft of their Manual for Load Rating and Permits for the U.S. Grant Bridge to ODOT. This submission also included a set of linked Excel worksheets which allowed for the entry of pre-defined and user-defined vehicle information (e.g., axle spacing and weights) as well as impact factors such that load rating could be achieved for permit purposes of special overload cases. In the file called GirderRating_HS20_2010.XLS, it seems as if the edge girders fail various capacity checks in various tabs (e.g., I-fact (beg) (crack)). Most commonly, the segments do not pass the lateral bracing check for a braced noncompact section (see Equation 10-101 and Table 10.48.2.1A, AASHTO Specifications).

Back of Envelope Calculation for Capacity at 2S for USG using Plans Only

Segment labelled as "Cracked" = Noncomposite
because the concrete decking does not pass the allowable stress rating.
Then:

	Width,b	Thickness,t	b/t	Compactness Check	
Bottom Flange	30"	2.5"	12	< 18.4, for fy=50	PASS
Top Flange	17.5"	2.25"	7.8	< 18.4, for fy=50	PASS

	Depth,D	Thickness,t	D/t	Compactness Check	
Web	75"	1"	75	< 86, for fy=50	PASS

Bracing	Distance,L	Radius Gyration,r	L/b	Compactness Check	
Noncomposite	300"	6.72"	45	< 28, for M1=Mu	FAIL

Bracing, Noncomp	Area, A	Beam Depth,d	Ld/A	Braced Check	
Bottom Flange	75 sqin	79.75"	319 < 400, for fy=50		PASS
Top Flange	39 sqin	79.75"	613 < 400, for fy=50		FAIL

For Negative Moment, use the Yield Capacity and
For Positive Moment, use the Unbraced Capacity by Equation 10-103c.

?

which is what I was doing to date with the rating of Negative Moment regions.

Figure 8.8: Beam Checks, Segment 2S, Negative Moment, US Grant Bridge (UCII, 2013)

Back of Envelope Calculation for Capacity at CLS for USG using Plans Only

Segment labelled as "Cracked" = Noncomposite
because the concrete decking does not pass the allowable stress rating.
Then:

	Width,b	Thickness,t	b/t	Compactness Check	
Bottom Flange	30"	1.75"	17	< 18.4, for fy=50	PASS
Top Flange	17.375"	1.75"	10	< 18.4, for fy=50	PASS

	Depth,D	Thickness,t	D/t	Compactness Check	
Web	75"	1.25"	60	< 86, for fy=50	PASS

Bracing	Distance,L	Radius Gyration,r	L/b	Compactness Check	
Noncomposite	300"	6.05"	50	< 28, for M1=Mu	FAIL

Bracing, Noncomp	Area, A	Beam Depth,d	Ld/A	Braced Check	
Bottom Flange	53 sqin	79.75"	453 < 400, for fy=50		FAIL
Top Flange	30 sqin	79.75"	800 < 400, for fy=50		FAIL

For both cases, use the Unbraced Capacity by Equation 10-103c.

?

Figure 8.9: Beam Checks, Segment CLS, Positive Moment, US Grant Bridge (UCII, 2013)

In addition to the lateral bracing check, many segments of the edge girders due not pass the compression flange check for the bottom flange (see Equation 10-93 and 10-100, Tables 10.48.1.2A and 10.48.2.1A, AASHTO Specifications).

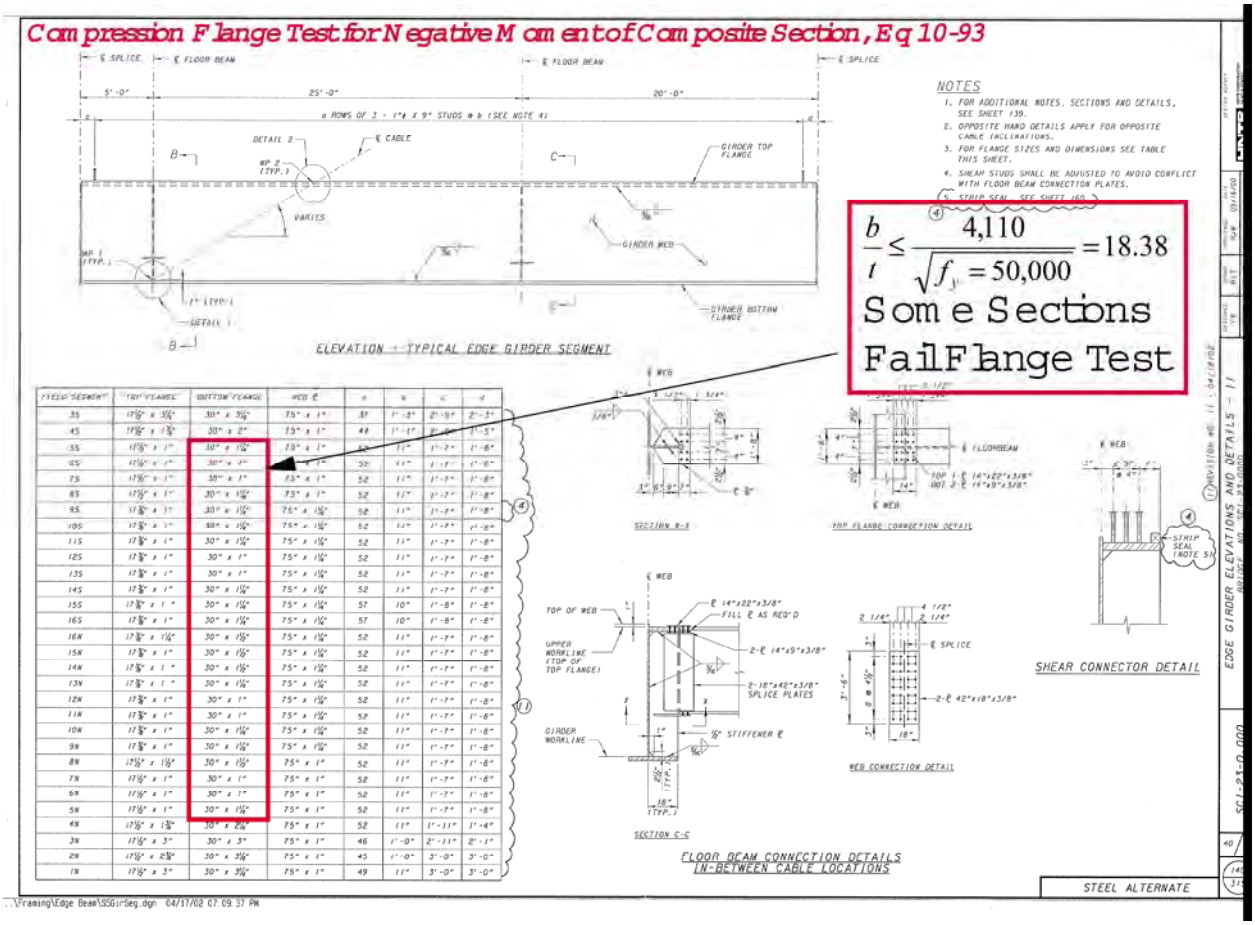

Figure 8.10: Compression Flange Test, Edge Girder Segments, US Grant Bridge (UCII, 2004)

The lateral bracing check fails due to the large spacing between the floorbeams for lateral bracing of the edge girders. Note that this is traditionally not applied to a composite section in positive moment, as the compression flange (i.e., the top flange) is braced by the composite concrete decking; however, this file found that most segments failed this capacity check, irregardless of its moment. It is surmised that the designers chose to be conservative and simply assumed a noncomposite or "cracked" case for all segments such that no bracing is provided by the decking in this regard. Hence, the capacity is reduced in the file GirderRating_HS20_2010.XLS to that computed for a partially braced member (see Equation 10-103c, AASHTO Specifications). Unfortunately, it is not entirely clear as to which reduced capacity of several listed is considered in their rating; so, to be conservative, we will assume here the smallest value listed for a given segment in Column AM (entitled "Final Mr for Unbraced Compression Flange") for the capacity of the edge girder segments and subsequent load factor ratings shown in Figures 8.11 through 8.13.

It must also be noted that HNTB states in their Manual that temperature and time dependent effects such as shrinkage, creep, and losses were considered in their analysis. In addition, the deadload and PT forces are taken at day 10,000 to account for the end of pre-stress losses; however, this is not the worst-case scenario at many locations of the structure (e.g., most notably at the very critical KYAL segment due to the very large negative moment from the pulldowns embedded in the Kentucky abutment during construction, which is relaxed over time due to long term effects). As in the above ratings, we will analyze the present structure (i.e., not Day 10,000) based upon measured sensor and test results to date.

An initial or draft calculation of the ratings with these reduced capacities was conducted and presented to ODOT in 2013. As with a similar prior teleconference with HNTB, it was decided that the analysis should only consider the marked lanes (and not the two large shoulders) as per the old Ohio Bridge Manual (see Section 902.5, Bridge Design Manual, ODOT, 2003). In addition, the bridge would now be considered only for HS20 laneload.

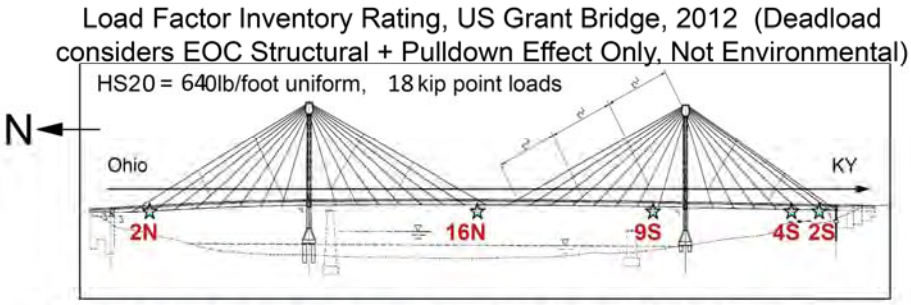

Table of Rating Factors, UnBraced Capacity for both +M and –M, No Axial Forces

Segment	2012 –M LL	2012 +M LL
2N	1.49	2.30
16N		1.61
9S	5.01	
4S		2.05
2S	1.61	

2 Marked Lanes only.
HS20 Laneload (not HS25).

DL measured thru 2012.
LL measured in 2012 by test.

Capacity reduced due to
Failed lateral bracing beam check.
Capacity taken from HNTB files as
Mr for Unbraced Compression Flange.

Figure 8.11: Inventory HS20 LF Rating, Structural DL Only, P=0, US Grant Bridge (UCII, 2013)

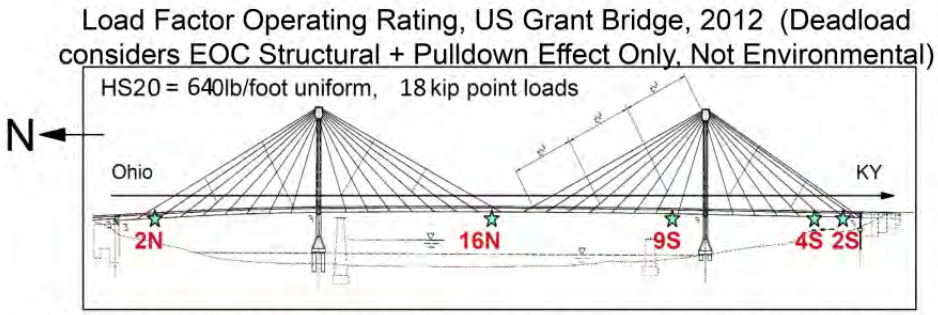

Table of Rating Factors, UnBraced Capacity for both +M and –M, No Axial Forces

Segment	2012 –M LL	2012 +M LL
2N	2.49	3.83
16N		2.69
9S	8.40	
4S		3.41
2S	2.69	

2 Marked Lanes only.
HS20 Laneload (not HS25).

DL measured thru 2012.
LL measured in 2012 by test.

Capacity reduced due to
Failed lateral bracing beam check.
Capacity taken from HNTB files as
Mr for Unbraced Compression Flange.

Figure 8.12: Operating HS20 LF Rating, Structural DL Only, P=0, US Grant Bridge (UCII, 2013)

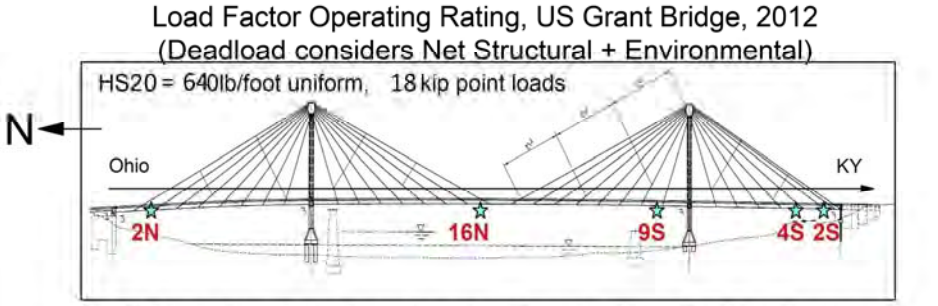

Table of Rating Factors, UnBraced Capacity for both +M and –M, No Axial Forces

Segment	2012 –M LL	2012 +M LL
2N	2.14	4.29
16N		1.29
9S	6.23	
4S		3.14
2S	1.37	

2 Marked Lanes only.
HS20 Laneload (not HS25).

DL measured thru 2012.
LL measured in 2012 by test.

Capacity reduced due to
Failed lateral bracing beam check.
Capacity taken from HNTB files as
Mr for Unbraced Compression Flange.

Figure 8.13: Operating HS20 LF Rating, Structural +LT DL, P=0, US Grant Bridge (UCII, 2013)

8.6 Allowable Stress Rating of Stays

As discussed further in Chapter 10, there were several tests of the bridge stays conducted by UCII and VSL at various stages of construction. For example, Figure 8.14 compares the results from VSL lift off tests conducted in 2006 versus those estimated by the B&T erection analysis. They are relatively close at most stays; however, there are clear differences between estimates and actual field conditions due to both as-built changes from the plan as well as differences between theoretical calculation and actual field measurements.

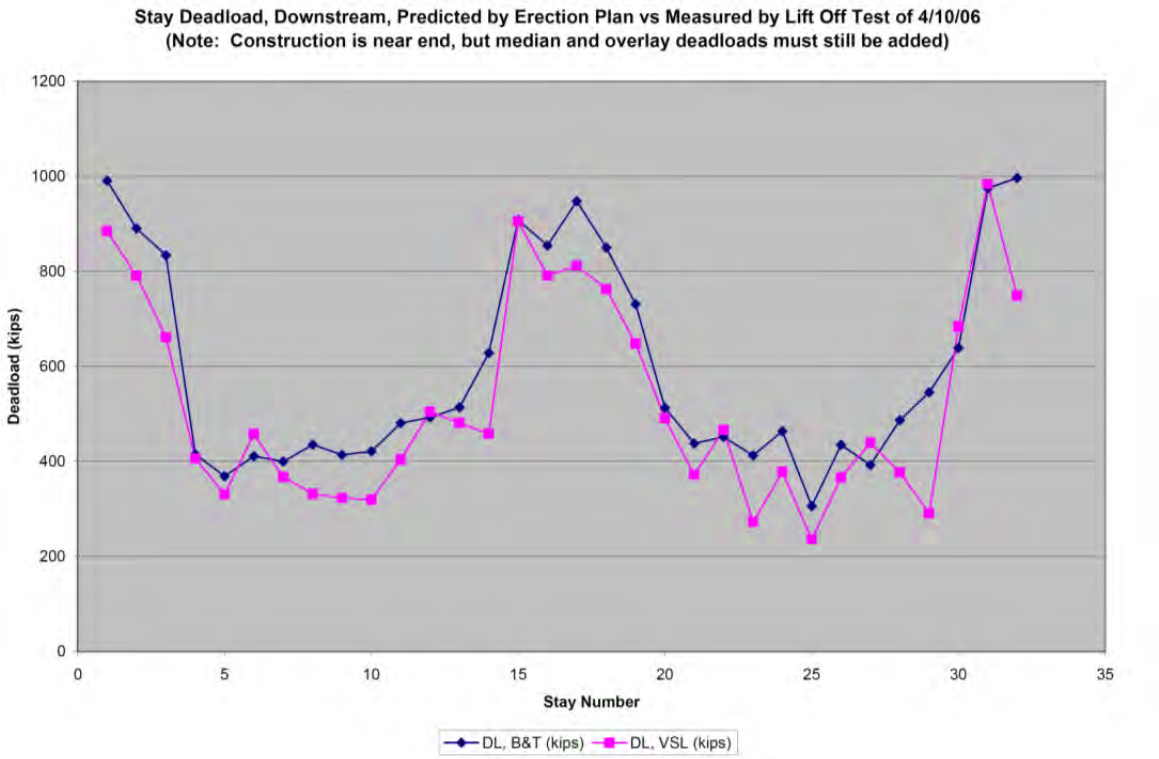

Figure 8.14: Differences between Erection Plan Estimates and Actual Test Results for Stay Deadload Force, US Grant Bridge (UCII, 2006)

Based upon the allowable stress for the stays listed in design plans, Figure 8.15 illustrates the stay rating based upon field test measurement of deadload when using the capacities listed in the design plans. Several stay ratings fell below unity and, hence, there was a reconsideration of the allowable stress for the stays based upon several references, including a more recent PTI Specification (2000) where the resistance factor was raised to 60% for strength and 85% for service. It should be noted that if the allowable stress is raised simply to 50% of gross ultimate tensile strength (GUTS), then all the stays would have passed rating in Figure 8.15. In 2010, the designer HNTB used a 50% GUTS allowable stress for inventory rating purposes. They list East (or Upstream) Stay 16N as the critical stay with an inventory rating of 1.35, based upon their structural model discussed above. Our stay test results were generally within 10% of those predicted by the B&T erection analysis (see Chapter 10); hence, our field ratings should be within 10% of those determined by the HNTB Manual.

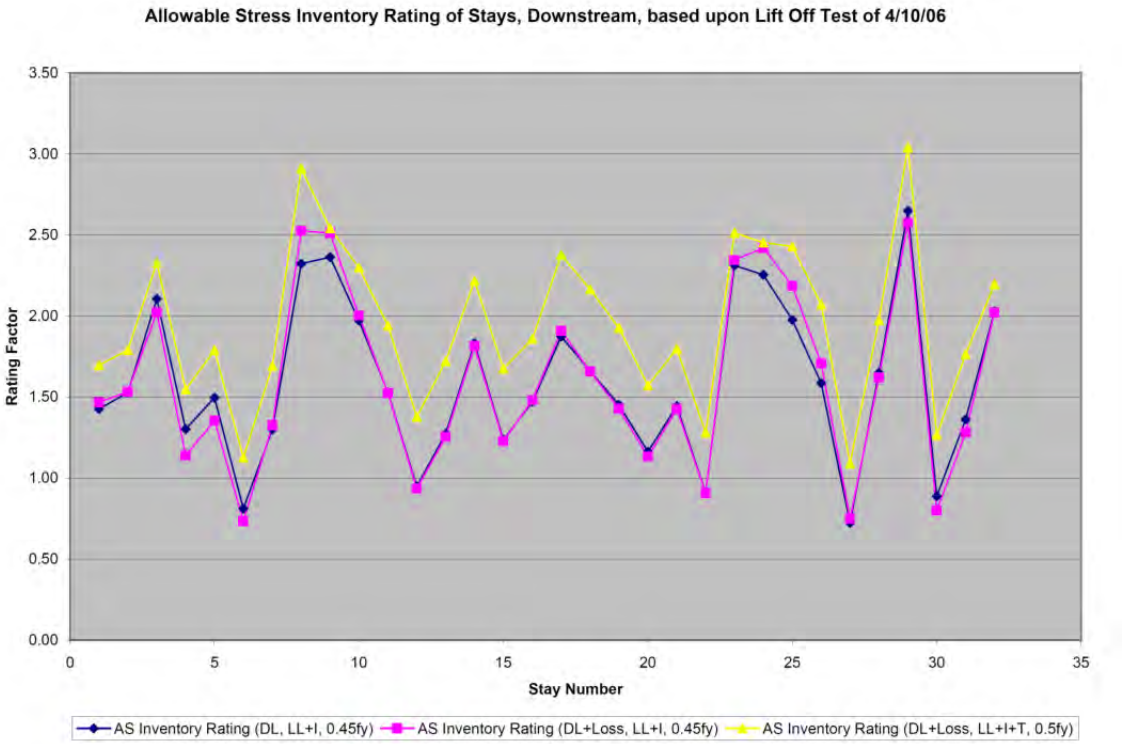

Figure 8.15: AS Rating of Stays using Design Capacities, US Grant Bridge (UCII, 2006)

For an analytical rating of the exterior pulldown strands, please see Chapter 7.

8.7 Conclusions and Recommendations

An inventory HS25 rating using both the allowable stress (see Figures 3.2 and 3.3) and load factor (see Figures 3.6 and 3.7) methods was formulated for both the composite and noncomposite or cracked case for each section as defined by the stations used by both HNTB and B&T. Each section was analyzed by each method at the bottom flange, top flange, cast-in-place (CIP) decking immediately above the edge girder, and for the deck panel adjacent to the edge girder which is to include the effect of the post tensioning (PT) force reported by B&T. In addition, each of these members was analyzed under both the positive and negative liveload moment reported by HNTB (see Figures 6.1 and 6.2).

Initially, the rating formulations were conducted with both bending moment and axial force stresses added together; this allowed both effects to be considered simultaneously. In addition, the axial force is greatly diminished near the abutments and centerline of the structure, which also happens to be the locations of the lowest rated sections of the bridge; so, axial force was only somewhat reducing the controlling rating values.

However, load factor design has commonly separated bending moment and axial force effects in the standard rating calculation. Upon review of the design manuals by HNTB, it seemed that this convention was also intended in the design of this bridge. Given that the axial force was only somewhat affecting the controlling rating values, it was decided to follow this convention.

Many of the sections have a bottom flange whose dimensions are such that the section will fail the compression flange check for compact and even braced sections. Many of the sections have lateral bracing (e.g., floorbeams) which does not meet the specification for the compression flange of a compact nor even a braced section. Without some guidance from the designer, we reduced the ultimate moment for negative moment regions to the yield limit state due to this concern.

Accordingly, Figure 8.2 tabulates both the measured (RF = 1.11) and designed (RF = 1.13) load factor rating at the instrumented sections of the US Grant bridge. This inventory rating was formulated using the measured deadload and superimposed deadload (DL) from the vibrating wire strain gages, both with and without the measured liveload (LL) response from the moving truckload tests, for the instrumented sections at the End of Construction (EOC) in October, 2006. For the same stations, an inventory rating (shown in blue) was formulated using the analytical estimates of the erected deadload by B&T (version 3) and the design liveload by HNTB for comparison. The measured load factor rating remained about the same (RF = 1.18) based upon field measurements of both deadload and liveload; however, the critical location switched from the center span to the Kentucky abutment due to the field restoration of the pulldowns.

During our Project Review with ODOT in 2009, we were asked to report ratings in two distinct fashions: 1) deadload based only upon EOC structural condition (RF = 1.26), and 2) deadload which incorporates both EOC structural condition and any/all other long-term effects and events that were not included within the EOC data (RF = 1.15): seasonal cycle upon the bridge (e.g., thermal, boundary conditions), creep and shrinkage effects on the concrete CIP joint, the initial repairs at the Kentucky abutment, etc. Of these, the main effect is the seasonal cycle; however, all are actual measured stresses that would constitute a reduction in capacity and lead to the most conservative estimate of the load rating.

In 2010, the designer HNTB provided a draft of their Bridge Analysis and Rating Report for the U.S. Grant Bridge to ODOT. A global model of the entire structure was used to calculate the internal demand forces for various structural components of the bridge, including the edge girders, cable stays, deck panels, floor and strut beams. In their rating report, HNTB reported that the bridge just barely reached an HS20 inventory rating (RF = 1.0) using Load Factor Method, with the most critical location identified as the West Girder of Segment 15N. Given that our deadloads and liveloads are not sufficiently different to cause such a reduction in our ratings, the reduction must come from capacity (see Appendix to Chapter 3 for more details).

In 2011, HNTB provided a written a draft of their Manual for Load Rating and Permits for the U.S. Grant Bridge to ODOT. Most commonly, the segments do not pass the lateral bracing check for a braced noncompact section (see Equation 10-101 and Table 10.48.2.1A, AASHTO Specifications). Hence, the capacity is reduced to that computed for a partially braced member (see Equation 10-103c, AASHTO Specifications). Unfortunately, it is not entirely clear as to which reduced capacity of several listed is considered in their rating; so, to be conservative, we will assume here the smallest value listed for a given segment in Column AM (entitled "Final Mr for Unbraced Compression Flange") for the capacity of the edge girder segments and subsequent load factor ratings (RF = 1.49). This inventory assessment only considers the marked lanes (and not the two large shoulders) for HS20 laneload and structural deadloads. An operating assessment was made (RF = 1.29) which also included environmental and other long-term deadload effects.

In 2010, the designer HNTB redefined the allowable stress for the stay cables as 50% of gross ultimate tensile strength (GUTS) for inventory rating purposes. They list East (or Upstream) Stay 16N as the critical stay with an inventory rating of 1.35, based upon their structural model discussed above. Our stay test results were generally within 10% of those predicted by the B&T erection analysis; hence, our field ratings should be within 10% of those determined by the HNTB Manual.

In Chapter 7, the load factor rating of the pulldown strands was found to be 2.0 under static truckload; however, we know that laneload will be a larger response and hence control for ratings purposes. Unfortunately, this cannot be estimated directly from the static truckload test results; however, if an analytical version of the laneload were provided for the strands, it could be easily scaled according to these test results and then used for ratings purposes. In any case, we will find that these rating results are comparable to those found using the strain gages on the exterior girders and, hence, the pulldowns are of similar condition to that of the superstructure itself.

REFERENCES

1. AASHTO, *Guide Specification for Strength Evaluation of Existing Steel and Concrete Bridges.* American Association of State Highway and Transportation Officials, Washington, D.C., 2002.
2. AASHTO, *Manual for Condition Evaluation of Bridges.* American Association of State Highway and Transportation Officials, Washington, D.C., 1994.
3. AASHTO, *Guide Specification for Distribution of Loads for Highway Bridges.* American Association of State Highway and Transportation Officials, Washington, D.C., 1994.
4. PTI, *Guide Specification for Cable Stay Design, Testing, and Installation.* Post Tensioning Institute, Phoenix, Arizona, 2000.
5. ODOT, *Bridge Design Manual*, Ohio Department of Transportation, Columbus, Ohio, 2003.

6. Howard, Needles, Tammen, and Bergendoff (HNTB), Design Calculations for the U.S. Grant Bridge, 2000.
7. Buckland & Taylor (B&T), Superstructure Erection Submission for U.S. Grant Bridge, Rev. 3, 2004.
8. Howard, Needles, Tammen, and Bergendoff (HNTB), Bridge Analysis and Rating Report, U.S. Grant Bridge, 2010.
9. Howard, Needles, Tammen, and Bergendoff (HNTB), Manual for Load Rating and Permits, U.S. Grant Bridge, 2011.
10. A. Helmicki, and V. Hunt, “Instrumentation of the US Grant Bridge for Monitoring of Fabrication, Erection, In-service Behavior, and to Support Management, Maintenance, and Inspection,” Project Review, ODOT Central Office, 2004.
11. A. Helmicki, and V. Hunt, “Instrumentation of the US Grant Bridge for Monitoring of Fabrication, Erection, In-service Behavior, and to Support Management, Maintenance, and Inspection,” Instrumentation Meeting, ODOT District Office, 2005.
12. A. Helmicki, and V. Hunt, “Instrumentation of the US Grant Bridge for Monitoring of Fabrication, Erection, In-service Behavior, and to Support Management, Maintenance, and Inspection,” Project Review, ODOT Central Office, 2006.
13. A. Helmicki, and V. Hunt, “Instrumentation of the US Grant Bridge for Monitoring of Fabrication, Erection, In-service Behavior, and to Support Management, Maintenance, and Inspection,” Project Review, ODOT Central Office, 2007.
14. A. Helmicki, and V. Hunt, “Instrumentation of the US Grant Bridge for Monitoring of Fabrication, Erection, In-service Behavior, and to Support Management, Maintenance, and Inspection,” Project Review, ODOT Central Office, 2009.
15. A. Helmicki, and V. Hunt, “Instrumentation of the US Grant Bridge for Monitoring of Fabrication, Erection, In-service Behavior, and to Support Management, Maintenance, and Inspection,” Project Review, ODOT Central Office, 2012.
16. A. Helmicki, and V. Hunt, “Instrumentation of the US Grant Bridge for Monitoring of Fabrication, Erection, In-service Behavior, and to Support Management, Maintenance, and Inspection,” Project Review, ODOT Central Office, 2013.
17. Lichtenstein, A.G., "Bridge Rating Through Nondestructive Load Test." *Proposed Manual for Bridge Rating through Load Testing,* NCHRP 12-28(13)A, August, 1992.
18. Lichtenstein, A.G., “Manual for Bridge Rating through Load Testing,” *NCHRP Research Results Digest*, No. 234, Transportation Research Board, National Research Council, Washington, D.C., November, 1998.
19. Hunt, V. *Nondestructive Evaluation and Health Monitoring of Highway Bridges*. Doctoral Dissertation, Department of Electrical and Computer Engineering, University of Cincinnati, Cincinnati, OH, December, 2000.

Chapter 9 Stay Vibration

9.1 Introduction

Several experiments were performed during various stages of construction to determine the capability of using traditional vibration techniques to estimate cable tensions with the non-traditional cable sheathing system of this structure (Kangas, 2009). The bridge has a pair of single towers from which the inclined cables are stretched out, in a modified fan system, to support the longitudinal girders. The girder to girder floor beams are uniformly spaced along the length of the bridge at a typical distance of 7.6 m, with the cables attached at each alternate floor-beam location.

There are 64 total cables divided into 2 parallel rows numbered 1 to 32 from Kentucky to Ohio and labeled upstream (U) and downstream (D). The stays consist of multiple, parallel strands and each strand consists of seven 1.5-cm twisted steel wires arranged in a hexagonal pattern. The composite strands are individually greased and sheathed to prevent rusting, and the strands are then contained within a protective polyethylene (PE) cover pipe to protect them from the environment. The number of strands for each stay ranges from 15 to 54 and cable lengths vary from 60.0 to 142.3 m. Figure 9.1 shows a plan overview of the US Grant Bridge.

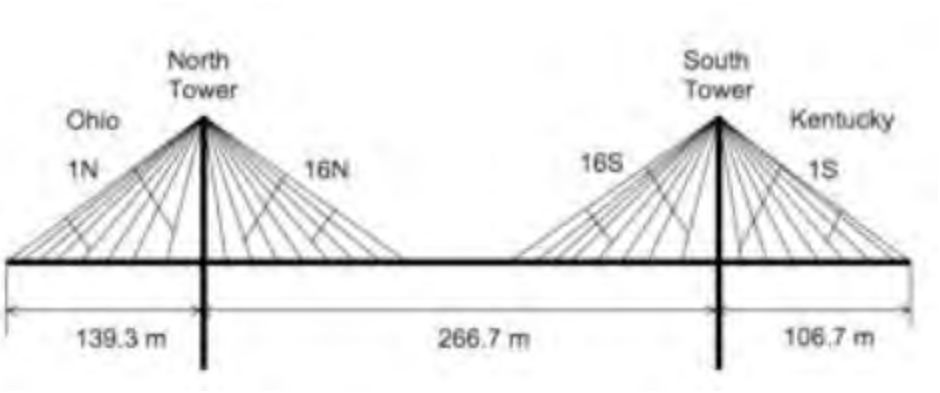

Figure 9.1: Plan Overview of the US Grant Bridge

The stays do not use grout as corrosion inhibitor, and since there is no guarantee that the sheath and strands will move in unison, a series of tests were conducted to verify that measuring cable motion at the sheath is applicable. These tests were designed to investigate the effects of sensor placement, excitation levels, thermal effects and cable inclination. Also, because this bridge uses cable cross-ties (Figure 9.2) to limit cable motion, tests were done before and after the installation of these ties to see if accurate estimates of tension could be made with these ties in place.

Figure 9.2: US Grant Stay Cable with Helical Surface Treatment and Cross-ties

9.2 Cable Vibration and Force Estimation

To estimate cable force, cable vibrations are measured by placing accelerometers on the cable's protective cover pipe which is assumed to move in unison with the internal wire strands. The measured vibrations are used to create auto-correlation functions, calculated only using the positive time lags, and therefore only retaining information that pertains to the positive (stable) poles. These identified correlations are subsequently used as basis functions within a stochastic subspace identification algorithm to extract the Eigen frequencies of the cables' measured response. Figure 9.3 shows typical measured cable acceleration and its corresponding auto-correlation used to identify cable resonant frequencies. To identify the resonant cable frequencies, the stochastic algorithm computes Eigen frequencies for varying model orders. The returned Eigen frequencies, that are consistent for various model orders, are selected for calculation of cable force.

Figure 9.4 shows an example of the Eigen frequencies estimated by the subspace algorithm, compared against the power spectrum, and created by the positive correlation lags. The simplest model to describe a member under tension assumes it behaves like a taut string and is described by the following equation:

$$f_n^s = \frac{n}{2L}\sqrt{\frac{T}{m}} \qquad \text{(Equation 9.1)}$$

where f_n^s is the nth harmonic frequency of vibration (Hz), and T, m and L are string tension (N), cable mass (kg/m), and cable free length (m), respectively.

This taut string approximation is not completely accurate for stay cables which have a degree of bending stiffness (EI), and cable sag associated with them, where sag is represented by the parameter sag-extensibility (λ^2). Mehrabi accounted for these parameters within the following equation to describe the in-plane resonant frequencies:

$$\frac{f_n^{EI}}{f_n^s} = 1 + \frac{2}{\epsilon} + \frac{4 + n^2\pi^2/2}{\epsilon^2} \qquad \text{(Equation 9.2)}$$

where

$$\epsilon = L\sqrt{\frac{T}{EI}} \qquad \text{(Equation 9.3)}$$

f_n^{EI} is the measured frequency of the nth harmonic (Hz)
f_n^s is the equivalent-taut string frequency of the nth harmonic (Hz)
ϵ is the dimensionless parameter related to the bending stiffness

The method for tension estimation implemented within this research follows the two-step method outlined by Peeters where non-linear least squares is used to simultaneously estimate ϵ and f_1^s from the identified cable frequencies, which are assumed to behave like f_n^{EI} in Equation 9.2. Knowing the cable length (L) and mass per unit length (m), the estimate of f_1^s can be used to calculate cable force according to Equation 9.1.

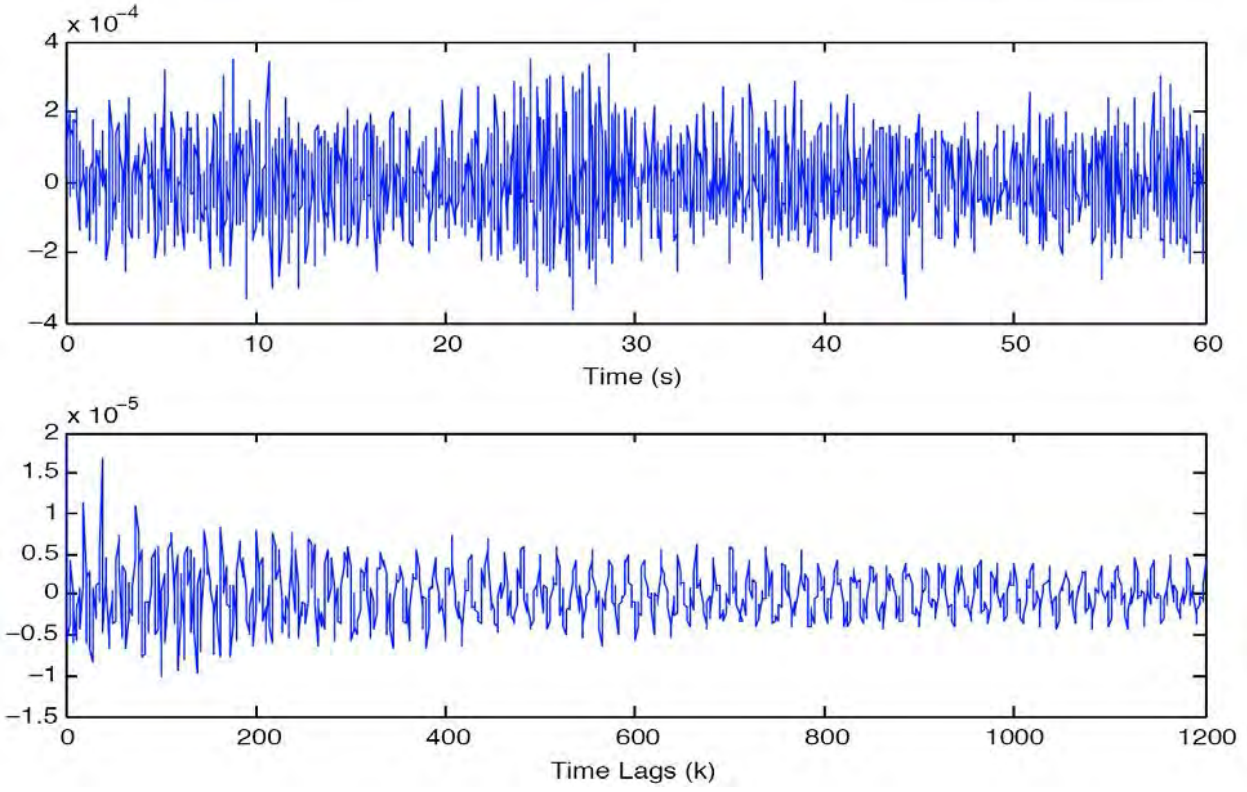

Figure 9.3: Typical Measured Cable Acceleration (top) and Auto-Correlation (bottom) (Kangas, 2009)

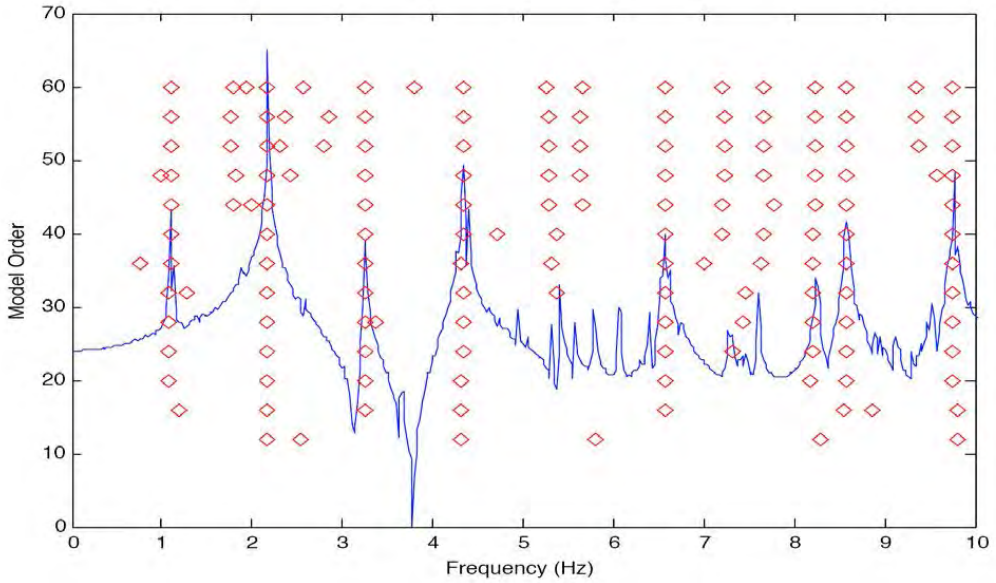

Figure 9.4: Typical Cable Eigen Frequencies (Kangas, 2009)

9.3 Tests before, and after Installation of Cross-Ties (9/14/06 and 9/26/06)

A preliminary baseline test was performed before the installation of the cable cross-ties. Most construction activities had finished prior to this test, however a few minor tasks still remained. To bring the bridge into its final profile, additional overlay was being applied to the bridge deck and minor adjustments to stay tension were being done, so the bridge was not in its final configuration during this test. Since most construction equipment had been removed prior to this trip, this was the first test performed where all of the stays were accessible.

Figures 9.5 and 9.6 show the calculated tensions from this test as well as the percentage difference between design tension values and the calculated tension values for in-plane and out-of-plane. As observed from the figures, the resulting tensions from this series of tests agree well with the design values, although there were a few outliers. Cables 9S, 12S, 9N and 13N differ from design tensions by greater than 10%. It should be noted that minor adjustments were being made to the bridge deck and to the cables themselves, so at the time of testing the cables were not tensioned to their “final” value. Since exact tensions were not known at the time of test, a possibly more insightful study for this test would be the comparison between in-plane and out-of-plane tension estimates. Figure 9.7 shows the percentage difference these two tension estimates for each of the 32 cable tested. In-plane and out-of -plane estimates show a great deal of consistency with the differences being confined to less than +/- 3%.

Based on the results of this test, the exclusion of sag-extensibility in tension calculations did not cause a discrepancy between in-plane and out-of-plane tension estimates. This indicates that the effect of cable sag at US Grant is minimal, which may be due to its construction designs. Following current design trends, the stays do not use cement grout as a corrosion inhibitor. Instead of grout, the strands are individually greased and sheathed, greatly reducing the weight of the stay, which in turn has reduced cable sag.

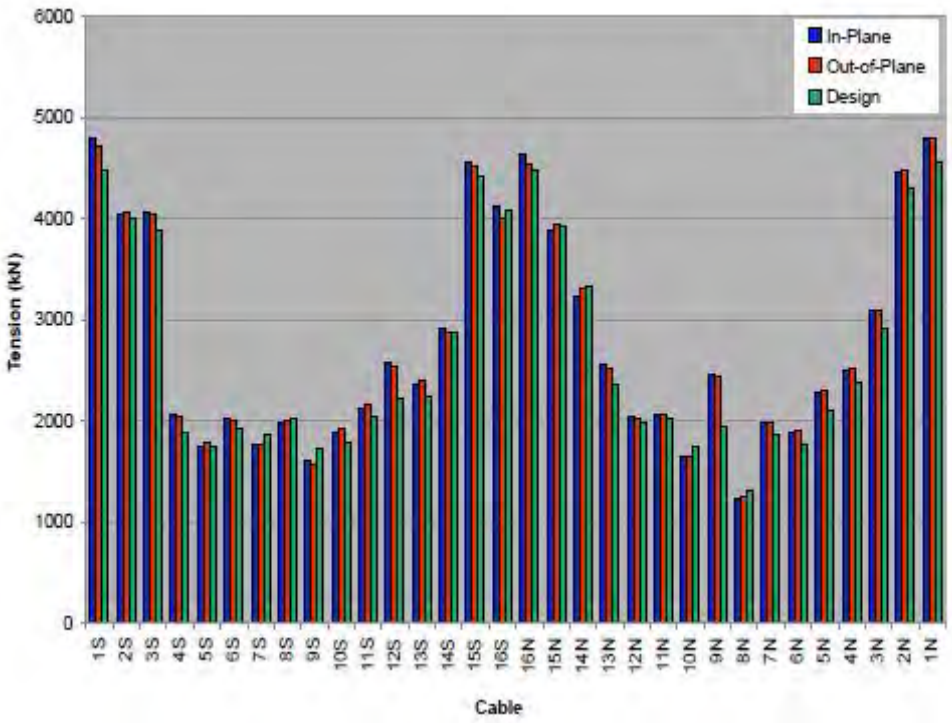

Figure 9.5: Estimated Tension versus Design Tension for the US Grant Bridge Stays (9/14/06)

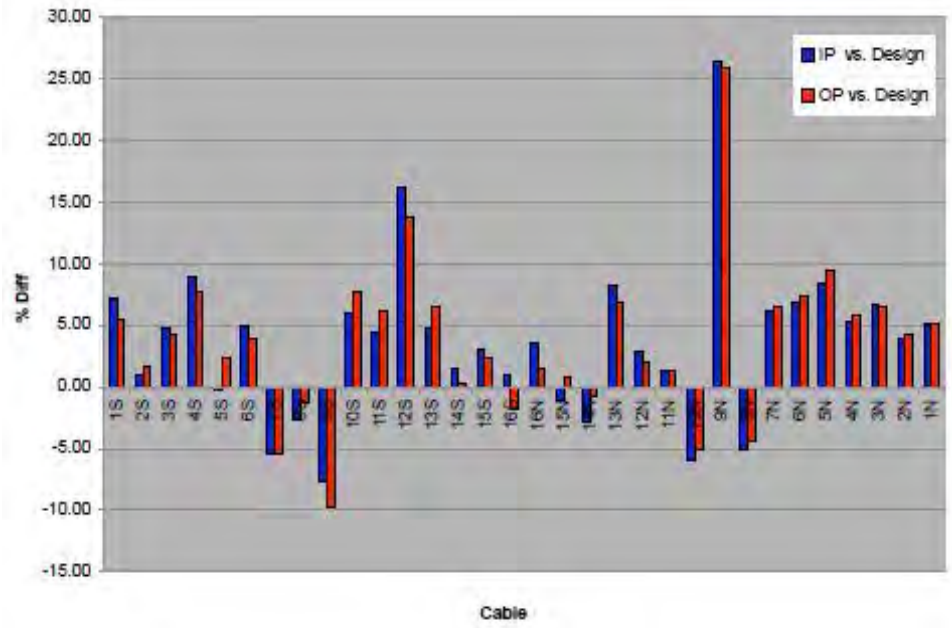

Figure 9.6: Difference between Calculated Tensions & Design Tensions for the US Grant Bridge Stays (9/14/06)

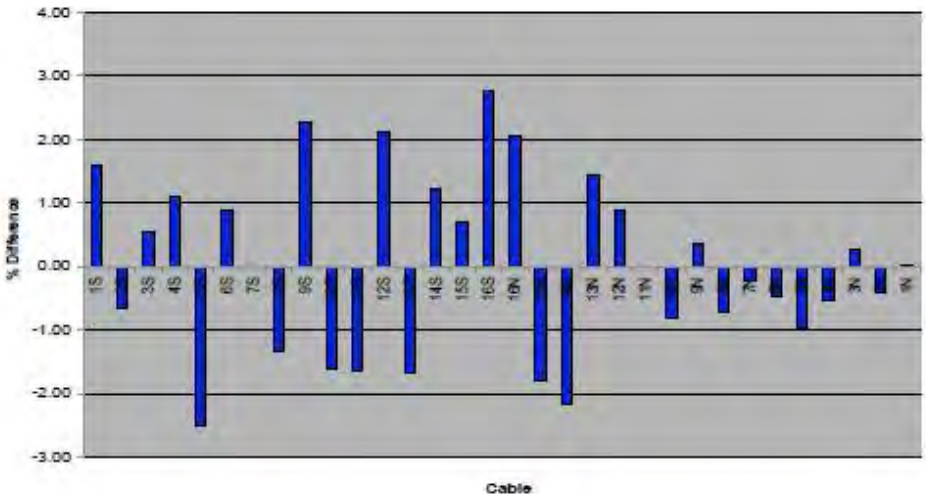

Figure 9.7: Difference between In-Plane & Out-of-Plane tensions for the US Grant Bridge (9/14/06)

Following the installation of the cable cross-ties another round of stay tests were conducted. These tests were performed to determine the ability to accurately estimate cable tension with these ties in place. The test setup from the previous field test was left unchanged, with accelerometers mounted on the sheath to measure in-plane and out-of-plane motion for all 32 downstream stays.

Figure 9.8 shows the cable spectrums from these two sensor locations compared against the simulated cable model for Cable 1S. The out-of-plane sensor captured a nice harmonic sequence, however the same is not true of the in-plane sensor. Since the configuration of the ties does not constrain out-of-plane motion this effect is not unexpected. It is interesting to note that there are some well defined peaks within the in-plane spectrum. Some of the peaks even appear to be located close to frequencies related to harmonic cable motion, mostly around 4 Hz. However the non-uniform frequency spacing of the peaks and the overall poor quality of the in-plane spectrum bring its usefulness into question. These characteristics were common for all the cables tested, indicating the in-plane sensors should not be used for tension estimation.

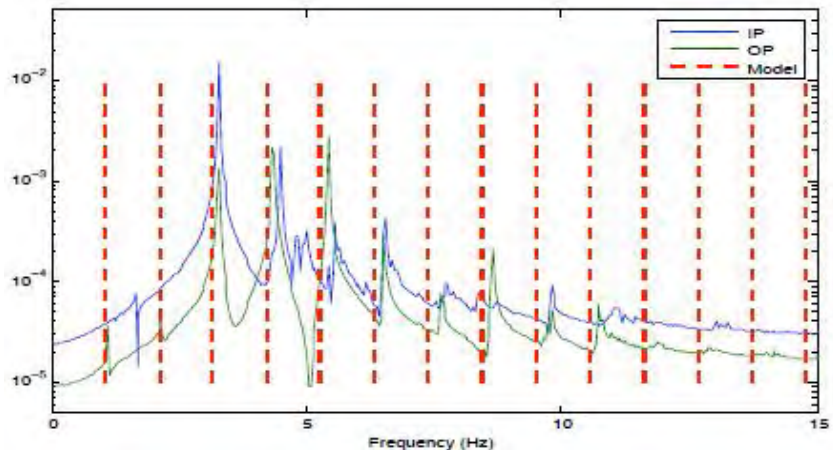

Figure 9.8: Effect of Cable Ties on Cable Response for the US Grant Bridge

Due to the poor quality of the in-plane cable spectrums, tension estimates were calculated from the out-of-plane spectrums only. These tensions and their comparison against design tensions are shown in Figure 9.9, while Figure 9.10 shows the difference in out-of-plane tensions before and after the ties were installed. The majority of these cable tensions are within +/- 5%, although a few are greater than that, namely cables 10S, 9N and 10N. These cables are located next to the southern and northern towers, respectively. Considering that minor construction events were still occurring, it seems these differences in tension may be attributed to ongoing adjustments to the structure and cables.

Based on the results from these tests, the installation of the ties did not prevent accurately estimating cable forces. However, only out-of-plane cable vibrations revealed harmonic behavior; in-plane measurements did not provide useful information. Hence, unless the ties have been removed prior to stay testing, any future measurements will only consider out-of-plane motion.

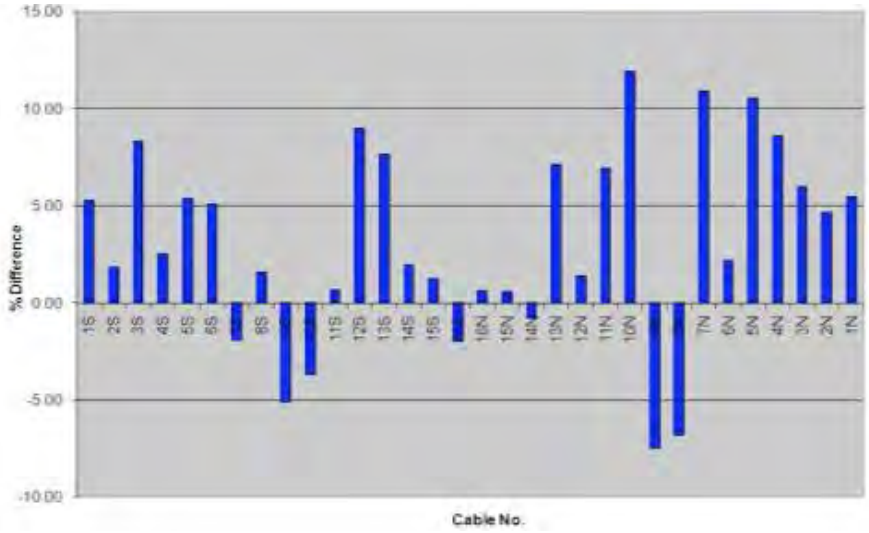

Figure 9.9: Difference between Calculated and Design Tensions (9/26/06)

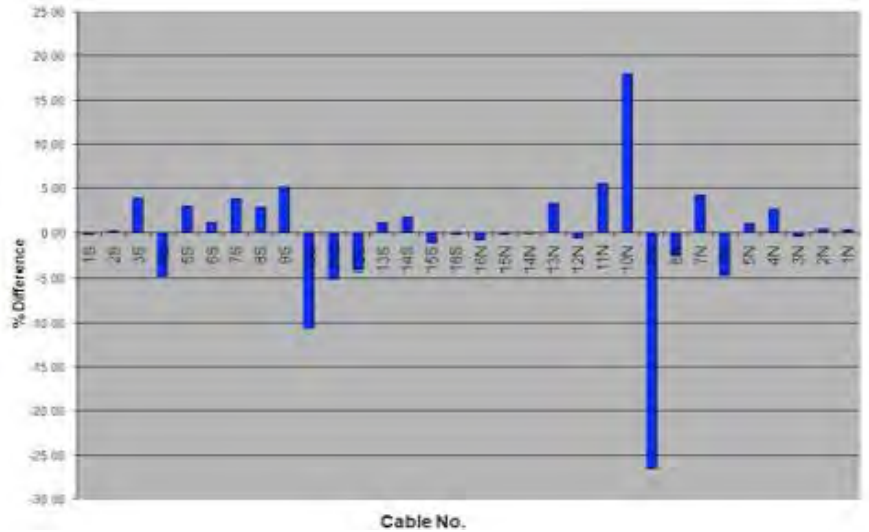

Figure 9.10: Comparison of Out-of-Plane Tensions before/after ties (9/14 vs 9/26)

9.4 Effects of Sensor Placement – 7/25/05

The first set of sensor-placement tests was performed on a stay, Cable 6S, that had been erected and its sheath was permanently set into place as shown in Figure 9.11 (left). In-plane and out-of-plane motion was measured under ambient conditions with two pairs of accelerometers: a lower pair, mounted approximately 10 feet above deck level and a second set, installed approximately one-third of the way up the stay. Since contact between the sheath and strands only existed due to sag, and these contact locations are unknown, multiple sensor locations were selected to see if cable motion could be accurately, and consistently, measured at the sheath.

An investigation of Figure 9.11 (right) shows that there are many well-defined peaks within the cable's frequency spectrum, some that coincide with the model estimates (vertical lines) and some that do not. This test was performed during active construction and these non-harmonic frequencies may correspond to excitation from construction equipment, or a result of some non-composite sheath/strand interaction. Regardless of input source, these non-harmonic frequencies were eliminated from consideration by comparing the spectrum to the frequencies predicted by the cable model. The frequency separation between harmonic and non-harmonic peaks, within the spectrum, makes it easy to determine which peaks correspond to harmonic motion.

Table 9.1 shows the individual frequencies and calculated tensions for each sensor location. Looking at this table, the following conclusions can be made:

1. Frequencies/tensions are consistent between upper/lower sensors.
2. Tensions compare favorably with the designer's predicted values, differing by less than 2%
3. Accurate tension estimates can be obtained by measuring cable motion at the sheath.

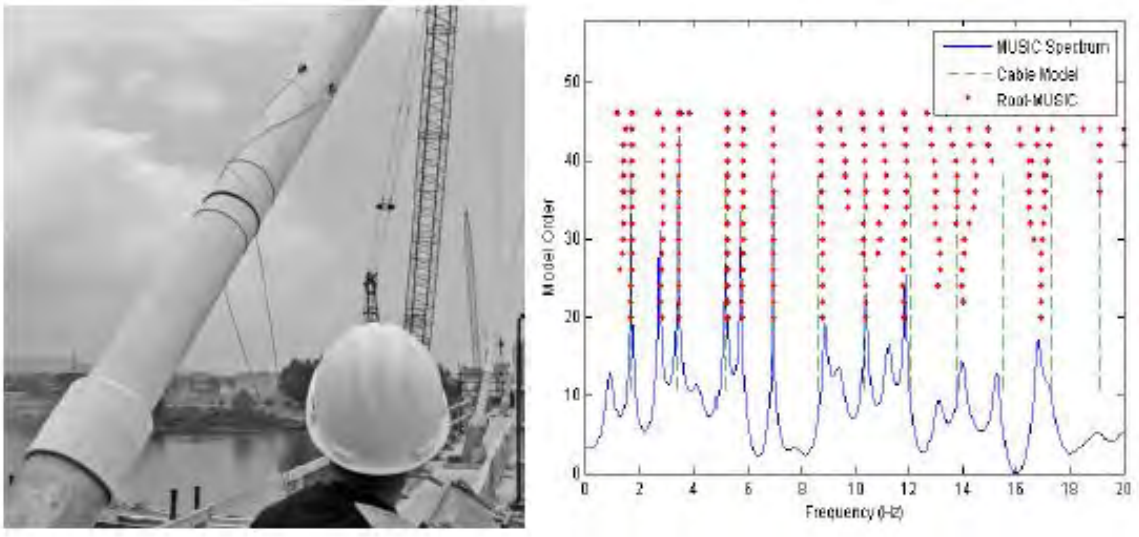

Figure 9.11: Lower set of Sensors on Sheath (left) and Spectrum of In-Plane Lower Sensor compared to the Finite Difference Simulation (right) for all Sensor Locations

Table 9.1: Harmonic Frequencies and Tensions for Cable 6S of the US Grant Bridge

Harmonic No	Model	IP Lower	OP Lower	IP Upper	OP Upper
1	1.72	1.71	1.71	1.74	1.74
2	3.43	3.46	3.47	3.47	3.47
3	5.15	5.20	5.07	5.18	5.05
4	6.87	6.91	6.84	6.91	6.84
5	8.60	8.67	8.52	8.67	8.56
6	10.33	-	10.24	-	10.10
7	12.07	11.92	11.72	11.89	11.79
8	-	13.89	-	-	13.58
Tension Calc. (kN)	-	1937	1885	1922	1882
Tension Design (kN)	1922				
% Diff.	-	0.78	-1.93	0.00	-2.06

9.5 Effects of Cable Inclination & Cable Sag - 4/14/06

A subset of the 64 cables at U.S Grant was selected based on the criteria that they be representative of the collection of cable lengths, masses and angles. An accelerometer was also mounted on the deck, near the anchor of each stay, to identify any interaction between the superstructure and the stay. Figure 9.12 shows a comparison of the superstructure frequency spectrum and the cable spectrum for three of these cables. None of the locations showed sufficient deck energy to drive the cable at an arbitrary, non-resonant frequency. Comparing these spectrums and looking at the results shown in Table 9.2, the following conclusions can be made:

1. Regardless of cable, the deck and cable spectrums have very few peaks that occur at frequencies common to both. This indicates that the deck does not appear to induce stay motion.
2. Cable angle does seem to have an influence on cable response. The “cleanest” response of the nine cables tested was from cable 15S, which had the smallest angle. Also, measured cable responses become more “noisy” for the shorter and more vertical cables, making it difficult to identify an equal number of harmonics. This is apparent by looking at Figure 9.12, where cable 8S is the shortest cable tested and after 8Hz there are no distinguishable peaks that correspond to harmonic motion.
3. Although cable angle does influence the number of identifiable cable harmonics, this angle does not affect the ability to estimate cable tension. Assuming a uniform distribution of sheath mass, accurate tension estimates were made for all nine cables tested.

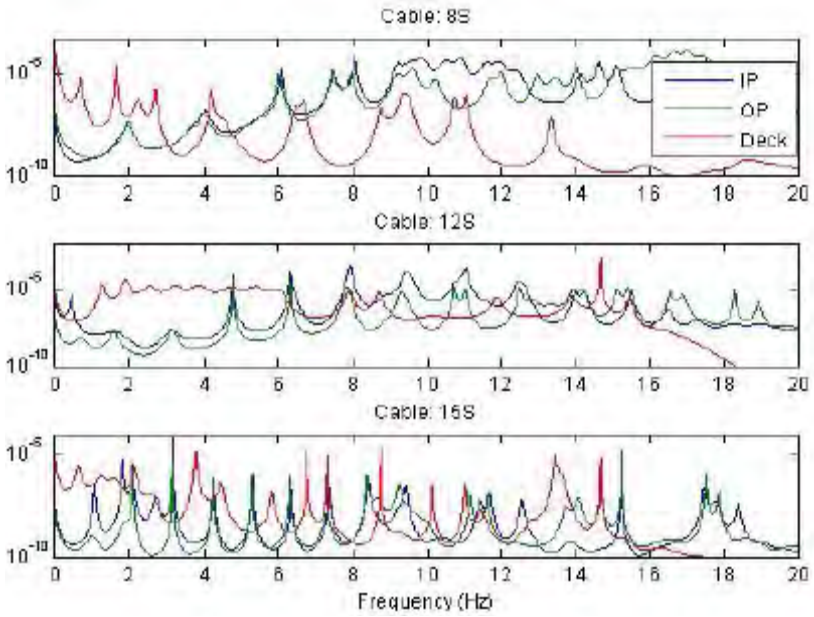

Figure 9.12: A Plot of In-Plane Frequency Spectrum, Out-of-Plane Frequency Spectrum and Deck Response for three US Grant Bridge Cables

Table 9.2: Harmonic Frequencies and Tensions for three US Grant Bridge Cables 4/14/06

Cable	Length (m)	Angle (Degrees)	Fund. Freq. (Hz)	Calculated Tension (kN)	Lift-off (kN)	% Diff
2S	120.4	30.1	1.02	3523	3523	0.00
3S	113.5	31.6	1.09	3003	2940	2.12
5S	87.9	40.9	1.36	1495	1472	1.51
6S	76.6	47.8	1.75	2033	2037	-0.22
8S	60.3	67.5	1.98	1490	1477	0.90
10S	66.7	56.6	1.70	1343	1428	-5.92
12S	87.4	40.7	1.56	2366	2246	5.35
13S	99.8	35.4	1.31	2251	2220	1.40
15S	126.5	28.0	1.05	4128	4030	2.43

9.6 Research Results and Conclusions

Before the opening of the US Grant Bridge, several rounds of field experiments were conducted to investigate the ability to estimate cable tensions using vibration-based measurements. Because the configuration of cable stays prevents direct measurement of the internal wire strands that comprise the stay, these measurements have been made by measuring the motion at the sheath. Traditionally cable stays have used grout as a corrosion inhibitor, so the sheath and strands were forced to have composite motion. Studies, however, had shown that this grout actually accelerated cable degradation. Hence, new stay designs

have eliminated grout and replaced this inhibitor with individually greased and sheathed strands or an epoxy resin directly applied to the strands. US Grant utilizes individually greased and sheathed strands and a high-density polyethylene (HDPE) sheath. Based on the series of experiments performed at US Grant throughout construction, it has been shown that accurate tension estimates could still be made by measuring cable motion at the sheath even with the cable cross-ties in place.

References

1. S. Kangas, “Modeling and Ambient Vibration Monitoring of Cable-Stayed Bridges” PhD Dissertation, Department of Electrical Engineering, University of Cincinnati, Cincinnati, OH, 2009.
2. S. Kangas, A. Helmicki, V. Hunt, R. Sexton, J. Swanson, "Cable-Stayed Bridges: A Case Study for Vibration-based Cable Tension Estimation", University of Cincinnati Infrastructure Institute, University of Cincinnati, OH, 2009.

Chapter 10 Modal Analysis

10.1 Introduction

This chapter discusses the design of small preliminary tests, data acquisition and parameter estimation using Operational Modal Analysis (OMA) techniques, and the validation and comparison of the results with Finite Element (FE) model-based predictions. One of the main reasons for the development of OMA is the problems faced while studying and characterizing large systems such as civil structures (bridges, buildings etc), using conventional Experimental Model Analysis (EMA) techniques. OMA technique differs from the traditional experimental modal analysis (EMA) as it tries to characterize the system on the basis of output-only response data, unlike EMA where both the input force and output response information are required.

10.2 Operational Modal Analysis of the USG Bridge

The final superstructure test of the bridge was designed with the help of findings based on the finite element model-based studies and few smaller tests that were conducted to ascertain the testing procedure, data acquisition and subsequent data processing methodologies. The final test parameters was comprised of sensor type, data acquisition parameters (frequency range of interest, sampling rate, test duration etc.), and sensor location.

Sensor locations for the final superstructure test are shown in Figure 10.1 and their corresponding locations are given in Table 10.1. These locations were chosen based on the FE model results which revealed the modes with high participation factors. Since most of these modes were vertical bending modes, acceleration was measured only in Z direction. Both the upstream and downstream sides of the bridge were instrumented in order to observe both the bending and torsional mode. Thus, there were three lines of sensors running along the length of the bridge; along the outer and inner girder on the upstream side and along the outer girder on the downstream side.

The sensors were placed at cable locations starting from 10 S to 16 N, including the sensor at the central span. Thus, a total of nine sensors, per sensor line, were located along the length of the bridge. In addition to these 27 sensors, 4 more sensors were placed at the locations corresponding to cable stays 5 N and 5 S at the outer girders on the upstream and downstream side, at the side spans. The purpose of putting these extra sensors was to help in distinguishing the modes which might have appeared similar in the central span with difference being more apparent in the side spans.

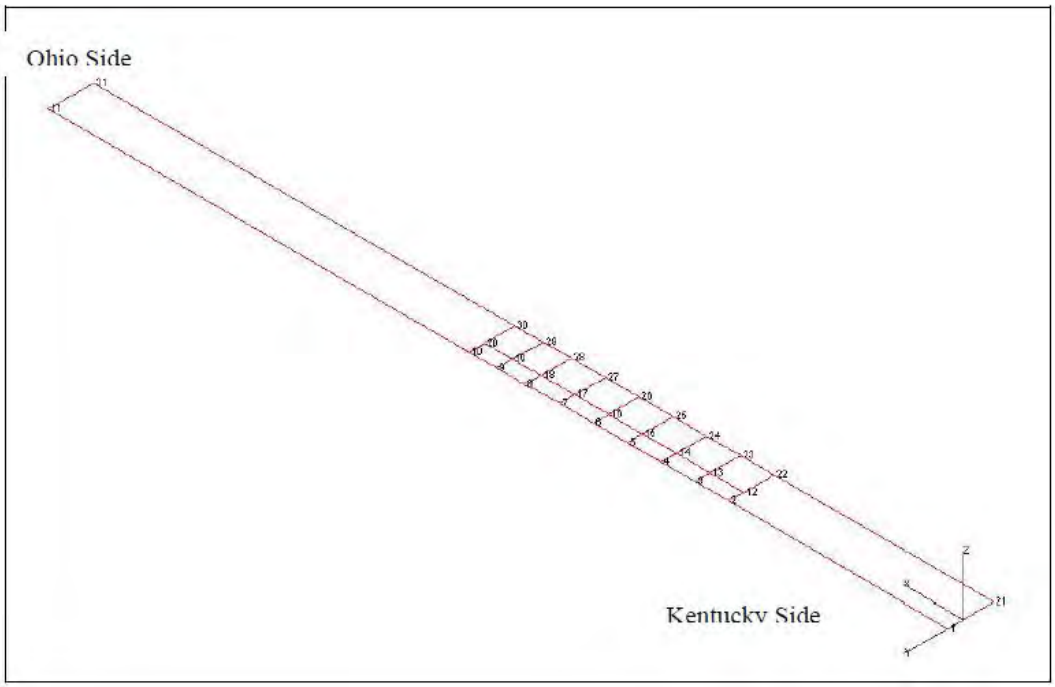

Figure 10.1 Sensor layout for final superstructure test

Table 10.1: Sensor Locations (Final Superstructure Test)

Sensor Label	Location on Bridge	Sensor Label	Location on Bridge	Sensor Label	Location on Bridge
1	Cable 5 NU Outer Girder			21	Cable 5 ND Outer Girder
2	Cable 10 NU Outer Girder	12	Cable 10 NU Inner Girder	22	Cable 10 ND Outer Girder
3	Cable 11 NU Outer Girder	13	Cable 11 NU Inner Girder	23	Cable 11 ND Outer Girder
4	Cable 12 NU Outer Girder	14	Cable 12 NU Inner Girder	24	Cable 12 ND Outer Girder
5	Cable 13 NU Outer Girder	15	Cable 13 NU Inner Girder	25	Cable 13 ND Outer Girder
6	Cable 14 NU Outer Girder	16	Cable 14 NU Inner Girder	26	Cable 14 ND Outer Girder
7	Cable 15 NU Outer Girder	17	Cable 15 NU Inner Girder	27	Cable 15 ND Outer Girder
8	Cable 16 NU Outer Girder	18	Cable 16 NU Inner Girder	28	Cable 16 ND Outer Girder
9	Central Span Outer Girder	19	Central Span Inner Girder	29	Central Span Outer Girder
10	Cable 16 SU Outer Girder	20	Cable 16 SU Inner Girder	30	Cable 16 SD Outer Girder
11	Cable 5 SU Outer Girder			31	Cable 5 SD Outer Girder

NU – North Upstream ND – North Downstream SU – South Upstream SD – South Downstream

Two sets of data were collected and the data acquisition parameters were set as following

1. Sampling rate of 40 Hz
2. Frequency range of 0 – 15 Hz
3. Test duration (first dataset) of 60 minutes
4. Test duration (second dataset) of 10 minutes

While collecting the first dataset, the only forces exciting the bridge were the wind and the river flow. For the second dataset a van was driven on downstream side of the bridge during the full 10 minute duration of the test (Figure 10.2).

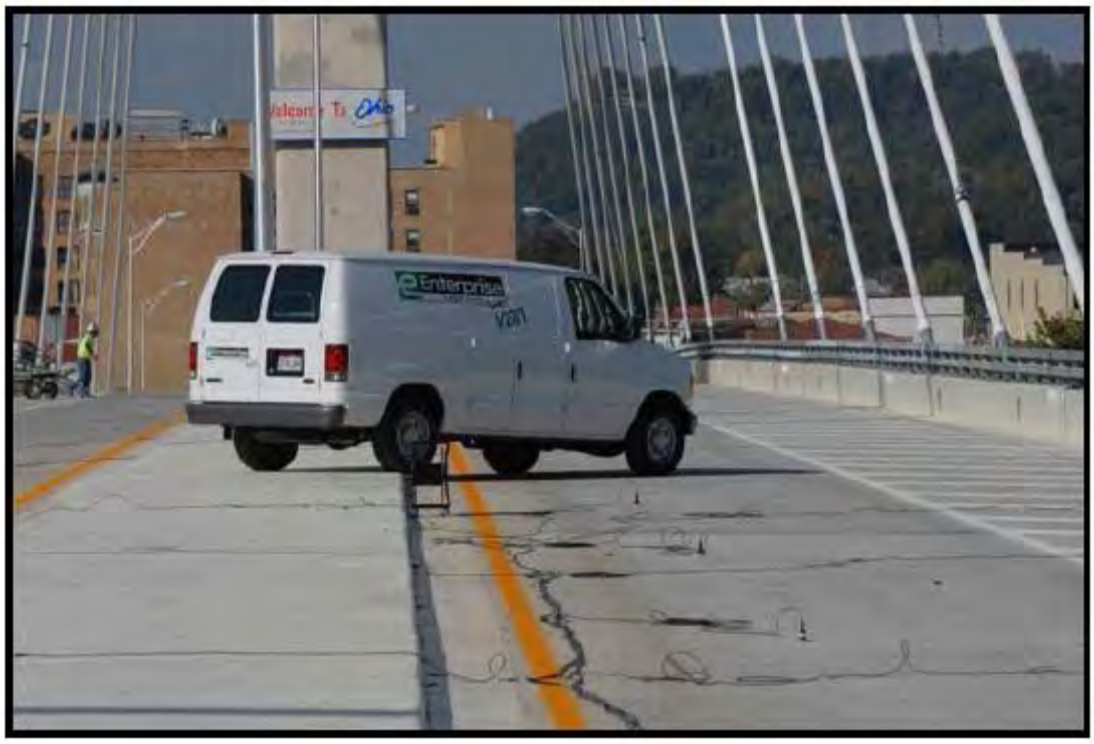

Figure 10.2 Second Operational Modal Analysis test with Van

10.3 Operational Modal Analysis - Enhanced Mode Indicator Function (OMA-EMIF) - based Parameter Estimation

The data collected was processed to obtain the power spectrum using the Welch Periodogram method. A block size of 2048 was used along with a Hanning window, and 3 cyclic averaging (Chauhan et al 2008). A typical auto-power spectrum is shown in Figure 10.3. The Short Time Fourier Transform (STFT) helped verify data consistency plots (Figure 10.4) before carrying out the parameter estimation. Data collected from various sensors was observed to be consistent except for a few channels where either the data had to be multiplied by a calibration factor, or certain portions that were inconsistent had to be chopped off. Furthermore, it was observed, during the analyses of the datasets, that driving the van over the bridge resulted in better signal-to-noise ratio in comparison to the case when bridge is excited only by means of natural sources (wind) only.

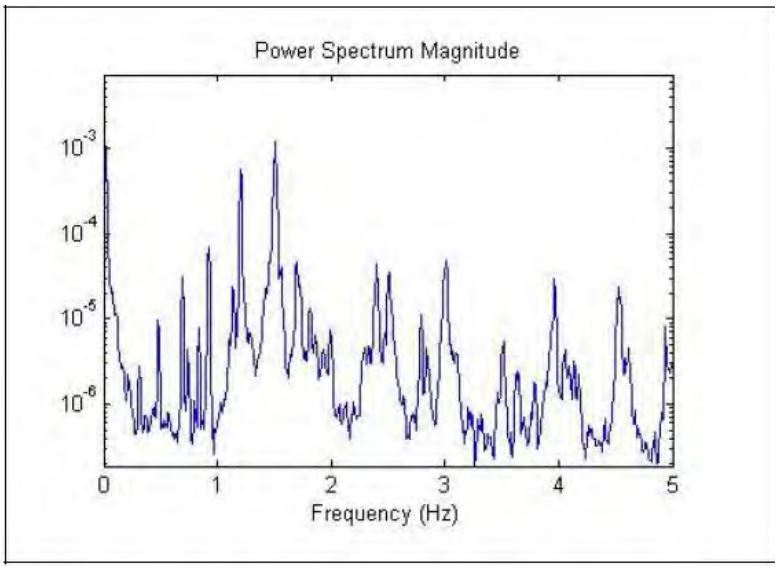

Figure 10.3 Typical auto-power spectrum

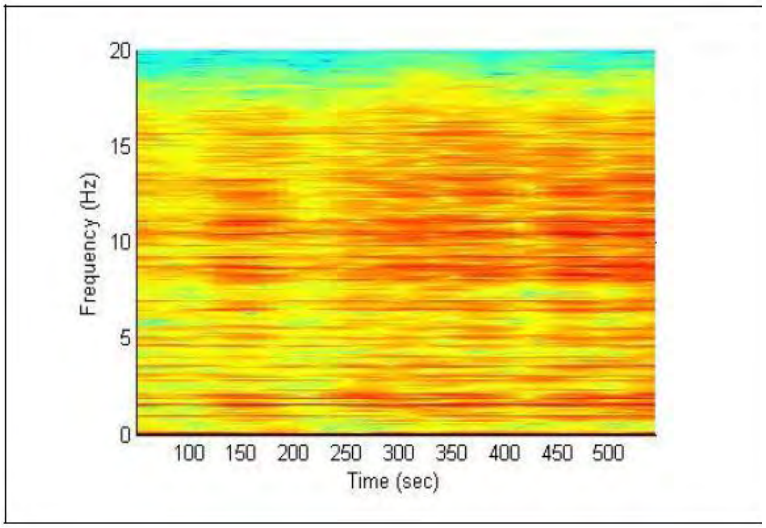

Figure 10.4 Typical Short Time Fourier Transform (STFT) plot of data collected by an accelerometer

The power spectrum-based Complex Mode Indicator Plot (CMIF) plot is shown in Figure 10.5. The parameter estimation process was carried out using the OMA-EMIF algorithm (Chauhan et al 2008), while the estimated parameters are listed in Table 10.2. A comparison of the selected modes among themselves was also carried out using the Modal Assurance Criterion (Helyen 1997), and the MAC plot is shown in Figure 10.6. The MAC plot shows that most modes are fairly independent of each other. However, the MAC plot modes at 1.1414 and 1.2068 Hz and the torsion modes at 0.742 and 0.929 Hz (shown in grey and orange in Table 3) appeared to be

similar though these are well separated in frequency. A possible reason proposed, was that these modes could be similar in mid span, where most of the sensors were instrumented, but different in the side spans. Instrumenting the mid spans would, therefore, not yield substantial distinction between these modes.

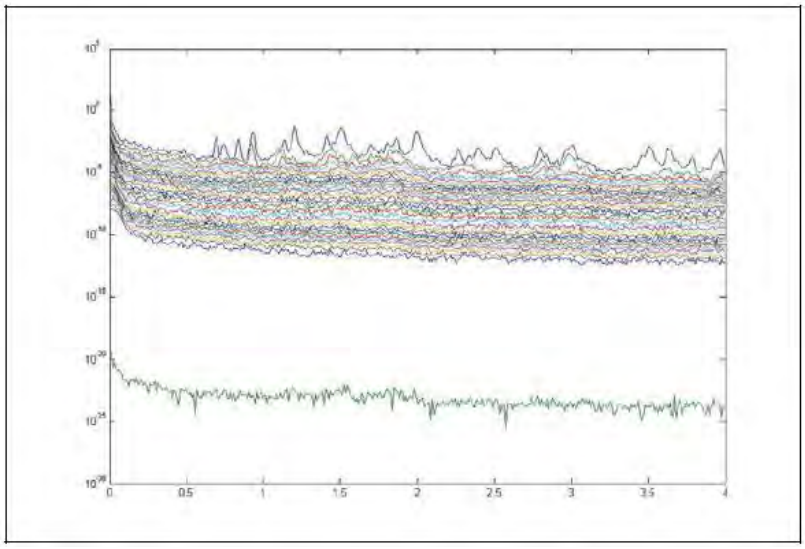

Figure 10.5 Complex Mode Indicator Function (CMIF) plot of second dataset (Final superstructure test)

Table 10.2: Estimated modal parameters

Frequency (Hz)	Damping (% Critical)	Description
0.4966	1.3182	Vertical
0.6982	1.8078	Vertical
0.7418	1.8808	Torsion
0.8424	2.1355	Vertical
0.8995	1.1372	Vertical
0.9296	1.2494	Torsion
1.1259	1.2018	Torsion
1.1414	0.8501	Vertical
1.2068	1.0884	Vertical
1.4107	0.9113	Torsion
1.4444	0.9153	Torsional (Probably Ken. Sidespan)
1.5177	1.4354	Vertical

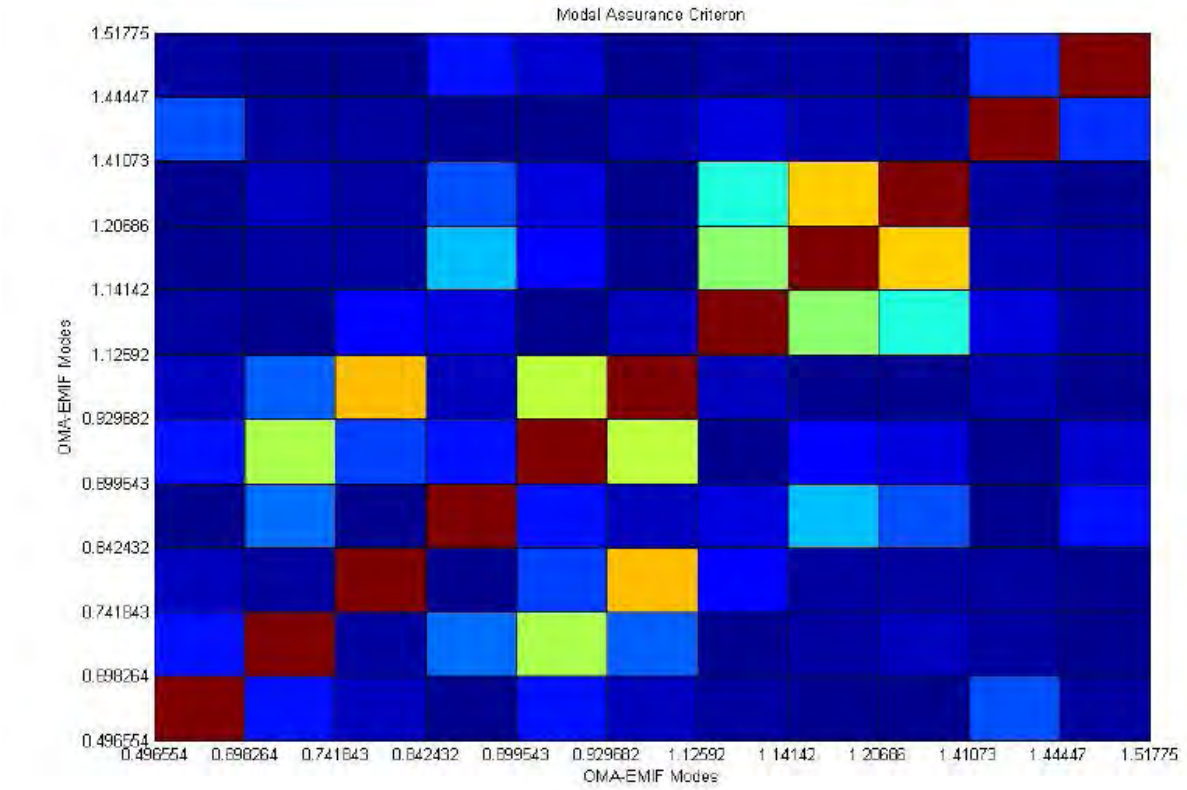

Figure 10.6 Auto Modal Assurance Criteria (MAC) plot between the various modes obtained using Operational Modal Analysis based on the Enhanced Mode Indicator Function (OMA-EMIF)

Table 10.3 shows the comparison of the FE model-based prediction of bridge modes with the experimentally obtained modes. Only the modes having large modal participation factor, based on finite element analysis, were considered for MAC comparison (Table 10.4). From Table 10.3, it can be observed that most of the bending modes compared well with the finite element prediction, within error limits. Since the girder stiffness correction in the finite element model was directed at correcting the flexural response, and owing to the relative importance of bending modes as compared to torsion modes, the torsional response of the bridge didn't match well as compared to the bending response.

The experimentally obtained 1st bending mode as indicated in the table was obtained from the second preliminary test. This mode was not observed in the final superstructure test, perhaps because of the low signal-to-noise ratio. This was considered as one of the shortcomings of the operational modal analysis, as mode observability depended considerably on favorable ambient conditions.

Table 10.3: Comparison of Finite Element Method (FEM) and Operational Modal Analysis (OMA) modes

FEM Modes				OMA Modes	
Description	Remarks	Freq	Modal participation Factor (Z Dir.)	Freq	Descr.
Bending-1	**Center span + OH span**	**0.2936**	**1.4270**	0.31	B
Tower Sway		0.3443	0.0000	-	-
Tower Anti Sway		0.3842	0.0000	-	-
Bending-2	**All spans**	**0.4827**	**5.5860**	**0.4966**	**B**
Deck Lateral	Center span	0.5942	0.0000	-	-
Torsion-1	**Center span + small torsion in end spans**	**0.6786**	0.0000	**0.7418**	**T**
Bending-3	**All spans**	**0.7052**	**21.6690**	**0.6982**	**B**
Torsion-2	Center span + OH span + small torsion in KY span	0.7971	0.0000	-	-
Bending-4	**KY span + Center span + small bending in OH span**	**0.8150**	**4.6240**	**0.8424**	**B**
Torsion-3	Center span + small torsion in end spans	0.8391	0.0000	-	-
Bending-5	**Center span + small bending in end spans**	**0.9230**	**12.9690**	**0.8995**	**B**
				0.9296	T
Torsion-4	KY span + Center span + small torsion in OH span	0.9511	0.0000		
Torsion-5	Center span + KY span + small torsion in OH span	1.0201	0.0000		
				1.1259	T
Bending-6	**OH span + Center span + small bending in KY span**	**1.0855**	**1.7710**	**1.1414**	**B**
Torsion-6	OH span + small torsion in center span and KY span	1.1678	0.0000		
Bending-7	**All spans**	**1.1749**	**0.0150**	**1.2068**	**B**
Torsion-7	All spans	1.2571	0.0000		
				1.4107	T
				1.4444	T
Bending-8	**All spans**	**1.4233**	**0.9020**	**1.5177**	**B**

Table 10.4: Modal Assurance Criteria (MAC) between Operational Modal Analysis (OMA) and Finite Element Method (FEM) bending modes

FEM (Hz)	OMA (Hz)	MAC
0.483	0.497	0.88
0.704	0.698	0.91
0.815	0.842	0.60
0.924	0.899	0.84
1.087	1.141	0.69
1.178	1.207	0.89

Additionally, time domain and frequency domain OMA algorithms were also applied to the collected data, for comparing their performance with the OMA-EMIF algorithm. Both Poly-reference Time Domain or PTD and Rational Fraction Polynomial in z domain (RFPz) algorithms are high order algorithms, PTD being in time domain while RFP-z is in the frequency domain. Table 10.5 lists the frequency and damping estimates obtained using the two algorithms along with the estimates of the OMA-EMIF algorithm.

Table 10.5: Rational Frequency Polynomial (RFP-z) and Poly-reference Time Domain (PTD) estimates

RFP-z		PTD		OMA-EMIF	
Frequency	Damping	Frequency	Damping	Frequency	Damping
0.315	3.940	0.322	4.156	-	-
-	-	-	-	0.4966	1.3182
0.697	1.617	0.694	1.468	0.6982	1.8078
0.741	1.242	0.736	1.238	0.7418	1.8808
0.841	2.147	0.834	1.425	0.8424	2.1355
0.917	1.860	-	-	0.8995	1.1372
0.932	1.219	0.925	0.997	0.9296	1.2494
1.098	1.410	-	-	1.1259	1.2018
1.140	1.504	1.127	1.211	1.1414	0.8501
1.207	0.983	1.198	0.687	1.2068	1.0884
1.413	0.780	1.402	0.868	1.4107	0.9113
1.447	0.897	1.435	0.855	1.4444	0.9153
1.516	1.386	1.502	1.341	1.5177	1.4354

Results from the table show that both algorithms were able to estimate the mode around the 0.315 Hz frequency, which was not estimated by the OMA-EMIF algorithm. Furthermore, PTD was not able to identify two modes (highlighted in Table 10.5) which were estimated by RFP-z and OMA-EMIF algorithms. Also, it was discovered that the 0.49 Hz mode was only estimated by OMA-EMIF algorithm. The Auto MAC plots for PTD and RFP-z are shown in Figures 10.6 and 10.7.

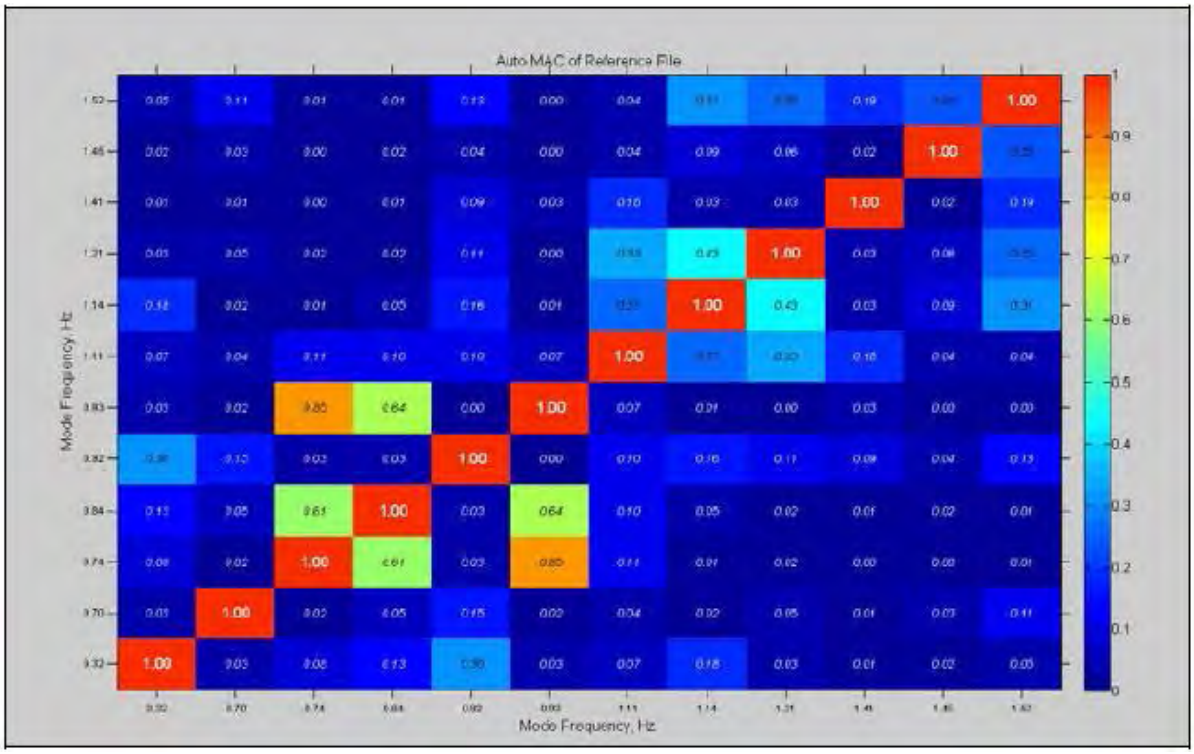

Figure 10.6 Auto Modal Assurance Criteria for Rational Fraction Polynomial in *z* domain estimates

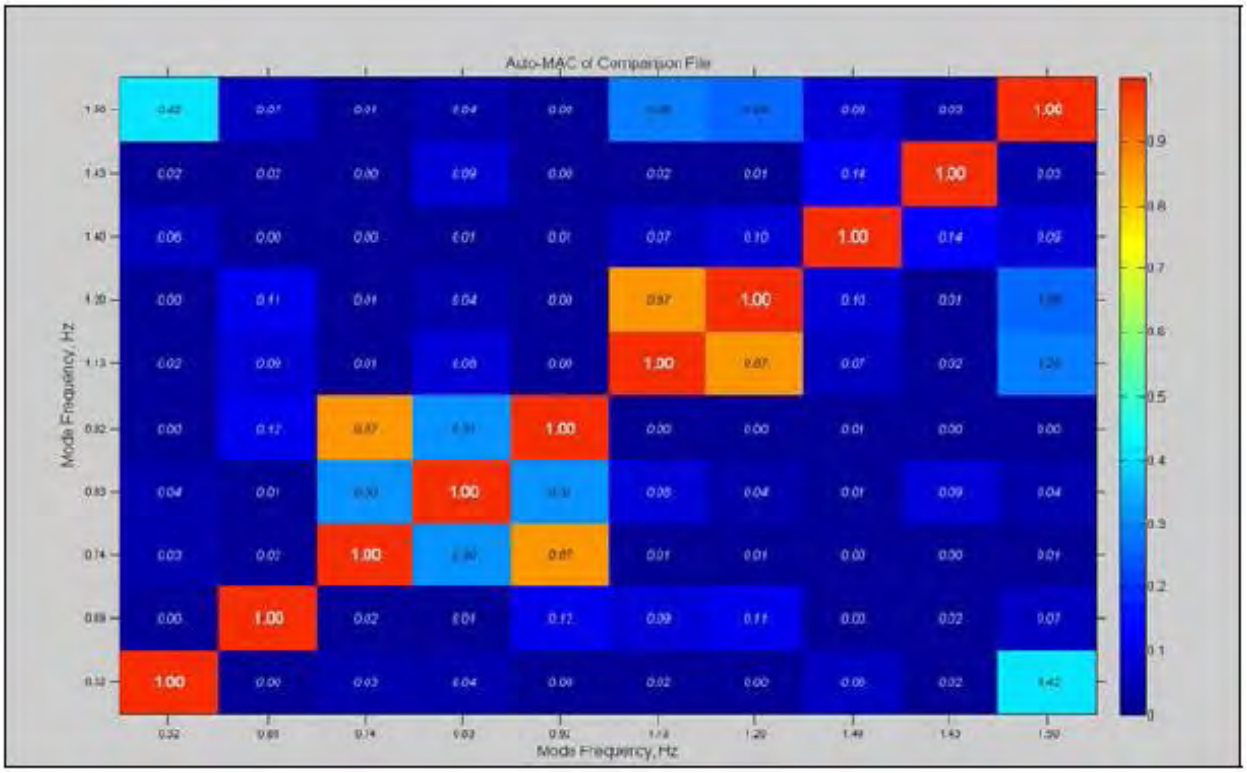

Figure 10.7 Auto Modal Assurance Criteria for Poly-reference Time Domain estimates

In Table 10.6, the cross MAC values between the various modes estimated by the three algorithms is presented. Some modes (highlighted in the table) have low cross MAC values or are not identified by some algorithms, indicating that the estimation of these modes is not consistent through the various algorithms. However, most of the bending modes (except for the 0.89 Hz mode) were identified satisfactorily. It should be noted that emphasis was laid, while designing the OMA set up, to observe these modes which were found to have high mass participation factor as per the finite element study.

Table 10.6: MAC Comparison between various OMA Algorithms

Frequency	OMA-EMIF/RFP-z	OMA-EMIF/PTD	RFP-z/PTD
0.31	-	-	0.169
0.49	-	-	-
0.69	0.756	0.686	0.903
0.74	0.644	0.789	0.850
0.84	0.117	0.279	0.816
0.89	0.012	-	-
0.93	0.988	0.985	.0979
1.12	0.324	-	-
1.14	0.645	0.876	0.687
1.20	0.999	0.998	0.999
1.41	0.486	0.606	0.756
1.44	0.597	0.732	0.841
1.51	0.980	0.986	0.997

10.4 Research Results and Conclusions

Based on the finite element studies, the modes with the high value of modal participation factors were identified. These modes were mostly bending modes and more critical than other modes. This knowledge from the FE model was combined with the findings of smaller pretests to design the final superstructure test. The importance of designing the final test in this manner comes from the fact that the chosen set up was optimum for the intended purpose which helped in reducing set up time, instrumentation and sensor requirement etc.

Also, the OMA-EMIF algorithm was used to obtain the modal parameters from the acquired data and these modes matched the finite element-based predictions, well within limits. The frequencies for the torsion modes don't match very well, and this is attributed to the inherent simplifications associated with the finite element model. In addition to OMA-EMIF, PTD and RFP-z algorithms were also applied to the collected data and their performance was also found to be satisfactory. The results of the various algorithms matched each other within error limits, thus providing more confidence in the estimated modal parameters.

References

1. S. Chauhan, J.S. Saini, S. Kangas, A.J. Helmicki, V.J. Hunt, and R.J. Allemang, "Application of OMA Algorithms to US Grant Bridge at Portsmouth, Ohio" Proceedings of International Modal Analysis Conference XXVI, Orlando, FL, 2008.
2. L.S. Heylen, "Modal Analysis Theory and Testing", PMA-K.U. Leuven, Belgium,1997.

Chapter 11 Website Design and Documentation

11.1 Introduction

A long term monitoring system has been installed in order to observe and evaluate environmental effects on the USG Bridge. This instrumentation package provided Ohio Department of Transportation (ODOT), University of Toledo (UT) and University of Cincinnati Infrastructure Institute (UCII) the ability to pull strain and temperature information about the bridge in a data-form which could easily be used to create plots over long periods of time (Kimmel et al 2009). Although the system provided strain and temperature information in a convenient format, the process involved manual data collection and required further work to create plots. A more automated approach to collecting, storing and plotting results was needed. A computer in the UCII laboratory was setup with customized data-logger software to make scheduled downloads of the bridges sensor data. These scheduled processes trigger various sets of programs to then load the collected data into a database for further analysis or plotting from web sites. With the data loaded into a database, ODOT, UT and UCII can plot sensor information from any web accessible device via a simple web browser. The ability to run programs on recently collected sensor data also provides the ability to alert the authorities of events if necessary. A diagram of the overall system described above is shown in Figure 11.1.

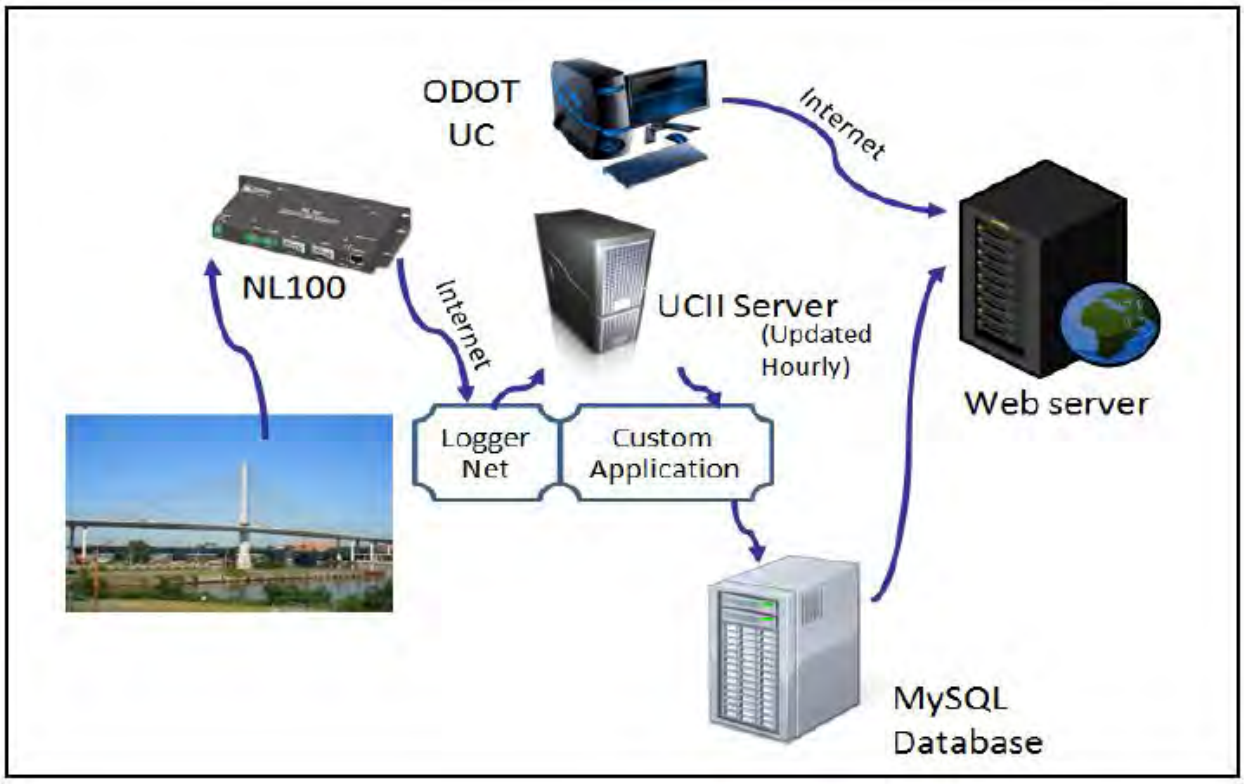

Figure 11.1: Complete Monitor System Diagram

11.2 Instrumentation

The current UCII long-term monitor for the USG Bridge consists of a Campbell Scientific CR10X data-logger, AM16/32 Relay Multiplexers, an NL100 Network Link interface, a Geokon Vibrating Wire Digital Signal Processor (DSP) interface and several Geokon Vibrating Wire Gages (VWG) embedded in the concrete. Figure 11.2 is a schematic showing the gage layout at each section of each lane of the bridge and the locations on the bridge where sensors are installed.

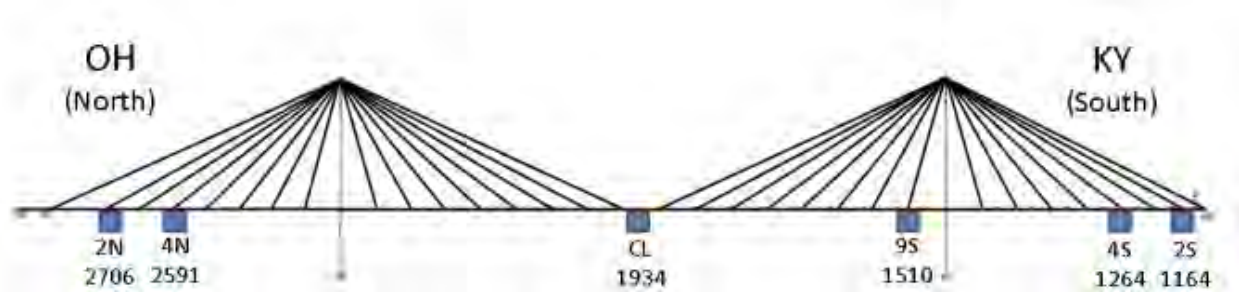

Figure 11.2 Segment Sensor Locations

11.3 Data Collection

The data collection and storage portion of the monitoring system is setup to take measurements every 30 minutes and store that information for download. Once stored by the data logger, the data is then ready for collection which can be carried out in various ways. The remote collection of data from the bridge is done using a dedicated computer with a dedicated internet connection which links to the NL100 device located at the bridge. Scheduling the automatic collection of the data is done using the LoggerNet software provided by Campbell Scientific.

The bridge health monitor incorporates a standard process for formatting and warehousing the collected data from the bridge. In order for the data downloaded from the CR10X to integrate into a database, some custom scripts were written which include a Python script for reformatting strings to dates, and another, for pushing the formatted data to a database. The driving script which calls all the others is a shell script which is what gets initiated by LoggerNet and also archives all collected data from the CR10X.

Making the collected data accessible via the web means warehousing the data in a database. This not only makes the data accessible but also makes sections or slices of specific data easily attainable. The database design was based on requirements of typical requests on the data and how those requests would best be handled. The database resides on a Department of Electrical Engineering server which was already running MySQL database server software. The LoggerNet software has a feature which allows for custom scripts to run after scheduled data collection tasks. The driving shell script for this system calls several scripts each with a specific purpose. Since this sequence is executed after each data collection, the database always

maintains the latest sensor data and can be used for real time monitoring of the bridge. Figure 11.3 shows a summary of the data collection process.

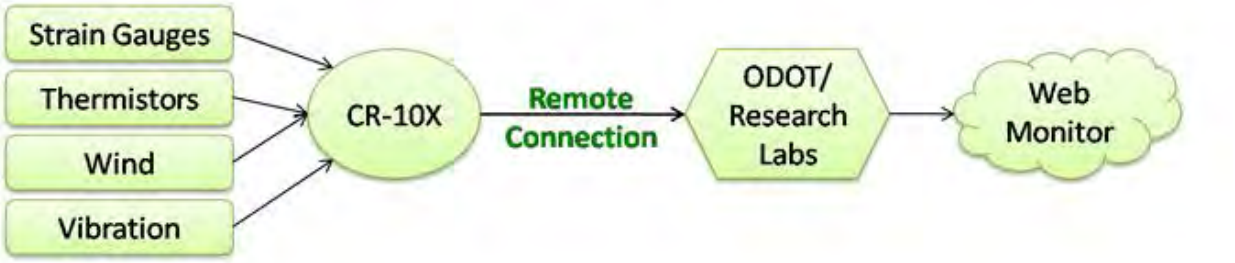

Figure 11.3 Data Collection Process for the USG Bridge

11.4 Website

The front door of this project is the web site which provides the tool for monitoring the bridge's health. Not only does the site provide the health monitoring but also provides information about all the equipment used and locations of installed sensors. To make navigating the site easy for the targeted audience, its design was based on the ODOT home page (http://www.dot.state.oh.us/). The web site's main sections include equipment information, installation information and monitoring. The navigation through the site is accomplished with a standard set of links on the left side that are always present. These links take you to the main sections of the web site and back to the main description page. The entire website is inaccessible by the general public and requires authorization by a username and password. Since the website is part of an ODOT funded project and was developed for UT and UCII researchers and ODOT staff to view, the website is limited to those personnel.

The monitor section of the web site is the most interactive and important section of the monitor and allows for further analysis of gage readings. The monitor page is the location used to examine and plot readings from various sensors on the bridge. The goal here was to provide a user-friendly interface to plot the strain readings but ultimately resulted in a page composed of a schematic of gage locations, a user input page, and a customizable graphing utility. Figure 11.4 shows the schematic used on the monitor page and a screen shot of the rest of the monitor page where the user input is handled. As shown the sensors installed on the bridge are listed on the left, which can be selected for plotting on a graph during a specified time frame. Temperature can also be plotted by selecting the check box next to it instead of Stress or Strain. Once all of the desired parameters are chosen, the "Graph" button is selected to produce plots based on the input parameters. A maximum of eight sensors can be plotted and each is plotted in different colors. You can also export the data in a comma separated value (CSV) format for use in other external graphing programs by selecting the "Export" button.

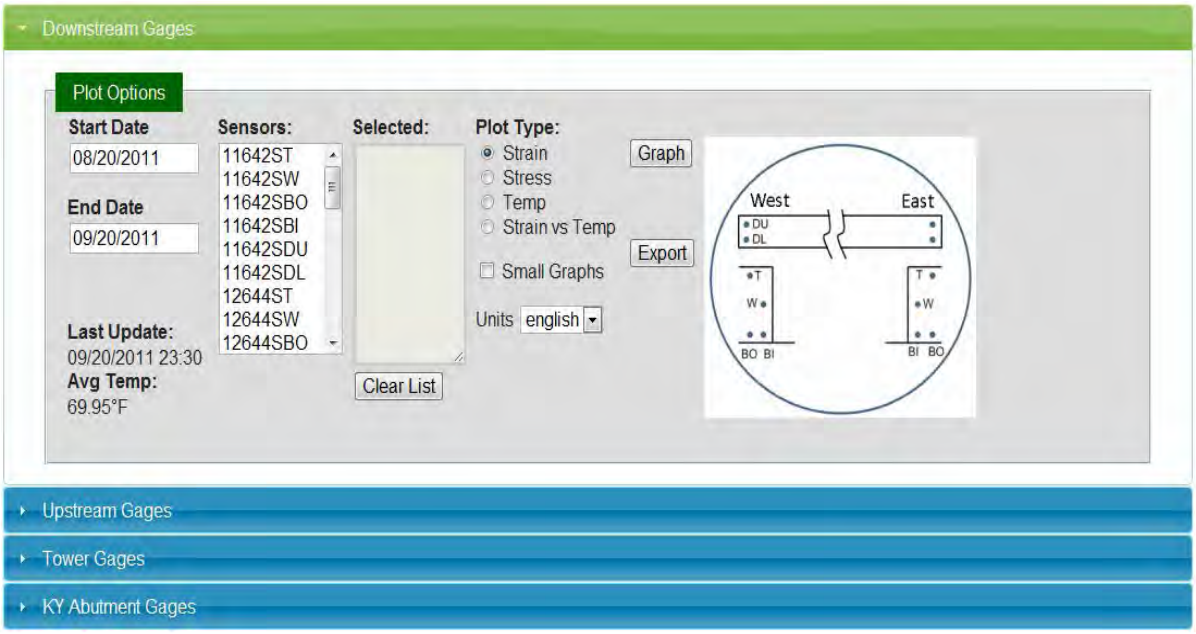

Figure 11.4 Monitor Website

When the vibrating wire gages are installed they are set at a value near its midrange per the manufacturer's operating manual which varies from gage to gage. Figure 11.5 displays the strain, and Figure 11.6, temperature plots of two sensors.

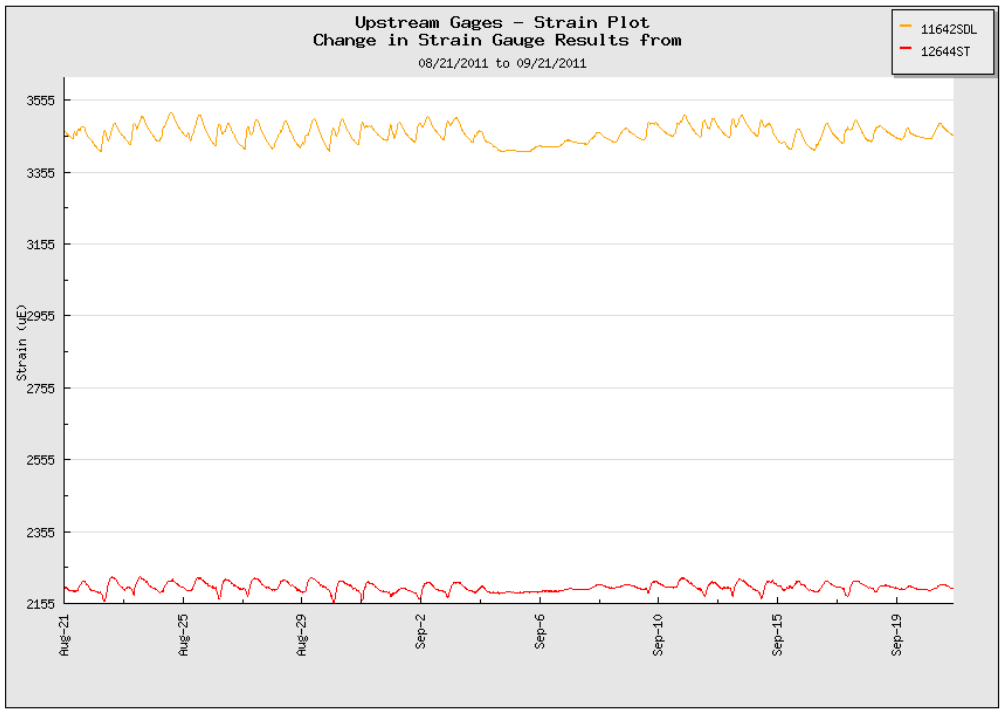

Figure 11.5 Web Monitor Sample Strain Plots

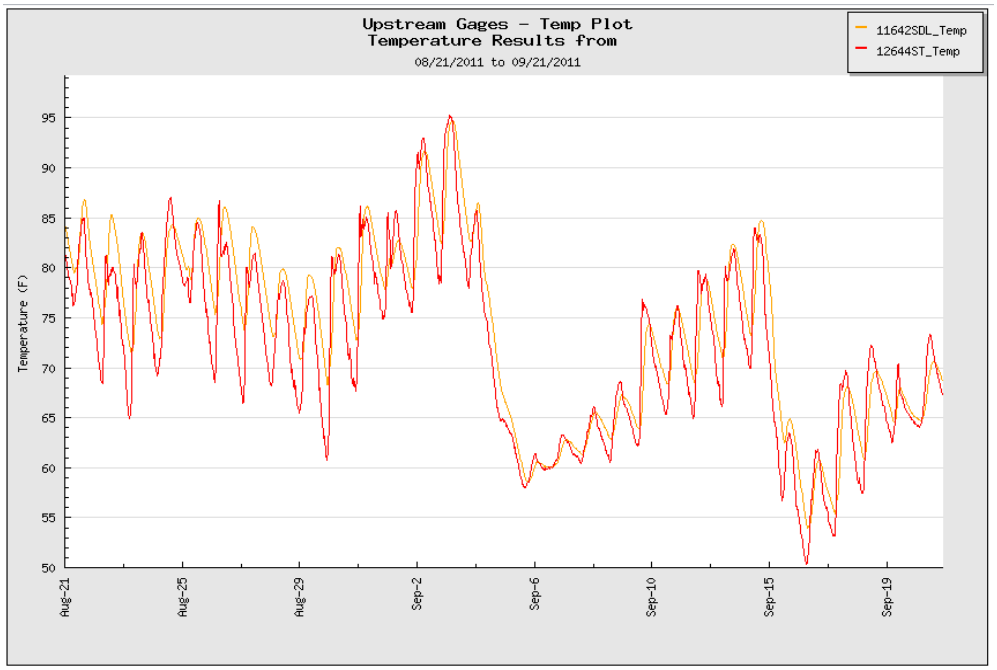

Figure 11.6 Web Monitor Sample Temperature Plots

11.5 Conclusion

This automated long-term health monitoring system for bridges is highly customizable and modular thus making it possible to add additional gages or other data driven devices. One main reason is the utilization of the existing manufacturer's software in a customized fashion. The most important and potential stopping point for such a system is remote connectivity but with modern devices such as cell phones even fairly remote locations can be connected. The use of open-source software and web standards also makes the system more apt to future customizations and additions. Currently the system consists of the following modules: data collection, data analysis and storage, and the web interface.

The data collection and warehousing of gage readings means not only can officials do further analysis of the bridges health but a historical archive of bridge performance is recorded. Plotting of strain data for multiple sensors over varying time frames means ODOT and UCII can further analyze the health of certain sections or the bridge as a whole over seasonal changes. High speed connectivity allows for more frequent data collection which enables close to real time monitoring of the bridge and conditions like cold weather or icing. This also allows for a close to real time model of the bridge for possible fault detection and warning.

References

1. G. Kimmel, J. Kumpf, V. Hunt, J. Swanson, A. Helmicki, "Automated Health Monitoring of an Aged and Deteriorated Truss," Proceedings of ASNT Fall Conference and Quality Testing Show, Columbus, OH, October, 2009.

Chapter 12 Conclusions and Future Work

12.1 Conclusions

The replacement of the US Grant Bridge over the Ohio River in Portsmouth, OH, was initiated by the Ohio Department of Transportation (ODOT) in 2001 when the original bridge was closed and demolished, and its substitute opened on October 16, 2006. The new structure consists of 9 spans, including a 875' main span crossing the Ohio River, for an overall bridge length of 2,155'. The design of this replacement structure is a steel cable stay design with steel girders and floor-beams supporting a post-tensioned concrete deck system nearly 65' wide carrying one lane of traffic in each direction. Each of the two main pylons/support towers are 288' above the waterline and the main span deck sits more than 85' above the Ohio River.

Research Plan

The initial tasks for the research project included modeling, sensor suite design and ordering of supplies and equipment. The first phase was to involve instrumentation of the towers at the traffic and cable anchor elevations as the construction process reached these locations. A select set of precast panels were chosen to be instrumented at the fabrication shop and critical steel frames at the staging yard near the construction site. The proposed design was such that a main cabinet for the on-site dedicated data systems would be installed at a secured and accessible location on the bridge, while a weather station would be installed at/upon one of the towers to characterize the environmental conditions at the structure. The first frame and panel was expected to be erected in July, 2002 and the final frame and panel in March, 2003. As the instrumented sections were erected, University of Cincinnati Infrastructure Institute (UCII) researchers worked with the contractor to route and connect the sensor cabling through a network of conduit and junction boxes to the main cabinet.

Also, dead-load effects would be recorded and long-term monitoring would begin as the sensors were connected to the data systems. In this manner, the responses to transverse and longitudinal post-tensioning of the panels would be measured and the stressing of the cable stays would be tracked for the given section and with successively erected sections of the bridge. Similarly, a set of dynamic experiments would be conducted to characterize the structure's response to ambient (e.g. wind) forces and effects, and to it.

Preliminary Design

Proper arrangements were made with the general contractor for the necessary assistance and access at the site, while minimizing any disruption to the construction work or its schedule. However, environmental loadings (i.e. wind, temperature, etc.), and traffic/in-service loadings were employed after construction without any need for contractor assistance. Detailed instrumentation and testing plan designs were developed in close consultation with ODOT officials, bridge designers, and construction contractors. Where possible, the researchers employed proven, off-the-shelf, turn-key components to assemble the pieces of the proposed monitor. This was to minimize monitor development time and maximize reliability.

In order to meet stated objectives, a weather station, together with a suite of vibrating wire and resistive strain gages, and accelerometers, were used at selected critical sections. Where possible, all gaging were placed embedded in (i.e., attached to rebar, etc.) or affixed on (i.e. tack-welded or epoxied to steel surfaces, etc.) the structure as construction proceeded.

Key variables that were monitored include:

- Weather conditions (i.e., temperature, precipitation, and wind direction and velocity).
- Cable acceleration in response to thermal, wind and traffic loads, in order to characterize vibration levels and mechanisms. Loads and stresses were calculated in order to ensure proper tensioning and positioning.
- Acceleration of selected deck sections in response to thermal, wind, and traffic load to compare with the designed frequencies of its movement, and to resolve any coupling with the stay movements themselves.
- Longitudinal stress of selected exterior girder and deck sections, particularly at abutments, pylons, and mid-span (high moment regions), in response to thermal, wind, and traffic load. These were used to monitor stress levels as compared to the design values and movement of the neutral axis of the section, and to obtain information on the integrity of the designed level of composite action.
- Thermal cross section of exterior girders and decking sections, over time, to resolve the environmental responses and internal strains of the structural components, and separate them from traffic responses.

A schedule of regular and automated monitoring, controlled truckload tests, and ambient cable vibration studies were also developed for the purposes of structural identification. The monitor and controlled tests/studies utilized installed sensor suites, and yielded the necessary information for comparison with design values as well as to calibrate finite element models of the structure. Such models were useful in determining the bridge response, globally, and interpolating responses at locations where gages were not mounted, developing trend lines for bridge response over time to understand long term behavior of structural systems, and provide a response-prediction tool which can be used for rating and issuance of overload permits, etc.

UCII researchers prioritized the many possible events of concern that may occur throughout the construction and service of this bridge, and winnowed the critical sections down to only five due to budget constraints. Existing design calculations and erection analyses were used to specifically identify the five critical sections to instrument, test, and monitor these variables during the life of the bridge. Allowable stress rating of the exterior girder section identified three minima of concern for the bottom flange in terms of positive moment and three for the cast-in-place (CIP) joint/decking above the girder in terms of negative moment. There was three of each, corresponding to each span of the structure. They do not necessarily coincide with each other, due to the very nature of a stayed structure and its staged construction; however, the middle and Ohio spans are proximate.

The Kentucky span is not a coincidence due to its large negative moment occurring near the end of construction when the bridge is weighed down and tied at the abutment in order to achieve the designed vertical profile for the structure. The ratings were also important because they enabled the identification of sections which may actually be classified as “cracked” (according to the designer) or non-composite. Note that the ratings for the pre-cast deck panels are also considered, which includes the post-tensioning to considerably improve the rating over the CIP joint/decking.

Finite Element Model

A three dimensional model, able to represent the real bridge geometry accurately, as well as having the ability to simulate symmetrical and unsymmetrical loading, was needed. Two finite element analysis packages were used depending on the desired response. The initial part of the research was conducted using SAP2000 version 7.44 (and version 10.0 later on) and the latter part of the study was conducted in ABAQUS, owing to limitations of SAP2000 to handle the involved complexities of the problem.

Besides the bridge deck, which behaves as a very stiff planar diaphragm, all components of the bridge are essentially linear elements. Therefore, the bridge components were idealized using linear elements, be it beam or truss. The beams at the deck level (i.e. longitudinal girders, cross beams and stringer beams) were modeled using three-dimensional BEAM elements, while the bridge deck was modeled using SHELL element with modifications to account for the fact that the girders carry all the axial forces, and nothing goes into the deck. The centerlines of the girder cross-section and the bridge deck are not aligned at the same horizontal plane, but the finite element model was developed assuming that both lie at the same plane. This simplification facilitates modeling efforts, but also leads to modeling deviations since the differences in the center of mass and center of rigidity of the bridge deck section are not reflected. This deviation primarily arises out of the eccentricity of the girder center line from the deck center line. The stiffness contribution due to the offset of the longitudinal girders from the center-line of the deck was accounted for by computing equivalent increased stiffness of the longitudinal girders. Also, the beam-beam shear connections were modeled as appropriate moment releases, ensuring that no moment are transferred between beams.

The pylons were modeled as three-dimensional beam elements, starting off at the pile-cap level, and cables were modeled as either One Element Cable Stay (OECS) or the Multi Element Cable Stay (MECS) formulation depending on the utility of the analysis. In SAP2000, OECS enabled the study of various installation effects for the tuned mass dampers’ global response, while both OECS and MECS were used for frequency extraction, computations involving cable vibrations, dynamic interaction effects, and dynamic sequence analysis in ABAQUS. When conducting a dead load analysis and eigenvalue extraction studies, as observed for the USG Bridge, it was sufficient to model the deck panels using single SHELL elements. For an equivalent static version of moving load analysis, however, it became imperative to model the deck panels using multiple deck elements, in order to allow accurate placement of truck loads.

The primary loading on a cable-stayed bridge comes from the self weight of the various elements, the cable pre-tensions and the vehicular loading, while the dynamic component arises due to the lateral loads associated with wind or seismic activity. Live load on the bridge consisted of HS20 truck and lane loading as per AASHTO standard specifications. In order to obtain accurate results, the equivalent static live load analysis was conducted with 97 load locations. The response from the various load cases were then overlapped appropriately to arrive at a realistic envelope of element responses. It was observed that slight discrepancies occurred at few locations, which were attributed to the modeling assumptions both by the designer and in the analysis.

The OECS model enabled the computation of superstructure frequencies and the corresponding modes. It was observed that the frequencies for the bending modes and corresponding mode shapes matched fairly well as compared to that of the torsional mode which had less correlation. For the US Grant Bridge, Operational Modal Analysis (OMA) tests were designed primarily to extract the structural frequencies accurately, while gathering some information on mode shapes. An array of 65 accelerometers was installed on bridge deck, with the arrangement designed to provide information on both the bending as well as torsion modes. Some preliminary tests were conducted to ascertain the suitability of the sensors and the adopted procedure, and then a final test was conducted. Again, the frequencies and mode shapes of the bending modes matched very well, but the torsion modes did not, for earlier-mentioned reasons.

Construction Loads

A significant amount of effort was expended in this project to measure, record, and interpret the behavior of the steel framing and composite concrete decking system during construction. This included monitoring the induced stresses and strains, where and when they occurred, and investigating causative effects. The main components of the framing system, namely the edge girders and the cast-in-place concrete strip directly above them, were comprehensively instrumented and continuously monitored during the construction of the bridge (see Figure 3.8). Instrumented monitoring commenced immediately before the segment was erected onto the bridge, through any temporary stressing or profiling with the stays or post-tensioning strands, placement of the precast concrete deck panels, during the concrete pour and curing of the cast-in-place strips, and as other segments were installed on either side of its respective tower, throughout most stages of its construction and into (and beyond) service on October 16, 2006.

The measured long-term strain/stress observed in March, 2009 are tabulated and compared to the equivalent deadload predictions by B&T. These values would include not only deadload and the superimposed deadload of the items installed in the Summer of 2006 (e.g., parapet, median, overlay, etc.), but also any and all other long-term effects that are evident (e.g., creep, shrinkage, degradation, initial repairs to the Kentucky pulldowns, etc.). Since all such stresses are treated the same by the Load Factor Method of analysis, we combine them here. Note that for most of the instrumented segments there is relative agreement between measured and estimated values.

Little to no change was observed in the average long-term value for each gage between 2009 and 2012 results; however, there was a positive moment induced locally near the Kentucky abutment due to the installed exterior pulldowns in 2011. There is little to no effect from creep (or any other long-term effect except the obvious seasonal response cycle) which contradicts the expected negative moment due to creep as predicted by the analysis of B&T.

Truckload Testing Results

ODOT provided four tandem-axle dump trucks to conduct the truck load tests. The trucks were placed in one of the static positions from the test plan and at least three readings were recorded from each sensor. It took about 10 minutes to test each position because the CR-10X loggers required about 2 minutes to scan the all of the vibrating wire gages and there was always some delay in positioning the trucks. A set of readings with no load on the bridge was recorded periodically during the test to cancel out any environmental effects in the results.

The moving truckload tests were conducted after the static tests, throughout the remainder of the afternoon. One truck was selected and the other trucks were returned to the garage. One person with a walkie-talkie took the passenger seat of the truck. The truck driver was to start north of the bridge, accelerate to a speed of about 20mph, center the truck in the test lane, and maintain that speed (and lane) for the entire length of the bridge. Upon reaching the south abutment, the truck would immediately brake to stop short of the intersection just south of the bridge. Two high-speed data acquisition systems were deployed at the northern sensor station (i.e., 2N). Data collection at 200Hz was manually triggered to commence as the front tire reached the north expansion joint and concluded when the back tire reached the southern expansion joint. Data was collected as the truck ran each marked lane and shoulder; then, the data systems would be relocated to the next sensor station, and the entire set of tests run again.

Upstream and downstream edge girders have comparable response to truckload; however, the thermal response for some gages (e.g., web) dwarfs the liveload response. Composite action is clearly evident in all test results, with a greater slope in the strain profile and hence large effective deck width than predicted by analysis. Laneload results control over the truckload results and are used as the liveload response in the rating analysis of the structure. Measured results are slightly less than the conservative predictions of the design analysis, with two exceptions at the middle span and Kentucky abutment. These locations should be especially observed during inspection for unexpected signs of distress.

After the bridge was opened to service in 2006, the Kentucky abutment and backwall began to exhibit cracking that started near the beam seat but became pervasive with increasing length and width over each subsequent inspection. It was believed that the source of this degradation was field modification to the location and installation of the steel pulldowns internal to the abutment. ODOT provided for immediate field rehabilitation of this installation, including the use of additional welding at the beam seat to resist further movement, which seemed to abate further cracking at the abutment. UCII then subsequently conducted another truckload test in order to observe/validate the effectiveness of the rehab and compare with expected design

values. After rehab of the Kentucky abutment, measured results are now equal to or slightly less than the conservative predictions of the design analysis.

A major rehabilitation of the Kentucky abutment pulldowns was conducted in 2011 in order to further examine, stiffen, and provide redundancy in the form of structural strands exterior to the abutment affixed to the edge girders and secured with rock anchors. HNTB designed the rehab and Brayman contracted the work. UCII installed additional instrumentation, along with any monitoring and truckload test results of same. A follow-up truckload test was conducted for comparison with previous test results, for verification of the continued performance of the structure and its new pulldowns, as well as to document the new baseline liveload response of the bridge. Measured results are slightly less than the conservative predictions of the design analysis, with the exception of the Kentucky abutment due to the addition of the exterior pulldowns and transverse bracing at Station 1S. In addition, there was a slight, unexplained change in influence line at Station 2S in 2012 as compared to the 2009 test results. These locations should be especially observed during inspection for unexpected signs of distress.

Pulldown Instrumentation and Testing

The goal of this part of the project was to install additional instrumentation at KYA on the US Grant bridge to monitor that location and track changes in its state of stress during and beyond the pending retrofit at that location. Vibrating wire gages were to be installed on both of the new upstream and downstream pull downs and at the abutment wall near KYA. Just as there was consistent behavior for the strain gages on the exterior girders over time, the strand and tilt meters show daily and seasonal cycles with very little drift over their deployment.

The measured results of the strand meters over the course of the static truckload tests yield similar conclusions as that found for the strain gages upon the exterior girders under static truckload. These results provide a liveload benchmark of the pulldown sensor package for future reference, and allow some rating analysis for the pulldowns themselves. Note that the response is compressive when the trucks are located in the span coincident with the sensors and tensile when the trucks are located in the adjacent or middle span of the bridge. Since the strands were pre-tensioned to act as pulldowns, compressive effects are not a concern in damaging the strands and only the tensile response that occurs for trucks located in the middle span needs to be analyzed.

The load factor rating of the strands was then found to be 2.0 under static truckload; however, we know that laneload will be a larger response and hence control for ratings purposes. Unfortunately, this cannot be estimated directly from the static truckload test results; however, if an analytical version of the laneload were provided for the strands, it could be easily scaled according to these test results and then used for ratings purposes. In any case, we will find that these rating results are comparable to those found using the strain gages on the exterior girders and, hence, the pulldowns are of similar condition to that of the superstructure itself.

Structural Analysis and Load Rating

An inventory HS25 rating using both the allowable stress and load factor methods was formulated for both the composite and noncomposite or cracked case for each section as defined by the stations used by both HNTB and B&T. Each section was analyzed by each method at the bottom flange, top flange, cast-in-place (CIP) decking immediately above the edge girder, and for the deck panel adjacent to the edge girder which is to include the effect of the post tensioning (PT) force reported by B&T. In addition, each of these members was analyzed under both the positive and negative liveload moment reported by HNTB.

Initially, the rating formulations were conducted with both bending moment and axial force stresses added together; this allowed both effects to be considered simultaneously. In addition, the axial force is greatly diminished near the abutments and centerline of the structure, which also happens to be the locations of the lowest rated sections of the bridge; so, axial force was only somewhat reducing the controlling rating values. However, load factor design has commonly separated bending moment and axial force effects in the standard rating calculation. Upon review of the design manuals by HNTB, it seemed that this convention was also intended in the design of this bridge. Given that the axial force was only somewhat affecting the controlling rating values, it was decided to follow this convention.

Many of the sections have a bottom flange whose dimensions are such that the section will fail the compression flange check for compact and even braced sections. Many of the sections have lateral bracing (e.g., floorbeams) which does not meet the specification for the compression flange of a compact nor even a braced section. Without some guidance from the designer, we reduced the ultimate moment for negative moment regions to the yield limit state due to this concern. Accordingly, we calculated both the measured (RF = 1.11) and designed (RF = 1.13) load factor rating at the instrumented sections of the US Grant bridge. This inventory rating was formulated using the measured deadload and superimposed deadload (DL) from the vibrating wire strain gages, both with and without the measured liveload (LL) response from the moving truckload tests, for the instrumented sections at the End of Construction (EOC) in October, 2006. For the same stations, an inventory rating was formulated using the analytical estimates of the erected deadload by B&T (version 3) and the design liveload by HNTB for comparison. The measured load factor rating remained about the same (RF = 1.18) based upon field measurements of both deadload and liveload; however, the critical location switched from the center span to the Kentucky abutment due to the field restoration of the pulldowns.

During our Project Review with ODOT in 2009, we were asked to report ratings in two distinct fashions: 1) deadload based only upon EOC structural condition (RF = 1.26), and 2) deadload which incorporates both EOC structural condition and any/all other long-term effects and events that were not included within the EOC data (RF = 1.15): seasonal cycle upon the bridge (e.g., thermal, boundary conditions), creep and shrinkage effects on the concrete CIP joint, the initial repairs at the Kentucky abutment, etc. Of these, the main effect is the seasonal cycle; however, all are actual measured stresses that would constitute a reduction in capacity and lead to the most conservative estimate of the load rating.

In 2010, the designer HNTB provided a draft of their Bridge Analysis and Rating Report for the U.S. Grant Bridge to ODOT. A global model of the entire structure was used to calculate the internal demand forces for various structural components of the bridge, including the edge girders, cable stays, deck panels, floor and strut beams. In their rating report, HNTB reported that the bridge just barely reached an HS20 inventory rating (RF = 1.0) using Load Factor Method, with the most critical location identified as the West Girder of Segment 15N. Given that our deadloads and liveloads are not sufficiently different to cause such a reduction in our ratings, the reduction must come from capacity.

In 2011, HNTB provided a written a draft of their Manual for Load Rating and Permits for the U.S. Grant Bridge to ODOT. Most commonly, the segments do not pass the lateral bracing check for a braced noncompact section. Hence, the capacity is reduced to that computed for a partially braced member. Unfortunately, it is not entirely clear as to which reduced capacity of several listed is considered in their rating; so, to be conservative, we will assume here the smallest value listed by HNTB for a given segment for the capacity of the edge girder segments and subsequent load factor ratings (RF = 1.49). This inventory assessment only considers the marked lanes (and not the two large shoulders) for HS20 laneload and structural deadloads. An operating assessment was made (RF = 1.29) which also included environmental and other long-term deadload effects.

In 2010, the designer HNTB redefined the allowable stress for the stay cables as 50% of gross ultimate tensile strength (GUTS) for inventory rating purposes. They list East (or Upstream) Stay 16N as the critical stay with an inventory rating of 1.35, based upon their structural model discussed above. Our stay test results were generally within 10% of those predicted by the B&T erection analysis; hence, our field ratings should be within 10% of those determined by the HNTB Manual.

Stay Vibration

Before the opening of the US Grant Bridge, several rounds of field experiments were conducted to investigate the ability to estimate cable tensions using vibration-based measurements. Because the configuration of cable stays prevents direct measurement of the internal wire strands that comprise the stay, these measurements have been made by measuring the motion at the sheath. Traditionally cable stays have used grout as a corrosion inhibitor, so the sheath and strands were forced to have composite motion. Studies, however, had shown that this grout actually accelerated cable degradation. Hence, new stay designs have eliminated grout and replaced this inhibitor with individually greased and sheathed strands or an epoxy resin directly applied to the strands. US Grant utilizes individually greased and sheathed strands and a high-density polyethylene (HDPE) sheath. Based on the series of experiments performed at US Grant throughout construction, it has been shown that accurate tension estimates could still be made by measuring cable motion at the sheath even with the cable cross-ties in place.

Structural Modal Analysis

Based on the finite element studies, the modes with the high value of modal participation factors were identified. These modes were mostly bending modes and more critical than other modes. This knowledge from the FE model was combined with the findings of smaller pretests to design the final superstructure test. The importance of designing the final test in this manner comes from the fact that the chosen set up was optimum for the intended purpose which helped in reducing set up time, instrumentation and sensor requirement etc.

Also, the OMA-EMIF algorithm was used to obtain the modal parameters from the acquired data and these modes matched the finite element-based predictions, well within limits. The frequencies for the torsion modes don't match very well, and this is attributed to the inherent simplifications associated with the finite element model. In addition to OMA-EMIF, PTD and RFP-z algorithms were also applied to the collected data and their performance was also found to be satisfactory. The results of the various algorithms matched each other within error limits, thus providing more confidence in the estimated modal parameters.

Website Design

This automated long-term health monitoring system for bridges is highly customizable and modular thus making it possible to add additional gages or other data driven devices. One main reason is the utilization of the existing manufacturer's software in a customized fashion. The most important and potential stopping point for such a system is remote connectivity but with modern devices such as cell phones even fairly remote locations can be connected. The use of open-source software and web standards also makes the system more apt to future customizations and additions. Currently the system consists of the following modules: data collection, data analysis and storage, and the web interface.

The data collection and warehousing of gage readings means not only can officials do further analysis of the bridges health but a historical archive of bridge performance is recorded. Plotting of strain data for multiple sensors over varying time frames means ODOT and UCII can further analyze the health of certain sections or the bridge as a whole over seasonal changes. High speed connectivity allows for more frequent data collection which enables close to real time monitoring of the bridge and conditions like cold weather or icing. This also allows for a close to real time model of the bridge for possible fault detection and warning.

12.2 Future Work

Given the concerns stated above regarding the capacity of the designed structure, UCII recommends regular maintenance and continued monitoring with the designed health monitoring system. In addition, special attention should be directed to the stations mentioned above during visual inspections (specifically, the Kentucky abutment and the middle of the center span). The maintenance manual calls for regular inspection and lift-off tests of select stays in order to check for any changes in their deadload force. Finally, we recommend a regular regimen of truckload tests for comparison with the baseline tests provided herein.